Report No. FRA - RT - 73 - 30

METROLINER
RIDE IMPROVEMENT PROGRAM

James M. Herring

FEBRUARY 1973

FINAL REPORT

Prepared for

FEDERAL RAILROAD ADMINISTRATION

Office of Research, Development and Demonstrations

Washington D. C. 20590

The contents of this report reflect the views of The Budd Company, Technical Center which is responsible for the facts and the accuracy of the data presented herein. The contents do not necessarily reflect the official views or policy of the Department of Transportation. This report does not constitute a standard, specification or regulation.

TECHNICAL REPORT STANDARD TITLE PAGE

1. Report No.	2. Government Accession No.	3. Recipient's Catalog No.
FRA - RT - 73 - 30		

4. Title and Subtitle	5. Report Date
METROLINER RIDE IMPROVEMENT PROGRAM	February 1973
	6. Performing Organization Code

7. Author(s)	8. Performing Organization Report No.
James M. Herring	PR-394

9. Performing Organization Name and Address	10. Work Unit No.
The Budd Company, Technical Center 300 Commerce Drive Fort Washington, Penna. 19034	11. Contract or Grant No. DOT-FR-10035
	13. Type of Report and Period Covered
12. Sponsoring Agency Name and Address Department of Transportation Federal Railroad Administration Washington, D. C.	Final Report
	14. Sponsoring Agency Code

15. Supplementary Notes

16. Abstract The objective of this program was to determine methods of improving the ride quality of the Metroliner railcars. Two levels of modifications were considered: first, modifications to the existing hardware and second, replacement of the present trucks. In the conduct of the program road tests, track measurement and laboratory dynamic tests were performed on the present Metroliner. The results of these tests were used to aid in the development of a dynamic simulation of the Metroliner, and assist in establishing the nature of track irregularities. Once developed, the simulation was used to evaluate modifications to the present Metroliner and new truck configurations.

17. Key Words	18. Distribution Statement
Railcar dynamics; Dynamic testing; ride comfort, system identification; railcar design, vibration; dynamic simulation	Document is available to the public through the National Technical Information Service, Springfield, Virginia 22151

19. Security Classif. (of this report)	20. Security Classif. (of this page)	21. No. of Pages	22. Price
Unclassified	Unclassified	184	

PREFACE

During the conduct of the program, significant contributions were made by The Federal Railroad Administration; The Analytic Computing Division, and The Loads Division of NASA Langley; The Penn Central Railroad; Battelle Memorial Institute; and ENSCO, Inc. We gratefully acknowledge the assistance of these organizations in contributing to the successful completion of this program.

TABLE OF CONTENTS

		Page
1.0	INTRODUCTION	1
	1.1 Objective	1
	1.2 Plan.	1
	1.3 Participating Organizations	3
2.0	DEVELOPMENT AND VERIFICATION OF THE SIMULATION . . .	4
	2.1 The Carbody Subsystem	5
	2.2 The Truck Subsystem	20
	2.3 The Power Transformer Subsystem	31
3.0	TRACK IRREGULARITY INPUTS.	41
	3.1 Wheelbase Dependent Inputs.	43
	3.2 Truck Spacing Dependent Inputs.	52
	3.3 Rail Joint Dependent Inputs	55
	3.4 Summary of Track Irregularity Inputs.	65
4.0	PERFORMANCE OF PRESENT METROLINER.	70
	4.1 Performance of Vertical Simulation of Present Metroliner.	71
	4.2 Performance of Lateral Simulation of Present Metroliner.	89
	4.3 Summary of Present Metroliner Performance . . .	120
5.0	MODIFIED DESIGN.	128
	5.1 Recommended Modifications to Present Metroliner	143
6.0	NEW TRUCK DESIGN	150
	APPENDIX: RAILCAR DYNAMIC SIMULATION (Bound under separate cover)	

LIST OF ILLUSTRATIONS

2.1-1	Carbody Subsystem	6
2.1-2	Carbody Subsystem Vertical Acceleration "A" End of Carbody	9
2.1-3	Carbody Subsystem Vertical Accelration	10
2.1-4	Carbody Subsystem Vertical Acceleration "B" End of Carbody	11
2.1-5	Truck Response During Vertical Carbody Test	13
2.1-6	Carbody Subsystem Lateral Acceleration "A" End of Carbody	15
2.1-7	Carbody Subsystem Lateral Acceleration Center of Carbody	16
2.1-8	Carbody Subsystem Lateral Acceleration	17
2.1-9	Carbody Subsystem Roll Acceleration "A" End of Carbody	18
2.2-1	Side View Metroliner Truck	21
2.2-2	End View Metroliner Truck	22
2.2-3	Plan View Metroliner Truck	23
2.2-4	Truck Subsystem Vertical Acceleration Truck Frame Assembly	26
2.2-5	Truck Subsystem Load Deflection Primary Suspension With Gear Coupling Connected and Disconnected	28
2.2-6	Truck Subsystem Vertical Dynamic Test With Gear Coupling Connected and Disconnected	29
2.2-7	Dynamic Spring Rate and Damping Capacity of Pirelli Spring	30
2.2-8	Truck Subsystem Roll Acceleration of Truck Frame Assembly	32
2.3-1	Power Transformer Subsystem	35
2.3-2	Power Transformer Subsystem Vertical Acceleration of Transformer	37

2.3-3	Power Transformer Subsystem Lateral Acceleration of Transformer.	38
2.3-4	Power Transformer Subsystem Roll Acceleration of Transformer	39
3.1-1	Track Irregularity Wave Length of Maximum Vertical Input	45
3.1-2	Road Test, Average Vertical Acceleration of Equalizer Beams on A End Truck Run #5	46
3.1-3	Track Irregularity Wavelengths of Minimum Vertical Input	48
3.1-4	Road Test, Laterial Acceleration of Journal Boxes on "A End" Truck Run #5	49
3.1-5	Road Test, Yaw Acceleration of Journal Boxes on "A End" Truck Run #5.	50
3.1-6	Road Test, Roll Acceleration of Equalizer Beams on "A End" Truck Run #5	51
3.1-7	Frequencies of Track Irregularities Where Maxima and Minima in Truck Wheel and Axle Assemblies Acceleration Occur VS Train Speed . . .	53
3.2-1	Frequencies of Track Irregularities Where Metroliner Truck Motion are in Phases and 180° out of Phase VS Train Speed.	54
3.3-1	Track Measurement, Right Alignment Run #4	56
3.3-2	Track Measurement, Right Profile Run #4.	57
3.3-3	Relationship of Left and Right Rail Profiles . . .	58
3.3-4	Track Measurement, Crosslevel Run #4	60
3.3-5	Track Measurement, Gage Run #4	61
3.3-6	Road Test, Vertical Acceleration of Equalizer Beams on "A End" Truck Run #4	62
3.3-7	Road Test, Lateral Acceleration of Journal Boxes on "A End" Truck Run #4	63
3.3-8	Road Test, Roll Acceleration of Equalizer Beams on "A End" Truck Run #4	64
3.3-9	Track Measurement, Right Profile Run #5.	66

3.3-10	Track Measurement, Right Alignment Run #5	67
3.3-11	Frequencies of Maxima Wheel Set Accelerations Due to Track Joints VS Train Speed	68
3.4-1	Frequencies of Dominant Railcar Inputs VS Train Speed	69
4.1-1	Present Metroliner Truck Frame Vertical Acceleration Due to Vertical Input	73
4.1-2	Road Test, Vertical Acceleration of Truck Bolster on "A End" Truck Run #5	74
4.1-3	Present Metroliner, Truck Frame Longitudinal Acceleration Due to Pitch Input	76
4.1-4	Road Test, Longitudinal Anchor Rod Forces on "A End" of Car Run #5	77
4.1-5	Present Metroliner, Carbody "A" End Vertical Acceleration Due to Vertical Input	78
4.1-6	Present Metroliner, Carbody "A End" Vertical Acceleration Due to Pitch Input	79
4.1-7	Road Test, Vertical Acceleration of Carbody Floor Over "A End" Left Bolster Spring Run #5 . . .	80
4.1-8	Road Test, Vertical Acceleration of Carbody Floor Over "A" End Right Bolster Spring Run #4 . .	81
4.1-9	Gain of Filter for Road Test.	83
4.1-10	Road Test, Vertical Acceleration of Truck Bolster on A End Truck Run #4	84
4.1-11	Road Test, Vertical Force Transmitted Through Bolster Spring on "A" End Truck, Right Side Run #4	85
4.1-12	Present Metroliner, Carbody Center Vertical Acceleration Due to Vertical Input	86
4.1-13	Road Test, Vertical Acceleration of the Carbody Floor at the Center Run #5	87
4.1-14	Road Test, Vertical Acceleration of the Carbody Floor at the Center Run #4	88
4.1-15	Present Metroliner, Carbody Center Vertical Acceleration Due to Pitch Input	90

4.1-16	Present Metroliner, Carbody Longitudinal Acceleration Due to Pitch Input	91
4.1-17	Present Metroliner, Transformer Vertical Acceleration Due to Vertical Input	92
4.1-18	Road Test, Vertical Acceleration of Power Transformer Mounted to Carbody Near Center Run #5	93
4.1-19	Present Metroliner, Transformer Vertical Acceleration Due to Pitch Input	94
4.1-20	Present Metroliner, Transformer Longitudinal Acceleration Due to Pitch Input	95
4.2-1	Present Metroliner, Truck Frame Lateral Acceleration Due to Lateral Input	97
4.2-2	Present Metroliner, Truck Frame Lateral Acceleration Due to Roll Input.	98
4.2-3	Present Metroliner, Truck Frame Lateral Acceleration Due to Yaw Input	99
4.2-4	Present Metroliner, Truck Frame Roll Acceleration Due to Roll Input	100
4.2-5	Present Metroliner, Truck Fram Roll Acceleration Due to Lateral Input	101
4.2-6	Present Metroliner, Truck Frame Roll Acceleration Due to Yaw Input	102
4.2-7	Present Metroliner, Carbody "A End" Lateral Acceleration Due to Lateral Input	103
4.2-8	Road Test, Lateral Acceleration of Carbody Floor Over "A" End Right Bolster Spring Run #1	104
4.2-9	Present Metroliner, Carbody "A" End Lateral Acceleration Due to Roll Input.	106
4.2-10	Present Metroliner, Carbody "A" End Lateral Acceleration Due to Yaw Input	107
4.2-11	Present Metroliner, Carbody Center Lateral Acceleration Due to Lateral Input	108
4.2-12	Road Test, Lateral Acceleration of Carbody Floor at Center Run #5.	109

4.2-13	Present Metroliner, Carbody Center Lateral Acceleration Due to Roll Input	110
4.2-14	Present Metroliner, Carbody Center Lateral Acceleration Due to Yaw Input	111
4.2-15	Present Metroliner, Carbody "A" End Roll Acceleration Due to Lateral Input	112
4.2-16	Present Metroliner, Carbody "A" End Roll Acceleration Due to Yaw Input	113
4.2-17	Present Metroliner, Carbody "A" End Roll Acceleration Due to Roll Input	115
4.2-18	Present Metroliner, Transformer Lateral Acceleration Due to Lateral Input	116
4.2-19	Present Metroliner, Transformer Lateral Acceleration Due to Roll Input	117
4.2-20	Present Metroliner, Transformer Lateral Acceleration Due to Yaw Input	118
4.2-21	Road Test, Lateral Acceleration of Bottom of Power Transformer Mounted to Carbody Near Center Run #5	119
4.2-22	Road Test, Yaw Accelerator of Journal Bores on "A" End Truck Run #8	121
4.2-23	Road Test, Lateral Acceleration of Journal Boxes on "A" End Truck Run #8	122
4.2-24	Road Test, Yaw Acceleration of Truck Frame on "A" End Truck	123
4.2-25	Road Test, Lateral Acceleration of Carbody Floor Over "A" End Right Bolster Spring	124
4.2-26	Road Test, Lateral Acceleration of the Carbody Floor at the Center Run #8	125
4.2-27	Road Test, Lateral Acceleration of Bottom of Power Transformer Mounted to Carbody Near Center.	126
5.0-1	Modified Design, Carbody "A end" Vertical Acceleration Due to Vertical Input	130
5.0-2	Modified Design, Carbody Center Vertical Acceleration Due to Vertical Input	131

5.0-3	Modified Design, Transformer Vertical Acceleration Due to Vertical Input	132
5.0-4	Modified Design, Carbody "A end" Lateral Acceleration Due to Lateral Input.	134
5.0-5	Modified Design, Carbody "A end" Lateral Acceleration Due to Roll Input	135
5.0-6	Modified Design, Carbody "A end" Lateral Acceleration Due to Yaw Input.	136
5.0-7	Modified Design, Carbody Center Lateral Acceleration Due to Lateral Input.	137
5.0-8	Modified Design, Carbody Center Lateral Acceleration Due to Roll Input	138
5.0-9	Modified Design, Carbody Center Lateral Acceleration Due to Yaw Input.	139
5.0-10	Modified Design, Carbody "A end" Roll Acceleration Due to Lateral Input.	140
5.0-11	Modified Design, Carbody "A end" Roll Acceleration Due to Yaw Input.	141
5.0-12	Modified Design, Carbody "A end" Roll Acceleration Due to Roll Input	142
5.0-13	Modified Design, Truck Frame Vertical Acceleration Due to Vertical Input	145
5.0-14	Modified Design, Truck Frame Longitudinal Acceleration Due to Pitch Input.	146
5.0-15	Modified Design, Carbody "A end" Vertical Acceleration Due to Pitch Input.	147
5.0-16	Modified Design, Carbody Center Vertical Acceleration Due to Pitch Input.	148
5.0-17	Modified Design, Carbody Longitudinal Acceleration Due to Pitch Input.	149
6.0-1	Effect of Truck Frequency, Carbody "A end" Vertical Acceleration Due to Vertical Input. . . .	152
6.0-2	Effect of Truck Frequency, Carbody Center Vertical Acceleration Due to Vertical Input. . . .	153

6.0-3	New Truck Design, Truck Frame Vertical Acceleration Due to Vertical Input	156
6.0-4	New Truck Design, Truck Frame Longitudinal Acceleration Due to Pitch Input	157
6.0-5	New Truck Design, Carbody A-end Vertical Acceleration Due to Vertical Input	158
6.0-6	New Truck Designs, Carbody A-end Vertical Acceleration Due to Pitch Input	159
6.0-7	New Truck Design, Carbody Center Vertical Acceleration Due to Vertical Input	160
6.0-8	New Truck Design, Carbody Center Vertical Acceleration Due to Pitch Input	161
6.0-9	New Truck Designs, Carbody Longitudinal Acceleration Due to Pitch Input	162
6.0-10	New Truck Designs, Transformer Vertical Acceleration Due to Vertical Input	163
6.0-11	New Truck Designs, Transformer Vertical Acceleration Due to Pitch Input	164
6.0-12	New Truck Designs, Transformer Longitudinal Acceleration Due to Pitch Input	165
6.0-13	New Truck Designs, Truck Frame Lateral Acceleration Due to Lateral Input	166
6.0-14	New Truck Designs, Truck Frame Lateral Acceleration Due to Roll Input	167
6.0-15	New Truck Designs, Truck Frame Lateral Acceleration Due to Yaw Input	168
6.0-16	New Truck Designs, Truck Frame Roll Acceleration Due to Roll Input	169
6.0-17	New Truck Designs, Truck Frame Roll Acceleration Due to Lateral Input	170
6.0-18	New Truck Designs, Truck Frame Roll Acceleration Due to Yaw Input	171

6.0-19	New Truck Designs, Truck Frame Lateral Acceleration Due to Lateral Input	172
6.0-20	New Truck Designs, Carbody A-end Lateral Acceleration Deu to Roll Input	173
6.0-21	New Truck Designs, Carbody A-end Lateral Acceleration Due to Yaw Input	174
6.0-22	New Truck Design, Carbody Center Lateral Acceleration Due to Lateral Input	175
6.0-23	New Truck Design, Carbody Center Lateral Acceleration Due to Roll Input	176
6.0-24	New Truck Designs, Carbody Center Lateral Acceleration Due to Yaw Input	177
6.0-25	New Truck Designs, Carbody A-end Roll Acceleration Due to Lateral Input	178
6.0-26	New Truck Designs, Carbody A-end Roll Acceleration Due to Yaw Input	179
6.0-27	New Truck Designs, Carbody A-end Roll Acceleration Due to Roll Input	180
6.0-28	New Truck Designs, Transformer Lateral Acceleration Due to Lateral Input	181
6.0-29	New Truck Designs, Transformer Lateral Acceleration Due to Roll Input	182
6.0-30	New Truck Designs, Transformer Lateral Acceleration Due to Yaw Input	183

LIST OF TABLES

2.1-1	Calculated Mass Properties of Metroliner Carbody Without Power Transformer	8
2.1-2	Metroliner Carbody Properties	19
2.2-1	Mass Properties of Metroliner Truck	25
2.2-2	Metroliner Truck Suspension Parameters	33
2.3-1	Mass Properties of Transformer.	36
2.3-2	Transformer Suspension Parameters	40
3.0-1	Summary of Road Test Locations	44
4.0-1	Simulation Input Configurations	72
4.3-1	Present Metroliner Resonances	127
5.0-1	Modified Transformer Parameters	129
5.0-2	Modified Truck Parameters	144
6.0-1	New Truck Parameters	155
6.0-2	High Frequency Truck Parameters	184

1.0 INTRODUCTION

1.1 Objective

The major objective of this program is to determine methods of improving the ride quality of the Metroliner through modifications of the dynamic configuration. For the program two levels of modifications are considered. The first level of modifications are achievable utilizing the existing hardware with suspension component modification or replacement. The second level of modifications allows, in addition to changes achievable with existing hardware, the introduction of a new truck configuration.

For the first level of modification, a series of recommendations and their effect on dynamic performance is presented. For the second level of modifications, a specification for a new truck is prepared and dynamic performance of the truck presented.

1.2 Plan

The program was centered around the development of a dynamic simulation of a Metroliner railcar subject to track irregularity inputs. Once developed, this dynamic simulation was systematically varied to evaluate the effect of suspension component modifications and alternate truck configurations. Based on these results, recommended modifications to the existing suspension component and the new truck requirements were established.

Two major test programs were performed in the conduct of the program to aid in the development and verification

of the dynamic simulation. A road test was performed on a single Metroliner car to examine the performance of suspension components in service, aid in establishing the nature of the inputs from track irregularities, and provide a baseline for ride quality. Supplementing this test, measurements of track irregularities over the road test course were performed to aid in establishing the inputs. In the laboratory, a series of shaker tests were performed on the identical Metroliner to aid in parameter identification and verification of the dynamic simulation. Supplementing these tests, shaker tests were performed on a few suspension components.

The major constraints which were imposed on the improvement program are:

1. The existing trackage and wayside clearance envelop shall be used.
2. The existing carbody shall be used.
3. The new truck configuration shall utilize the existing traction equipment and incorporate off tread friction braking.
4. The new truck structural configuration shall be of a design with proven passenger experience.

In the development of this program two major assumptions were made:

1. The railcar is assumed to be dynamically stable and the modifications recommended can be accomplished while maintaining dynamic stability.

2. Improvements in the ride quality of a single car will result in improvements in the ride quality of a train of cars.

This report describes the development and verification of the simulation using the laboratory test results, an analysis of the rail inputs using measured inputs from the road test and track measurements, the performance of the existing Metroliner with comparisons to road test results, the development and performance of the modified design, and the development and performance of the modified design with new trucks.

1.3 Participating Organizations

During the conduct of this program, major contributions were supplied by The Federal Railroad Administration, Battelle Memorial Institute, N.A.S.A. Langley, and ENSCO, Inc.

The Federal Railroad Administration, Rail Research Division, directed the Metroliner road test and track measurements in accordance with test plans developed by The Budd Company. ENSCO was responsible for the implementation of the Metroliner instrumentation and performance of the Metroliner road test and subsequent track measurements using the rail research cars. The laboratory tests were performed at The Budd Company Testing Laboratory with suspension component testing performed by Battelle Institute. The Analytic Computing Division, N.A.S.A. Langley performed the data reduction of the Metroliner road test results. The Loads Division,

N.A.S.A. Langley provided consultation during the development of the simulation by The Budd Company, performed the computer programing of the simulation, and ran the required simulation on their digital computer facility at Langley.

Three reports have been published concerning these efforts and are referenced in this report:

1. Metroliner Ride Data Collection System

   J. May, Report No. DOT-FR-72-11 ENSCO, Inc. July 1972

2. Supplement to Summary Report of Experimental Evaluation of Elastomeric LIM Truck Suspension Elements

   Battelle Memorial Institute (available through F.R.A.)

3. Summary of Metroliner Test Results

   J. Herring & P. Strong Report No. PB-208-284

   The Budd Company, February 10, 1972

2.0 DEVELOPMENT AND VERIFICATION OF THE SIMULATION

The simulation is a single railcar responding to inputs from track irregularities. The simulation is linear and the solutions are under steady-state conditions. Originally a non-linear simulation was considered, but was not pursued due to schedule requirements.

The simulation is composed of two models. The "vertical" model describes the vertical, longitudinal, and pitch motions of the railcar. The "lateral" model describes the lateral, roll and yaw motions of the railcar. The simulation was divided into five subsystems, the carbody vertically and laterally, the truck and the power transformer vertically

and laterally. The power transformer was included since its weight is comparable to the truck frame weight and is mounted on a suspension system under the carbody.

The development of the simulation was coordinated with a series of dynamic tests performed on the Metroliner in the laboratory. Dynamic tests were performed on the carbody subsystem, the truck subsystem and the transforner subsystems with boundary conditions identical to those of the subsystem simulations. The results of the laboratory tests were used to verify and identify parameters of the simulation of the five subsystems.

Once the subsystem simulations were verified, they were combined into the "vertical" and "lateral" railcar simulations.

A detailed description of the formulation and computer solution of the simulation is contained in Appendix A, Railcar Dynamic Simulation.

2.1 The Carbody Subsystem

The carbody subsystem consists of the carbody with the transformer removed resting on the truck secondary suspension with the primary suspension locked out. Figure 2.1-1 illustrates this subsystem and shows the location of the application of the dynamic force during the laboratory tests.

The carbody was simulated as seven rigid segments connected by flexible joints. Seven segments were chosen in anticipation that the first carbody bending modes would be significant. Additionally the seven segments correspond with the seven subdivisions of the carbody under floor sepa-

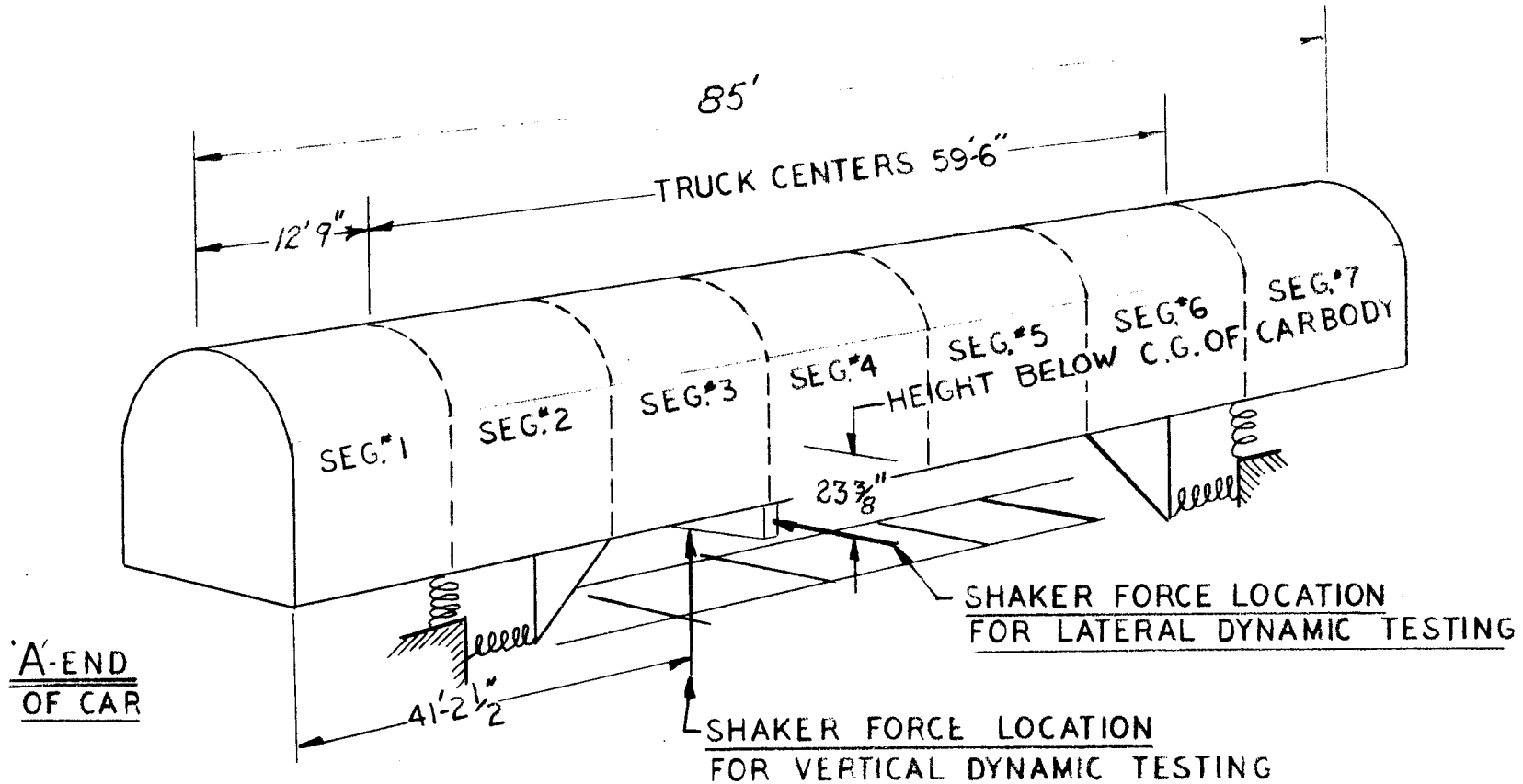

CARBODY SUBSYSTEM

FIGURE-2.1-1

rated by major cross bearers. These segments are shown on Figure 2.1-1. The transformer is attached under the 4th segment and the trucks between segments 1 and 2, and 6 and 7. Using the Metroliner design weight tables, the mass properties of the segments were computed and are tabulated in Table 2.1-1.

The carbody flexibility is defined by a series of influence coefficients. These coefficients were calculated in terms of the carbody modulus and area moment of inertia assuming the carbody has uniform stiffness. The damping of the carbody is described in terms of the structural damping coefficient.

The vertical carbody simulation has nine degrees of freedom; one vertical motion for the end of each segment and a common longitudinal motion for all segments. The lateral carbody simulation has 15 degrees of freedom, one roll motion for each segment and one lateral motion at the ends of the segments. The vertical or lateral motion at adjacent ends of connecting segments are assumed equal, requiring only one degree of freedom.

The vertical laboratory test results are compared to the "vertical" carbody subsystem simulation results in Figures 2.1-2, 2.1-3, and 2.1-4. In Figure 2.1-2, 2.1-3 and 2.1-4, the vertical acceleration on the center line of the car floor 4'4", 45'2-1/2" and 84'1" from the A end of the carbody is shown. In both experiment and simulation this is the acceleration in response to an input force

Table 2.1-1

Calculated Mass Properties of Metroliner Carbody

Without Power Transformer

Segment No.	Weight Lbs.	Segment Length In.	C.G. Location-Inches X *	Y **	Z ***	Radii of Gyration at C.G. in inches about X axis	Y axis	Z axis
1	17,790	150	446	-1.6	65.9	44.8	62.7	58.3
2	11,469	130	291	1.7	62.5	41.7	50.9	45.7
3	15,828	144	156	- .3	55.4	43.5	49.6	45.5
4	14,942	152	0	-4.3	69.1	43.8	51.9	47.4
5	17,195	144	-138	.3	50.8	42.1	49.0	43.4
6	14,556	144	-280	2.8	69.4	51.7	59.1	41.7
7	13,425	150	-447	- .6	66.2	44.7	63.0	57.1
Carbody	105,205		12.1	0.3	62.4	45.3	298.5	297.3

* origin at carbody center

** origin centerline of carbody

*** origin top of rail

CARBODY SUBSYSTEM

$$\frac{\text{VERTICAL ACCELERATION "A END" OF CARBODY}}{\text{VERTICAL APPLIED FORCE / CARBODY WEIGHT}} \left[\frac{gs}{g}\right] = \text{GAIN}$$

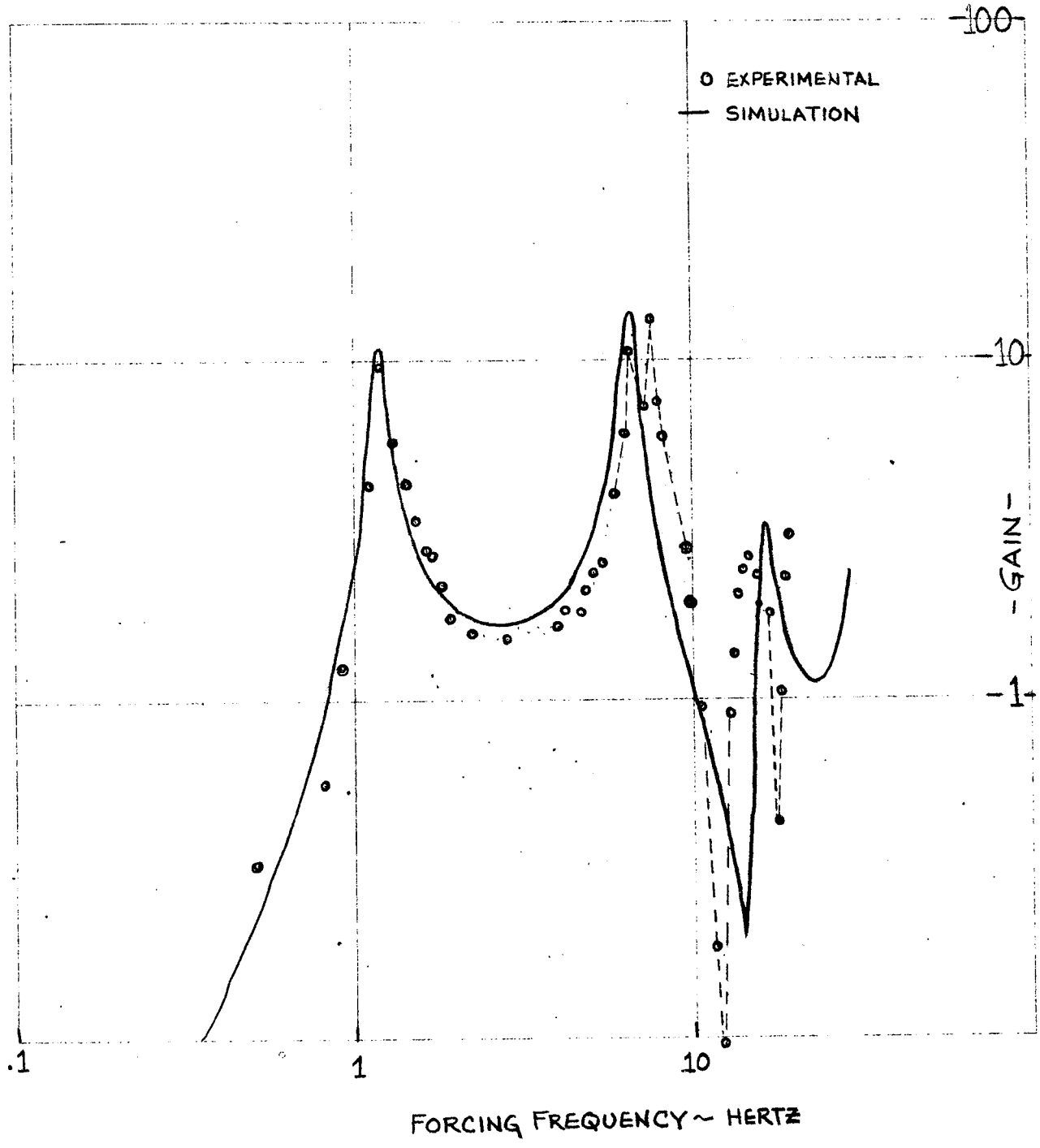

FIGURE 2.1-2

CARBODY SUBSYSTEM

$$\frac{\text{VERTICAL ACCELERATION "CENTER" OF CARBODY}}{\text{VERTICAL APPLIED FORCE / CARBODY WEIGHT}} \left[\frac{g_s}{g}\right] = \text{GAIN}$$

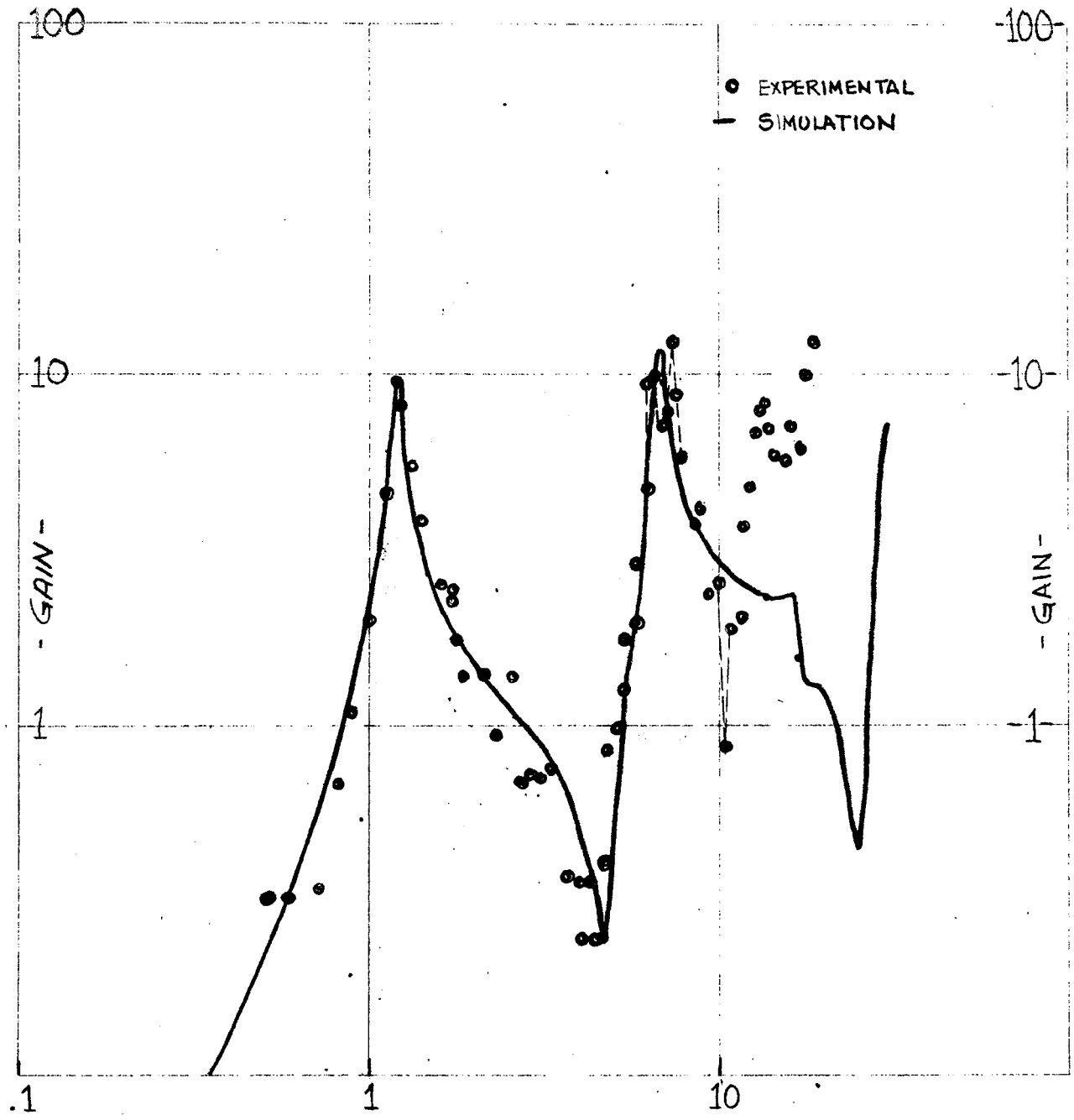

FIGURE 2.1-3

CARBODY SUBSYSTEM

VERTICAL ACCELERATION "B END" OF CARBODY / VERTICAL APPLIED FORCE / CARBODY WEIGHT $\left[\frac{g_s}{g}\right]$ = GAIN

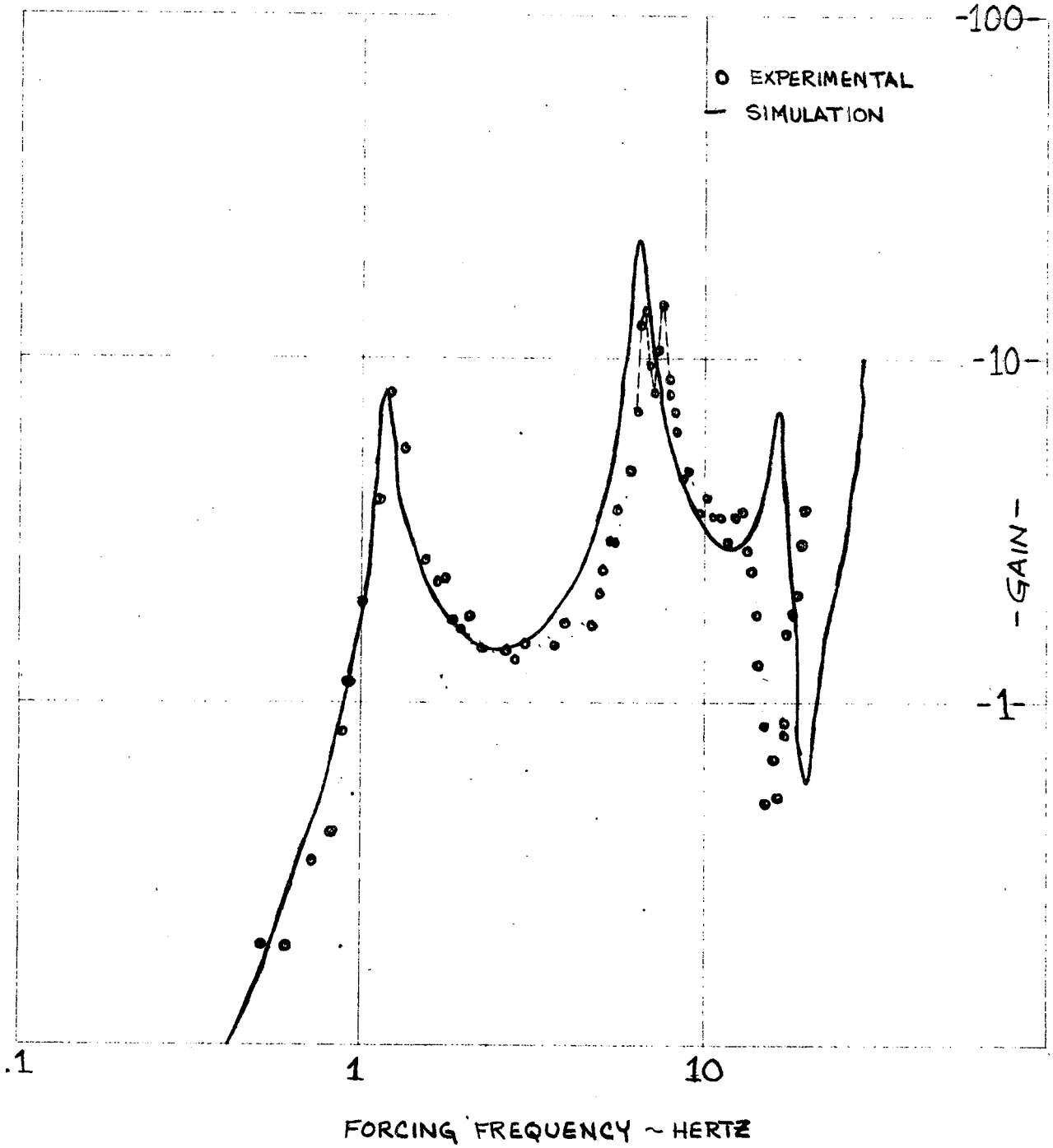

FIGURE 2.1-4

located as shown in Figure 2.1-1. The force is normalized in terms of acceleration by dividing the input force by the weight of the carbody. Relative maxima were experienced during the laboratory test at 1.2 hertz, 6.6 hertz, 7.4 hertz and 14.5 hertz. It was anticipated that a relative maxima should occur near 1.2 hertz due to the carbody rigid body resonance on the truck secondary suspension, and between 6 hertz and 8 hertz due to the carbody first mode bending resonance. The presence of two maxima in the 6 to 8 hertz range was due to the coupling of the longitudinal resonance of the truck on its anchor rods with the carbody bending. The longitudinal acceleration of the truck measured during the vertical testing is shown in Figure 2.1-5 with the input force normalized as described previously. As the carbody bends about its bending axis, a longitudinal motion is induced at the anchor rod/carbody connection a reasonable distance below the carbody bending axis. This induced motion excites the truck in the longitudinal direction. Using the reported value of the anchor rod longitudinal stiffness and the truck weight, the estimated longitudinal resonance of the truck is between 6.5 and 7 hertz which corresponds favorably to the experimental result. This coupling effect masks the experimental determination of the precise frequency of the carbody vertical bending resonance and reduces the measured gain at resonance, were this coupling removed. The required values of carbody stiffness and structural damping to achieve the simulation results of Figure 2.1-2 are:

TRUCK RESPONSE DURING VERTICAL CARBODY TEST

GAIN = $\frac{\text{Longitudinal Acceleration of "A" Truck Bolster}}{\text{Vertical Applied Force/Carbody Weight}}$ g's/g

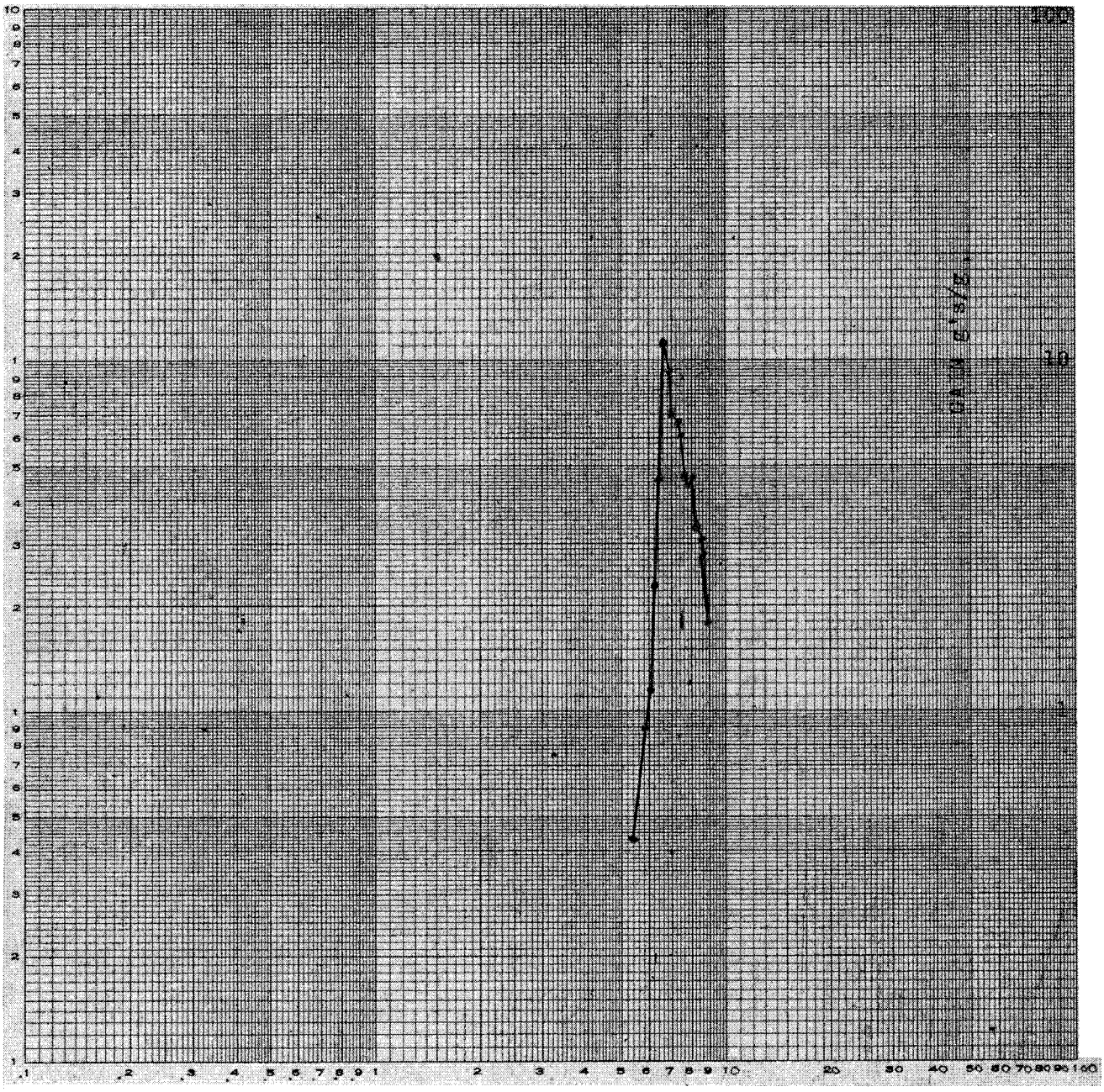

Frequency - hertz

FIGURE 2.1-5

vertical carbody stiffness (EI) 1.07×10^{12} lbs/in^2

vertical carbody structural damping coefficient .08

The value of the structural damping required appears high for structures of this type. The similar test, reported later, on the carbody laterally, resulted in a structural damping coefficient of .04. During this test no truck coupling was experienced.

Due to the uncertainty in the vertical carbody stiffness and structural damping, when a promising configuration was established, it was tested with carbody stiffnesses and damping which covers the range of uncertainty. These ranges are:

vertical carbody stiffness (EI) $1.07 - 1.17 \times 10^{12}$ lbs/in^2

vertical carbody structural damping coefficient .04 - .08

The lateral laboratory test results are compared to the "lateral" carbody subsystem simulation results in Figures 2.1-6, 2.1-7, 2.1-8 and 2.1-9.

In Figures 2.1-6, 2.1-7 and 2.1-8 the lateral acceleration on the centerline of the car floor 4'4", 45'2-1/2" and 84'1" from the A end of the carbody is shown. In both experiment and simulation this is the acceleration in response to an input force located as shown in Figure 2.1-1. The force is normalized in terms of acceleration by dividing the input force by the weight of the carbody. Relative maxima occurred at .7 hertz, 1.4 hertz, and 8 hertz as anticipated. The .7 hertz and 1.4 hertz maxima are the two rigid body lateral-roll resonances and the

CARBODY SUBSYSTEM

LATERAL ACCELERATION "A END" OF CARBODY / LATERAL APPLIED FORCE / CARBODY WEIGHT $\left[\frac{g's}{\frac{lb}{g}}\right]$ = GAIN

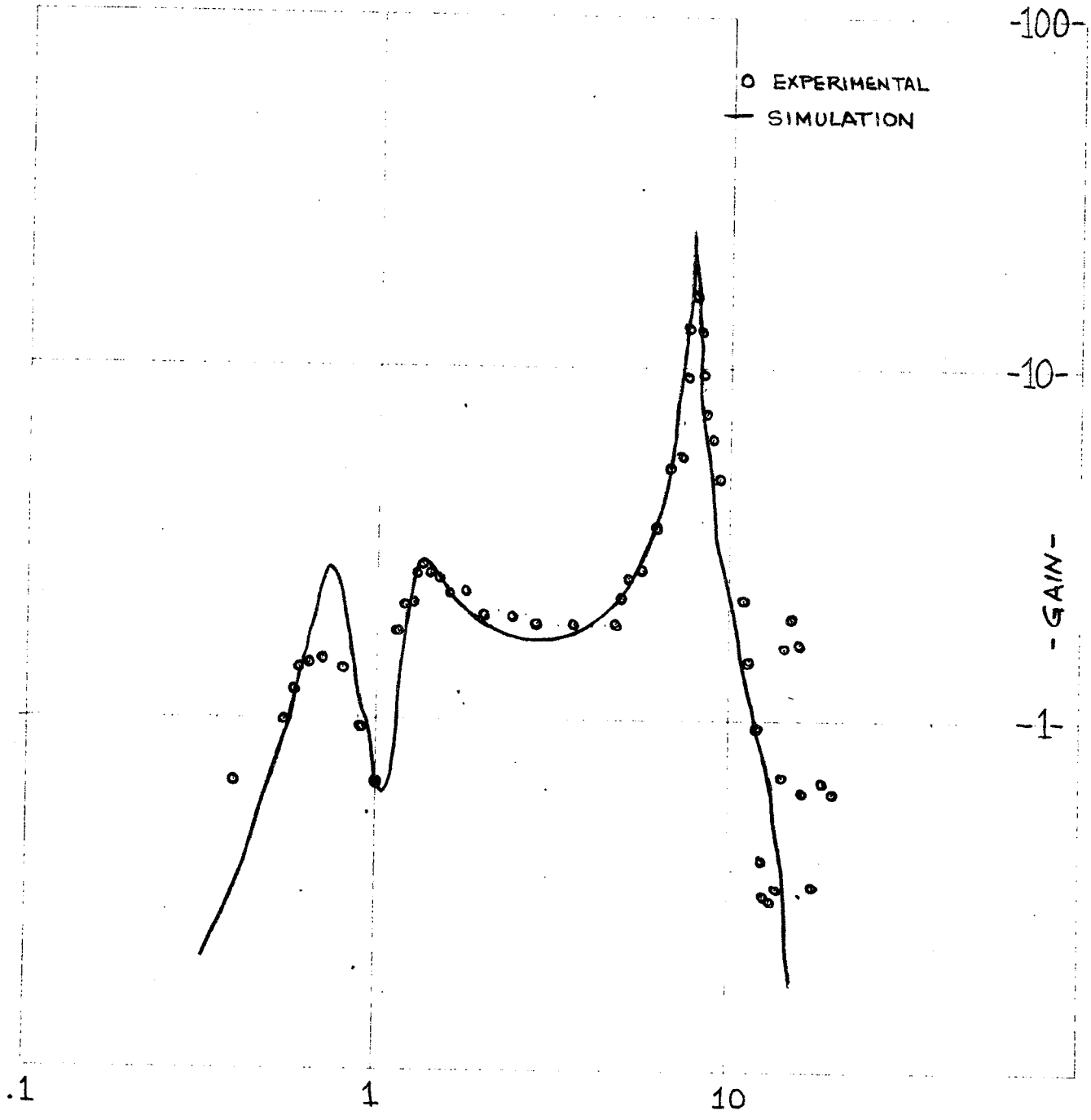

FIGURE 2.1-6

CARBODY SUBSYSTEM

LATERAL ACCELERATION "CENTER" OF CARBODY / LATERAL APPLIED FORCE / CARBODY WEIGHT $\left[\frac{g's}{g}\right]$ = GAIN

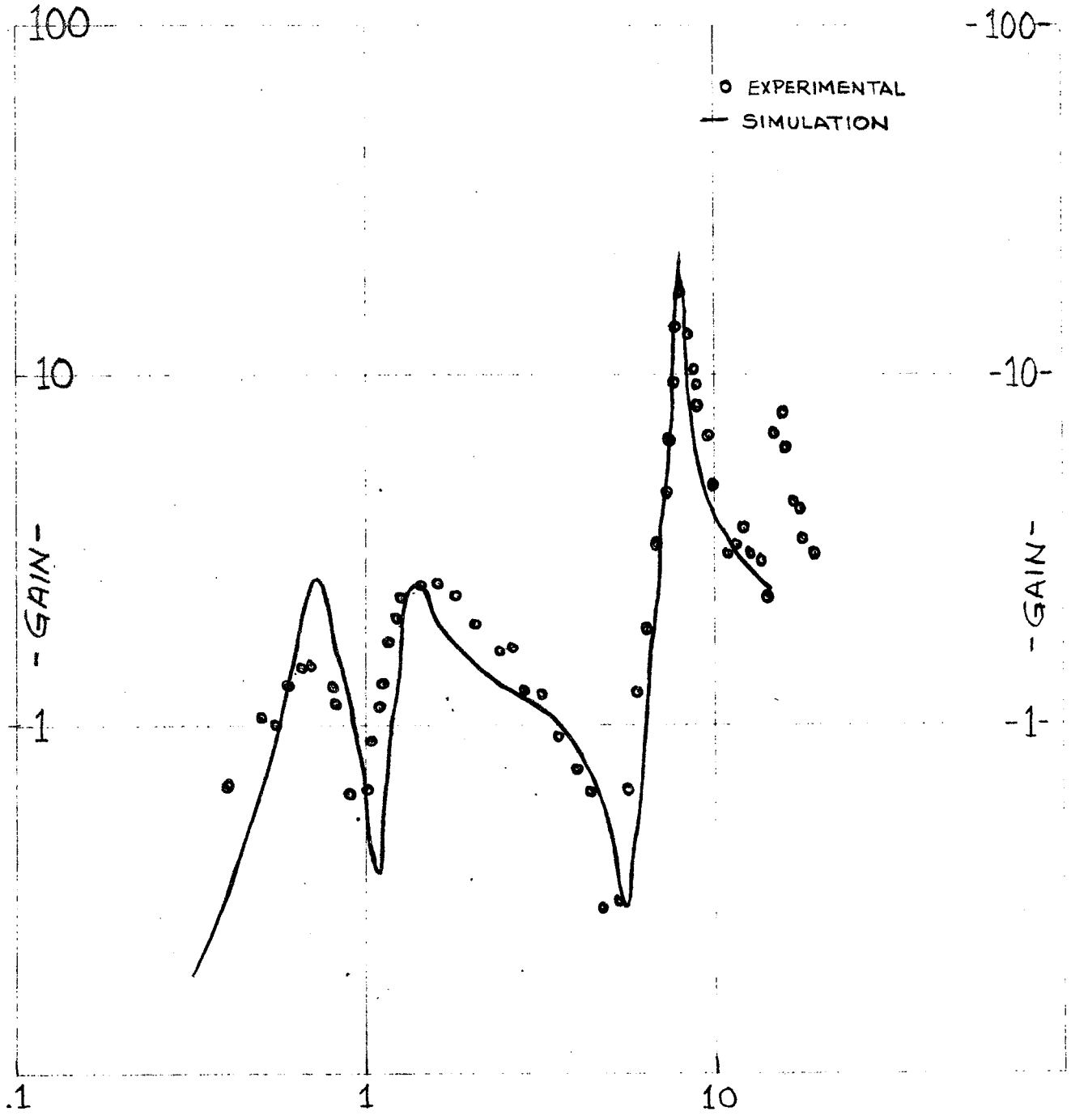

FIGURE 2.1-7

CARBODY SUBSYSTEM

LATERAL ACCELERATION "B END" OF CARBODY / LATERAL APPLIED FORCE / CARBODY WEIGHT $\left[\frac{g_s}{g}\right]$ = GAIN

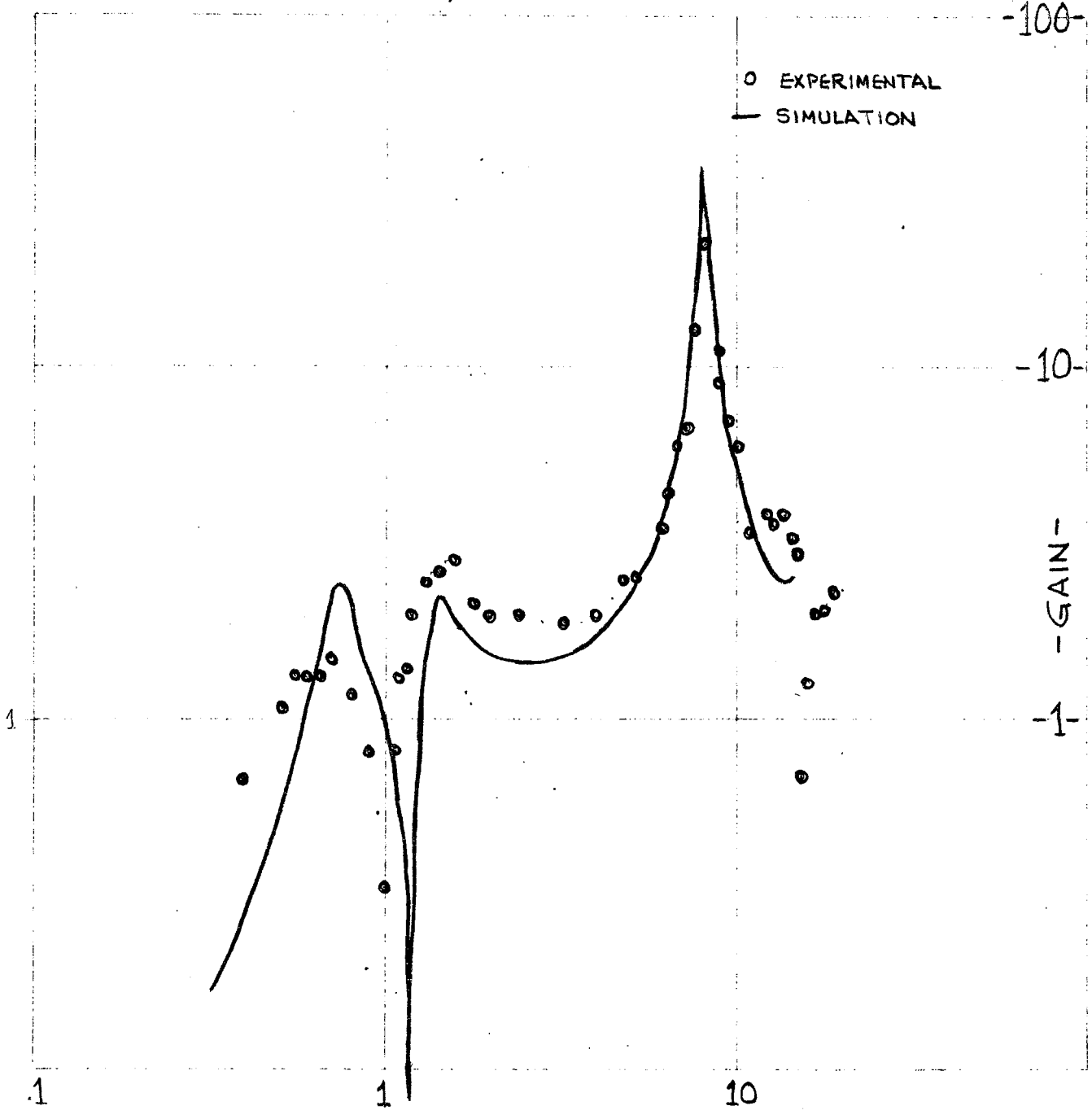

FIGURE 2.1-8

CARBODY SUBSYSTEM

RELATIVE ROLL ACCELERATION "A" END OF CARBODY / LATERAL APPLIED FORCE / CARBODY WEIGHT $\left[\frac{g's}{g}\right]$ = GAIN

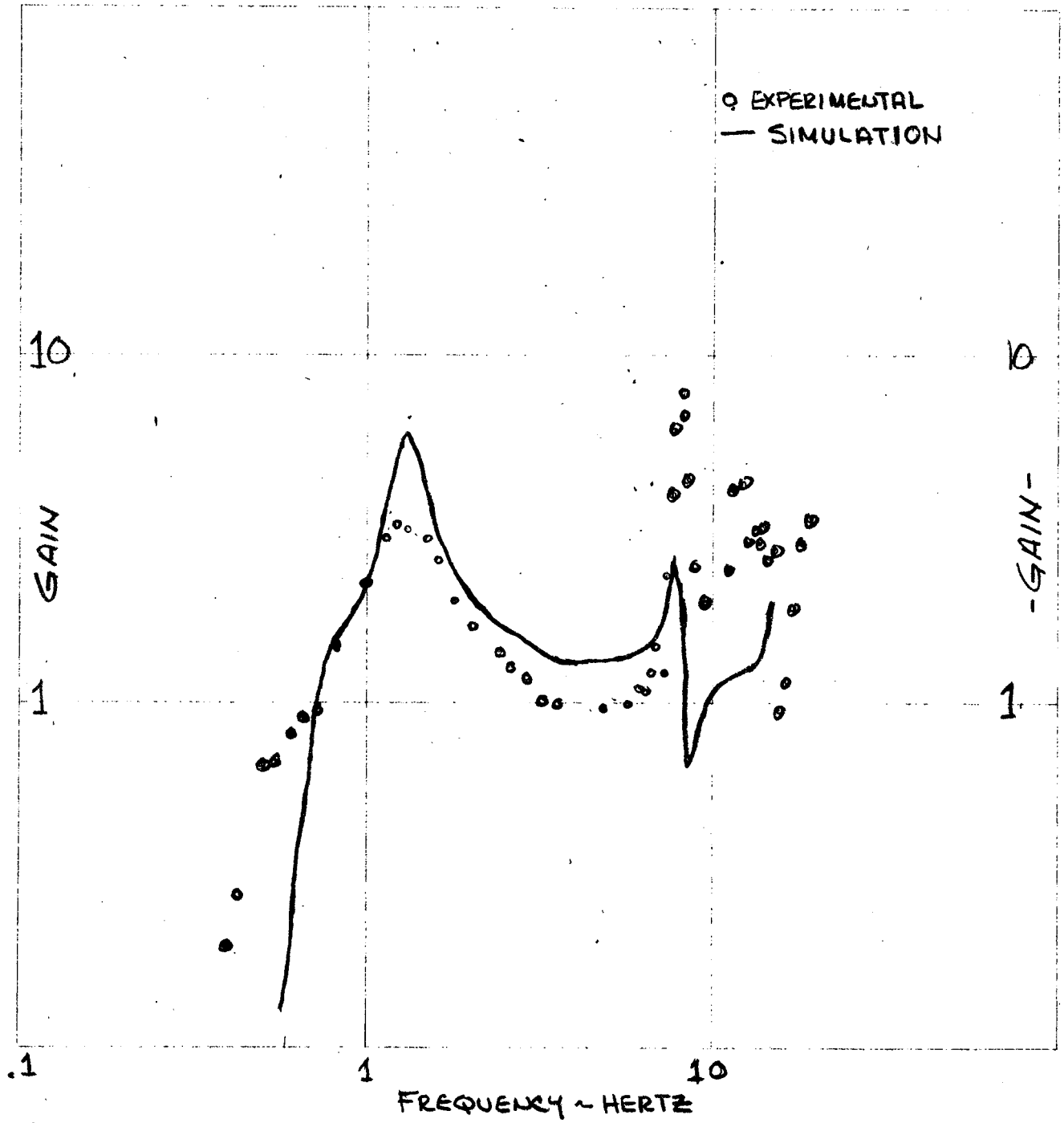

1g RELATIVE ROLL = 6.75 RAD/SEC^2

FIGURE 2.1-9

8 hertz maxima is the carbody lateral bending resonance. During the lateral laboratory test, additional accelerometers were located on the A end carbody floor to measure roll. The experimental and simulation results are shown in Figure 2.1-9 with the force normalized as previously described. The major disagreement between the experimental and simulation results under lateral forcing inputs, is the distribution of damping between the two rigid body lateral roll modes. In each case in the simulation insufficient damping was available in the lower mode. A similar disagreement occurred in the lateral transformer testing. Presently we are not able to identify the cause of this disagreement.

Table #2.1-2 is a summary of the vertical and lateral carbody properties used to simulate the existing Metroliner.

Table 2.1-2

Metroliner Carbody Properties

Vertical Carbody Stiffness (EI)	1.07×10^{12} lbs/in^2	*
Lateral Carbody Stiffness (EI)	1.58×10^{12} lbs/in^2	
Vertical Carbody Structural Damping Coefficient	.08	*
Lateral Carbody Structural Damping Coefficient	.04	

* refer to text for range of uncertainty

2.2 The Truck Subsystem

The truck subsystem consists of the truck with the carbody side of the secondary suspension system fixed.

The truck configuration is a generalized form of an equalizer beam truck. The truck includes two suspension systems, a primary suspension between the wheel and axle assemblies and the truck frame assembly, and a secondary suspension system between the truck frame assembly and the carbody. The major load in the secondary suspension is carried by the bolster coil spring. The air spring in parallel with the coil spring is designed to provide load leveling of the carbody under passenger load. During testing a nominal pressure of 5 psig was applied to the air spring to maintain contact with the spring seats. This pressure has a negligible effect on the secondary spring rate.

Within the truck frame assembly is a truck bolster which can yaw with respect to the truck frame. The bolster is attached to the carbody through longitudinal anchor rods. Across the primary suspension, the traction motor gear box is mounted. Figures 2.2-1, 2.2-2, and 2.2-3 are sketches of the existing truck showing major dimensions. For this simulation the truck wheels follow the vertical and lateral irregularities of the track. It is assumed that the wheel sets are performing in a stable manner and their displacements are controlled by track irregularities.

The truck subsystem simulation has seven degrees of freedom: vertical, pitch, longitudinal, lateral, roll,

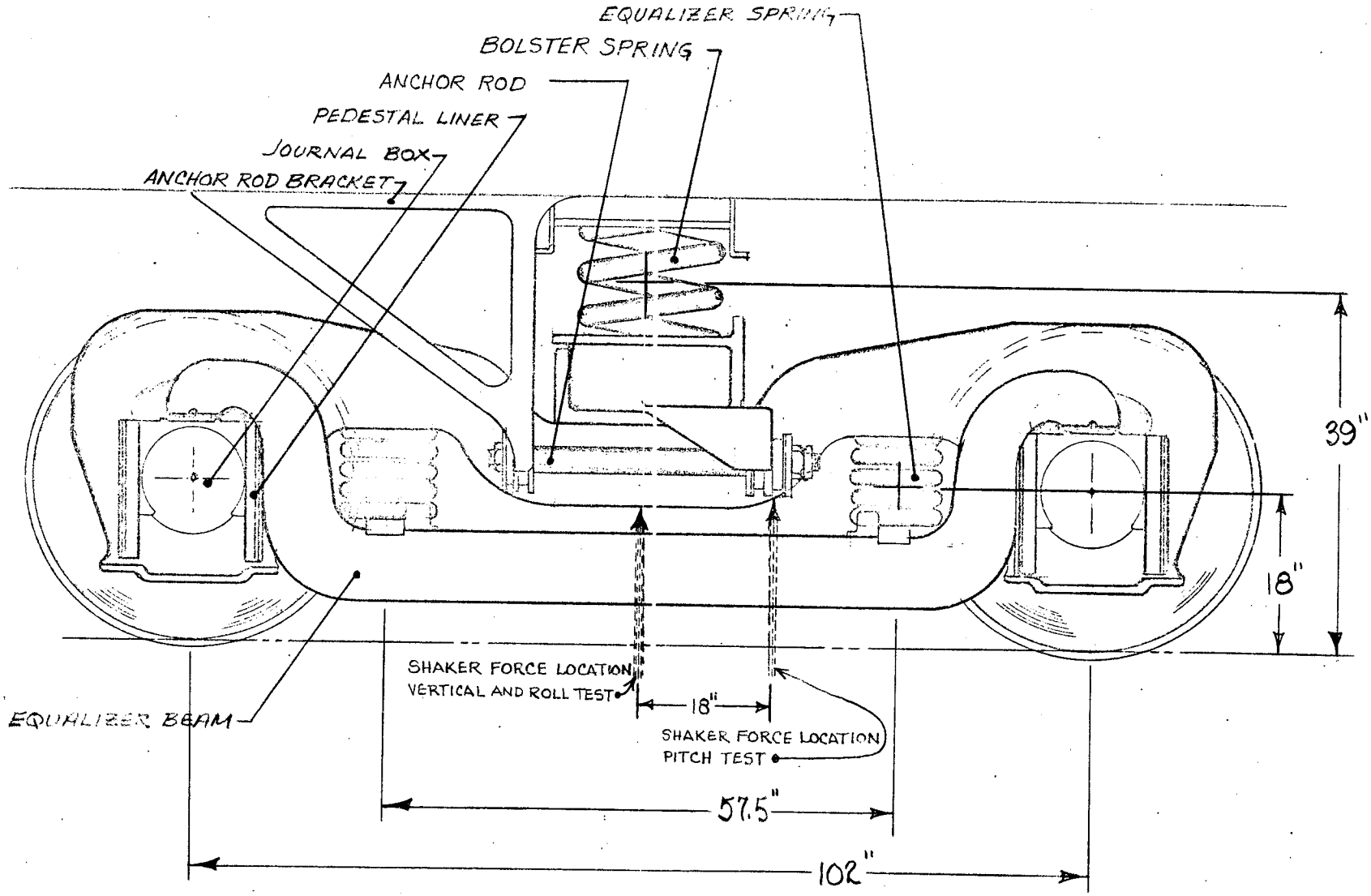

SIDE VIEW METROLINER TRUCK

FIGURE 2.2-1

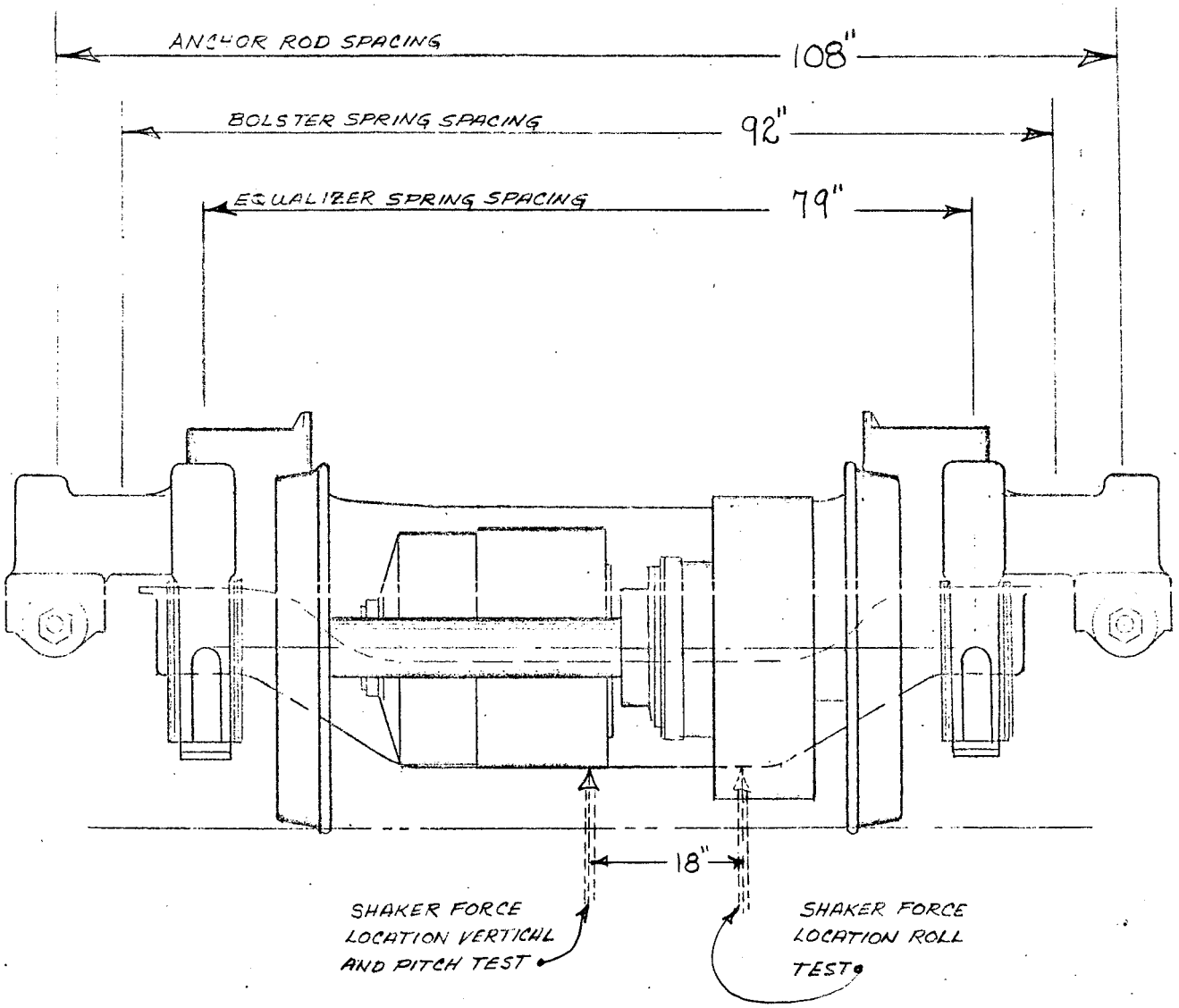

END VIEW METROLINER TRUCK

FIGURE 2.2-2

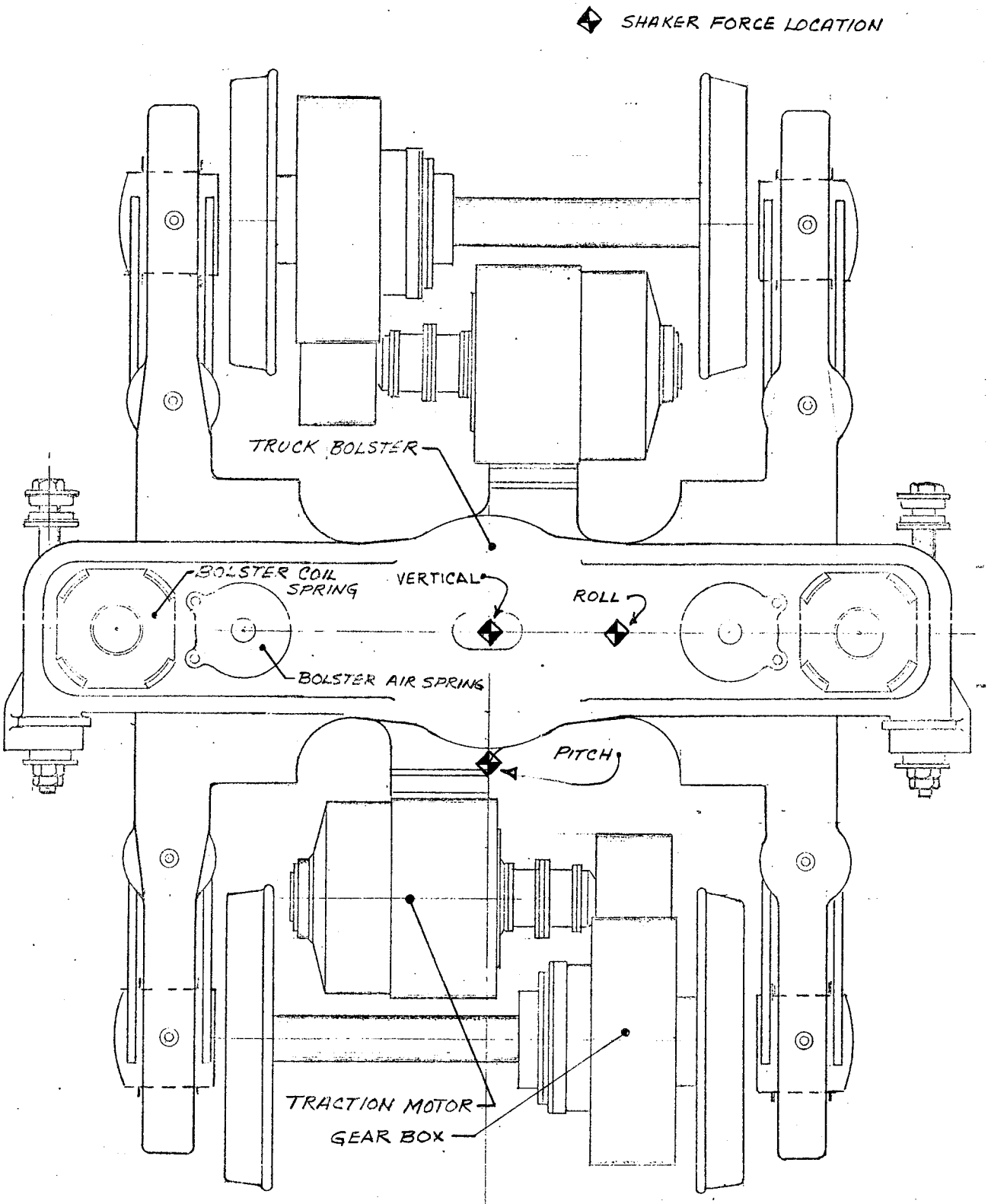

PLAN VIEW METROLINER TRUCK

FIGURE 2.2-3

yaw of the truck frame, and yaw of the truck bolster with respect to the truck frame. Using the Metroliner truck design weight tables, the mass properties of the truck were computed and are tabulated in Table 2.2-1.

The dynamic force during laboratory testing is applied to the truck frame assembly as shown in Figures 2.2-1, 2.2-2, and 2.2-3. The vertical test was performed with the dynamic force applied vertically at the geometric center of the truck frame.

The results of the vertical truck subsystem test is compared with the simulation results in Figure 2.2-4. The truck vertical subsystem resonance occurred at 9.5 hertz. This value is considerably higher than the anticipated vertical resonance of between 5.5 and 6 hertz based on the reported stiffness of the equalizer and bolster springs. The bolster vertical spring rate per truck based on the carbody subsystem vertical resonance of 1.2 hertz is 7740#/in. per truck. The vertical equalizer spring rate was reported to be 8000 to 9000#/in. per spring, or, considering four springs per truck, 32,000 to 36,000#/in. per truck. To achieve the 9.5 hertz vertical truck subsystem resonance assuming the primary suspension stiffness controlled by the equalizer springs, the stiffness of the equalizer springs would be 27,250#/in. per spring.

Two explanations for this difference were proposed First, the gear box connection across the primary suspension was appreciably increasing the primary suspension stiffness.

Table 2.2-1

Mass Properties of Metroliner Truck

Component	Weight in Pounds	C. G. Location - Inches			Radii of Gyration - Inches		
		Longitudinally From Truck Center	Laterally From Truck Center	Vertically Above Top of Rail	Longitudinal Axis Through C.G.	Lateral Axis Through C.G.	Vertical Axis Through C.G.
Truck Frame Assy. Less Motors & Truck Bolster	5,554.5	0.0	0.0	20.9	31.5	28.0	38.1
Truck Bolster	2,669.5	0.3	0.0	27.6	37.2	8.7	37.4
Traction Motor #1	2,086.0	34.0	10.5	19.5	9.3	8.6	9.3
Traction Motor #2	2,086.0	-34.0	-10.5	19.5	9.3	8.6	9.3
Total Truck Frame Assembly	12,396.0	0.0	0.0	21.9	28.6	28.1	37.5
Gear Box #1	787.5	45	18	18	9.6	12.9	9.6
Gear Box #2	787.5	-45	-18	18	9.6	12.9	9.6
Total Wheel & Axle Assembly	9,652.0	--	--	--	--	--	--
Total	23,623.0						

TRUCK SUBSYSTEM

VERTICAL ACCELERATION TRUCK FRAME ASSEMBLY / VERTICAL APPLIED FORCE / TRUCK FRAME ASSY WEIGHT $\left[\frac{g^s}{g}\right]$ = GAIN

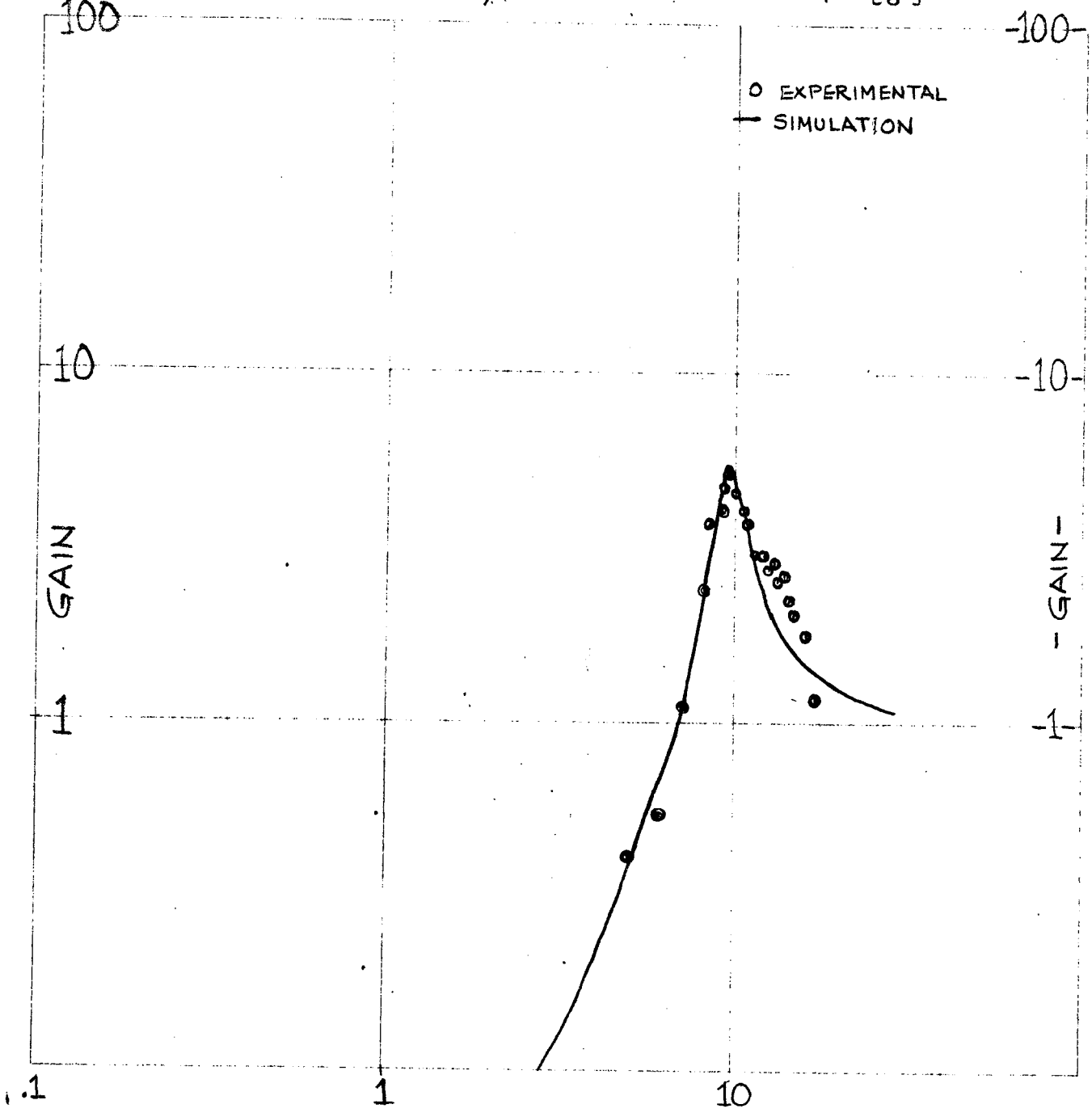

FORCING FREQUENCY ~ HERTZ

FIGURE 2.2-4

Second, the equalizer springs constructed from a coil spring encased in elastomeric material had appreciably increased in spring rate due to creep or aging of the elastomeric material.

To investigate the effect of the gear box connection, vertical static and dynamic tests were performed on the truck subsystem with the coupling between the motor and gear box disconnected. The results of the static tests are shown in Figure 2.2-5. For this test the carbody was not fixed. The results with the gear box coupling connected and disconnected are identical, with a nominal vertical static stiffness of 75,000#/in. per truck or 18,750#/in. per spring. The results of the vertical truck subsystem dynamic test with the coupling removed is shown in Figure 2.2-6. The results indicate the same vertical truck frame resonance with the coupling connected and disconnected. From these tests it was concluded that the motor gear box mounting had no effect on the vertical primary stiffness.

Further tests were performed on the equalizer spring by Battelle Memorial Institute. The results of their dynamic test is shown in Figure 2.2-7. These results indicate dynamic spring rates of 24,000#/in. for loads comparable to the vertical truck subsystem test. As a result it was concluded that the increased vertical stiffness of the primary suspension was due to the difference in the actual stiffness of the equalizer springs over the reported value. It should be

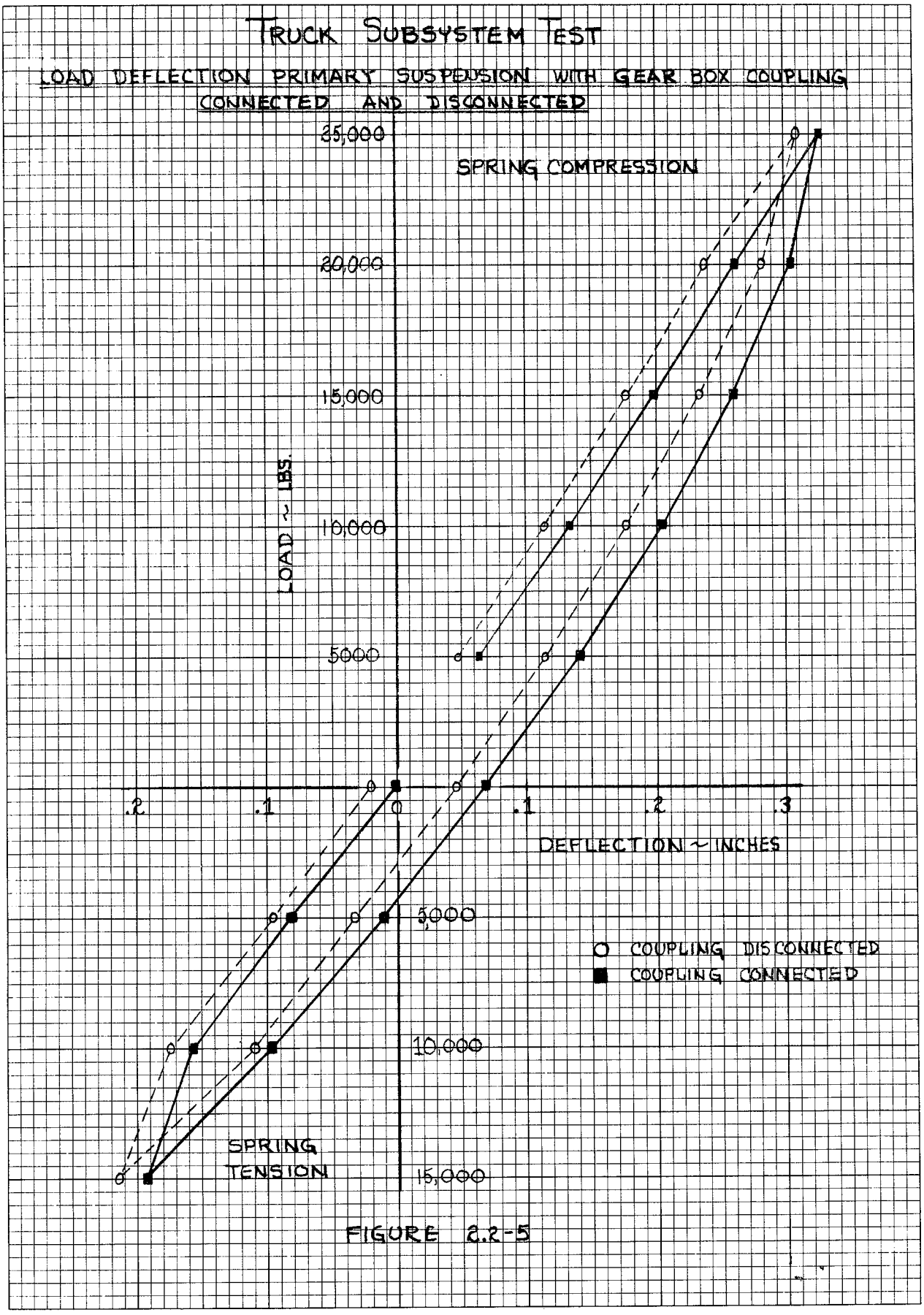
TRUCK SUBSYSTEM TEST
LOAD DEFLECTION PRIMARY SUSPENSION WITH GEAR BOX COUPLING CONNECTED AND DISCONNECTED
35,000
30,000
15,000
10,000
5000
SPRING COMPRESSION
LOAD ~ LBS.
.2
.1
0
.1
.2
.3
DEFLECTION ~ INCHES
5000
10,000
15,000
SPRING TENSION
COUPLING DISCONNECTED
COUPLING CONNECTED

FIGURE 2.2-5

TRUCK SUBSYSTEM TEST

VERTICAL DYNAMIC TEST WITH GEAR COUPLING CONNECTED AND DISCONNECTED

VERTICAL ACCELERATION OF TRUCK FRAME ASSEMBLY / VERTICAL APPLIED FORCE / TRUCK FRAME ASSY WEIGHT $\frac{g_s}{g}$ = GAIN

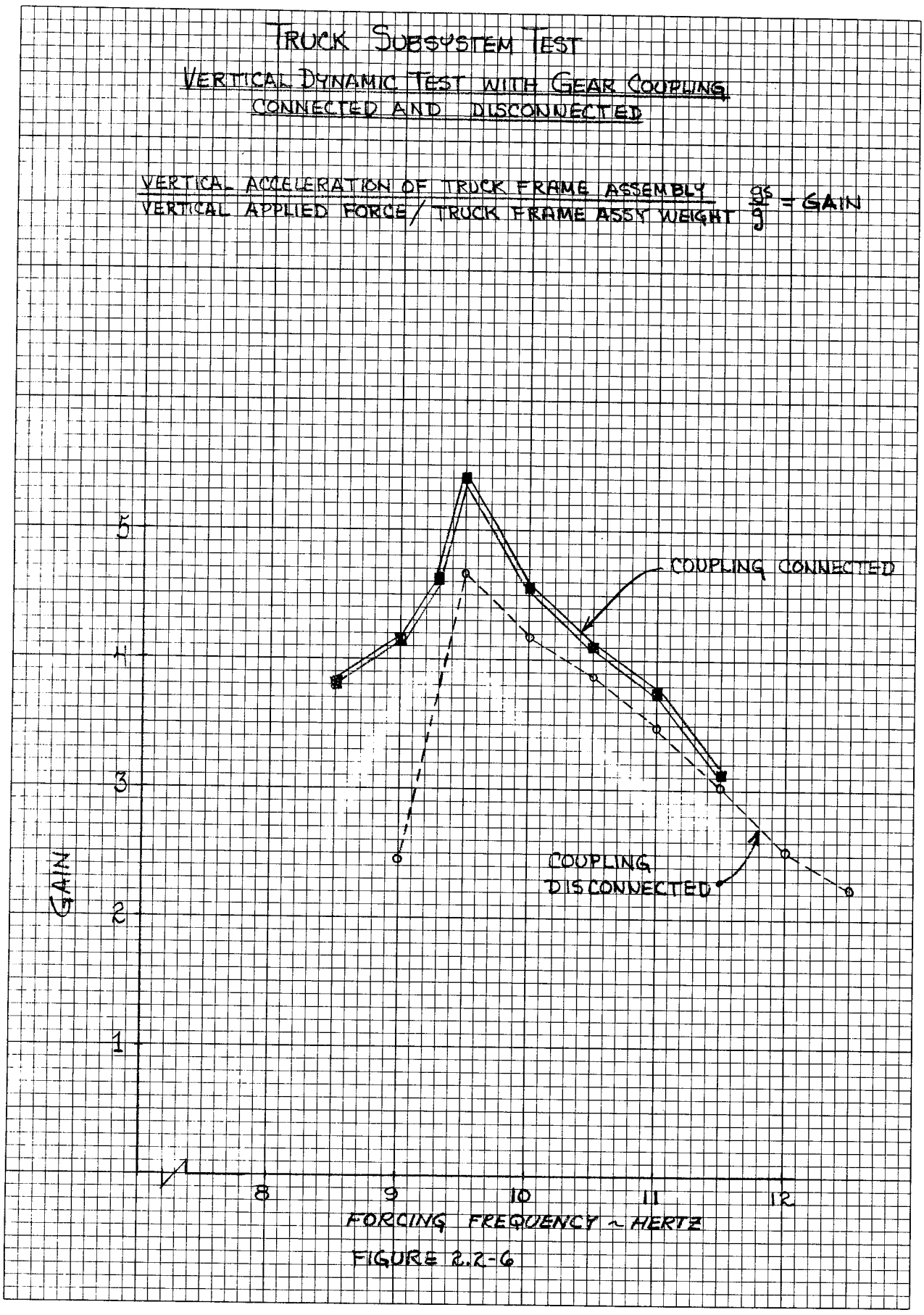

FIGURE 2.2-6

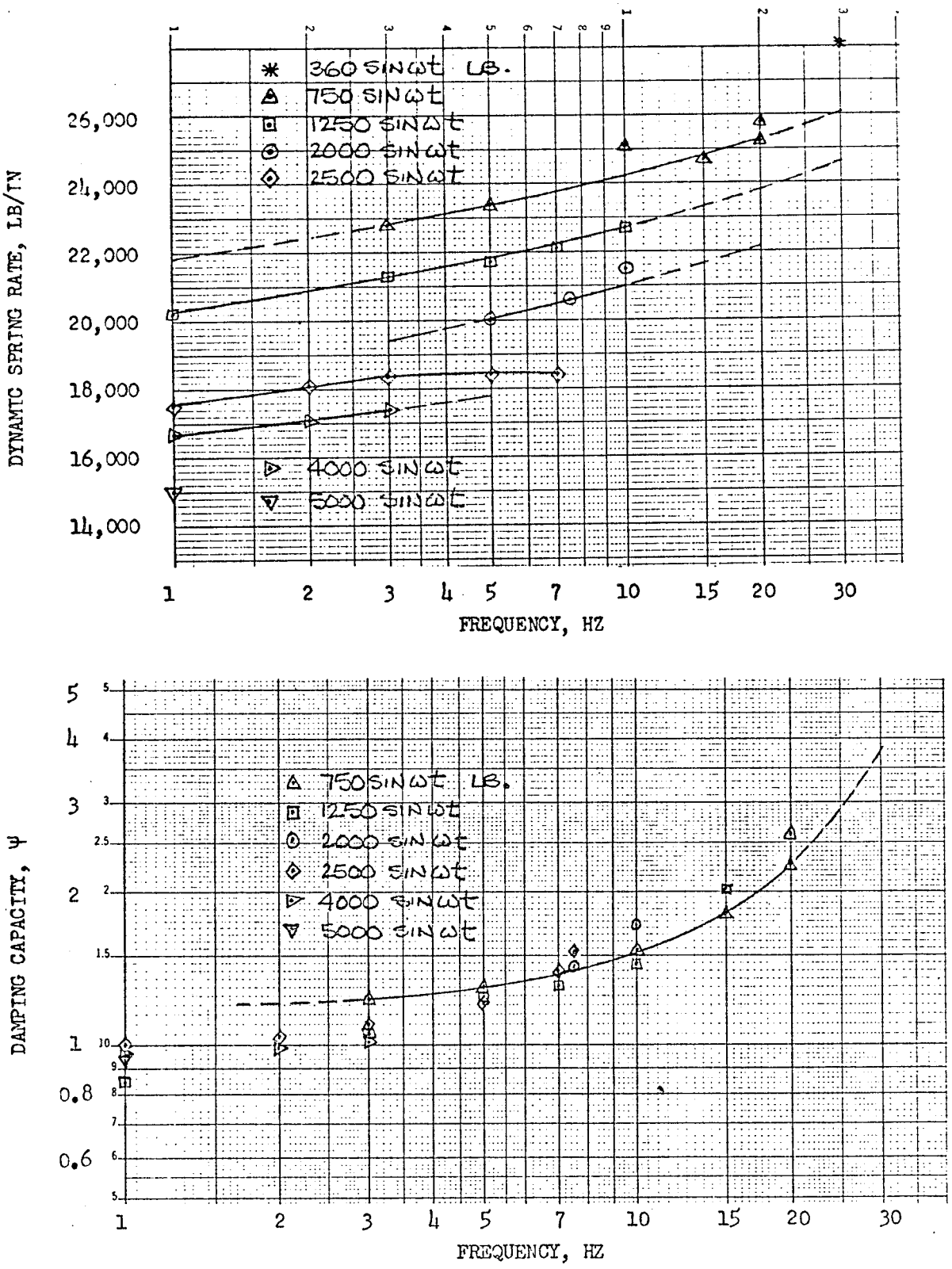

FIGURE 2.2-7 . DYNAMIC SPRING RATE AND DAMPING CAPACITY OF PIRELLI SPRING UNDER SINUSOIDAL LOAD AT 21,000 LB. PRELOAD

noted that the reported value was based on a short term static deflection curve of the spring.

The truck subsystem roll test was performed by exciting the truck frame in a combined vertical and roll mode by locating the shaker 18" laterally from the truck frame center. The roll acceleration experienced is compared with the simulation result in Figure 2.2-8. The truck frame roll resonance occurs at 15 hertz.

The truck subsystem pitch test was performed by exciting the truck frame in a combination vertical and pitch mode by locating the shaker 18" longitudinally from the truck frame centerline. During this test we were not able to obtain a reasonable pitch wave form. The wave form appeared to be mixed with a signal of 50 to 60 hertz. It is not electrical noise as the amplitude varies with forcing frequency and alternate instrumentation gave similar results.

Based on the matching of the simulation results to the truck subsystem and carbody subsystem tests, the vertical, lateral and longitudinal parameters of the truck secondary suspension and the vertical parameters of the truck primary suspension were identified. The lateral and longitudinal parameters of the primary suspension were estimated based on the equalizer springs lateral and longitudinal rate. The truck suspension parameters are tabulated in Table 2.2-2.

2.3 The Power Transformer Subsystem

The power transformer subsystem consists of the power transformer with the carbody end of the suspension mounts

TRUCK SUBSYSTEM

$$\frac{\text{RELATIVE ROLL ACCELERATION OF TRUCK FRAME}}{\text{VERTICAL APPLIED FORCE / TRUCK FRAME ASSY. WGT}}\left[\frac{g's}{g}\right] = \text{GAIN}$$

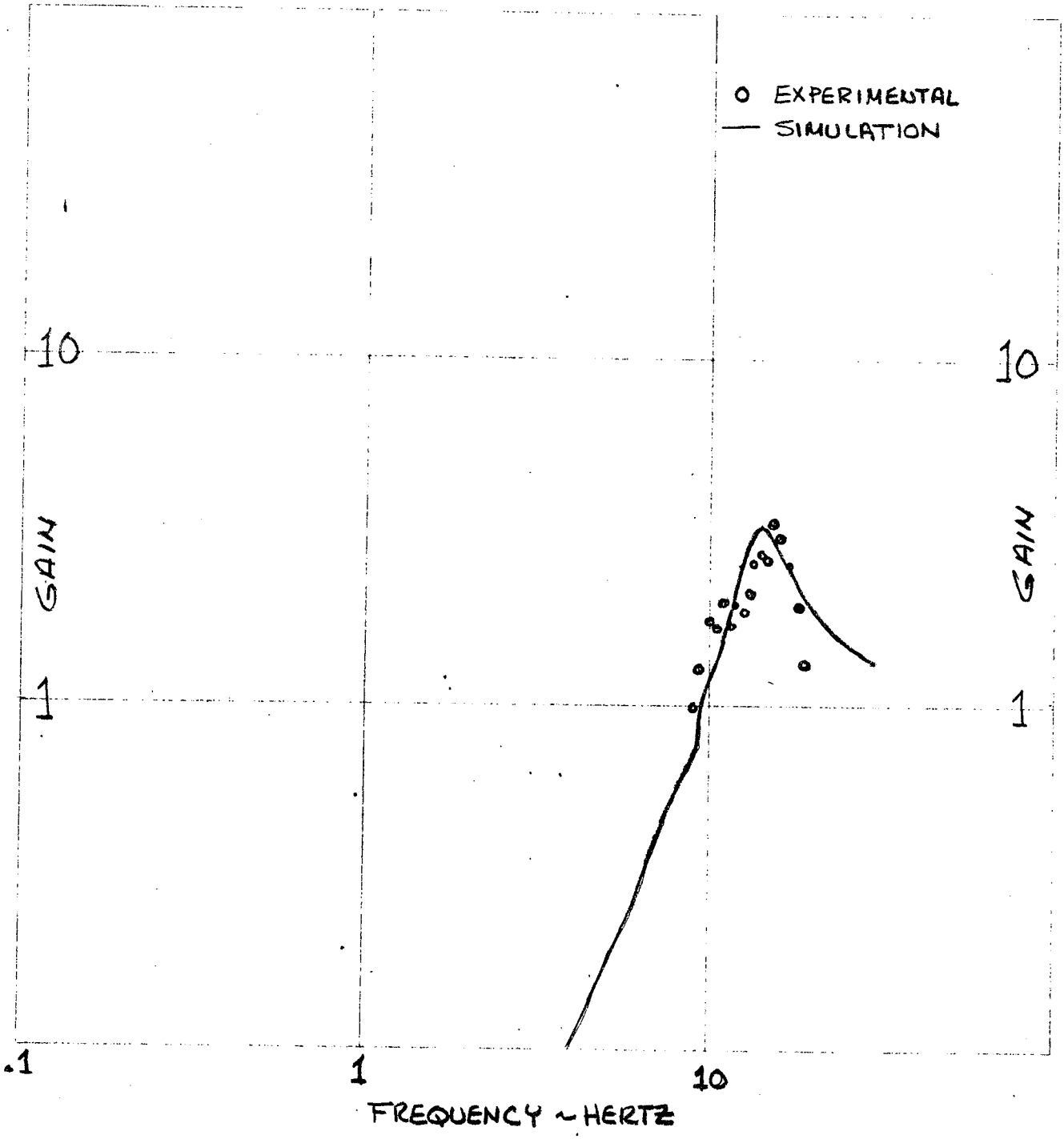

1 g RELATIVE ROLL = 8.17 RAD/SEC^2

FIGURE 2.2-8

Table 2.2-2

Metroliner Truck Suspension Parameters

	Primary Suspension System	Secondary Suspension System
Vertical Stiffness Per Truck	109,000#/in	7,740#/in
Lateral Stiffness Per Truck	55,800#/in *	3,386#/in
Longitudinal Stiffness Per Truck	55,800#/in *	96,660#/in
Vertical Damping Per Truck	260# sec/in	115# sec/in
Lateral Damping Per Truck	260# sec/in *	173# sec/in
Longitudinal Damping Per Truck	260# sec/in *	78# sec/in *

* Calculated

fixed. A sketch of the transformer subsystem is shown in Figure 2.3-1. The suspension mounts are elastomeric and act in shear vertically and laterally, and in tension and compression longitudinally. The mass properties of the transformer were calculated and are tabulated in Table 2.3-1.

The results of the vertical transformer test are compared with the vertical transformer subsystem simulation in Figure 2.3-2. The force is normalized in terms of acceleration, by dividing the force by the transformer weight. The transformer subsystem has a vertical resonance at 4.6 hertz.

The results of the lateral transformer test are compared with the lateral transformer subsystem tests in Figures 2.3-3 and 2.3-4.

The lateral results indicate two lateral-roll resonances at 3.6 hertz and 6.4 hertz. As in the case of the lateral carbody test, the major difference between test and simulation is the distribution of damping between the two lateral roll modes. In the simulation insufficient damping is available in the lower mode. A similar result occurred in the carbody subsystem test. Presently we are not able to identify the cause of this disagreement.

Based on the matching of the vertical and lateral test results, the vertical and lateral transformer suspension parameters were established. The longitudinal parameters were calculated. The transformer suspension parameters are tabulated in Table 2.3-2.

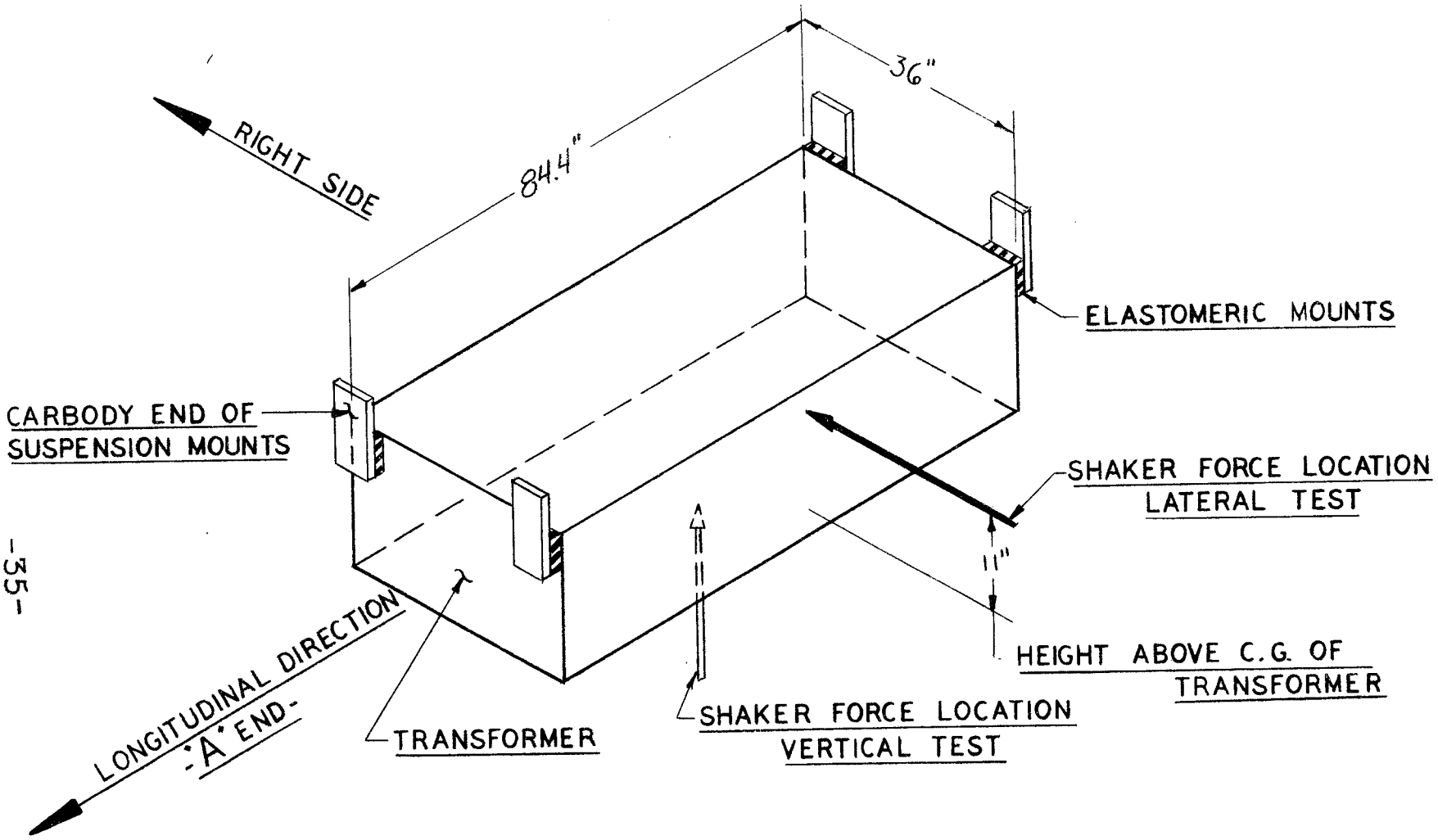

POWER TRANSFORMER SUBSYSTEM

FIGURE 2.3-1

Table 2.3-1

Mass Properties of Transformer

Weight	12,350 pounds
Longitudinal C.G Location from "A End" Mounts	42.2 inches
Lateral C.G Location from Right Side Mounts	18 inches
Vertical C.G Location Below Mounts	11 inches
Radius of Gyration about Longitudinal Axis	17.7 inches
Radius of Gyration about Lateral Axis	21.6 inches
Radius of Gyration about Vertical Axis	23.2 inches

POWER TRANSFORMER SUBSYSTEM

VERTICAL ACCELERATION OF TRANSFORMER / VERTICAL APPLIED FORCE / TRANSFORMER WEIGHT $\left[\frac{g^s}{g}\right]$ = GAIN

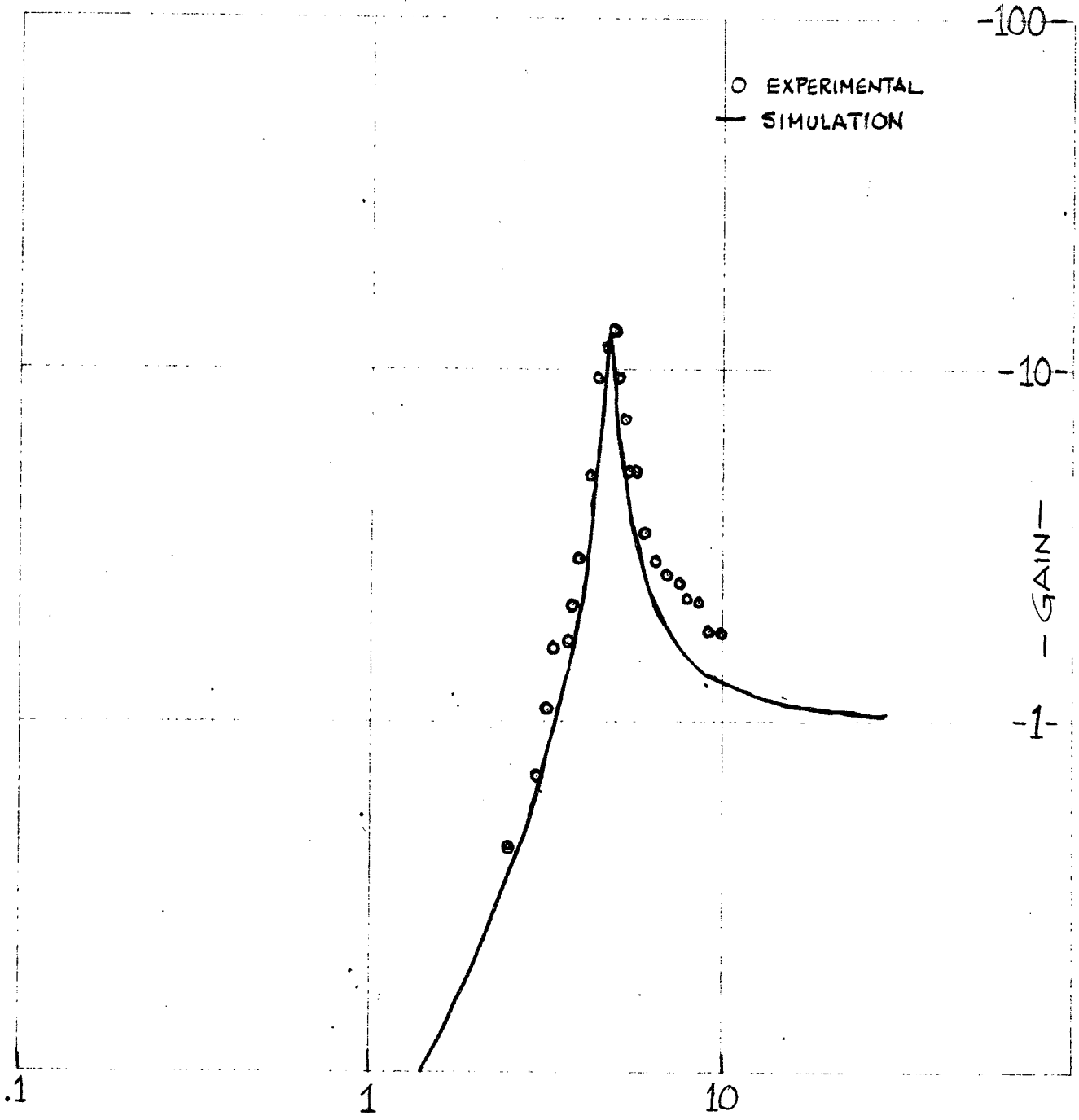

FIGURE 2.3-2

POWER TRANSFORMER SUBSYSTEM

LATERAL ACCELERATION OF TRANSFORMER C.G / LATERAL APPLIED FORCE / TRANSFORMER WEIGHT $\left[\frac{g_s}{g}\right]$ = GAIN

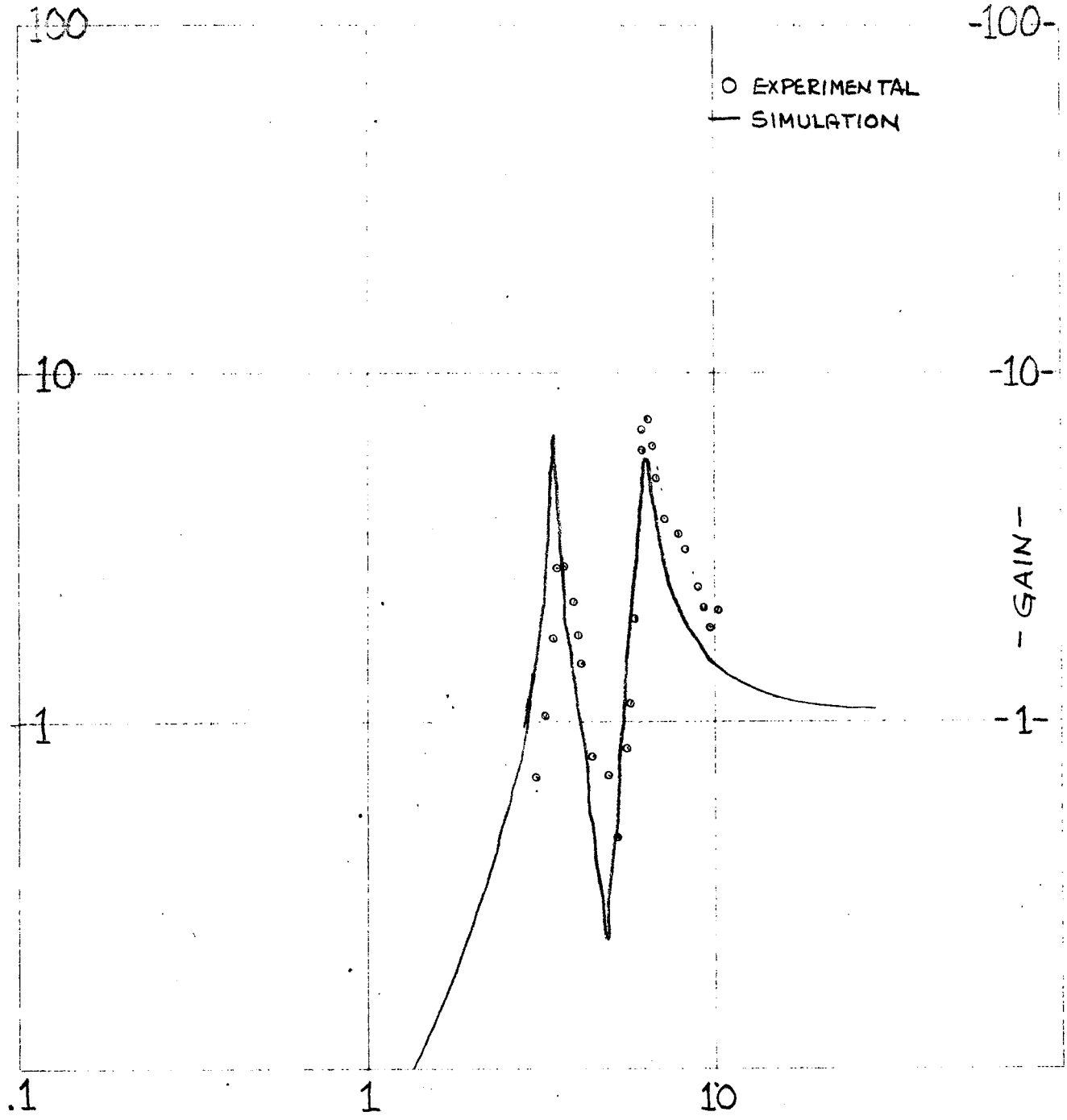

FIGURE 2.3-3

POWER TRANSFORMER SUBSYSTEM

RELATIVE ROLL ACCELERATION OF POWER TRANSFORMER / LATERAL APPLIED FORCE / TRANSFORMER WEIGHT $\left[\frac{g's}{g}\right]$ = GAIN

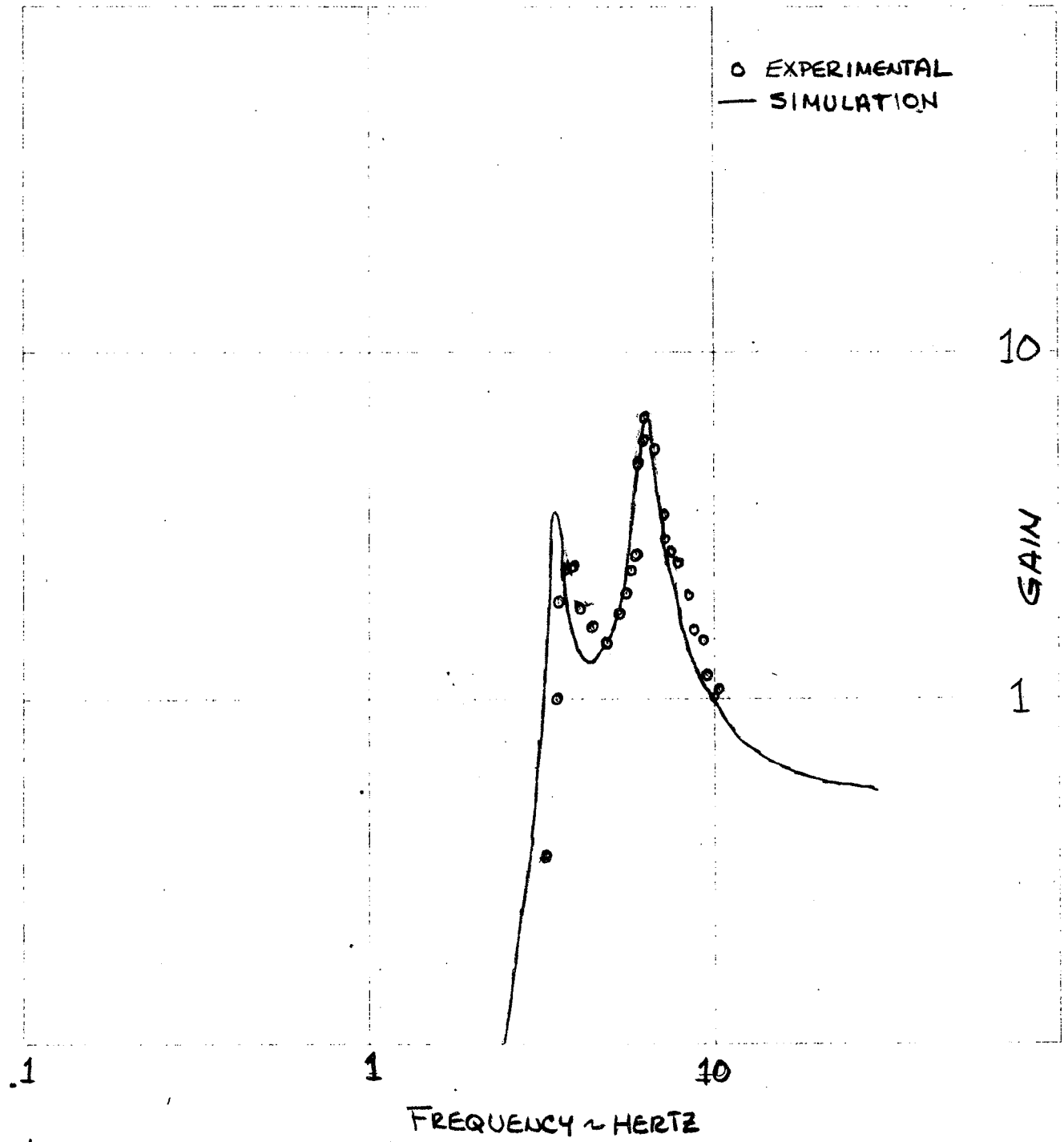

1g RELATIVE ROLL = 26.2 RAD/SEC²

FIGURE 2.3-4

TABLE 2.3-2

PRESENT POWER TRANSFORMER SUSPENSION PARAMETERS

Total System

Vertical Stiffness	28,800 lbs./in.
Lateral Stiffness	27,000 lbs./in.
Longitudinal Stiffness	260,000 lbs./in.
Vertical Damping	72 lbs.-sec./in.
Lateral Damping	72 lbs.-sec./in.
Longitudinal Damping	72 lbs.-sec./in.

3.0 TRACK IRREGULARITY INPUTS

Though at any one time the inputs to the rail car due to track irregularities consist of a mixture of vertical, longitudinal, lateral, pitch, roll and yaw of a single truck and combinations between the two trucks, for this study the inputs have been reduced to five major inputs (the simulation is capable of accepting any mixture). The major inputs considered are:

1. Vertical - both trucks translating vertically in phase
2. Pitch - both trucks translating vertically 180° out of phase
3. Lateral - both trucks translating laterally in phase
4. Roll - both trucks rolling in phase
5. Yaw - both trucks translating laterally 180° out of phase

Considering these major inputs, there are track irregularities of particular wave length where one or more of these inputs will dominate. The wave lengths are dependent on the wheelbase of the truck and the spacing between the truck centers.

To aid in establishing the nature of the track irregularity inputs, a road test on the Metroliner and track measurements were performed. Samples from six sections of track were analyzed and subsequently track profile measurements over these sections were performed. The six sections of track are described below.

Run #1 is a low speed run south of Baltimore station between milepost 97.25 and 98.25 on track #3. The speed through this location was between 31 and 45 miles per hour. This location was primarily chosen as a test case to check the data processing system and is included here as a sample of low speed performance. The track at this location is a mixture of continuously welded and bolted rail.

Run #4 is Stony Run between milepost 106.5 and 109.5 on track #3. The speed through this location was 105 MPH. This location is an example of operation over rough track. This location has 1 mile of continuously welded and 2 miles of bolted rail.

Run #5 is south of 30th Street Station, Philadelphia, between milepost 6.75 and 9.25 on track #3. The speed through this location was between 87 and 97 MPH. This location is an example of acceptable ride quality. The track at this location is continuously welded.

Run #6 is south of 30th Street Station, Philadelphia, between milepost 11.75 and 12.75 on track #3. The speed through this location was 103 MPH. This location is an example of performance on a curve when the carbody is riding on the lateral secondary suspension stops, by traveling at speeds greater than the balance speed of the curve. The track at this location is continuously welded.

Run #7 is entering Wilmington Station between milepost 25.25 and 26.75 on track #3. The speed through this location

is between 85 and 35 MPH. This location is an example of transient inputs, characterized as "lurch". The track at this location is continuously welded.

Run #8 is south of New Brunswick, N. J. between milepost 33 (N) and 34 (N) on track #3. The speed through this location is 105 MPH. This location is an example of what appears to be a lateral dynamic instability of the truck. The track at this location is continuously welded.

The conditions for each location are summarized in Table 3.0-1.

As previously stated, the Metroliner road test and track profile measurements were performed by ENSCO Inc. and reported in Metroliner Ride Data Collection System report No. DOT-FR-72-11. The description of the test sections, test setup, test results and data reduction procedures are described in Summary of Metroliner Test Results report No. PB-208-284.

3.1 Wheelbase Dependent Inputs

The average vertical acceleration of the wheel and axle assemblies of a single truck will have a relative maxima when the truck wheel base is some integer multiple of the track irregularity wave length as shown in Figure 3.1-1. Examining the road test results from track section five, this effect can be illustrated.

Figure 3.1-2 is the power spectral density of the average vertical acceleration of the wheel and axle assembly of the lead truck of the test car traveling at an average speed of

Table 3.0-1

Summary of Road Test Locations

Run	1	4	5	6	7	8
Mile Post Location Start	97.25	106.5	6.75	11.75	25.25	33(N)
Mile Post Location End	98.25	109.5	9.25	12.75	26.75	34(N)
Track No.	3	3	3	3	3	3
Speed (M.P.H.)	31 - 45	105	87 - 97	103	85 - 35	105

TRACK IRREGULARITY WAVE LENGTH AT WHICH
RELATIVE MAXIMA IN AVERAGE VERTICAL ACCELERATION
OF TRUCK WHEEL AND AXLE ASSEMBLY OCCUR

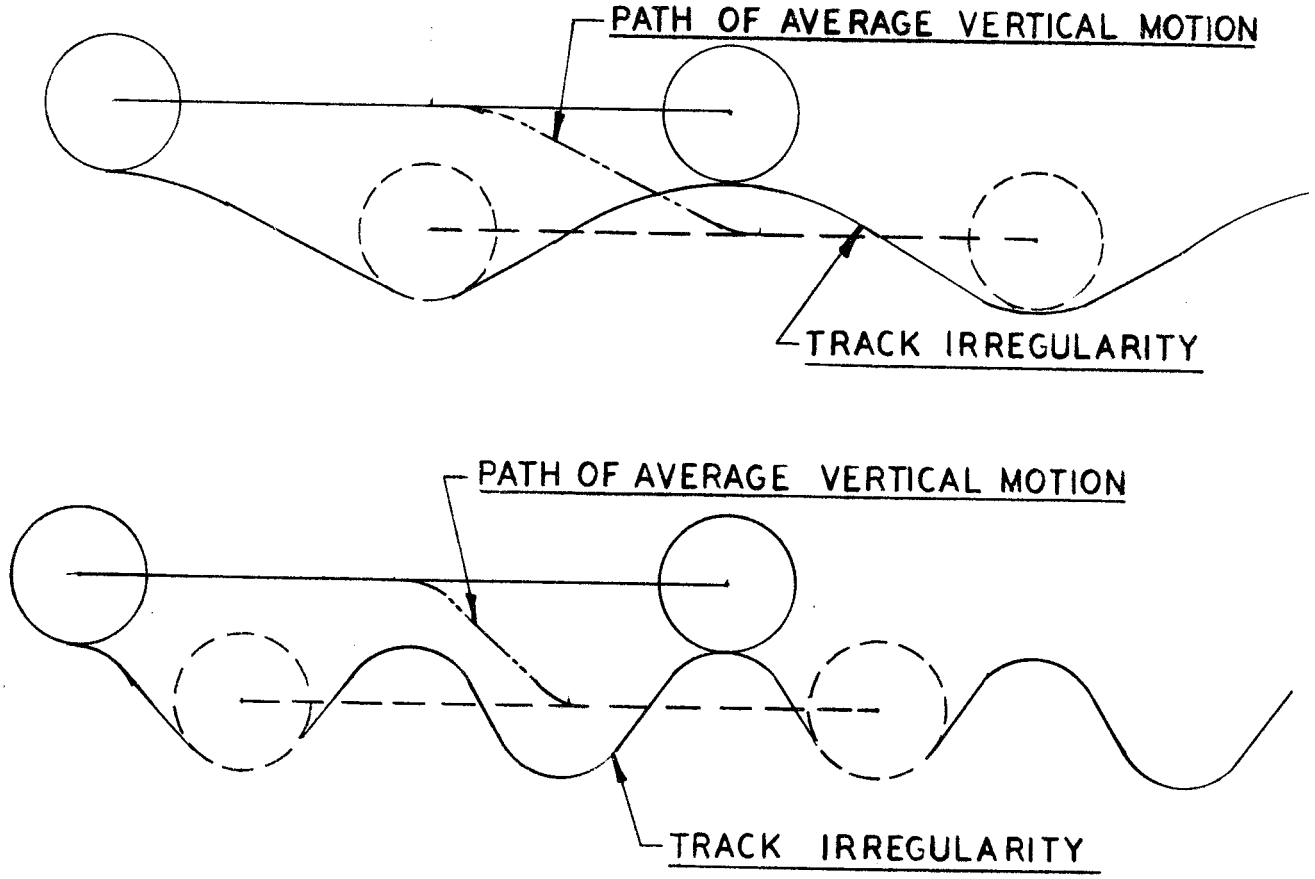

FIGURE 3.1-1

FIGURE 3.1-2

POWER SPECTRAL DENSITY OF AVERAGE VERTICAL ACCELERATION OF EQUALIZER BEAMS ON "A" END TRUCK

RUN NO. 5

FREQUENCY RESOLUTION = .1 hz

STANDARD DEVIATION = .19 gs

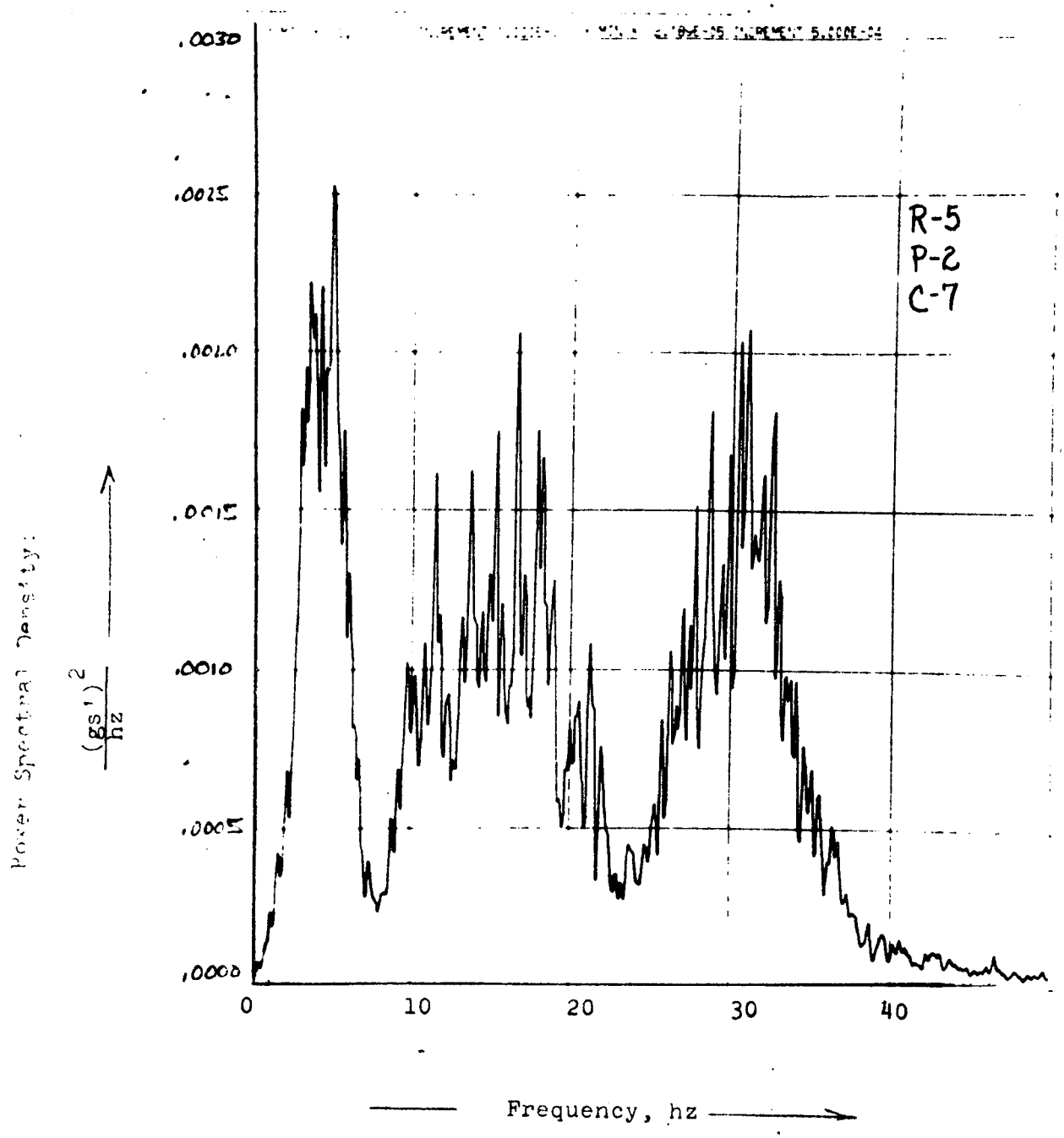

92 miles per hour. With the truck wheel base of 8'6" we would expect maximums in the vertical acceleration of the truck at track irregularity wave length of 8'6", 4'3", ...
At 92 miles per hour the frequency results from these wave lengths are 15.9 hertz and 31.7 hertz which is illustrated by the test result. Additionally, a minimum in the average vertical acceleration of the wheel assemblies should occur when the wave length of track irregularities is such that one wheel set is at a maxima and the other is at a minima as shown in Figure 3.1-3. This occurs at track irregularity inputs of 17', 5'8" .... At 92 miles per hour the frequency resulting from these wave lengths is 7.9 hertz and 23.8 hertz which correspond to the minima in vertical acceleration on Figure 3.1-2. The same effect can be seen in the average lateral of the wheel assemblies for track section five as shown in Figure 3.1-4.

Figure 3.1-5 is the power spectral density of the average yaw acceleration of the truck frame, determined by the difference in the lateral acceleration of the lead axle journal box and the trailing axle journal box of the truck, on track section five.

If we examine the yaw of the truck frame the situation should be reversed with relative maxima in yaw occurring at 7.9 hertz and 23.8 hertz and minimum yaw at 15.9 and 31.7 hertz for a speed of 92 MPH as shown in Figure 3.1-5.

Figure 3.1-6 is the power spectral density average roll acceleration of the truck frame assembly, determined by

TRACK IRREGULARITY WAVE LENGTH AT WHICH
RELATIVE MINIMA IN AVERAGE VERTICAL ACCELERATION
OF TRUCK WHEEL AND AXLE ASSEMBLY OCCUR

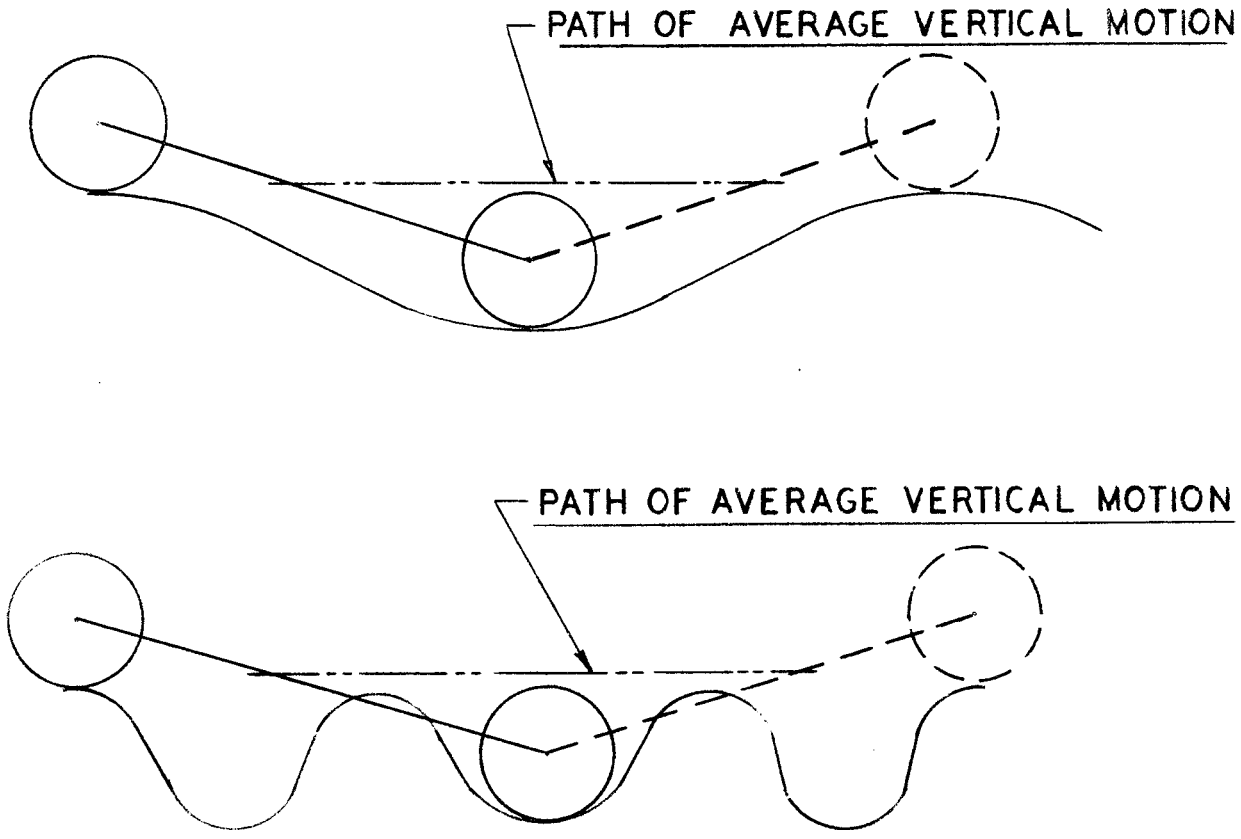

FIGURE 3.1-3

FIGURE 3.1-4

POWER SPECTRAL DENSITY OF AVERAGE LATERAL ACCELERATION OF JOURNAL BOXES ON "A" END TRUCK

RUN NO. 5

FREQUENCY RESOLUTION = .1 hz

STANDARD DEVIATION = .10 gs

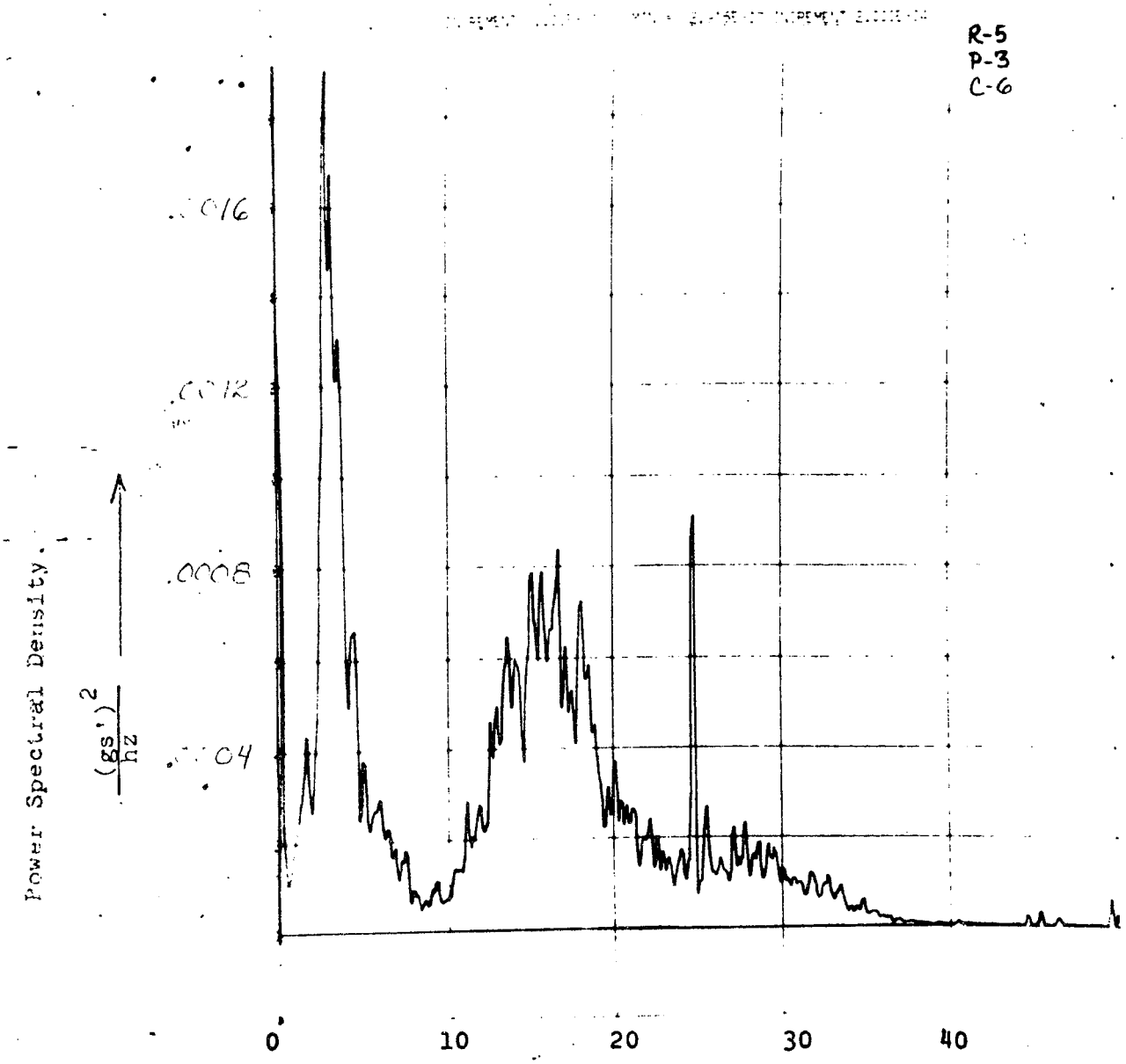

FIGURE 3.1-5

POWER SPECTRAL DENSITY OF AVERAGE YAW ACCELERATION OF JOURNAL BOXES ON "A" END TRUCK (1/2 the difference in lateral acceleration of the journal boxes.)

RUN NO. 5

FREQUENCY RESOLUTION = .1 hz

STANDARD DEVIATION = .10 gs

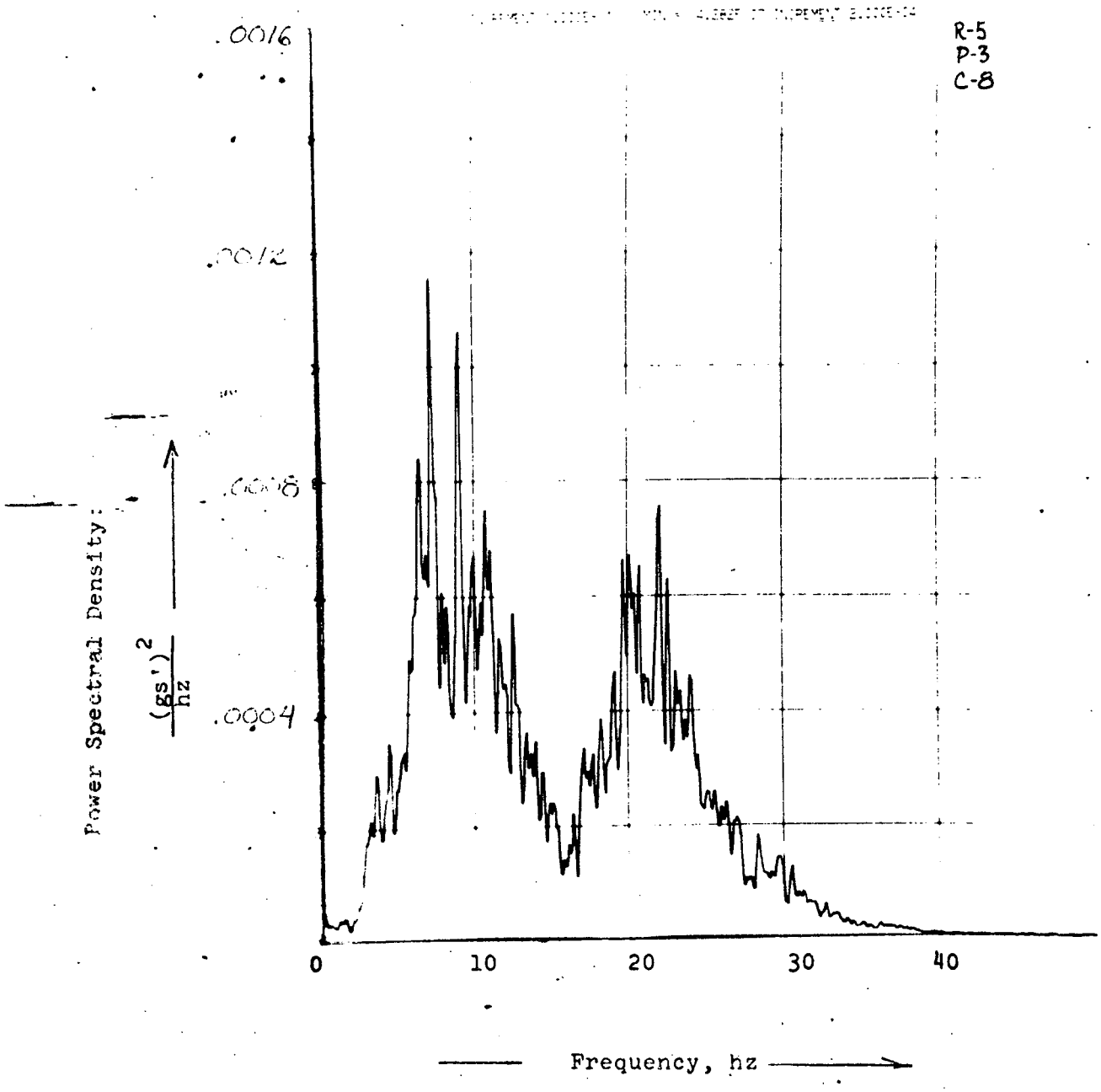

FIGURE 3.1-6

POWER SPECTRAL DENSITY OF AVERAGE ROLL ACCELERATION OF EQUALIZER BEAMS ON "A" END TRUCK (1/2 the difference in vertical acceleration of equalizer beams.)

RUN NO. 5

FREQUENCY RESOLUTION = .1 hz

STANDARD DEVIATION = .23 gs

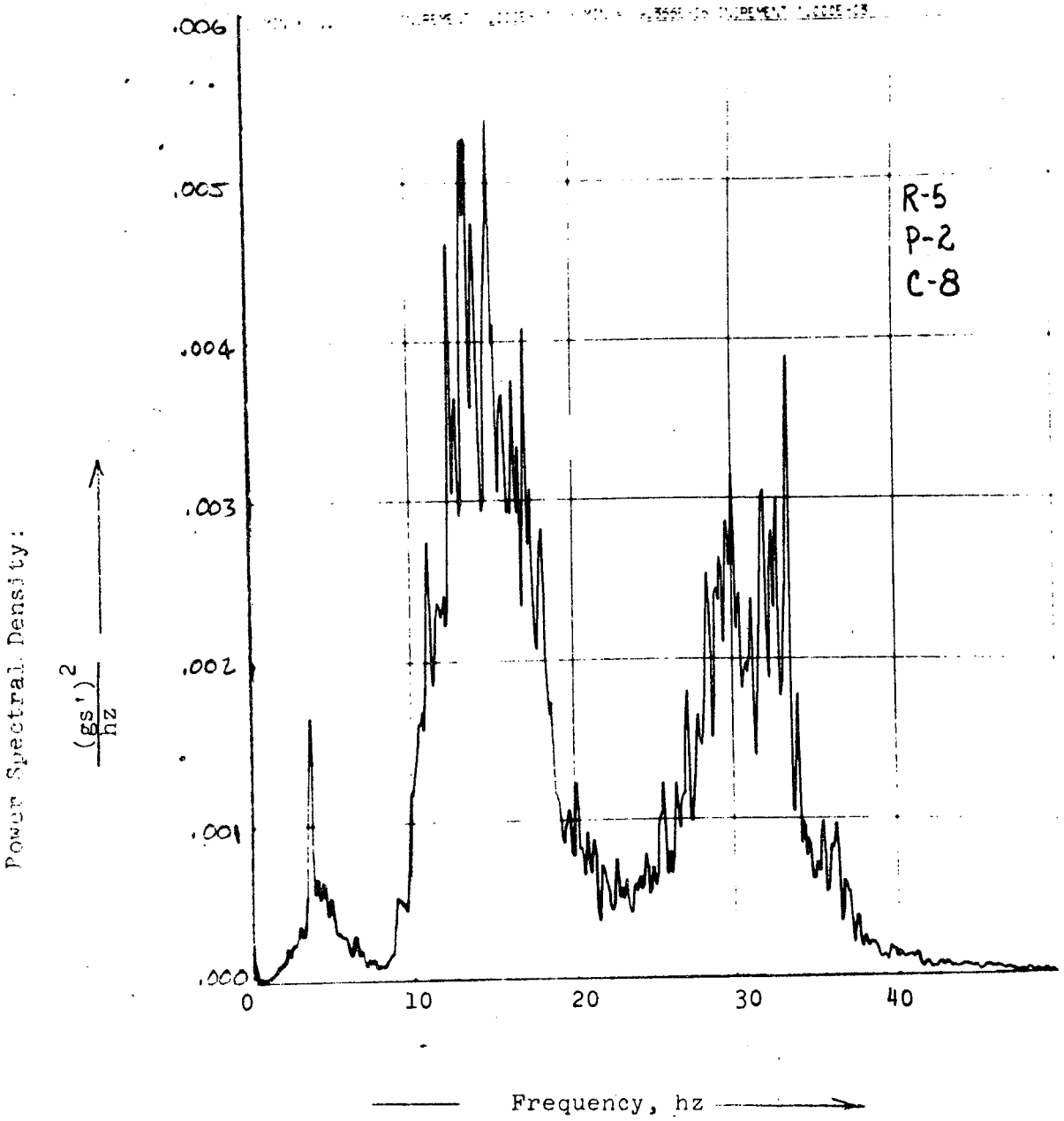

the difference of the average vertical acceleration of the left and right equalizer beams of the truck, for track section five. Since roll is primarily generated by vertical inputs, we would expect the average roll of the wheel assemblies to have maxima and minima similar to the vertical as shown in Figure 3.1-6.

The frequencies of track irregularities where relative maxima occur in the average vertical, lateral, roll, yaw and pitch accelerations of the truck frame assembly are plotted in Figure 3.1-7 for the Metroliner truck wheelbase of 8'6" as a function of train speed.

3.2 Truck Spacing Dependent Inputs

Using arguments similar to those developed in section 3.1, we can determine the wave lengths of track irregularities where the two railcar truck motions are in phase or 180° out of phase. Where the truck motions are in phase, relative maxima in the vertical, lateral, and roll inputs to the railcar should occur. Where the truck motions are 180° out of phase, relative maxima in yaw and pitch inputs to the railcar should occur.

With the Metroliner truck spacing of 59'6" relative maxima in the vertical, lateral and roll inputs should occur at track irregularity wave length of 59'6", 29'9", 19'10" ... The relative maxima in the yaw and pitch inputs should occur at track irregularity wave lengths of 119', 39.6' ....

In Figure 3.2-1 the frequencies of track irregularities where the Metroliner truck motion are in phase and

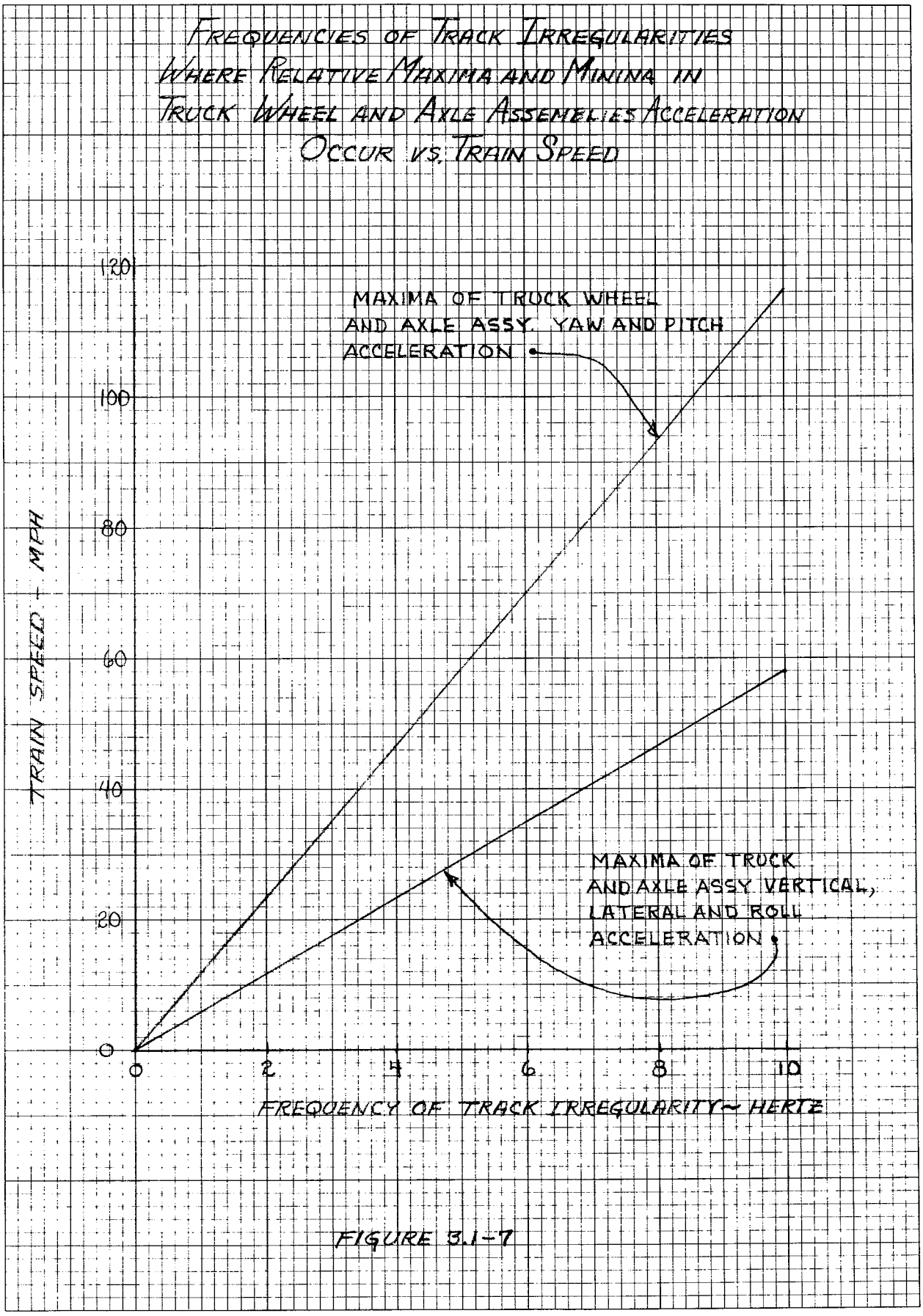
FREQUENCIES OF TRACK IRREGULARITIES
WHERE RELATIVE MAXIMA AND MINIMA IN
TRUCK WHEEL AND AXLE ASSEMBLIES ACCELERATION
OCCUR VS. TRAIN SPEED
120
100
80
60
40
20
0
TRAIN SPEED - MPH
MAXIMA OF TRUCK WHEEL
AND AXLE ASSY. YAW AND PITCH
ACCELERATION
MAXIMA OF TRUCK
AND AXLE ASSY VERTICAL,
LATERAL AND ROLL
ACCELERATION
0
2
4
6
8
10
FREQUENCY OF TRACK IRREGULARITY ~ HERTZ

FIGURE 3.1-7

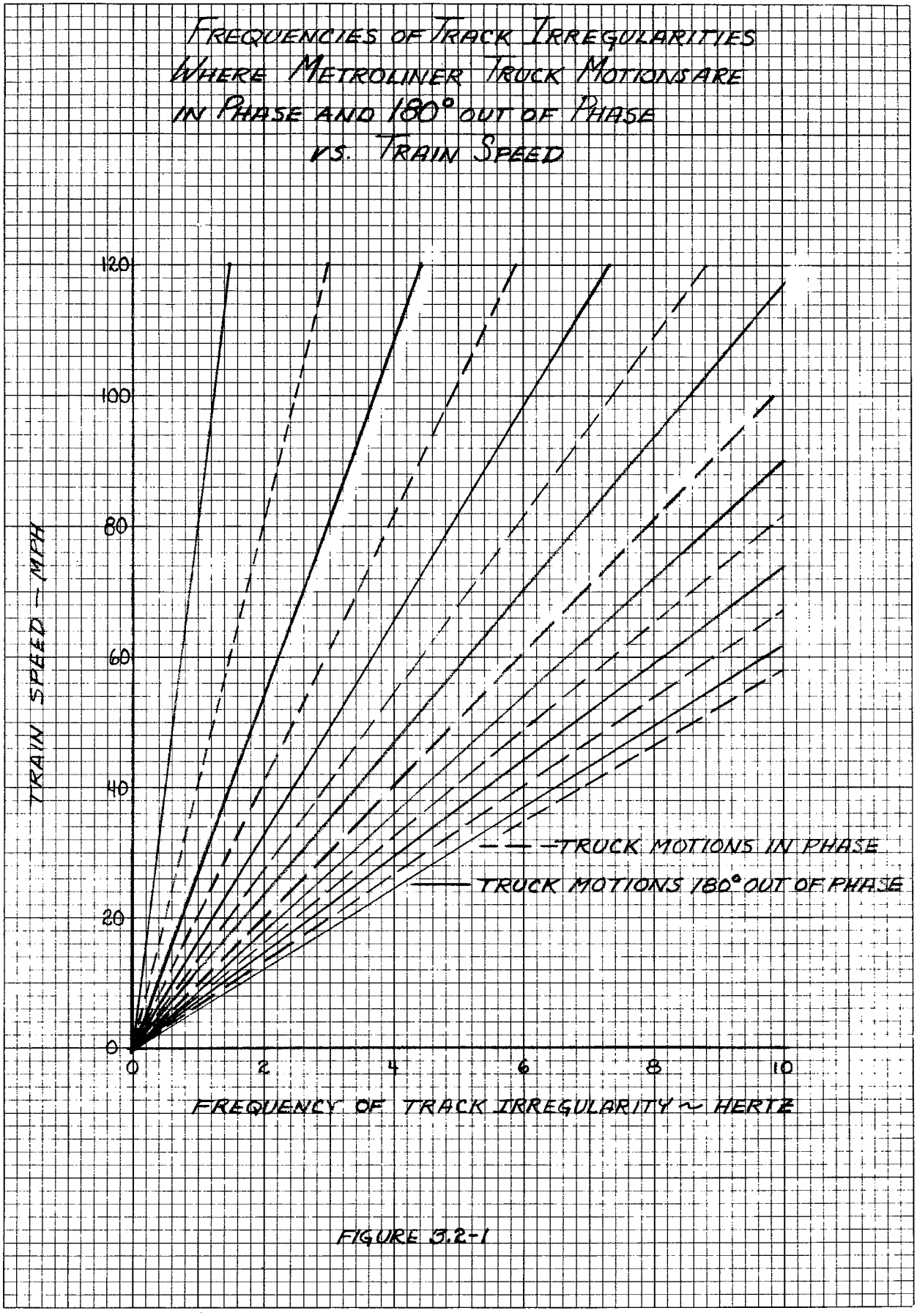
FREQUENCIES OF TRACK IRREGULARITIES
WHERE METROLINER TRUCK MOTIONS ARE
IN PHASE AND 180° OUT OF PHASE
VS. TRAIN SPEED
TRAIN SPEED — MPH
120
100
80
60
40
20
0
0
2
4
6
8
10
FREQUENCY OF TRACK IRREGULARITY ~ HERTZ
TRUCK MOTIONS IN PHASE
TRUCK MOTIONS 180° OUT OF PHASE

FIGURE 3.2-1

180° out of phase as a function of train speed are shown.

3.3 Rail Joint Dependent Inputs

Bolted rail is laid in 39 foot sections. The left rail joint is staggered 19.5 feet with respect to the right rail joint. Power spectral densities of rail measurements taken of the right bolted rail in track section four are shown in Figure 3.3-1 and 3.3-2. For this rail the dominate amplitudes of track irregularities in both alignment and profile occur at 39 feet, 19.5 feet, 13 feet and 9.75 feet wave lengths which are the fundamental second, fourth and sixth harmonics of the rail joint spacing. The rail profile and alignment wave form are symmetrical as no odd harmonics are evident.

A wheel set traveling along the track has an average vertical motion which is the average of the vertical position of the two rails, an average roll motion which is the average difference of the vertical position of the two rails, and an average lateral motion which is the average lateral position of the two rails. In Figure 3.3-3 the vertical amplitudes of the fundamental second, fourth and sixth harmonics of the right and left rail are shown with the left rail joint staggered 19.5 feet with respect to the right rail joint. For this track, the average vertical motion of a wheel set should have a relative maxima at wave lengths of 19.5 feet and 9.75 feet since when the wave forms of the two rails are added, the 39 foot fundamental and the 13 foot fourth

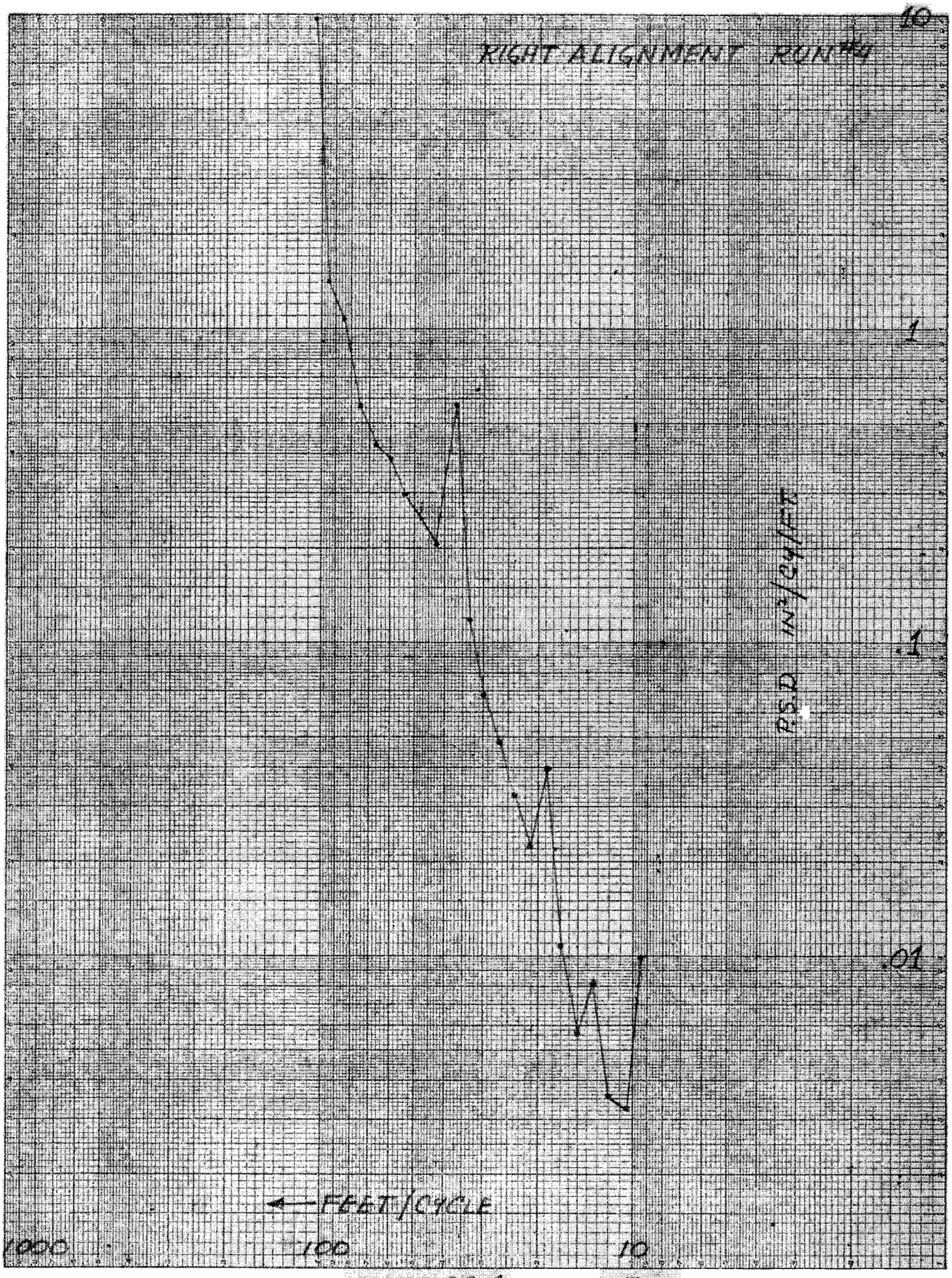
RIGHT ALIGNMENT RUN #4
10
1
.1
.01
P.S.D. in²/cycle/ft
← FEET/CYCLE
1000
100
10

FIGURE 3.3-1

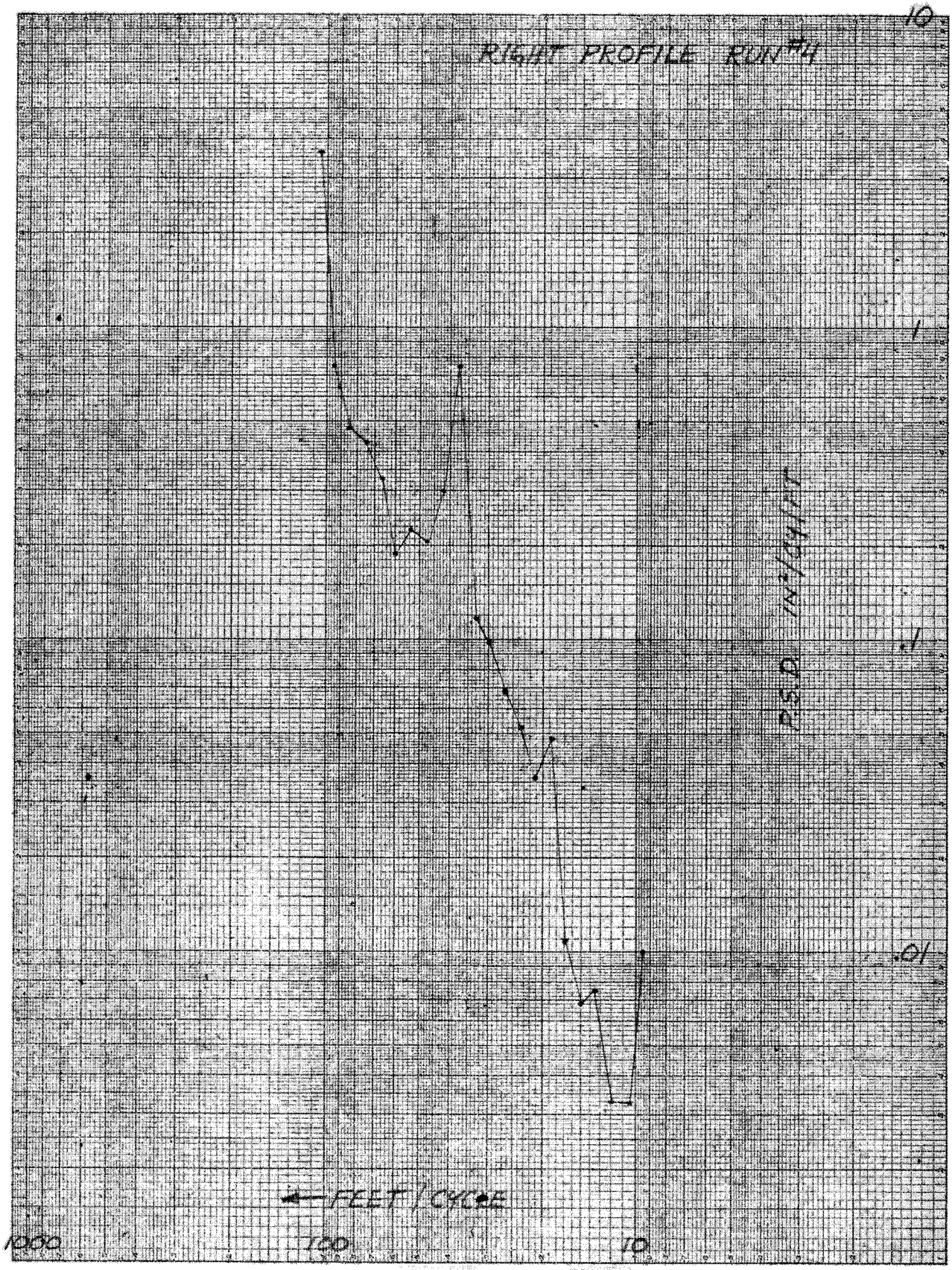
RIGHT PROFILE RUN #4
10
1
.1
.01
PSD FT²/IN/FT
FEET / CYCLE
1000
100
10

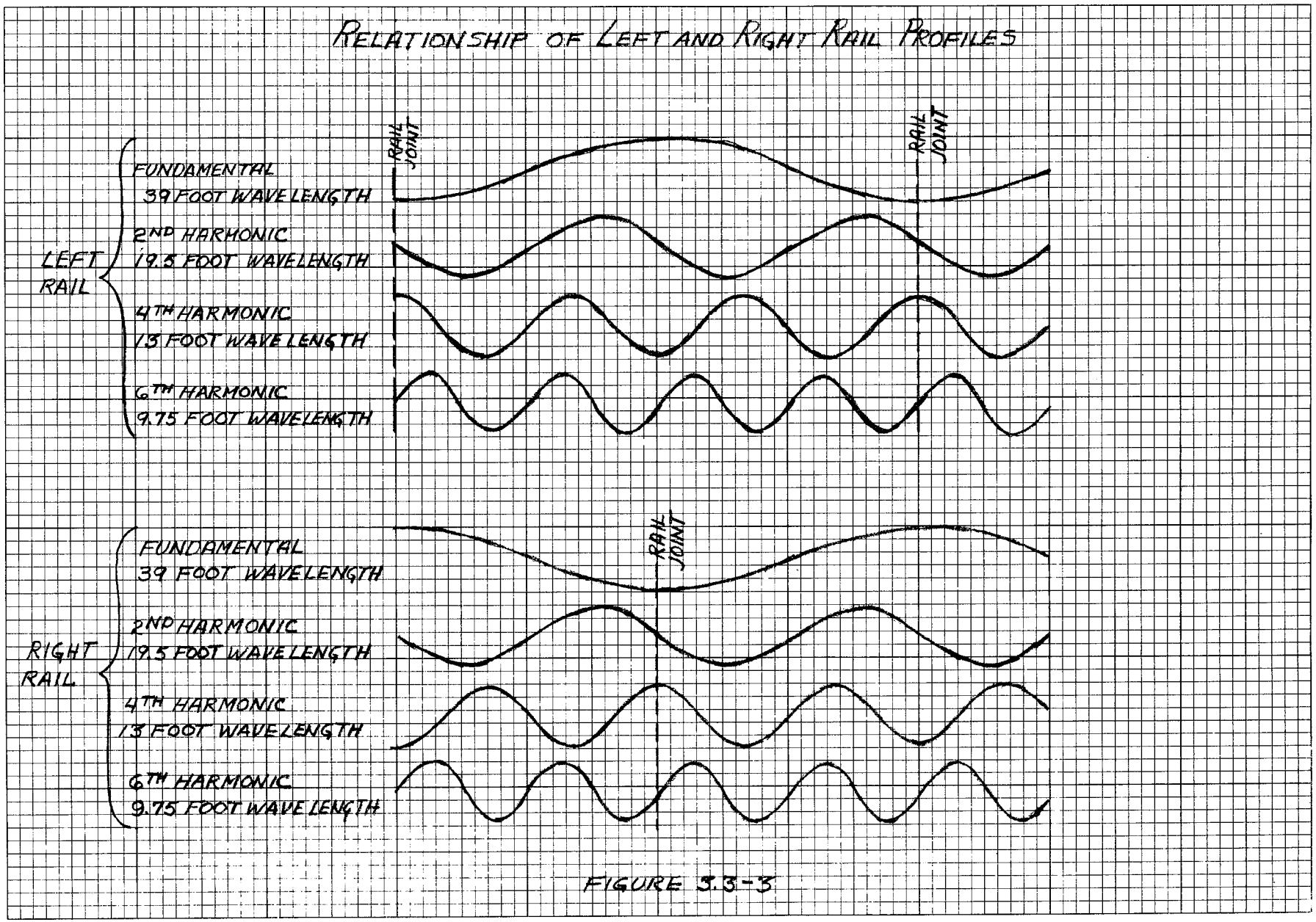
RELATIONSHIP OF LEFT AND RIGHT RAIL PROFILES
RAIL JOINT
RAIL JOINT
FUNDAMENTAL
39 FOOT WAVELENGTH
2ND HARMONIC
19.5 FOOT WAVELENGTH
LEFT RAIL
4TH HARMONIC
13 FOOT WAVELENGTH
6TH HARMONIC
9.75 FOOT WAVELENGTH
RAIL JOINT
FUNDAMENTAL
39 FOOT WAVELENGTH
2ND HARMONIC
19.5 FOOT WAVELENGTH
RIGHT RAIL
4TH HARMONIC
13 FOOT WAVELENGTH
6TH HARMONIC
9.75 FOOT WAVELENGTH

FIGURE 3.3-3

harmonic tend to cancel. The average roll motion of the wheel set should have a relative maxima at wave lengths of 39 feet and 13 feet, since when the wave forms of the two tracks are substracted the 19 foot second harmonic and 9.75 foot sixth harmonic tend to cancel.

The lateral alignment of the rails is similar to the vertical profile with the exception that the rail joints are either closer to the center of the track or further from the center of the track than a point on the rail midway between the joints. In either case, the resulting relationship between the left and right rail alignment is the same as shown in Figure 3.3-3 with the exception that the amplitude of the right rail is reversed. As a result, the average lateral motion of the wheel set should have a maxima at wave lengths of 39 feet and 13 feet since when the lateral alignments are added the second harmonic at 19.5 feet and the sixth harmonic at 9.75 feet tend to cancel.

The cross level measurements and gage measurements of track section four, Figures 3.3-4 and 3.3-5 respectively show dominate wave length amplitudes at 39 feet and 13 feet and the absence of the 19.5 foot wave length as anticipated.

Figures 3.3-6, 3.3-7 and 3.3-8 are power spectral densities of the average vertical, lateral and roll accelerations experienced by the truck wheel and axle assemblies traveling over track section four at an average speed of 105 MPH. The vertical acceleration, Figure 3.3-6 has

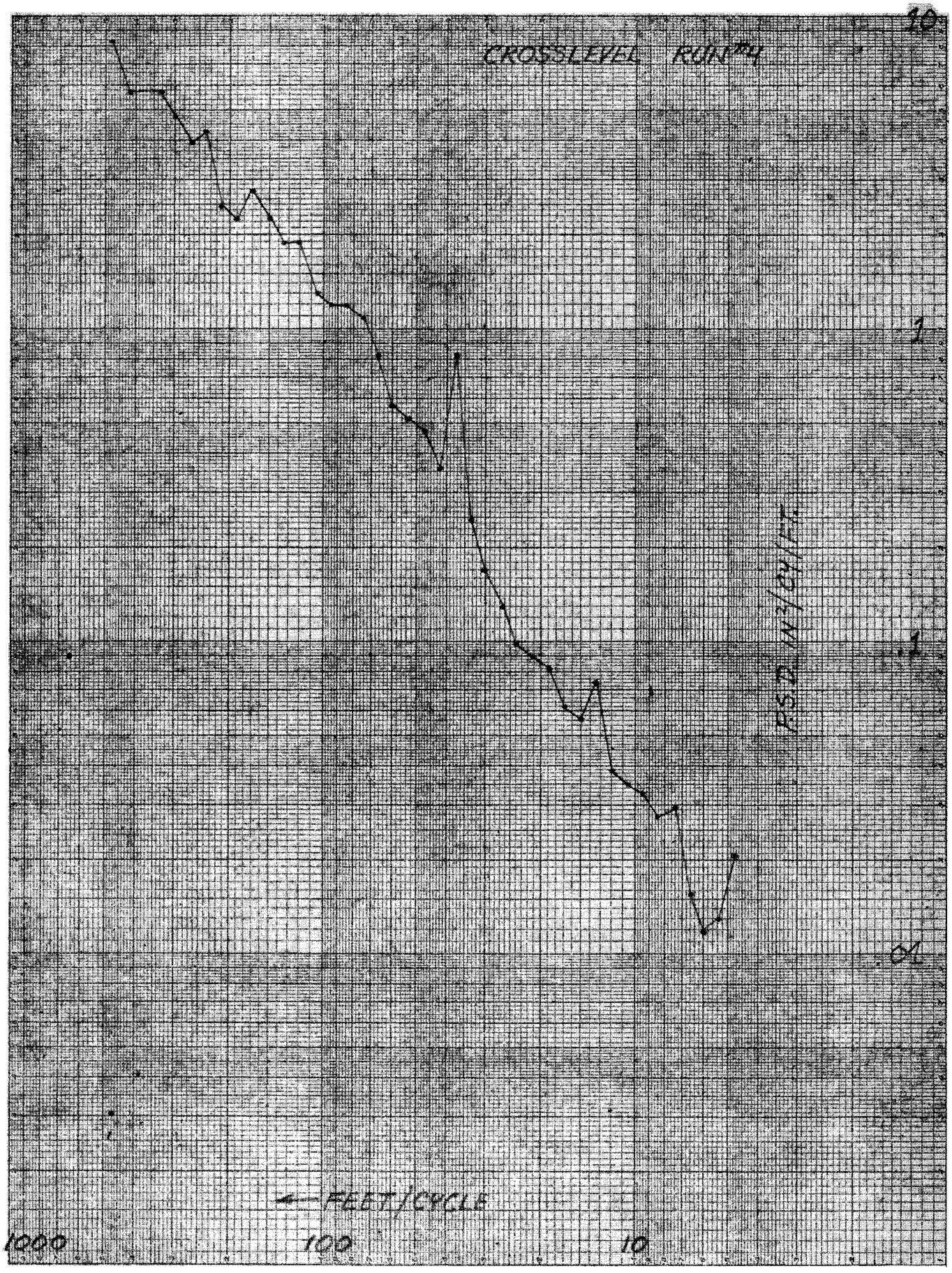
CROSSLEVEL RUN #4
10
1
.1
.01
P.S.D. IN²/CYCLE/FT.
← FEET/CYCLE
1000
100
10

FIGURE 3.3-4

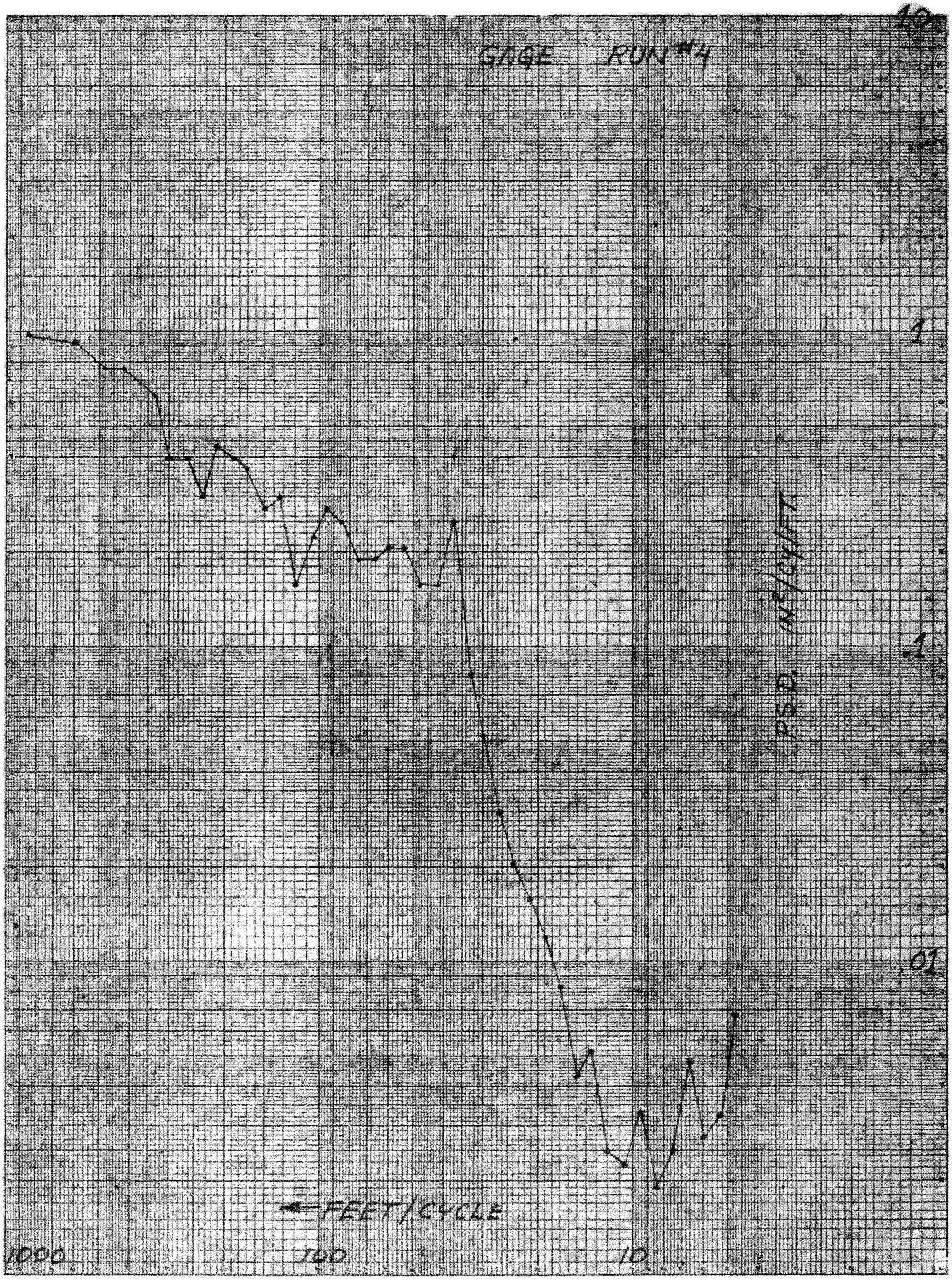

FIGURE 5.3-5

FIGURE 3.3-6

POWER SPECTRAL DENSITY OF AVERAGE VERTICAL ACCELERATION OF EQUALIZER BEAMS ON "A" END TRUCK

RUN NO. 4

FREQUENCY RESOLUTION = .1 hz

STANDARD DEVIATION = .36 gs

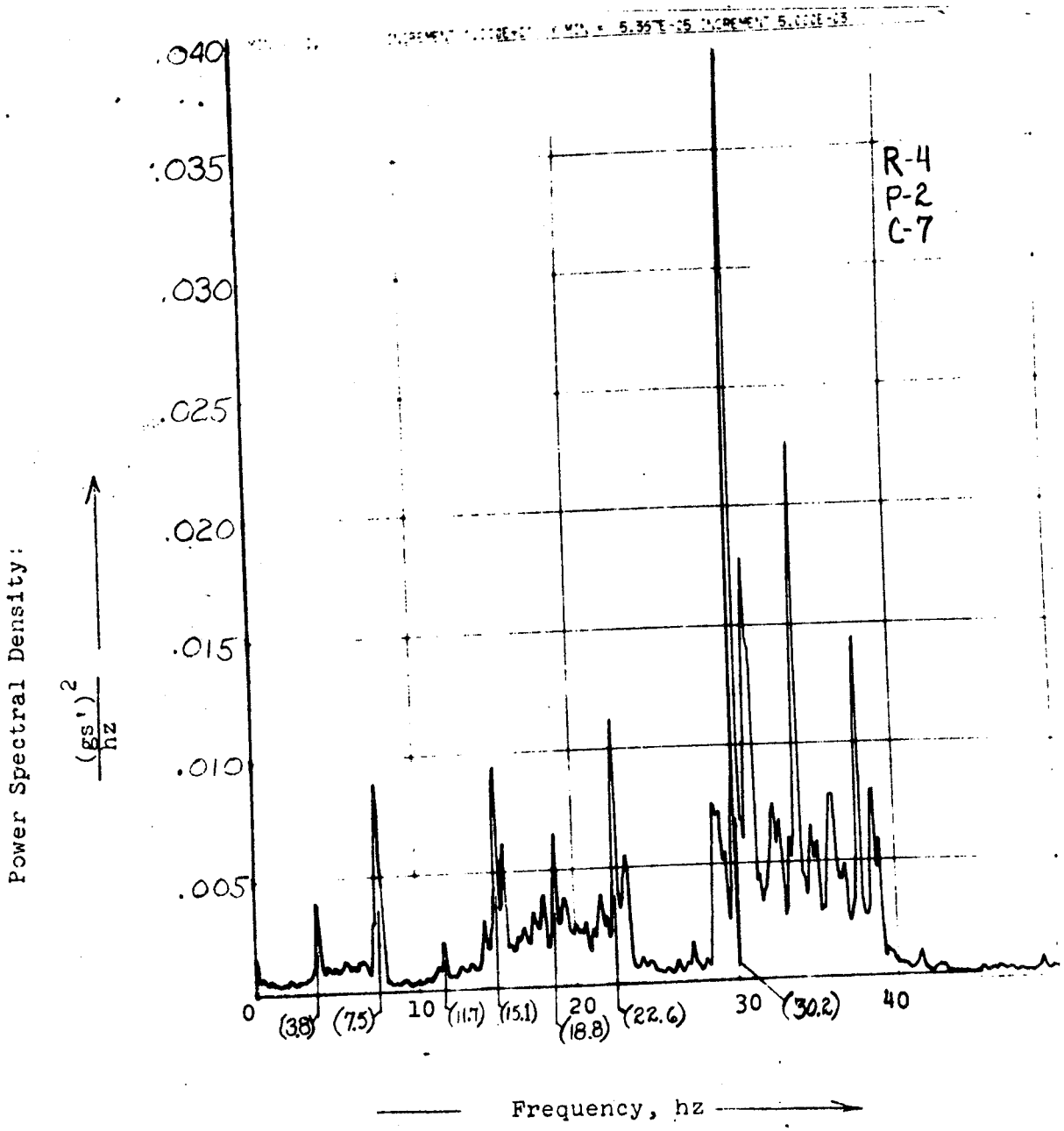

FIGURE 3.3-7

POWER SPECTRAL DENSITY OF AVERAGE LATERAL ACCELERATION OF JOURNAL BOXES ON "A" END TRUCK

RUN NO. 4

FREQUENCY RESOLUTION = .1 hz

STANDARD DEVIATION = .21 gs

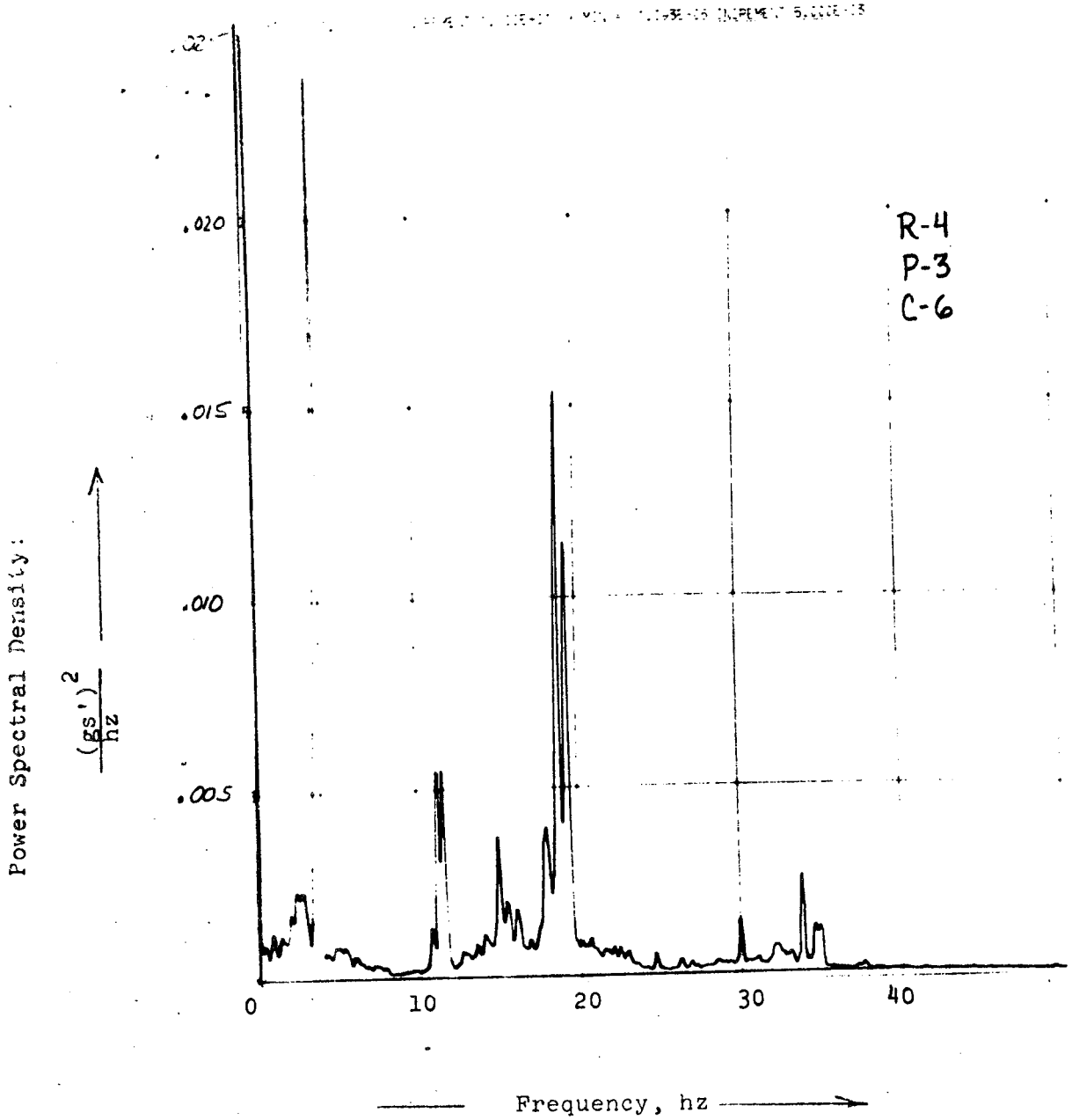

FIGURE 3.3-8

POWER SPECTRAL DENSITY OF AVERAGE ROLL ACCELERATION OF EQUALIZER BEAMS ON "A" END TRUCK (1/2 the difference in vertical acceleration of equalizer beams.)

RUN NO. 4

FREQUENCY RESOLUTION = .1 hz

STANDARD DEVIATION = .53 gs

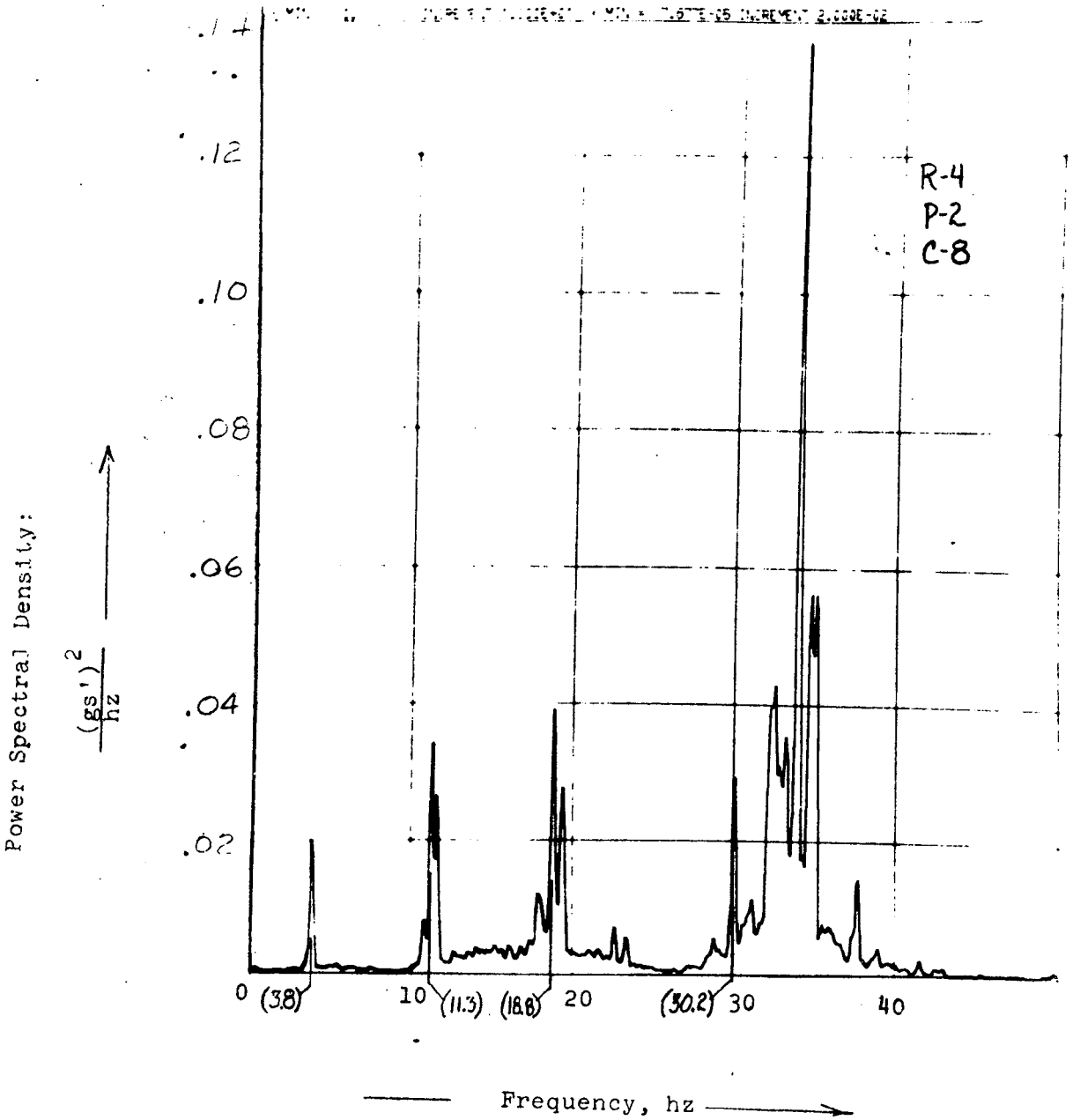

considerable energy at 7.8 hertz and 15.1, wave lengths of 19.7 feet and 10.2 feet as anticipated. The lateral and roll accelerations Figure 3.3-7 and 3.3-8 respectively has considerable energy at 3.8 hertz and 11.3 hertz wave lengths of 40.5 feet and 13.6 feet as anticipated.

The effects of the 39 foot rail joint spacing while dominate on this bolted rail section, are not limited to bolted track. Welded rail has characteristic similar to bolted rail as shown in Figures 3.3-9 and 3.3-10, the profile and alignment measurements of the right rail in track section five which is welded rail.

Figure 3.3-11 is a plot of the frequencies where maxima in the vertical, lateral and roll accelerations of a wheel set occur due to rail joint wave lengths as a function of train speed.

3.4 Summary of Track Irregularity Inputs

At a track irregularity wave length of 39 feet the effects of the truck spacing and rail joint discontinuities reinforce. At 39.67 feet a relative maxima in railcar pitch and yaw inputs occurs with the truck motions 180° out of phase. At 39 feet a relative maxima in lateral and roll acceleration of a wheel set occurs due to rail joint discontinuities. The combination of these two effects results in a dominate railcar yaw input. The railcar roll input is small since the trucks are rolling in opposition to each other. The frequency of the dominate railcar yaw input is shown in Figure 3.4-1 as a function of train speed.

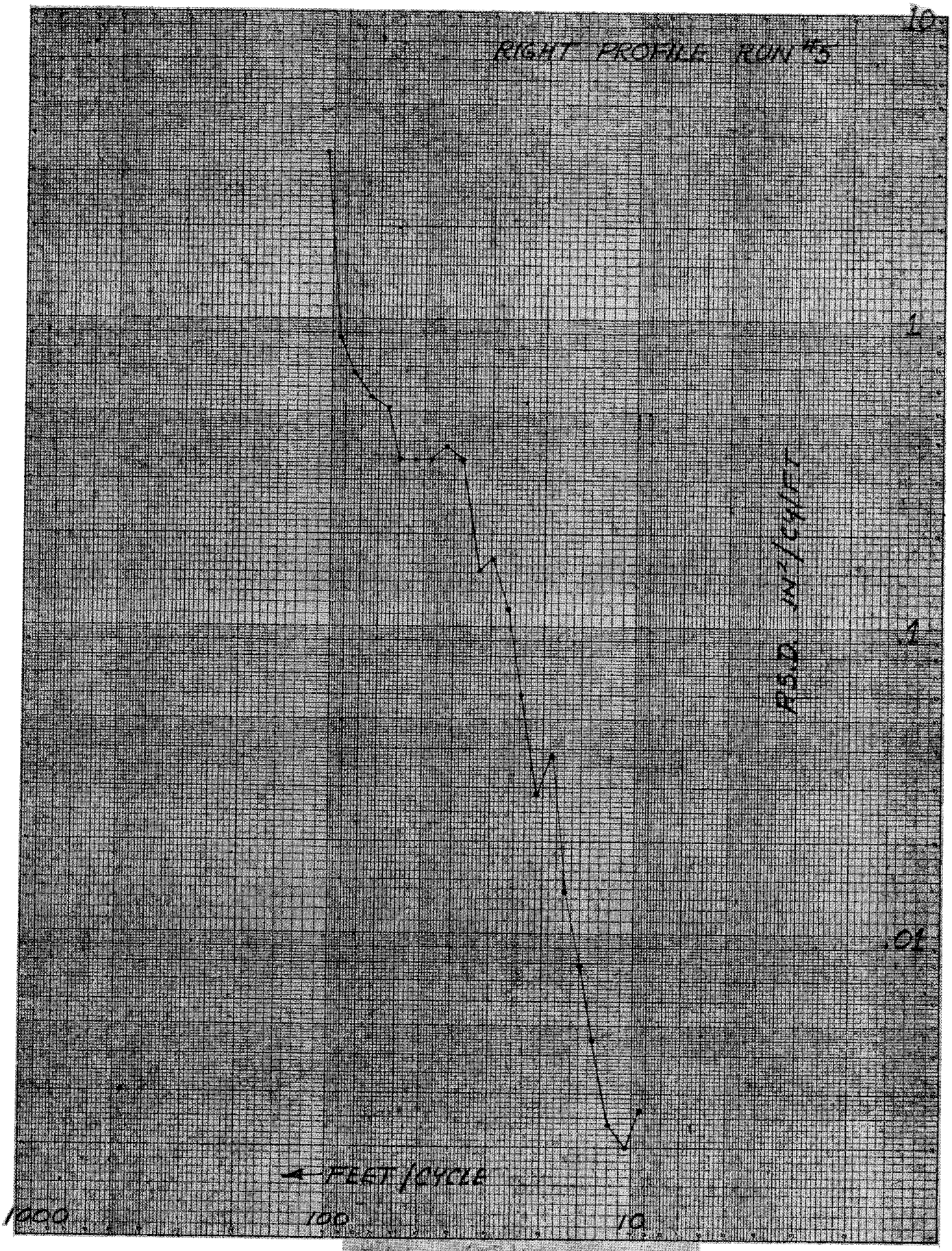

FIGURE 3.3-9

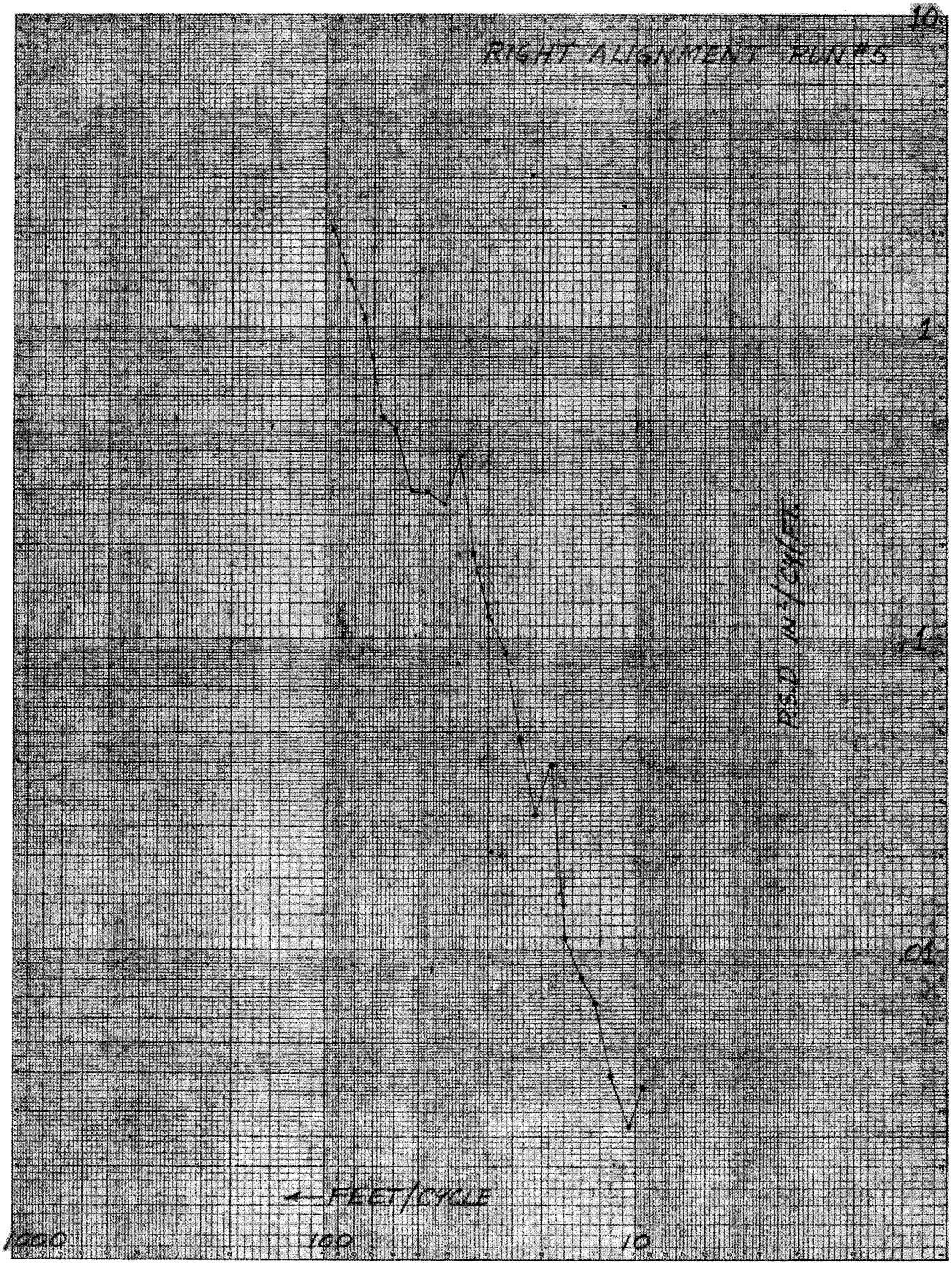
RIGHT ALIGNMENT RUN #5
10
1
.1
.01
PSD IN INCHES
← FEET/CYCLE
1000
100
10

FIGURE 3.3-10

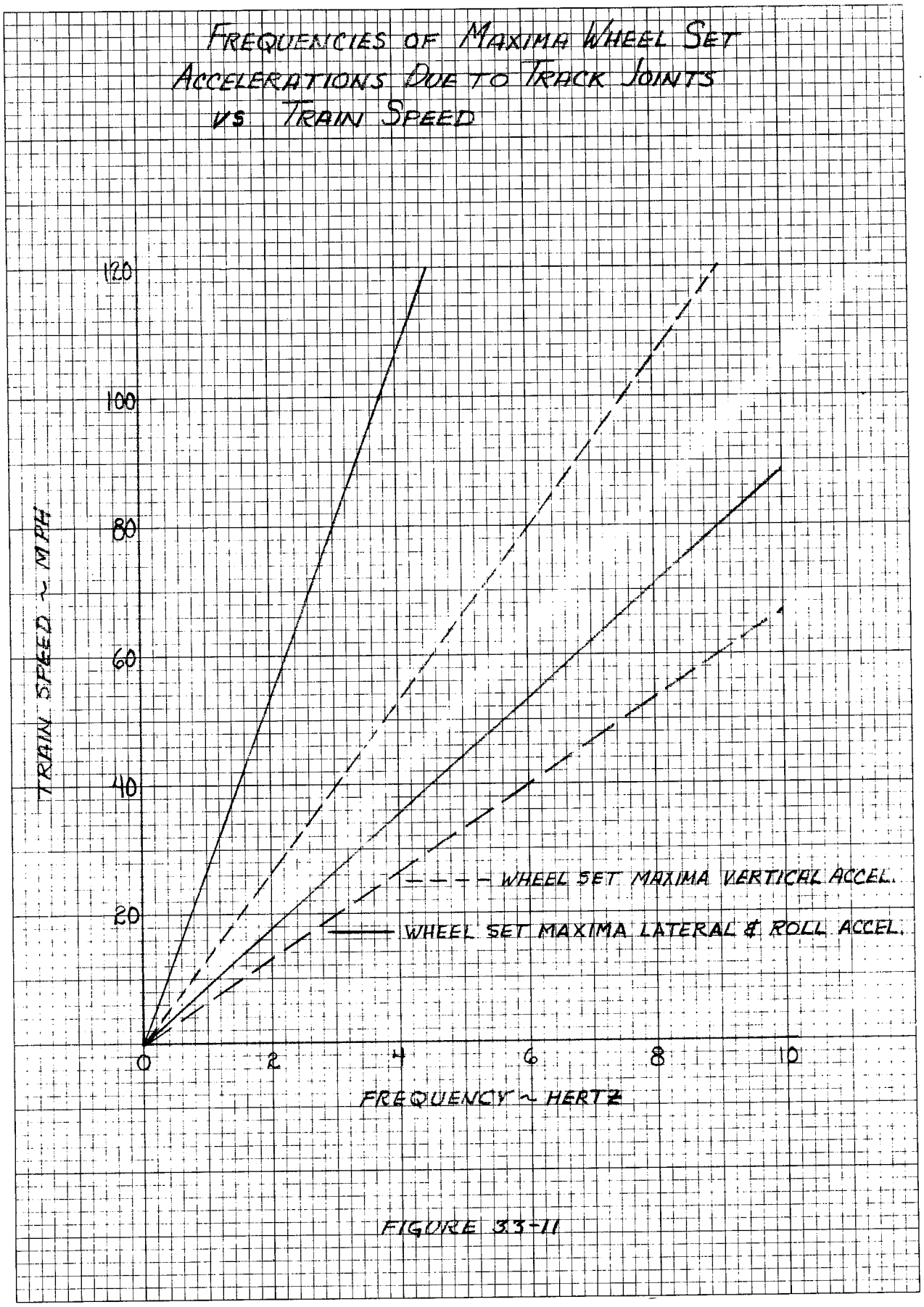
FREQUENCIES OF MAXIMA WHEEL SET
ACCELERATIONS DUE TO TRACK JOINTS
VS TRAIN SPEED
120
100
80
60
40
20
0
2
4
6
8
10
TRAIN SPEED ~ MPH
FREQUENCY ~ HERTZ
WHEEL SET MAXIMA VERTICAL ACCEL.
WHEEL SET MAXIMA LATERAL & ROLL ACCEL.

FIGURE 33-11

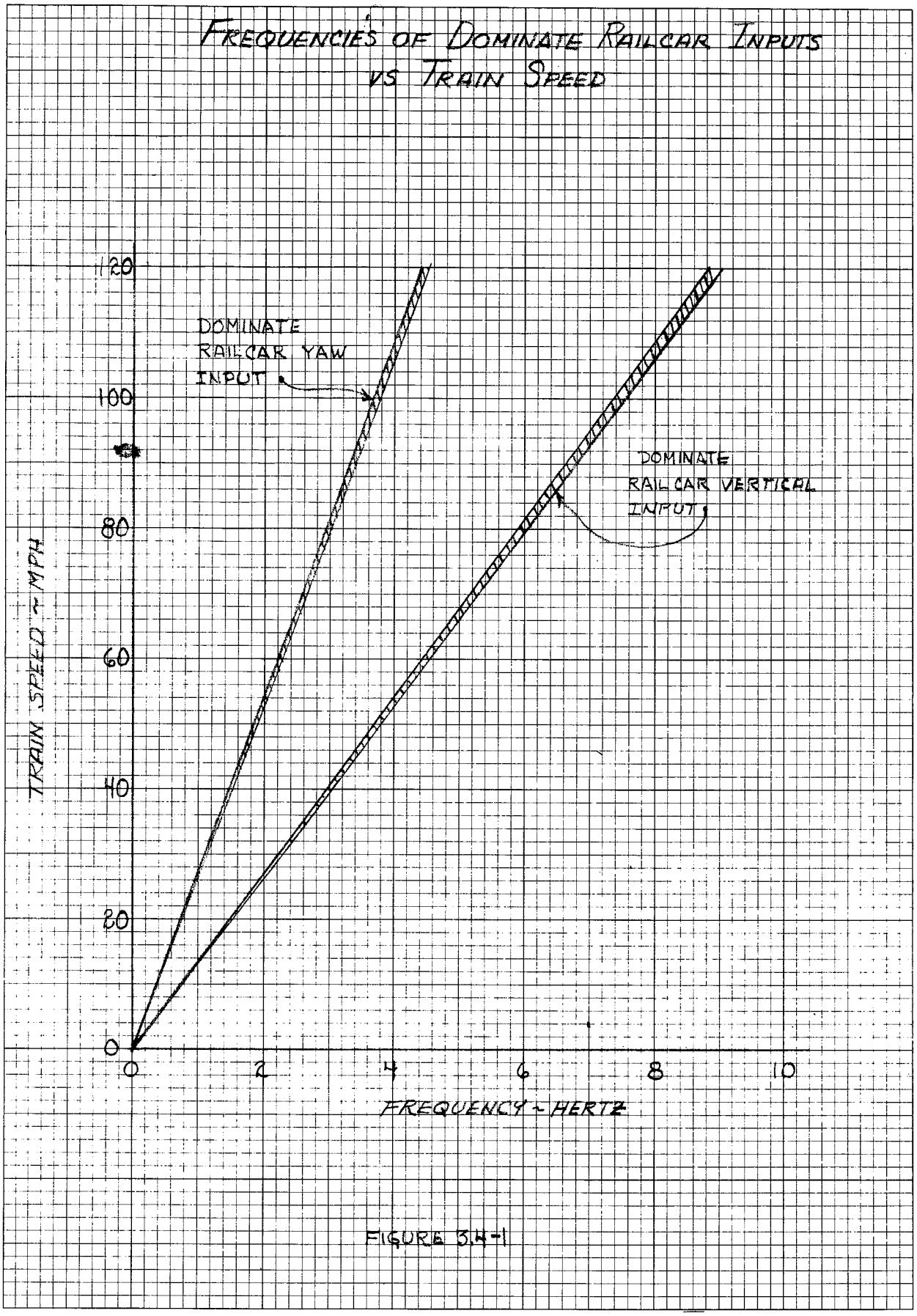
FREQUENCIES OF DOMINATE RAILCAR INPUTS
VS TRAIN SPEED
120
100
80
60
40
20
0
TRAIN SPEED ~ MPH
DOMINATE
RAILCAR YAW
INPUT
DOMINATE
RAILCAR VERTICAL
INPUT
0
2
4
6
8
10
FREQUENCY ~ HERTZ

FIGURE 3.4-1

At a track irregularity wave length of 19.5 feet, a second reinforcement of the truck spacing and rail joints occurs. At 19.83 feet a relative maxima in railcar vertical, lateral and roll input occurs with the truck motions in phase. At 19.5 feet a relative maximum in the vertical acceleration of a wheel set occurs due to rail joint discontinuities. The combination of these two effects results in a dominate railcar vertical input. The frequency of the dominate railcar vertical and yaw inputs is shown in Figure 3.4-1 as a function of train speed.

There are additional dominate yaw and vertical inputs at 13 feet and 9.75 feet respectively.

A minimum in the average vertical acceleration of the truck wheel and axle assembly occurs at a wave length of 17 feet or two times the truck wheelbase. If the truck wheelbase were increased from 8'6" to 9'9", the minimum in the average vertical acceleration of the truck wheel and axle assembly would occur at a wave length of 19.5 feet. This effect would tend to reduce the magnitude of the dominate vertical carbody input at 19.5 hertz and increase the magnitude of the dominate vertical carbody input at a wave length of 9.75 hertz. While a truck of this wheelbase is not considered in this program due to clearance constraints, this effect should be evaluated in the near future.

4.0 PERFORMANCE OF PRESENT METROLINER

The subsystem simulations described in section 2.0 are combined into the "vertical" railcar simulation and the

"lateral" railcar simulation. In this section we shall discuss the results of these simulations and make comparisons to road test results where practical.

The simulation results are presented as plots of the accelerations at various locations on the railcar resulting from input accelerations applied to the wheel and axle assemblies of the trucks, as a function of frequency. Five input configurations are used. These input configurations and values of input accelerations are tabulated in Table 4.0-1. Direct comparisons of the simulation results to the test results cannot be made since the test results are weighted by input amplitude variations with frequency as described in section 3.0. As a result, in comparing simulated and test results these input effects must be considered.

4.1 Performance of Vertical Simulation of Present Metroliner

Figure 4.1-1 is the vertical acceleration of the truck frame due to a vertical input. The resonance of the truck frame is 9.5 hertz. The truck frame isolates track irregularity inputs at frequencies above 13 hertz, and appreciably amplifies track irregularities in the 6 to 12 hertz range. Figure 4.1-2 is the measured vertical acceleration of the truck frame assembly from track section five. Comparing the truck frame acceleration to the input acceleration during that track section (Figure 3.1-2), there is considerable amplification between 5 and 13 hertz as indicated by the simulation.

Table 4.0-1

Simulation Input Configurations

Type of Input	"A end"Truck Wheel and Axle Assembly		"B end" Truck Wheel and Axle Assembly		Phasing Between "A end" and"B end" Truck Motions
	Magnitude	Direction	Magnitude	Direction	
Vertical	1g	vertical	1g	vertical	in phase
Pitch	1g	vertical	1g	vertical	180° out of phase
Lateral	1g	lateral	1g	lateral	in phase
Yaw	1g	lateral	1g	lateral	180° out of phase
Roll	8.4 rad/sec^2	roll	8.4 rad/sec^2	roll	in phase

PRESENT METROLINER

TRUCK FRAME VERTICAL ACCELERATION DUE TO VERTICAL INPUT

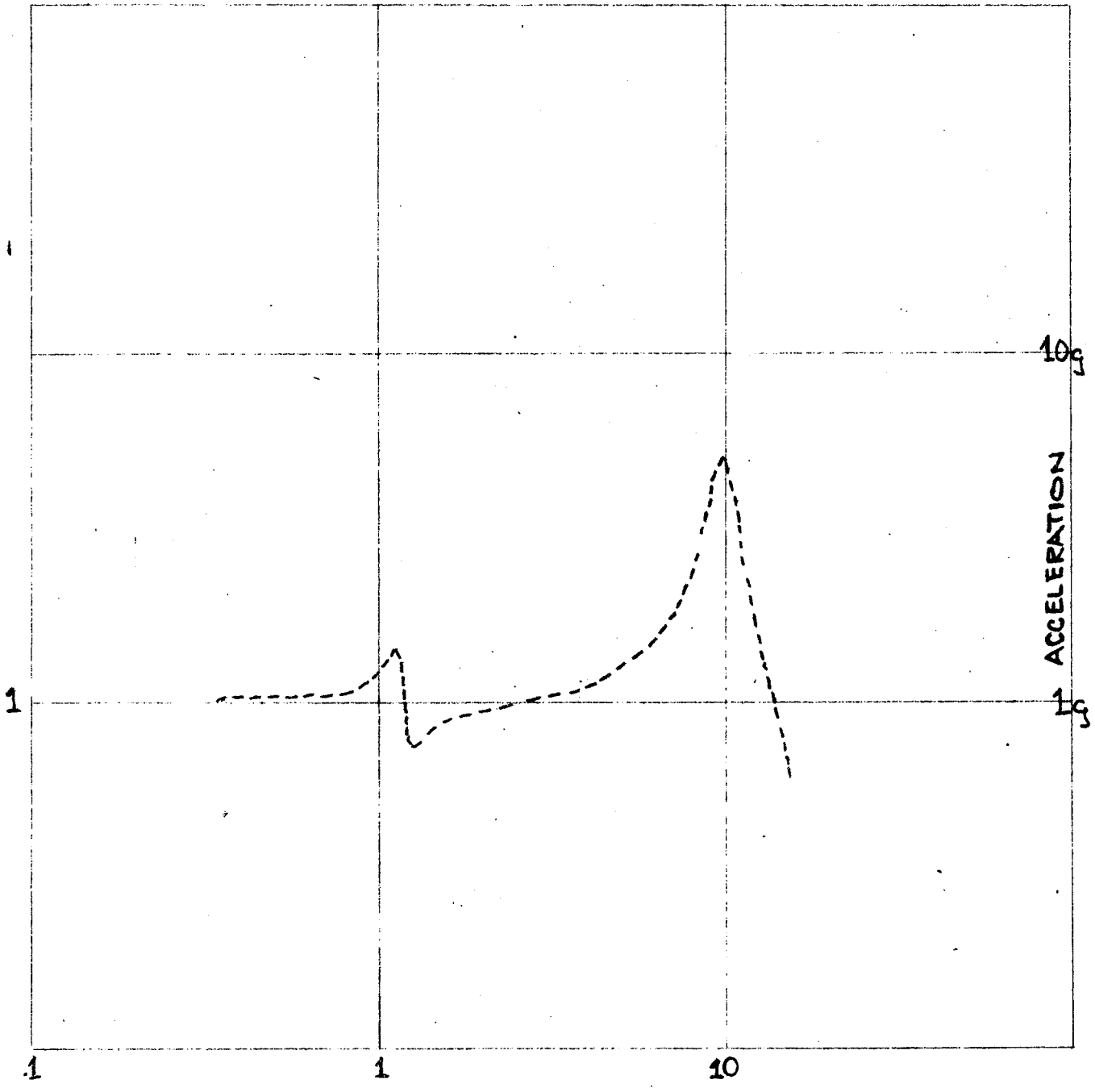

FREQUENCY - HERTZ

FIGURE 4.1-1

FIGURE 4.1-2

POWER SPECTRAL DENSITY OF VERTICAL ACCELERATION

OF TRUCK BOLSTER ON "A" END TRUCK

RUN NO. 5

FREQUENCY RESOLUTION = .1 hz

STANDARD DEVIATION = .21 gs

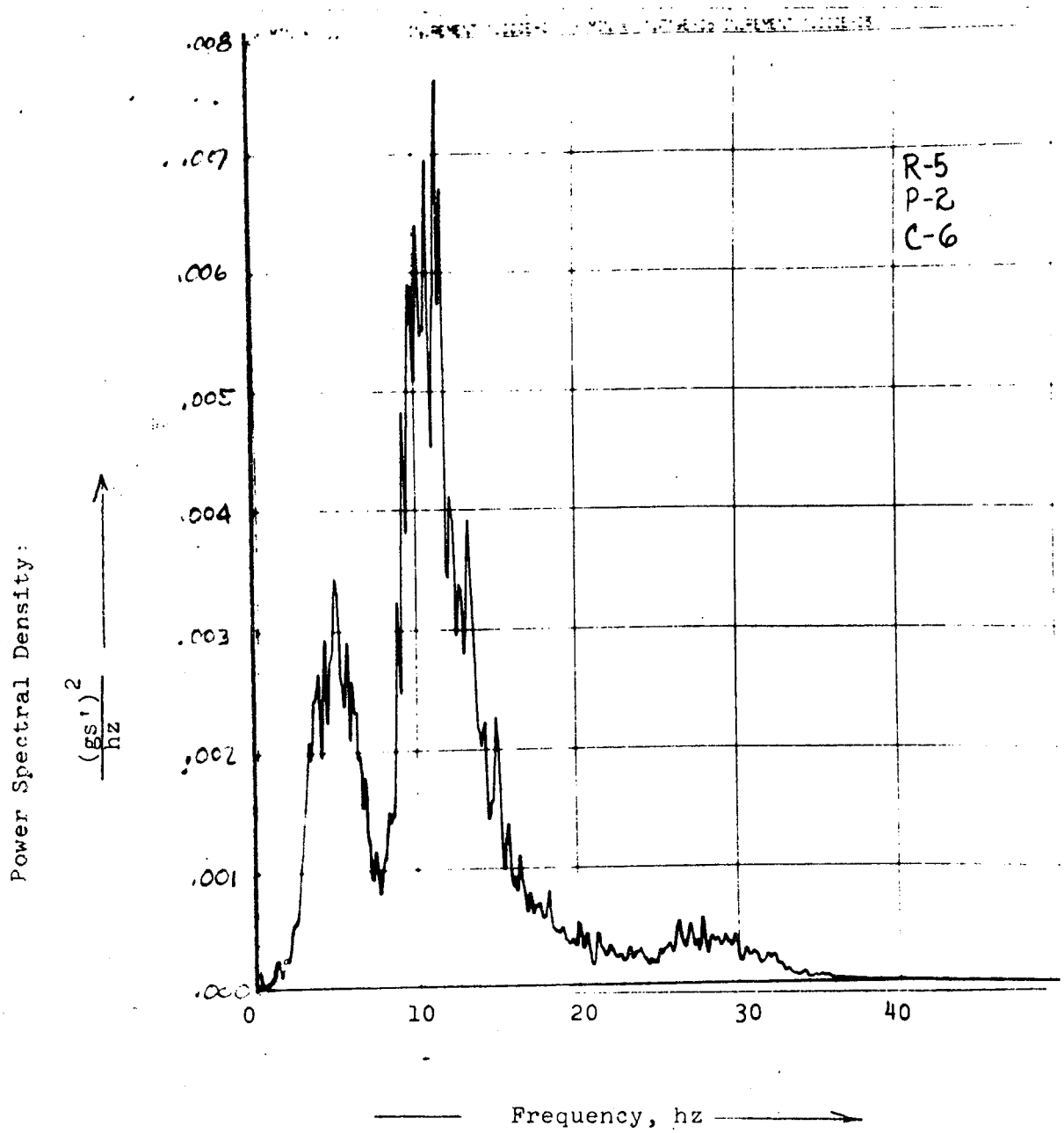

The longitudinal response of the truck frame assembly to pitch inputs is shown in Figure 4.1-3. The dominate peaks occur at 1.32 hertz, the pitch resonance of the carbody and 2.6 hertz the longitudinal resonance of the carbody on the anchor rods. During the road test the force in the anchor rods of the "A end" truck was measured. This force is related to the accelerations of the truck in the longitudinal direction. Figure 4.1-4, the average longitudinal force in the anchor rods on track section five, shows considerable energy at 1.4 hertz and 2.6 hertz similar to the simulation.

The simulated carbody accelerations at the "A end" of the carbody due to vertical and pitch inputs are shown in Figures 4.1-5 and 4.1-6. These results show resonances at 1.05 hertz the vertical carbody resonance, 1.32 hertz the pitch carbody resonance, 4.6 hertz the vertical transformer resonance, 7 hertz the vertical carbody bending resonance, and 9.5 hertz the vertical truck frame resonance. Figure 4.1-7 is the measured vertical acceleration of the carbody over the "A end" truck from track section five. This measured acceleration is dominated by energy at 1.14 hertz, a combination of vertical and pitch carbody resonance. The measured vertical acceleration of the carbody over the "A end" truck on track section four where considerable high frequency input energy was experienced is shown in Figure 4.1-8. This measurement shows considerable energy at 1.07 hertz the

PRESENT METROLINER

TRUCK FRAME LONGITUDINAL ACCELERATION DUE TO PITCH INPUT

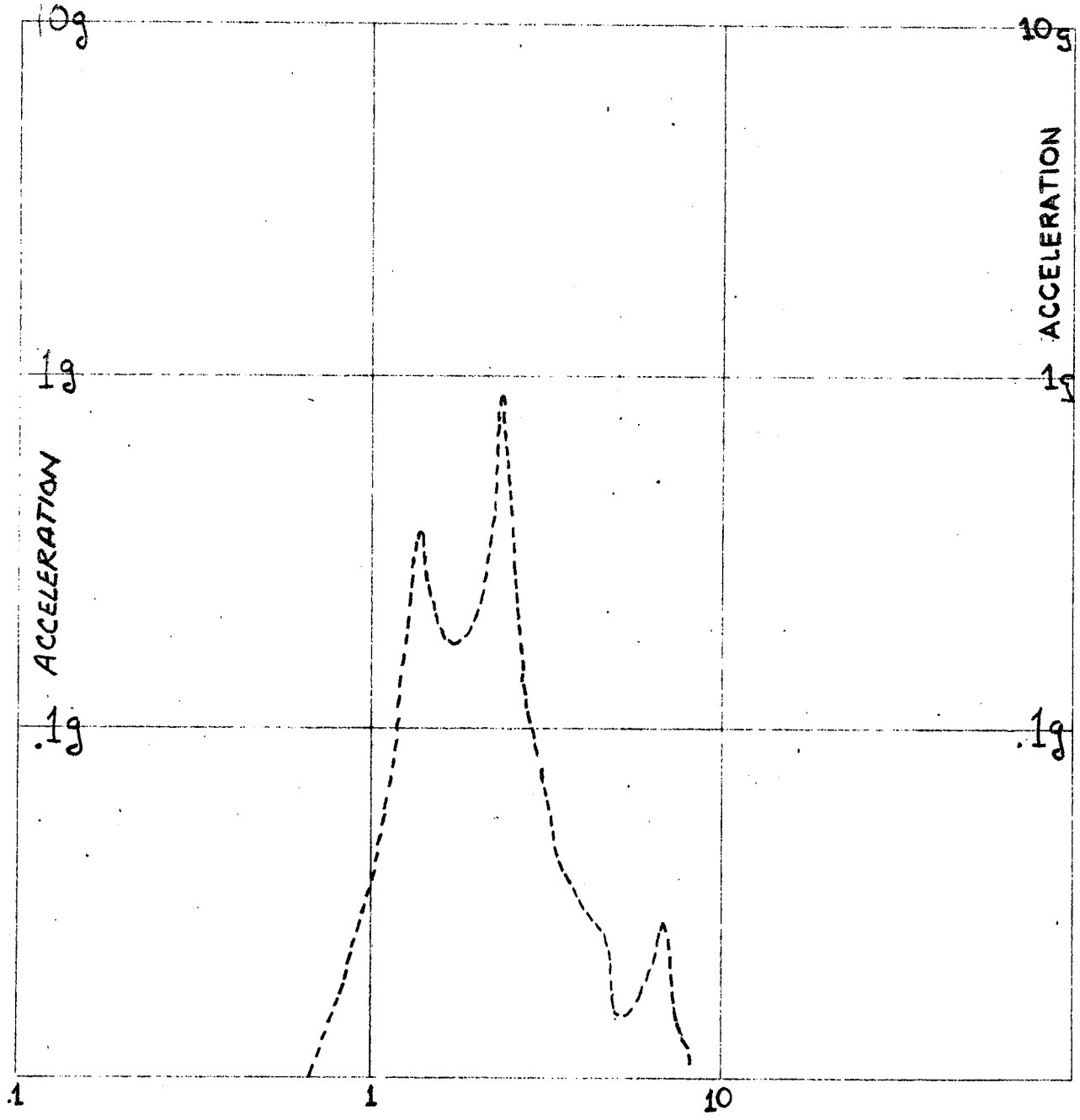

FIGURE 4.1-3

FIGURE 4.1-4

POWER SPECTRAL DENSITY OF RELATIVE AVERAGE LONGITUDINAL ANCHOR ROD FORCES ON "A" END OF CAR

RUN NO. 5

FREQUENCY RESOLUTION = .1 hz

STANDARD DEVIATION = .12 volts

CALIBRATION = pounds/volt

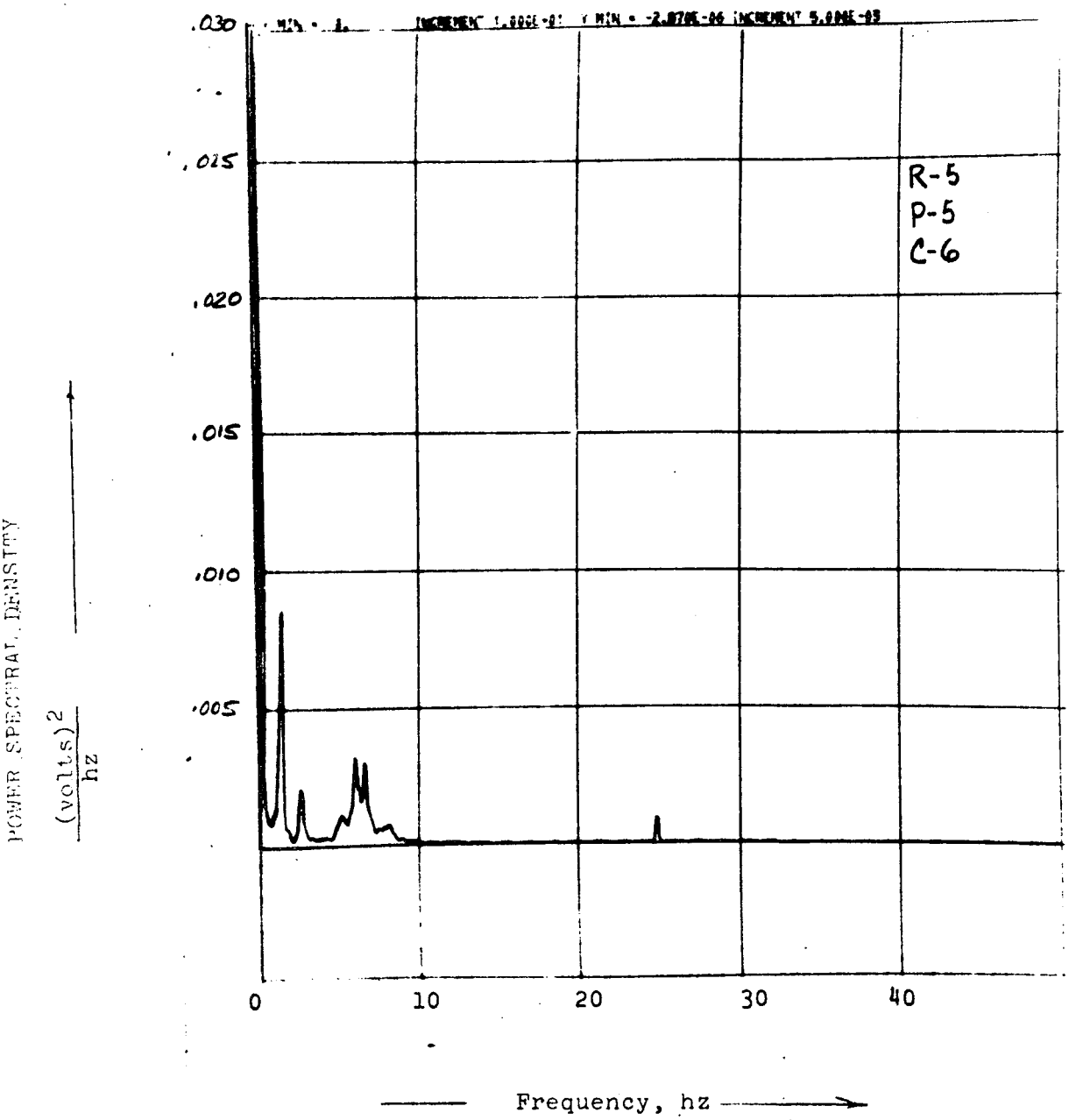

PRESENT METROLINER

CARBODY 'A' END VERTICAL ACCELERATION DUE TO VERTICAL INPUT

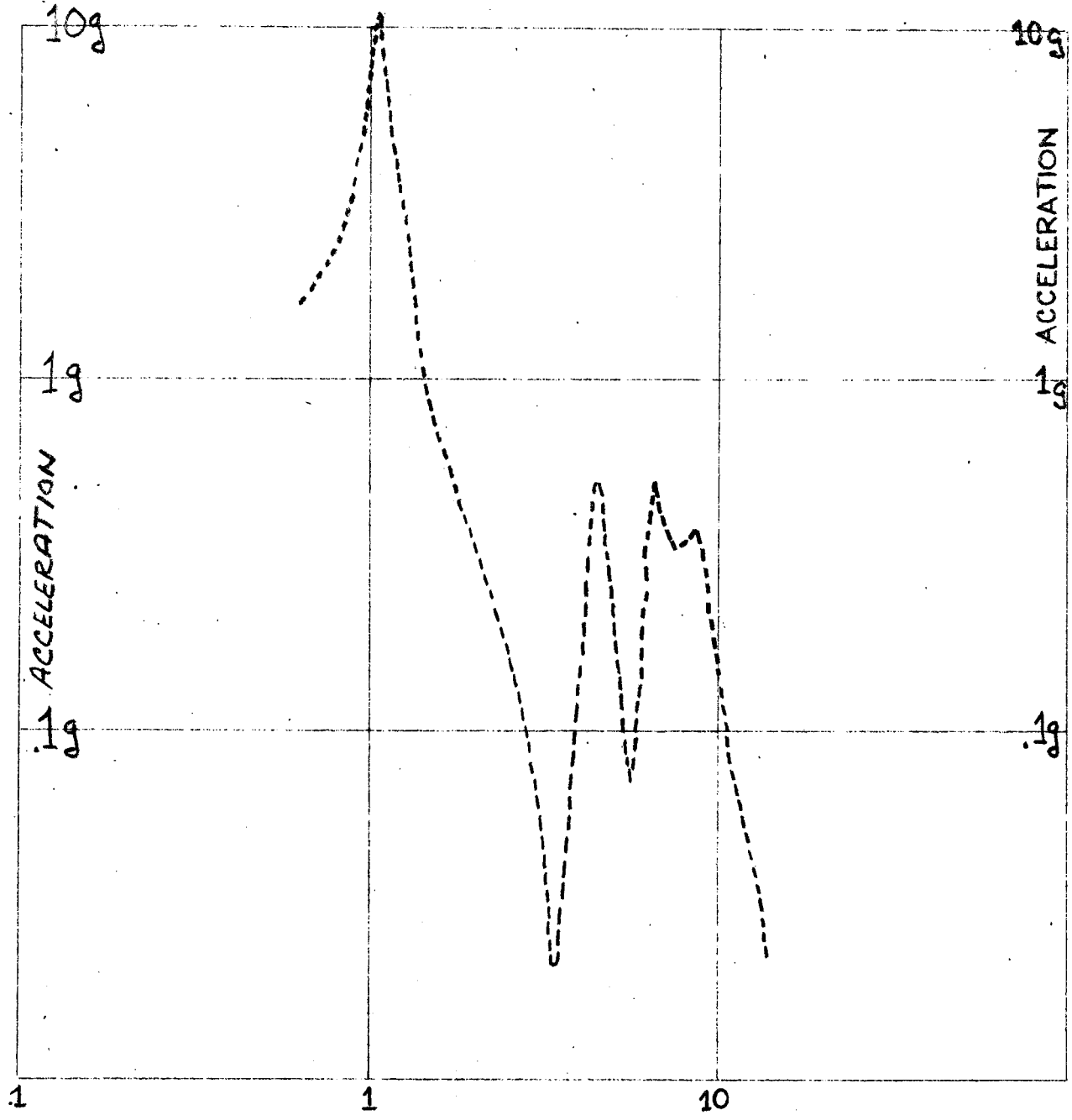

FIGURE 4.1-5

PRESENT METROLINER

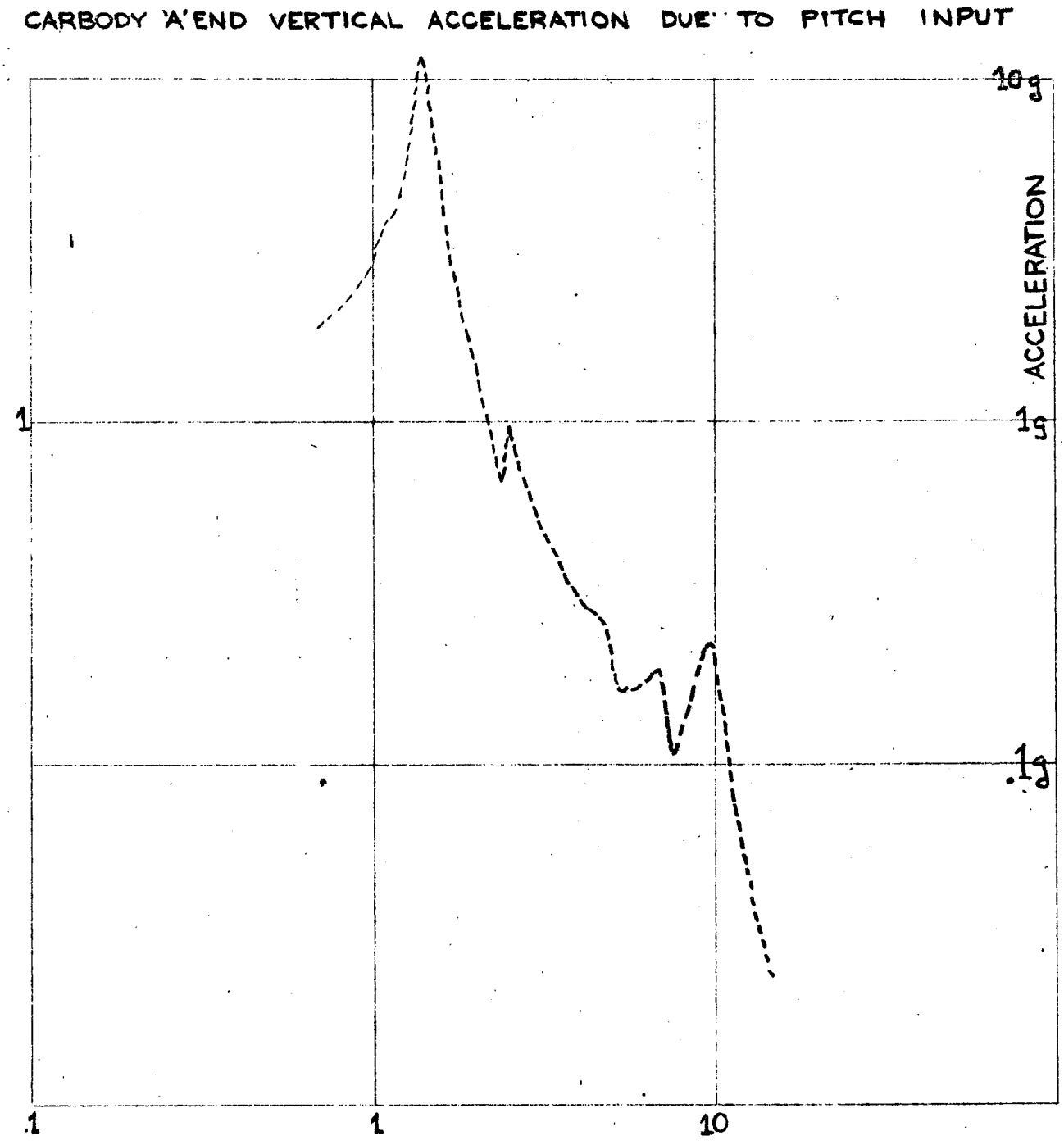

FIGURE 4.1-6

FIGURE 4.1-7

POWER SPECTRAL DENSITY OF VERTICAL ACCELERATION

OF CARBODY FLOOR OVER "A" END LEFT BOLSTER SPRING.

RUN NO. 5

FREQUENCY RESOLUTION = .1 hz

STANDARD DEVIATION = .065 gs

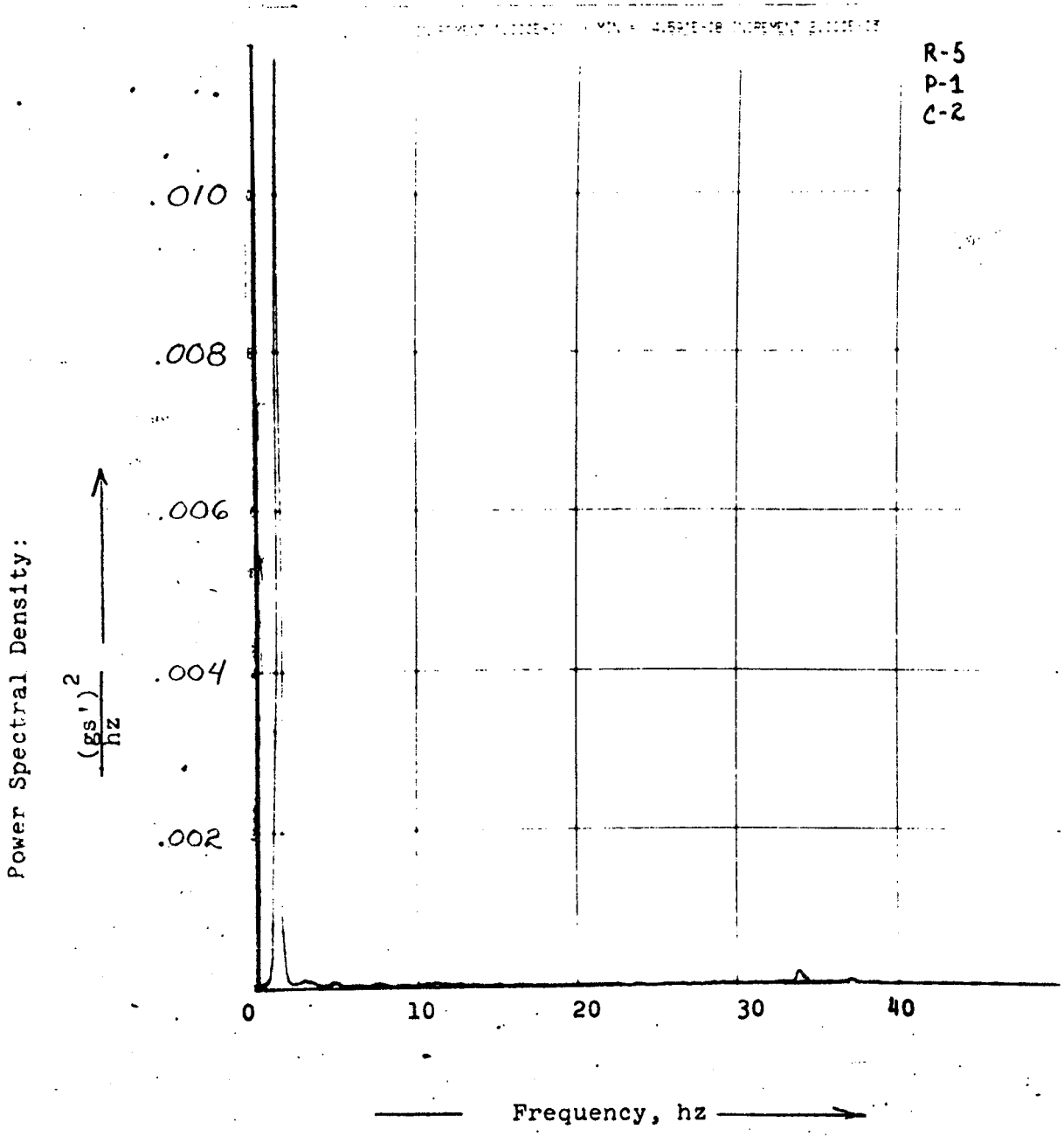

FIGURE 4.1-8

POWER SPECTRAL DENSITY OF VERTICAL ACCELERATION

OF CARBODY FLOOR OVER "A" END RIGHT BOLSTER SPRING

RUN NO. 4

FREQUENCY RESOLUTION = .1 hz

STANDARD DEVIATION = .063 gs

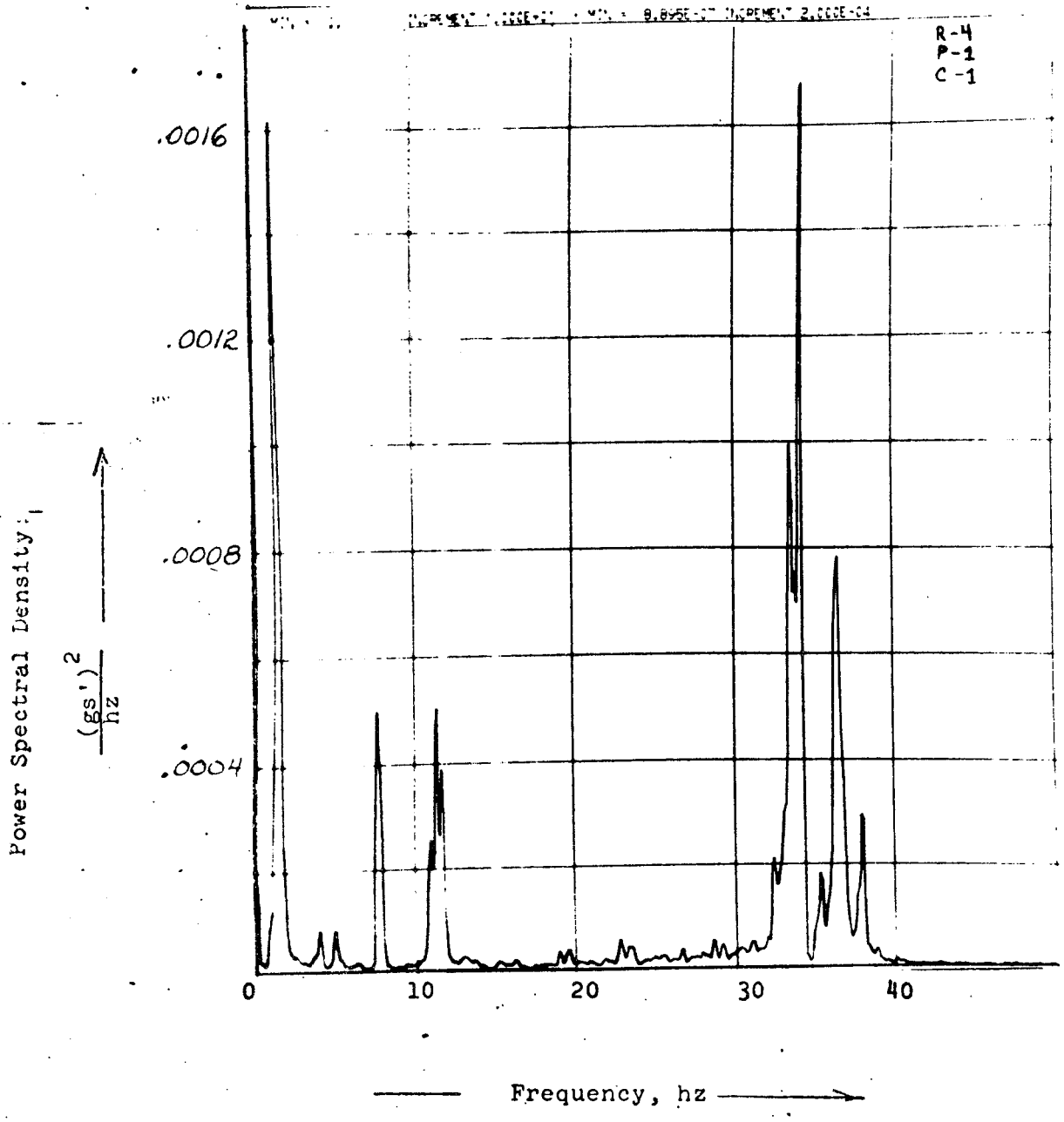

vertical carbody resonance and 4.9 hertz near the vertical transformer resonance. The energy at 3.9 hertz and 7.6 hertz is near the input acceleration peaks and as a result cannot be considered railcar resonances.

Figure 4.1-8 shows significant energy at 34 hertz and 36 hertz. The amount of energy at these frequencies is considerably higher than indicated since all the road test measurements were filtered as shown in Figure 4.1-9. Energy of this frequency was not transmitted from the truck frame (Figure 4.1-10) but is present in the bolster coil spring (Figure 4.1-11). Estimates of the surge frequencies of the two nested coil spring which make up one bolster coil spring set are 34 hertz and 36 hertz. Therefore, a reasonable explanation of this energy is surging of the bolster springs.

The simulated vertical acceleration at the center of the car to a vertical input is shown in Figure 4.1-12. The response is dominated by the carbody vertical rigid body resonance at 1.05 hertz, with a second resonance at 7 hertz, the vertical carbody bending resonance. Figure 4.1-13, the measured vertical acceleration at the center of the carbody in track section five, shows maxima at 1.07 the vertical carbody resonance, 4.6 hertz the vertical transformer resonance, and a split at 6.8 hertz and 7.5 hertz similar to that experienced in the laboratory test, due to the vertical carbody bending resonance and truck longitudinal resonance. In track section four, Figure 4.1-14, the carbody vertical

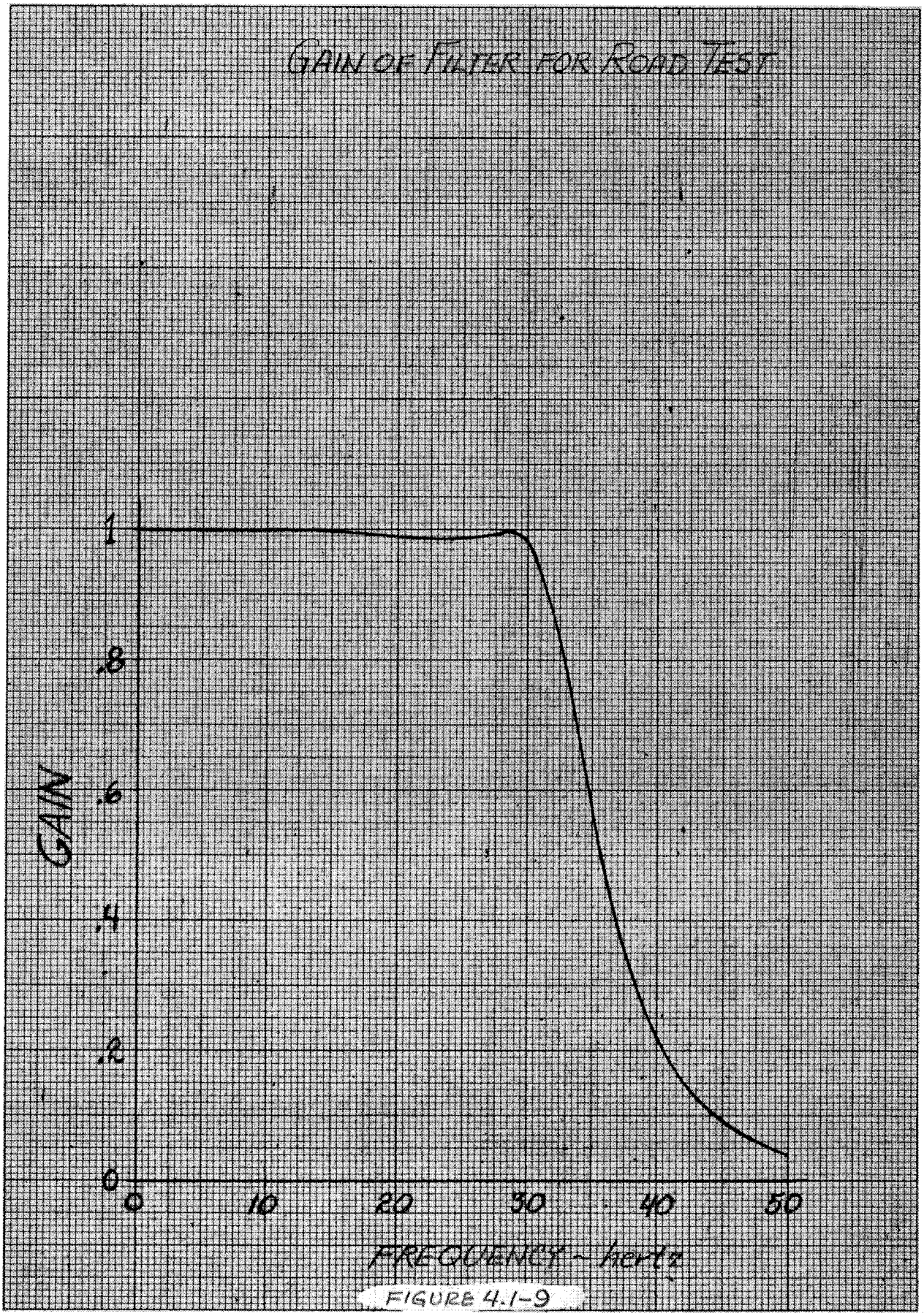
GAIN OF FILTER FOR ROAD TEST
GAIN
1
.8
.6
.4
.2
0
0
10
20
30
40
50
FREQUENCY - hertz

FIGURE 4.1-9

FIGURE 4.1-10

POWER SPECTRAL DENSITY OF VERTICAL ACCELERATION

OF TRUCK BOLSTER ON "A" END TRUCK

RUN NO. 4

FREQUENCY RESOLUTION = .1 hz

STANDARD DEVIATION = .24 gs

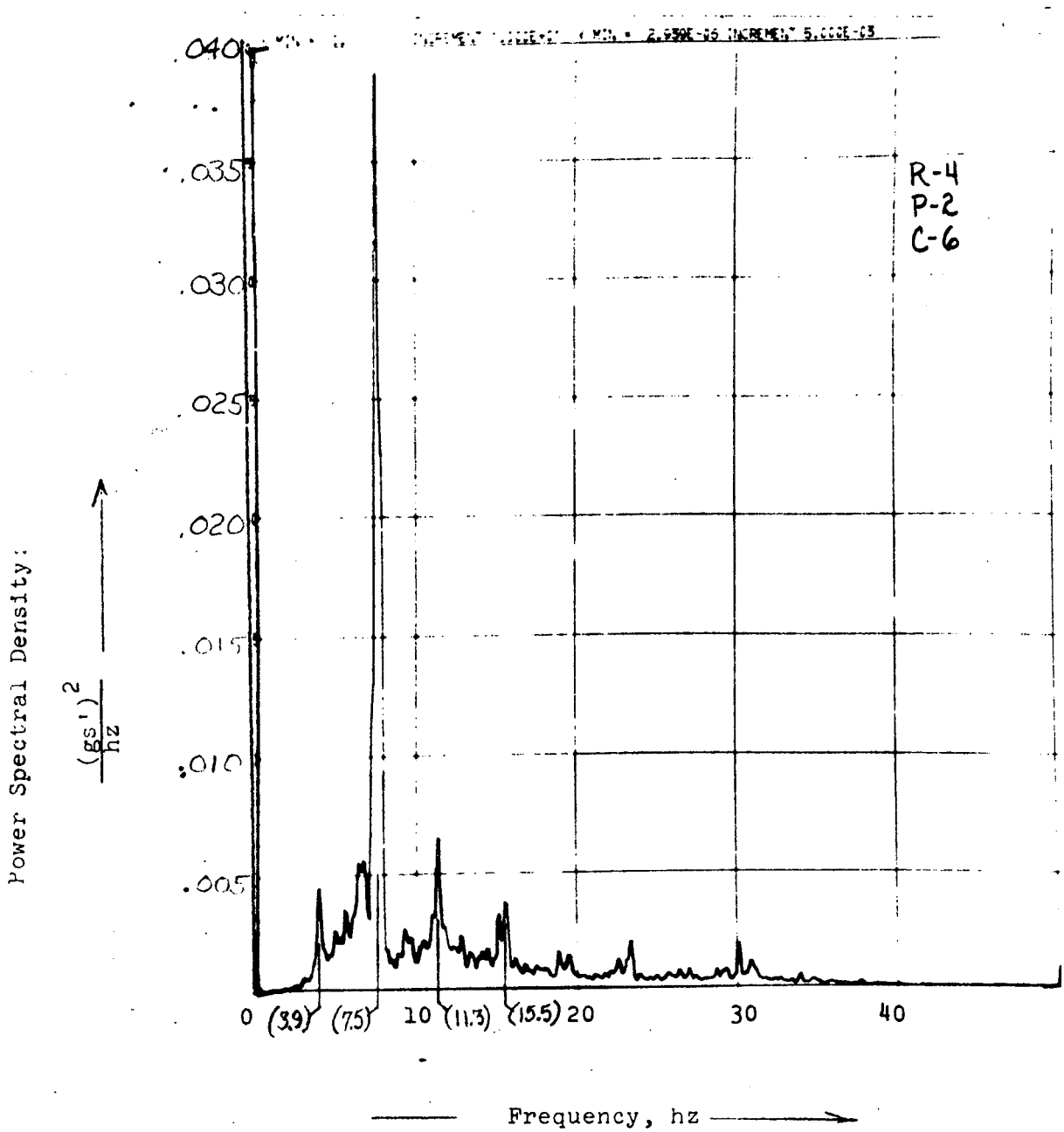

FIGURE 4.1-11

POWER SPECTRAL DENSITY OF RELATIVE VERTICAL FORCE

TRANSMITTED THROUGH BOLSTER SPRING ON "A" END TRUCK RIGHT SIDE

RUN NO. 4

FREQUENCY RESOLUTION = .1 hz

STANDARD DEVIATION = .15 volts

CALIBRATION = pounds/volt

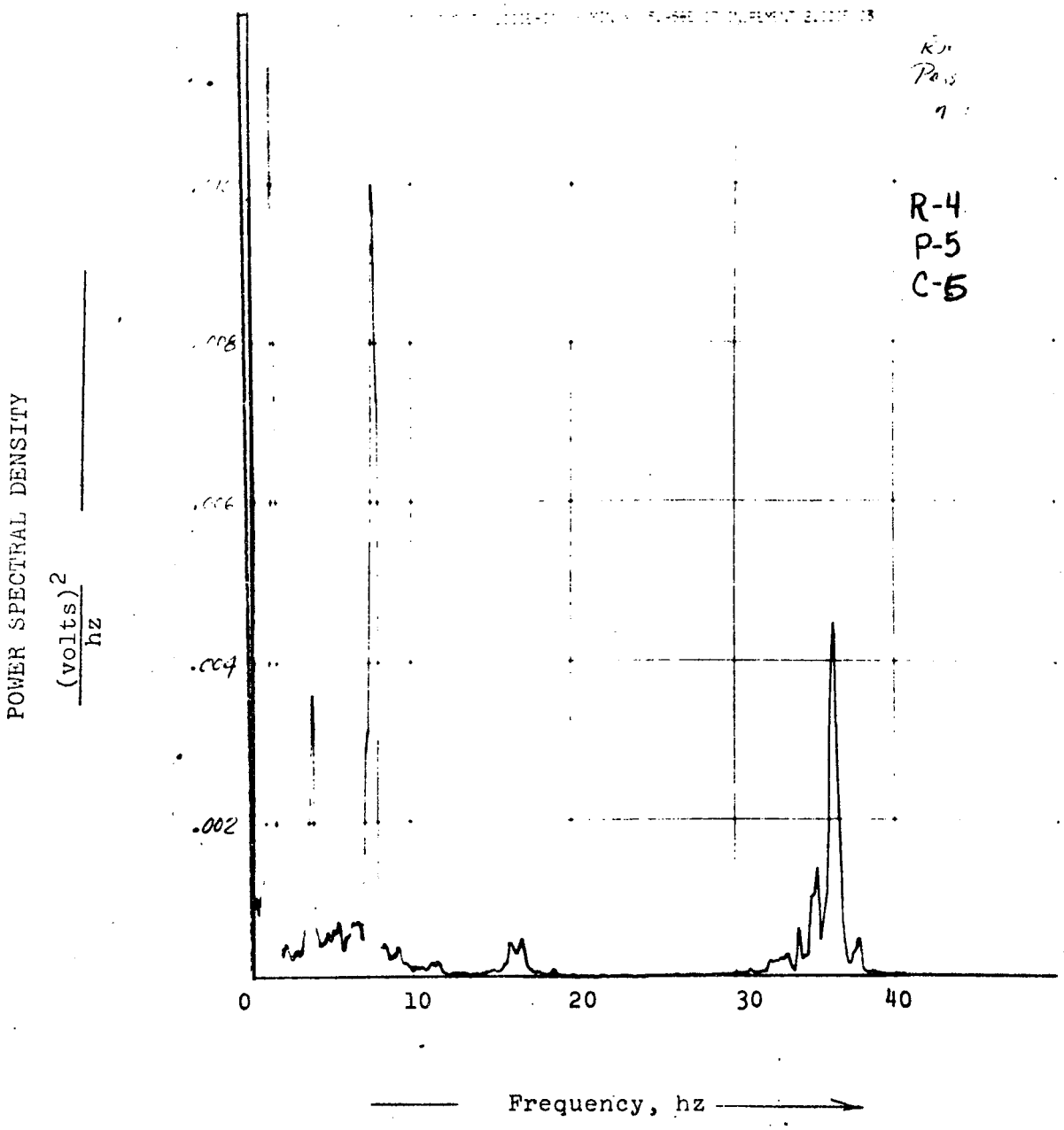

PRESENT METROLINER

CARBODY CENTER VERTICAL ACCELERATION DUE TO VERTICAL INPUT

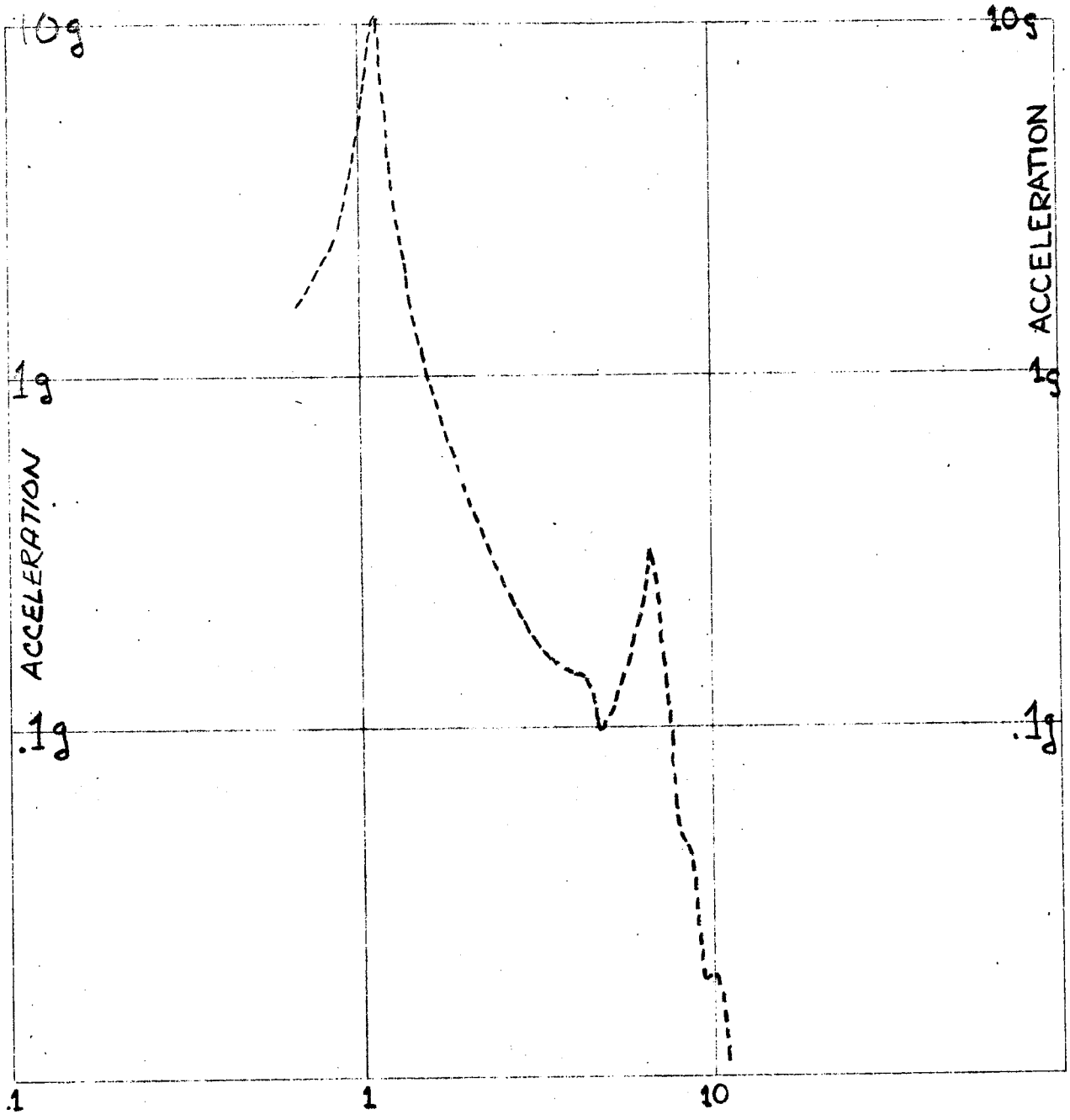

FREQUENCY - HERTZ

FIGURE 4.1-12

FIGURE 4.1-13

POWER SPECTRAL DENSITY OF VERTICAL ACCELERATION

OF THE CARBODY FLOOR AT THE CENTER

RUN NO. 5

FREQUENCY RESOLUTION = .1 hz

STANDARD DEVIATION = .021 gs

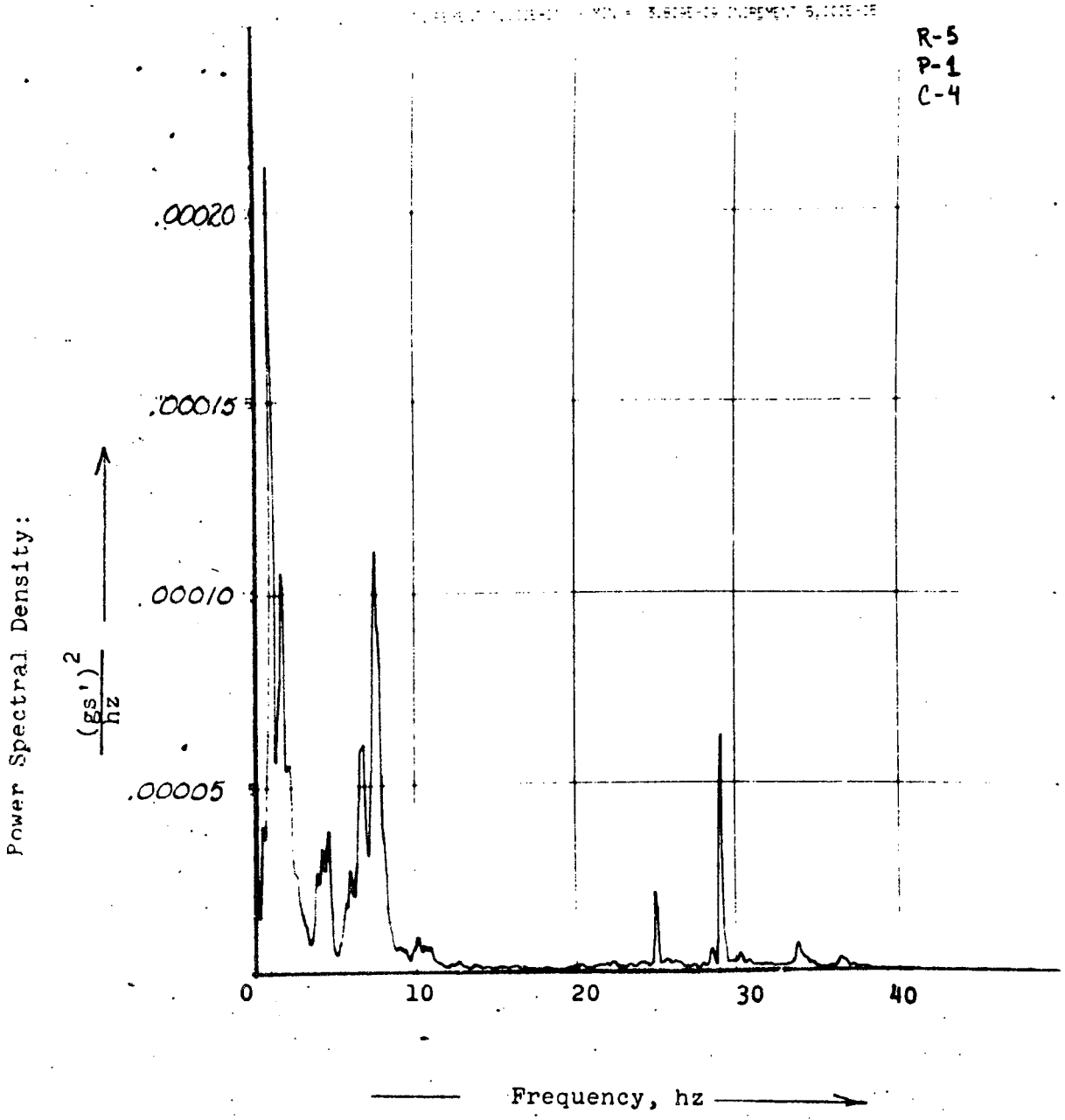

FIGURE 4.1-14

POWER SPECTRAL DENSITY OF VERTICAL ACCELERATION
OF THE CARBODY FLOOR AT THE CENTER

RUN NO. 4

FREQUENCY RESOLUTION = .1 hz

STANDARD DEVIATION = .039 gs

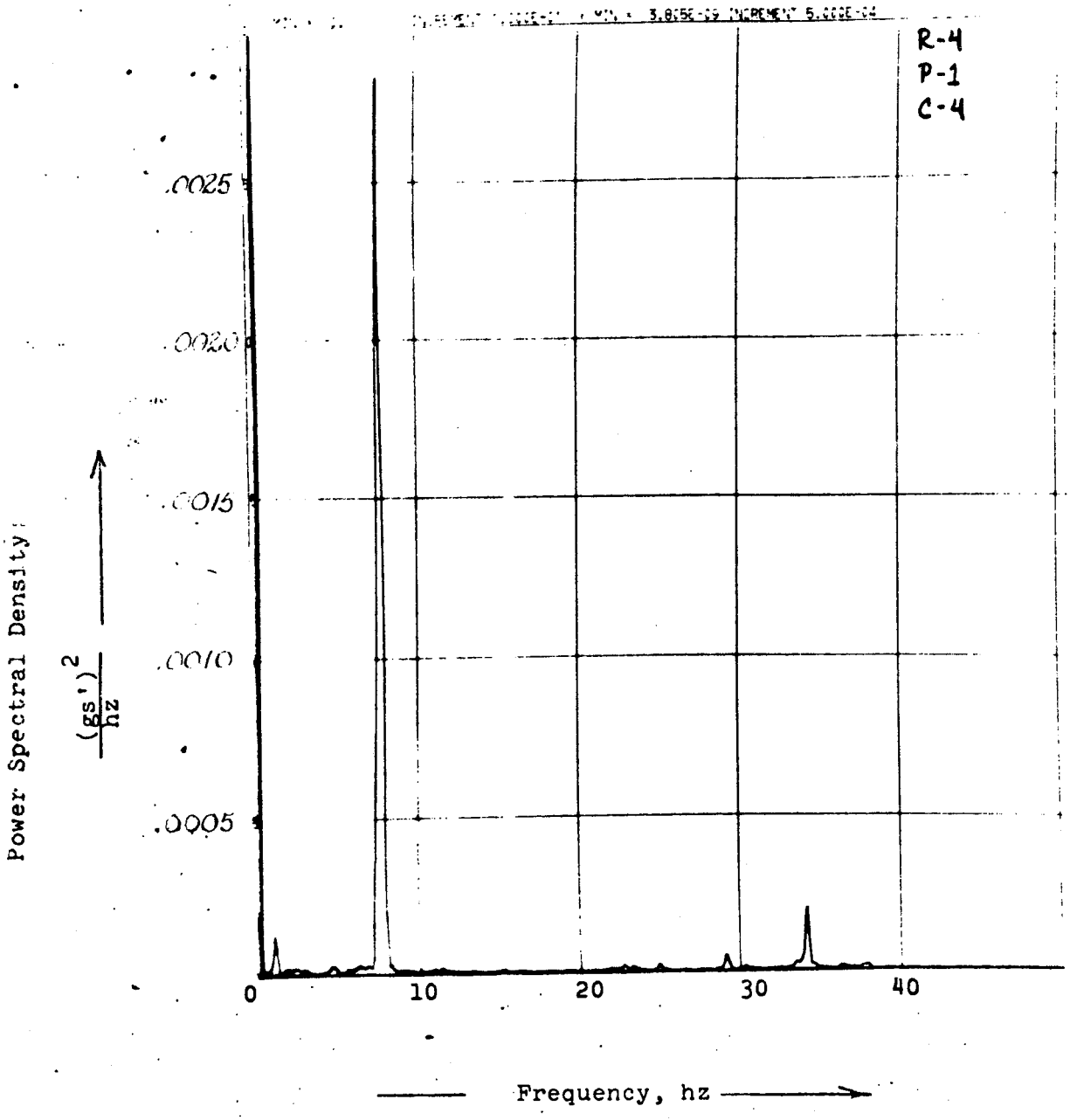

bending resonance dominates, due to the input energy spike near this resonance.

The simulated vertical acceleration of the carbody center to a pitch input, Figure 4.1-15, is considerably less than the response to the vertical input as would be expected.

The simulated longitudinal acceleration of the carbody to pitch input is shown in Figure 4.1-16 with two major resonances, the pitch carbody resonance at 1.32 hertz and the longitudinal carbody resonance on the anchor rods at 2.3 hertz.

The simulated vertical acceleration of the transformer to a vertical input, Figure 4.1-17, is dominated by the carbody vertical resonance at 1.05 hertz and the transformer vertical resonance at 4.6 hertz. The measured vertical acceleration of the transformer in section five, Figure 4.1-18, is dominated by the 4.6 hertz vertical transformer resonance. The simulated vertical transformer acceleration due to pitch, Figure 4.1-19, is considerably lower with basically the same result as the response to vertical input. The simulated longitudinal acceleration of the transformer due to pitch input, Figure 4.1-20, is similar to the carbody longitudinal response to pitch.

4.2 Performance of Lateral Simulation of Present Metroliner

The lateral simulation was tested with lateral, roll, and yaw inputs. Accelerations on the truck frame assembly, the carbody end and center, and the transformer are plotted

PRESENT METROLINER

CARBODY CENTER VERTICAL ACCELERATION DUE TO PITCH INPUT

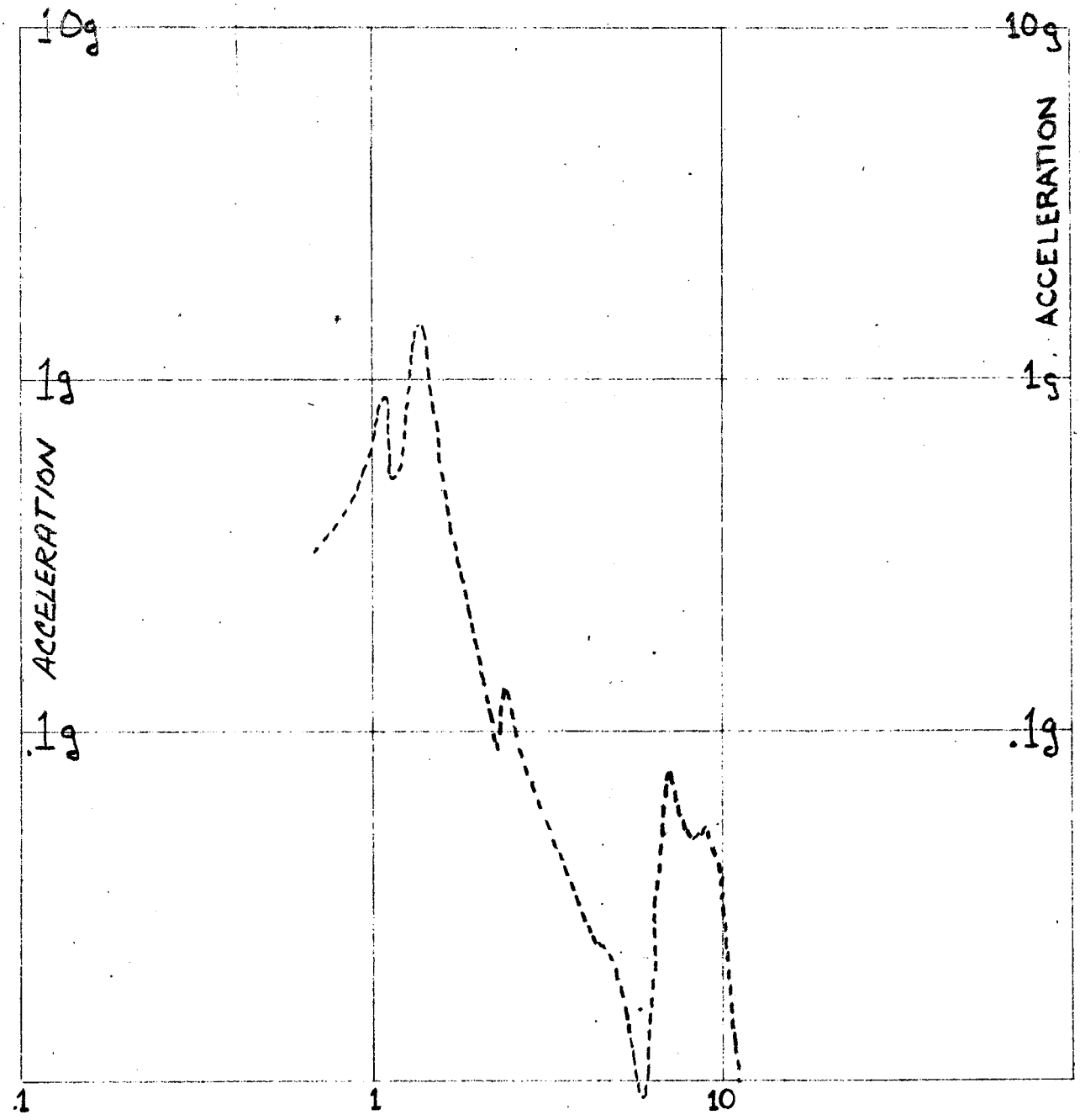

FREQUENCY - HERTZ

FIGURE 4.1-15

PRESENT METROLINER

CARBODY LONGITUDINAL ACCELERATION DUE TO PITCH INPUT

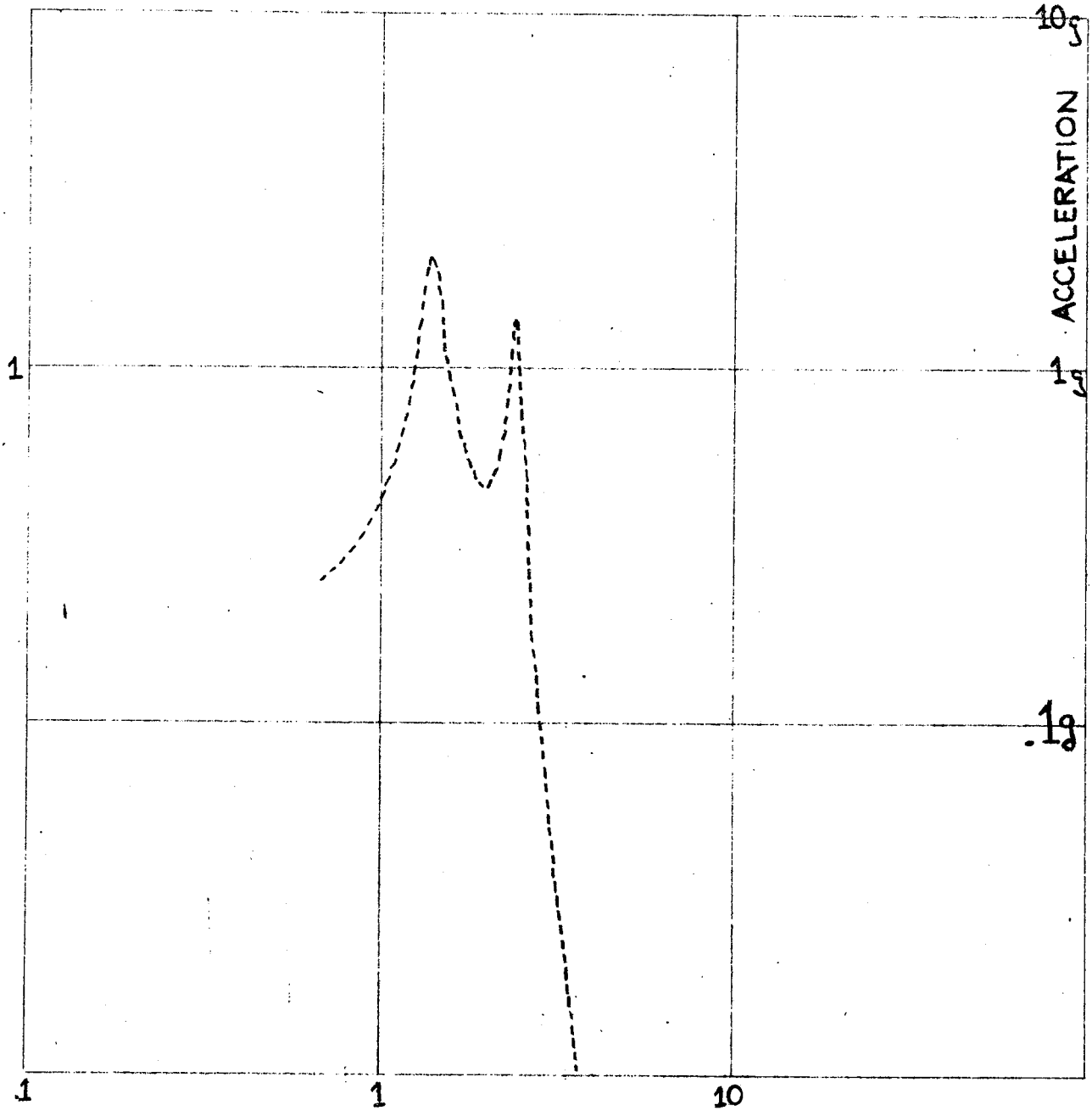

FREQUENCY - HERTZ

FIGURE 4.1-16

PRESENT METROLINER

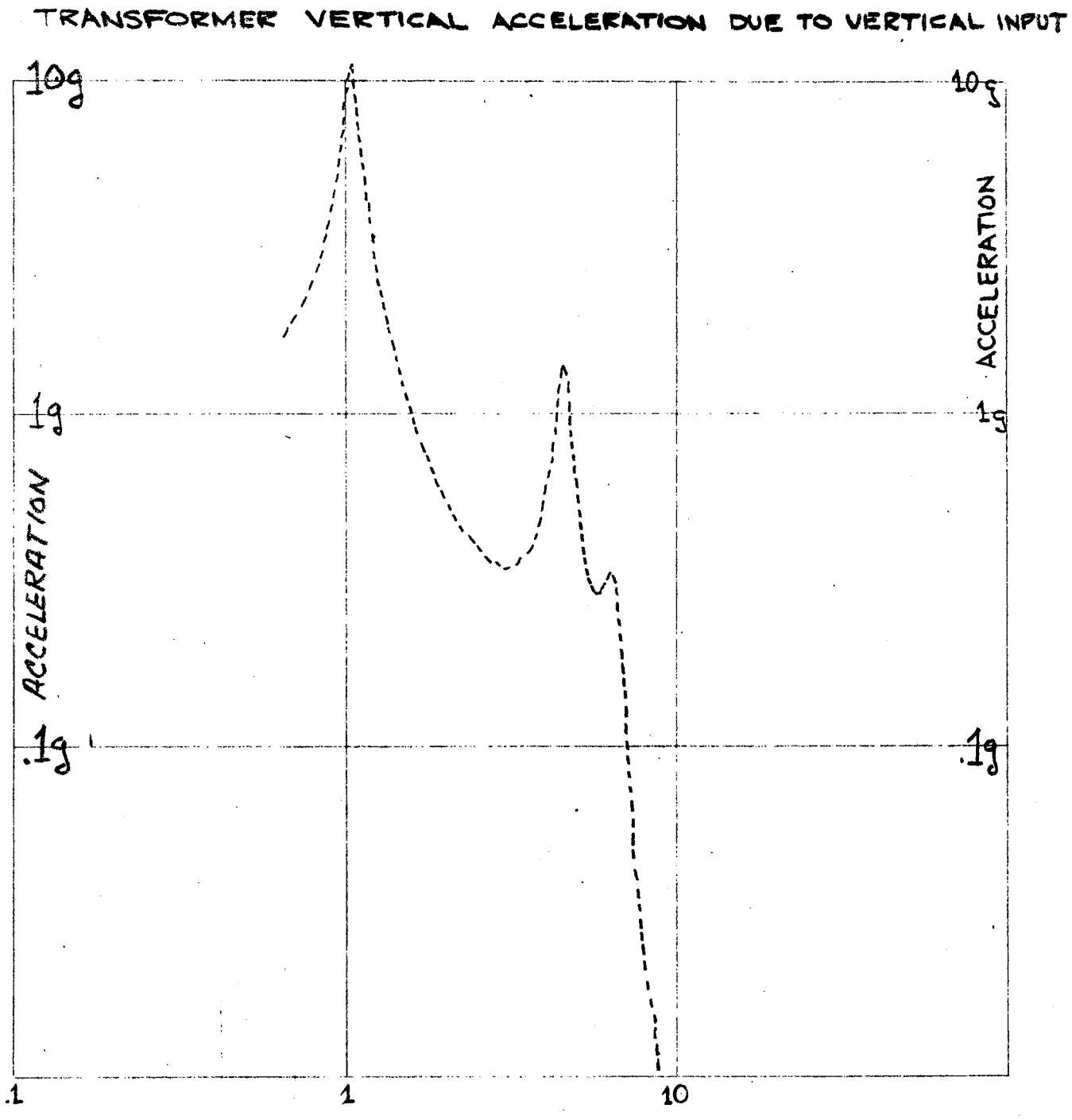

FIGURE 4.1-17

FIGURE 4.1-18

POWER SPECTRAL DENSITY OF VERTICAL ACCELERATION

OF POWER TRANSFORMER MOUNTED TO CARBODY NEAR CENTER

RUN NO. 5

FREQUENCY RESOLUTION = .1 hz

STANDARD DEVIATION = .043 gs.

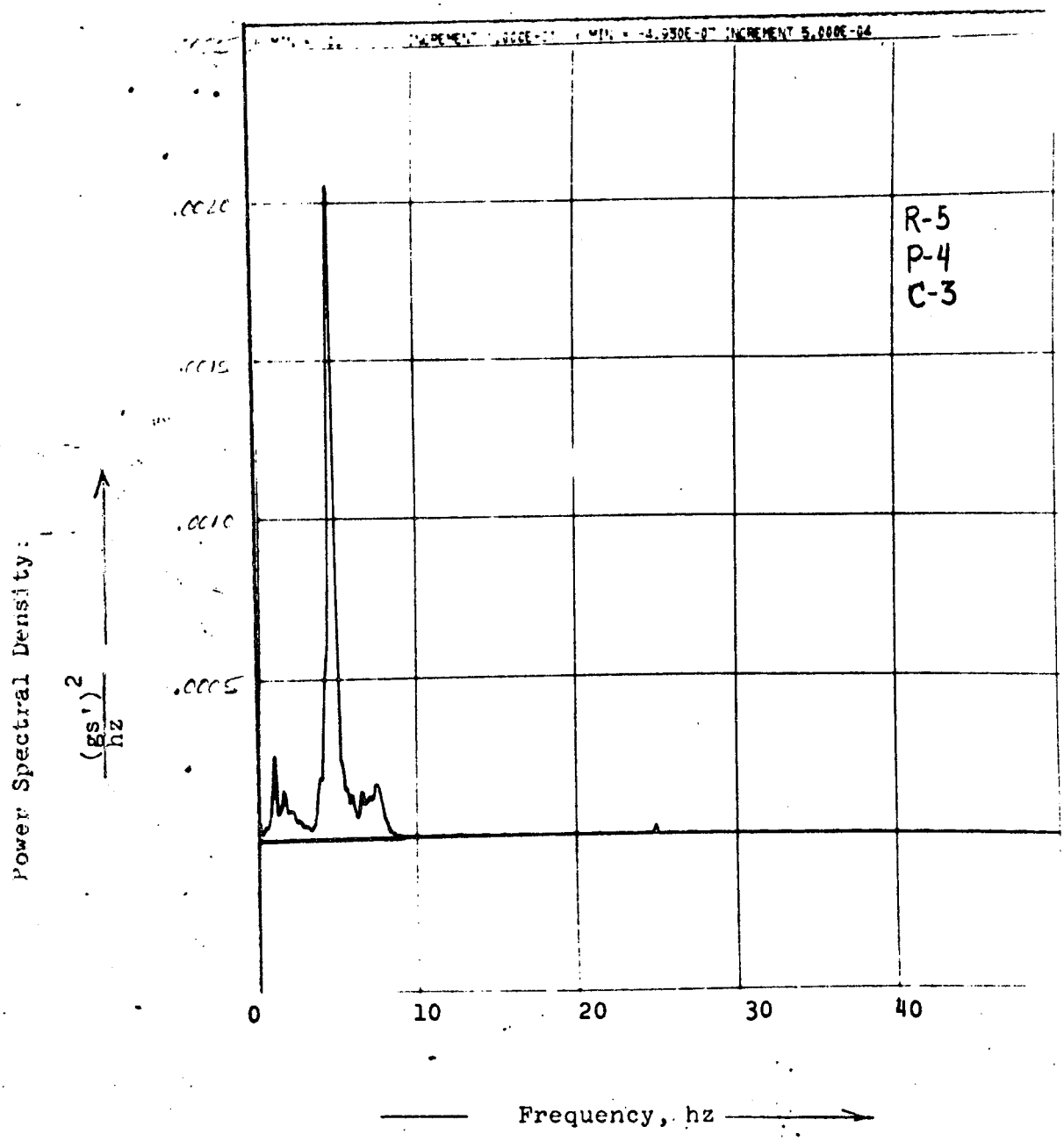

PRESENT METROLINER

TRANSFORMER VERTICAL ACCELERATION DUE TO PITCH INPUT

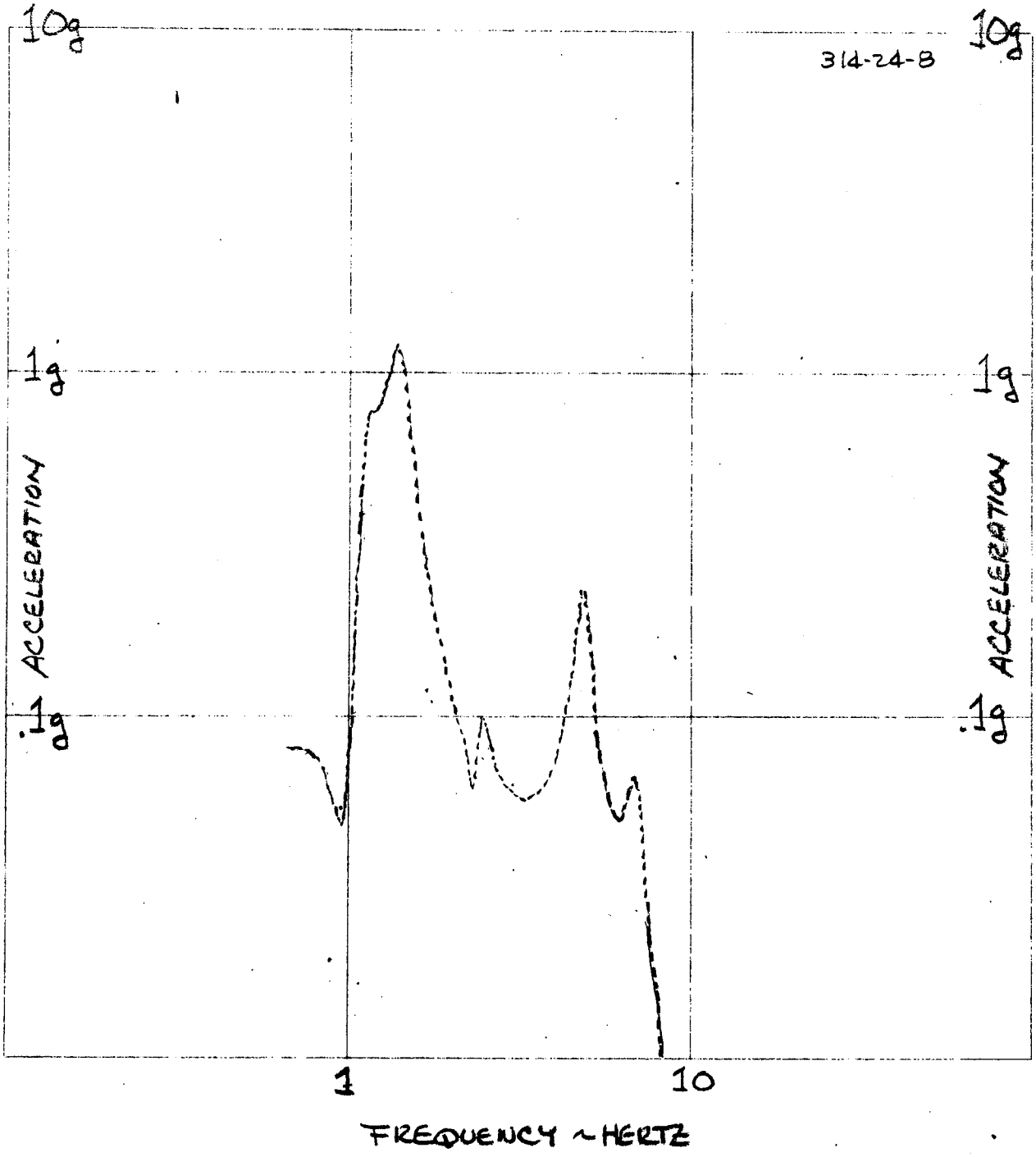

FIGURE 4.1 - 19

PRESENT METROLINER

TRANSFORMER LONGITUDINAL ACCELERATION DUE TO PITCH INPUT

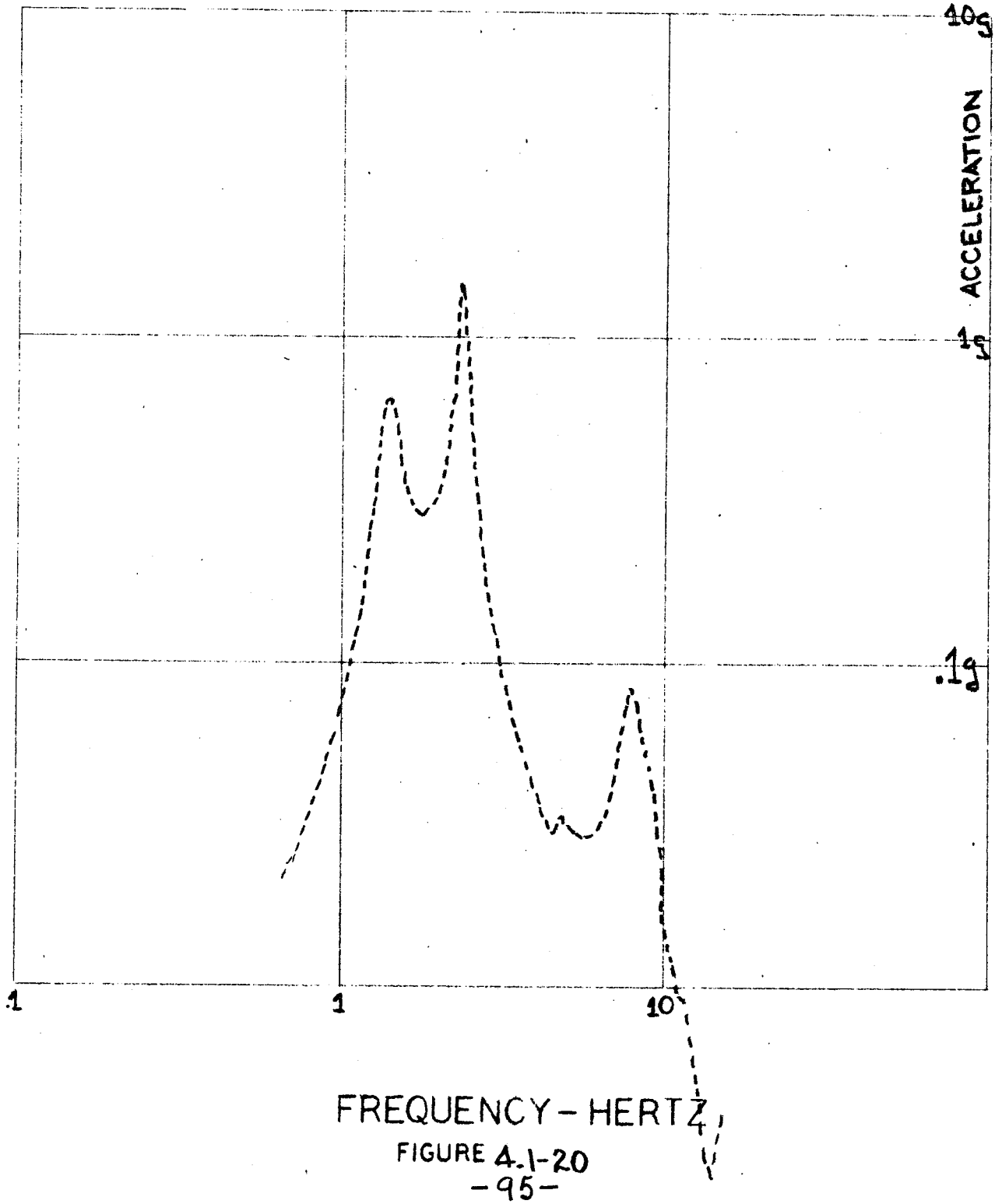

FIGURE 4.1-20

as a function of frequency with input acceleration level constant.

Figure 4.2-1 is the simulated lateral acceleration of the truck frame assembly to a lateral input. The result indicates appreciable magnification of the lateral inputs between 3.5 hertz and 8 hertz with isolation of lateral inputs above 9 hertz. The simulated lateral acceleration due to roll and yaw inputs, Figures 4.2-2 and 4.2-3, indicate the same result as the response to vertical input.

Figure 4.3-4 shows the simulated roll acceleration of the truck frame to a roll input. The roll resonance occurs at 13.0 hertz. The simulated truck frame roll acceleration due to lateral and yaw inputs, Figures 4.3-5 and 4.3-6, is dominated by a 7 hertz resonance as yet unexplained and 12.5 hertz the roll resonance.

The simulated lateral acceleration of the "A" end of the carbody to a lateral input, Figure 4.2-7, indicates resonances at .64 hertz and 1.2 hertz, the carbody lateral-roll modes; 3.6 hertz and 6 hertz, the transformer lateral-roll modes, and 8 hertz, the carbody lateral bending resonance. The lateral measured inputs for all sections of track, with the exception of track section one, contain high lateral inputs in the 3 to 4 hertz range due to the dominate 39 foot wave length lateral input discussed in section 3.4. Figure 4.2-8, the measured lateral acceleration of the "A" end carbody floor in track section one, shows the lower lateral

PRESENT METROLINER

TRUCK FRAME LATERAL ACCELERATION DUE TO LATERAL INPUT

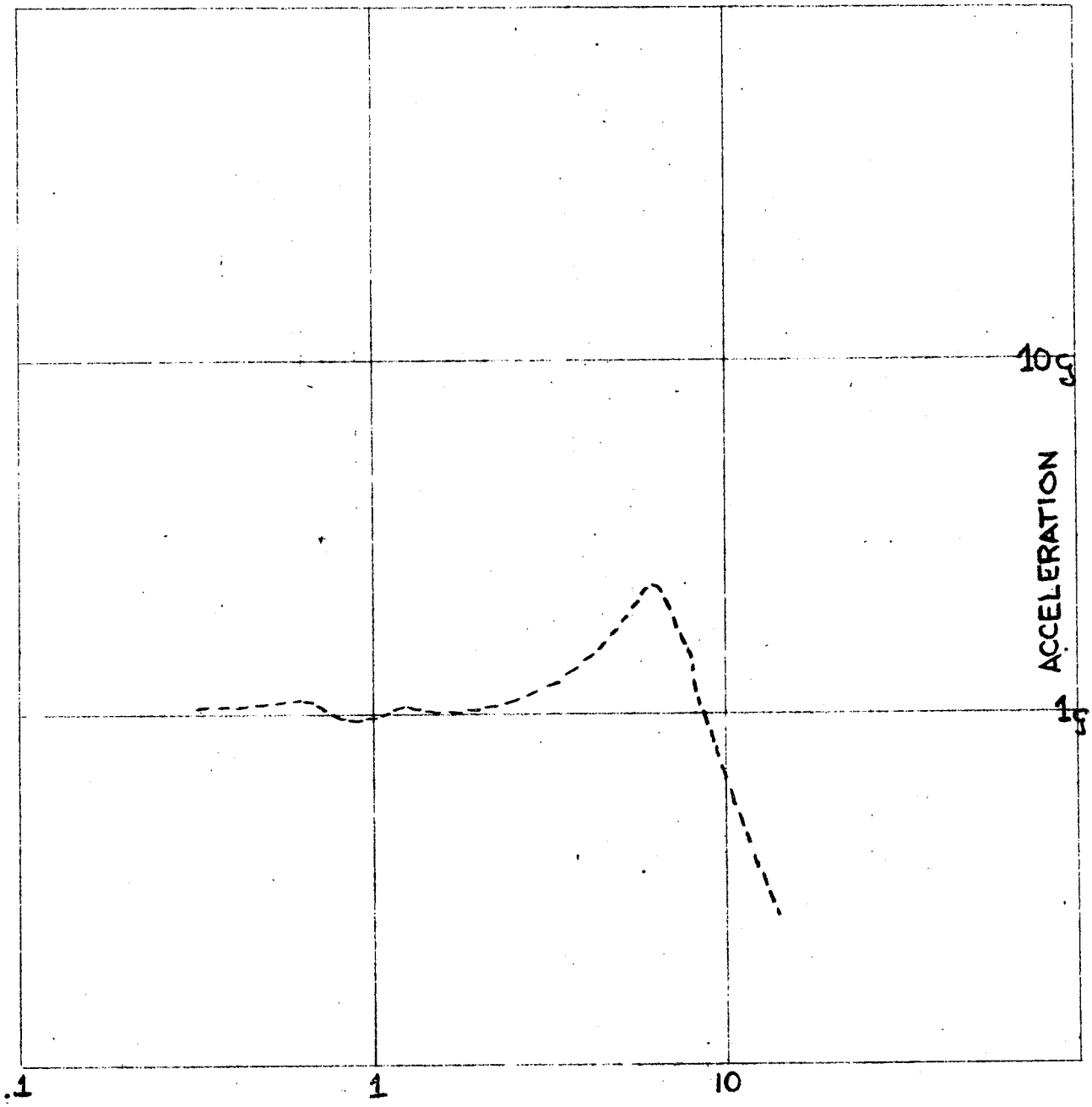

FREQUENCY - HERTZ

FIGURE 4.2-1

PRESENT METROLINER

TRUCK FRAME LATERAL ACCELERATION DUE TO ROLL INPUT

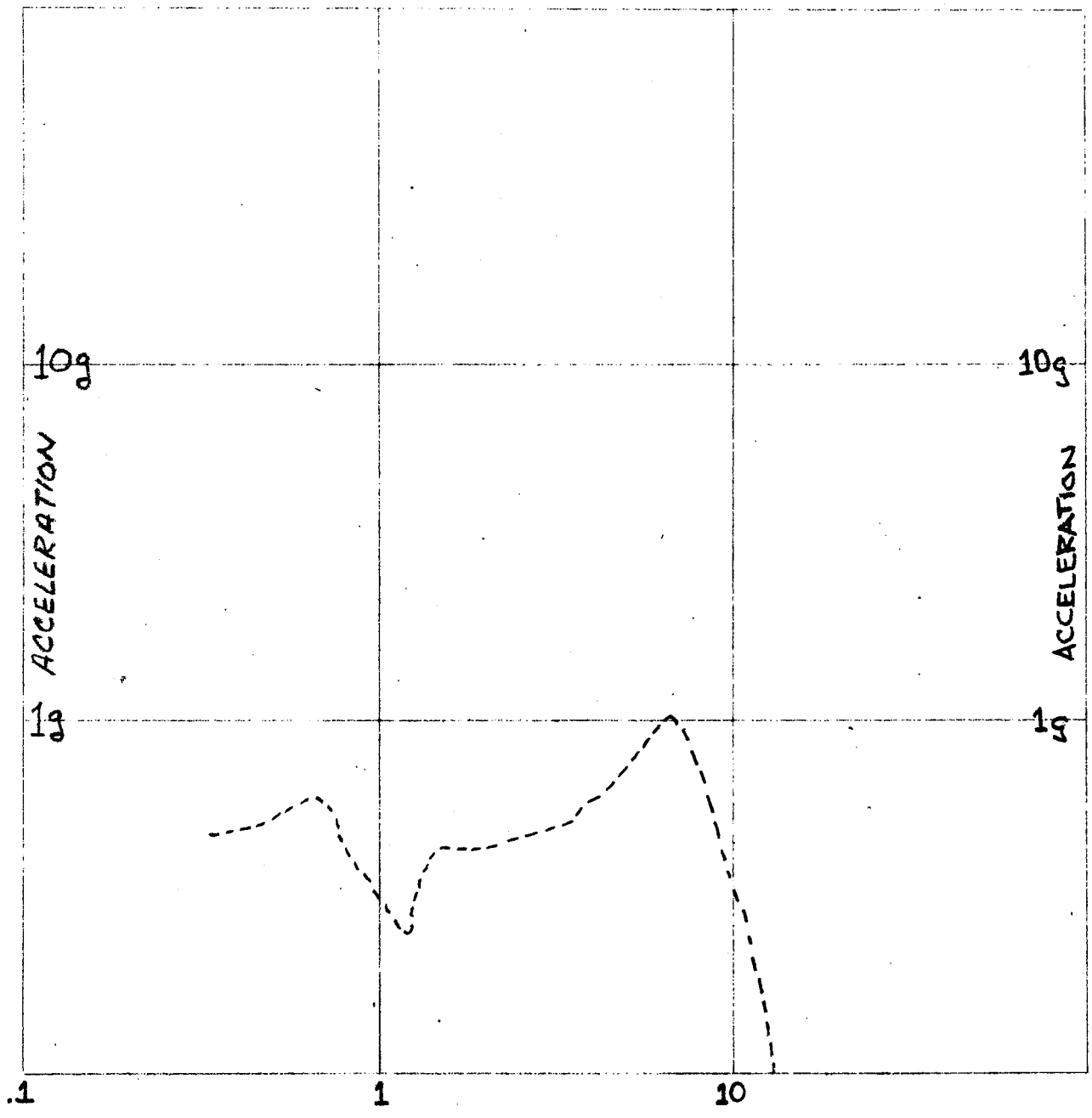

FIGURE 4.2-2

PRESENT METROLINER

TRUCK FRAME LATERAL ACCELERATION DUE TO YAW INPUT

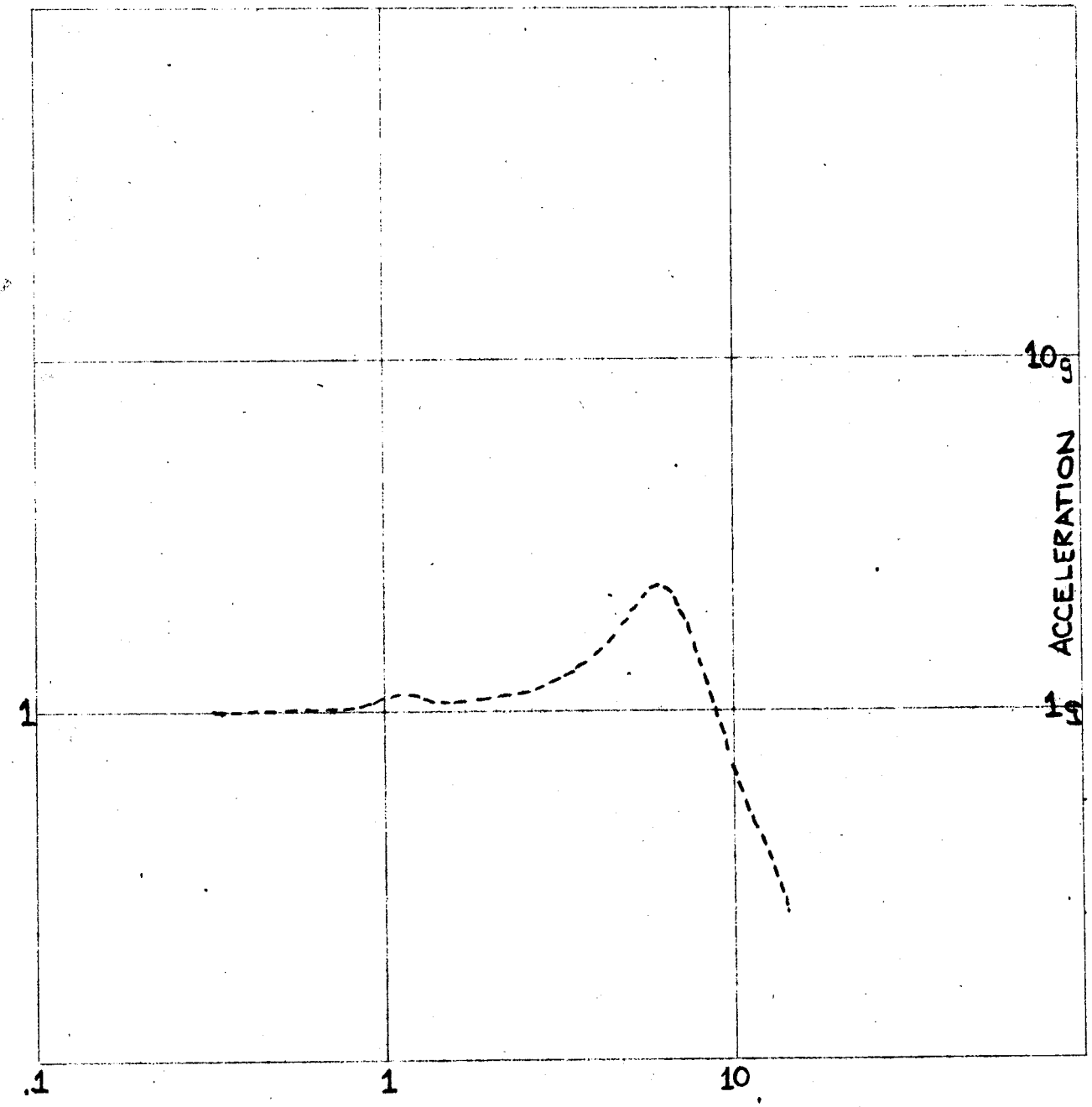

FREQUENCY – HERTZ

FIGURE 4.2-3

PRESENT METROLINER

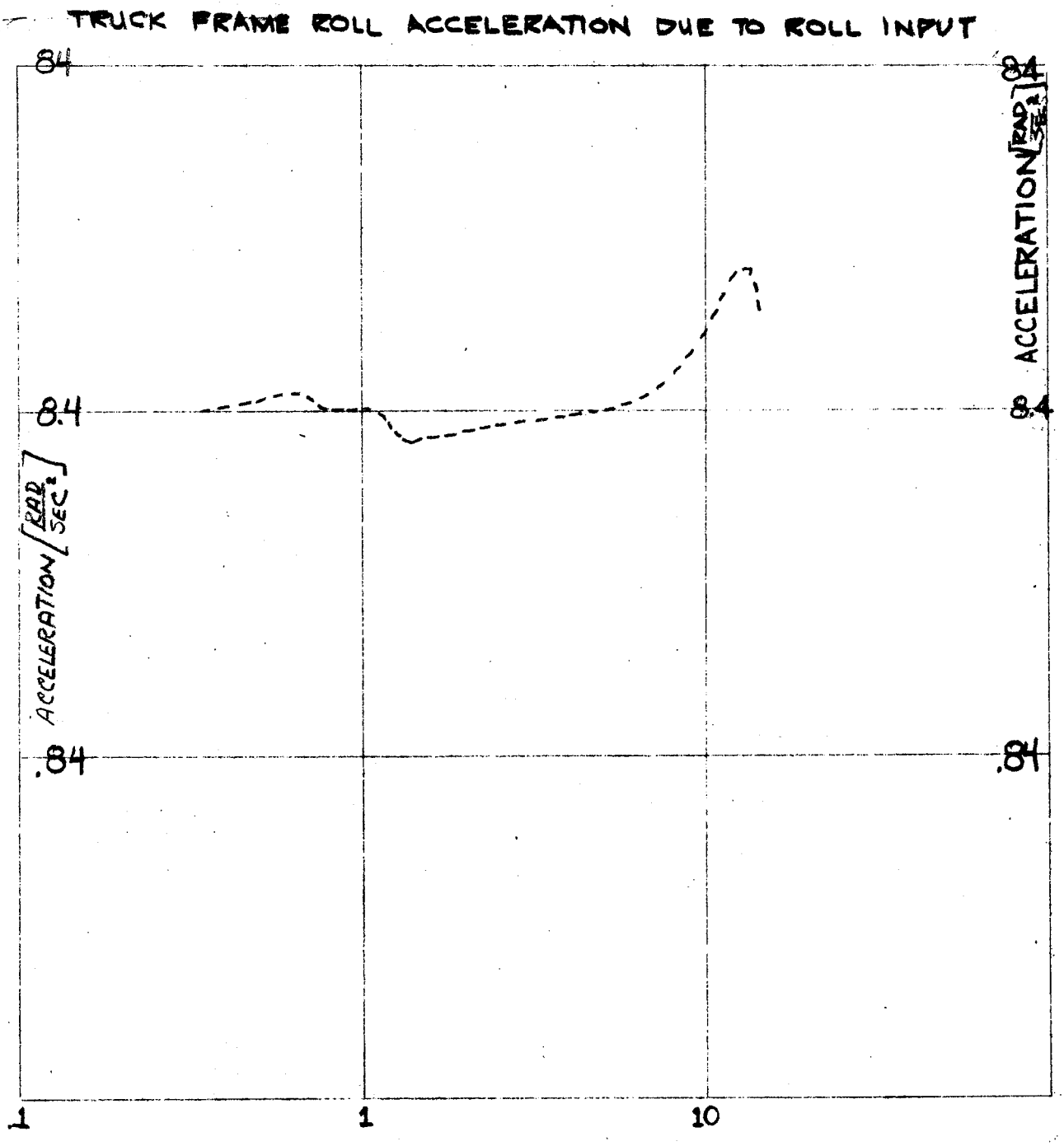

FIGURE 4.2-4

PRESENT METROLINER

TRUCK FRAME- ROLL ACCELERATION DUE TO LATERAL INPUT

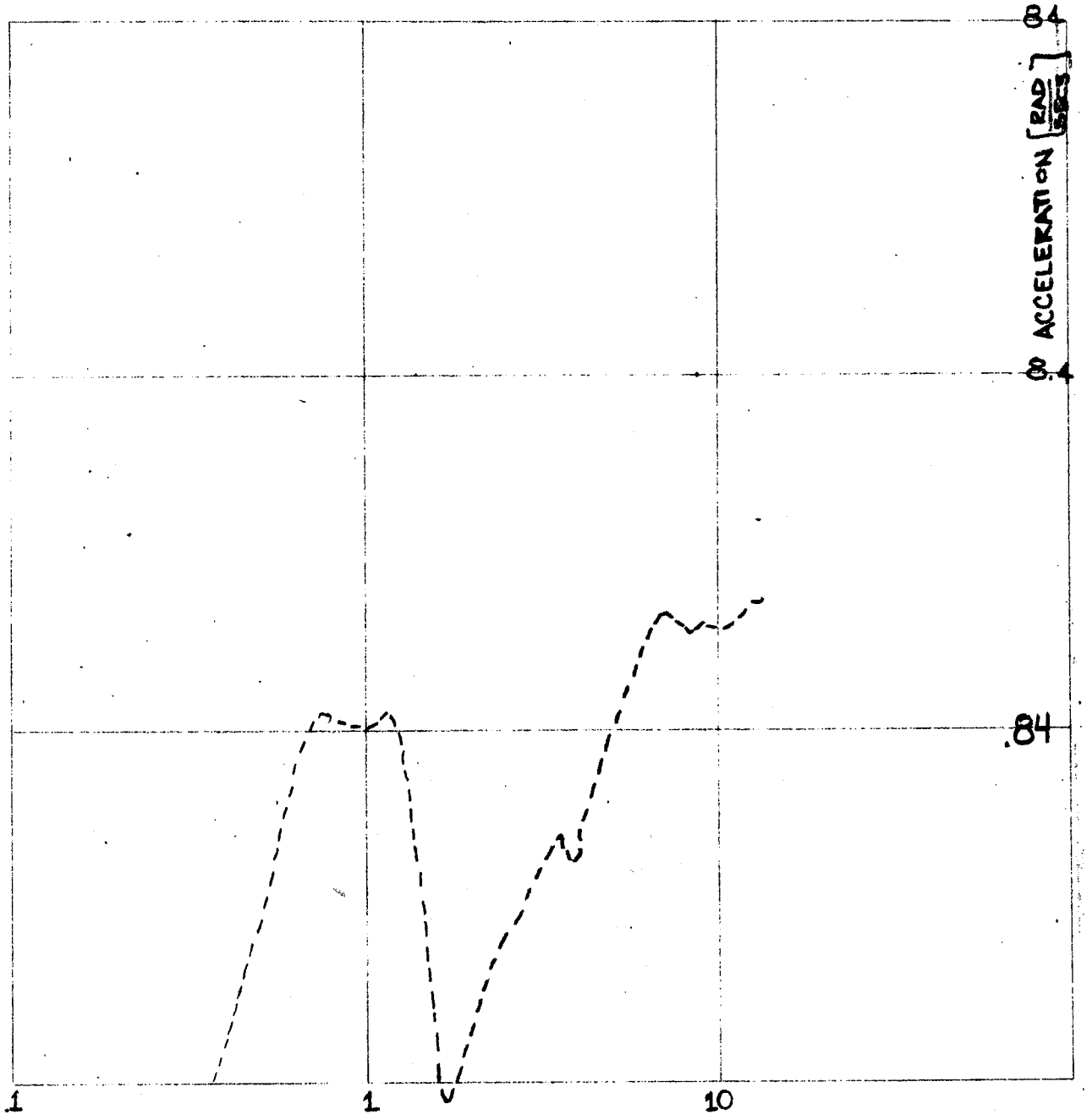

FREQUENCY - HERTZ

FIGURE 4.2-5

PRESENT, METROLINER

TRUCK FRAME ROLL ACCELERATION DUE TO YAW INPUT

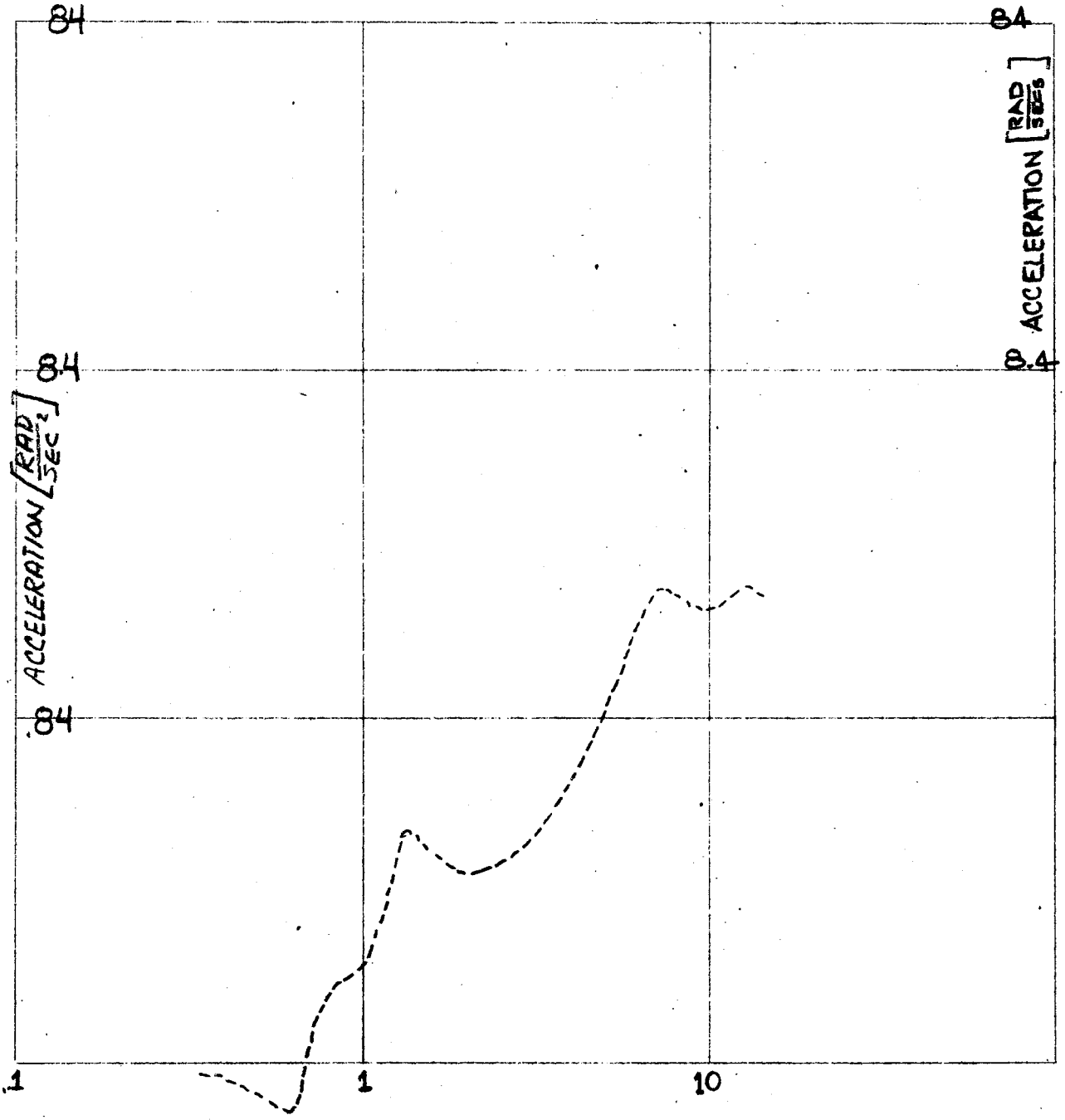

FREQUENCY – HERTZ

FIGURE 4.2-6

PRESENT METROLINER

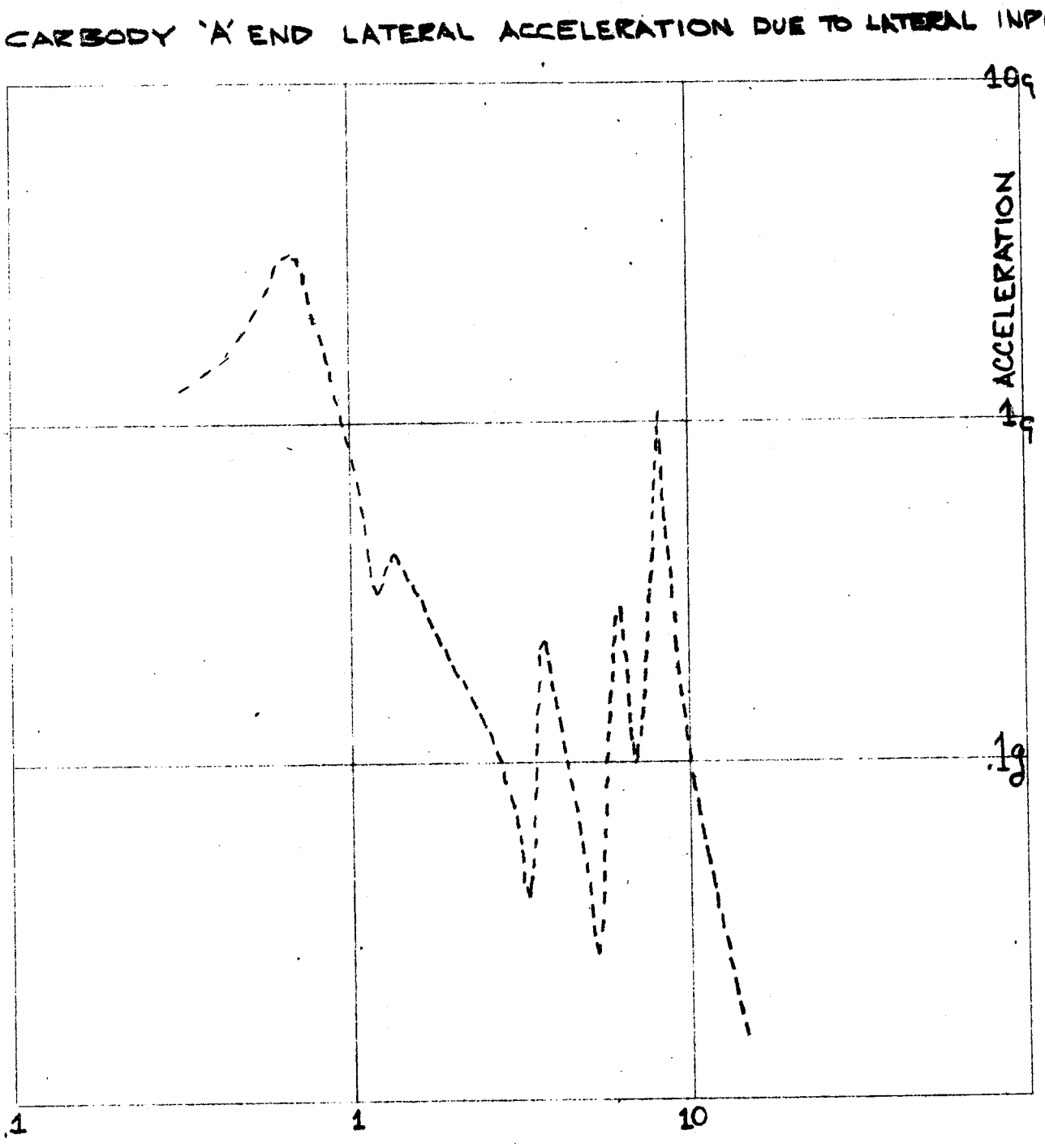

FIGURE 4.2-7

FIGURE 4.2-8

POWER SPECTRAL DENSITY OF LATERAL ACCELERATION
OF CARBODY FLOOR OVER "A" END RIGHT BOLSTER SPRING

RUN NO. 1

FREQUENCY RESOLUTION = .1 hz

STANDARD DEVIATION = .037 gs

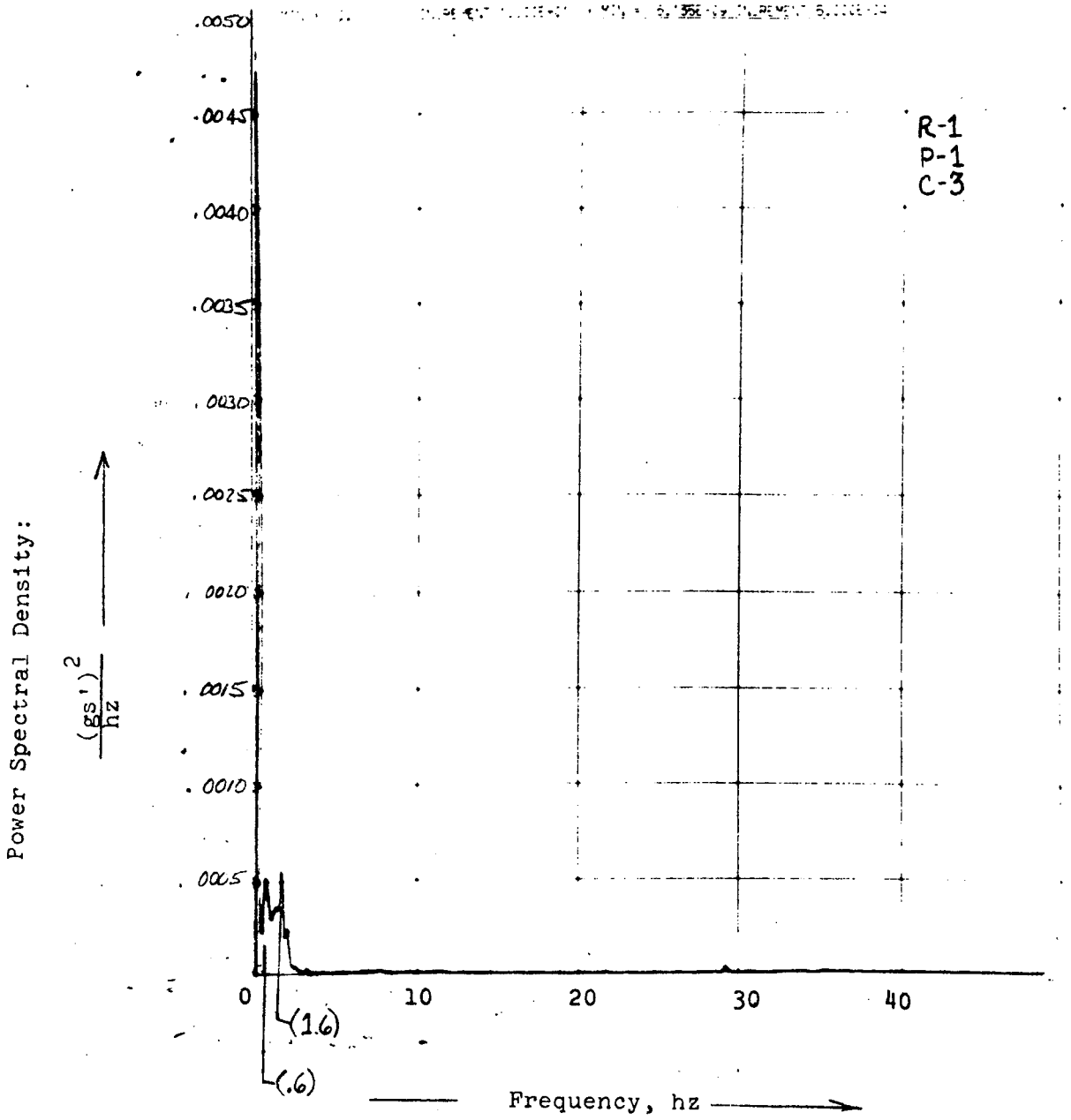

mode at .6 and the forced maximum of the 39 foot rail disturbance at 1.6 hertz.

The simulated lateral acceleration of the "A end" of the carbody to a roll input, Figure 4.2-9, is essentially the same as the response due to the lateral input.

The simulated lateral acceleration of the "A end" of the carbody to a yaw input, Figure 4.2-10, does not show a strong influence of the carbody bending resonance, as experienced in the two previous cases.

In the center of the carbody, the simulated lateral acceleration to a lateral input, Figure 4.2-11, is dominated by the lateral-roll carbody resonances at .65 and 1.25 hertz and the carbody lateral bending resonance at 8.4 hertz. Figure 4.2-12, the measured lateral acceleration at the center of the car on track section five, shows resonances at 3.8, 6.8 and 8.9 hertz which correspond to the 39 foot wave length dominate track input, the upper lateral-roll transformer mode and the carbody lateral bending mode. It is interesting to note that the lateral carbody bending resonance did not appear as a major response in the measurements made on the six track sections. The simulated lateral acceleration of the carbody center to roll and yaw inputs are shown in Figures 4.2-13 and 4.2-14.

The simulated roll acceleration of the "A end" of the carbody due to lateral and yaw inputs, Figures 4.2-15 and 4.2-16 respectively, is influenced primarily by the lateral-roll modes of

PRESENT METROLINER

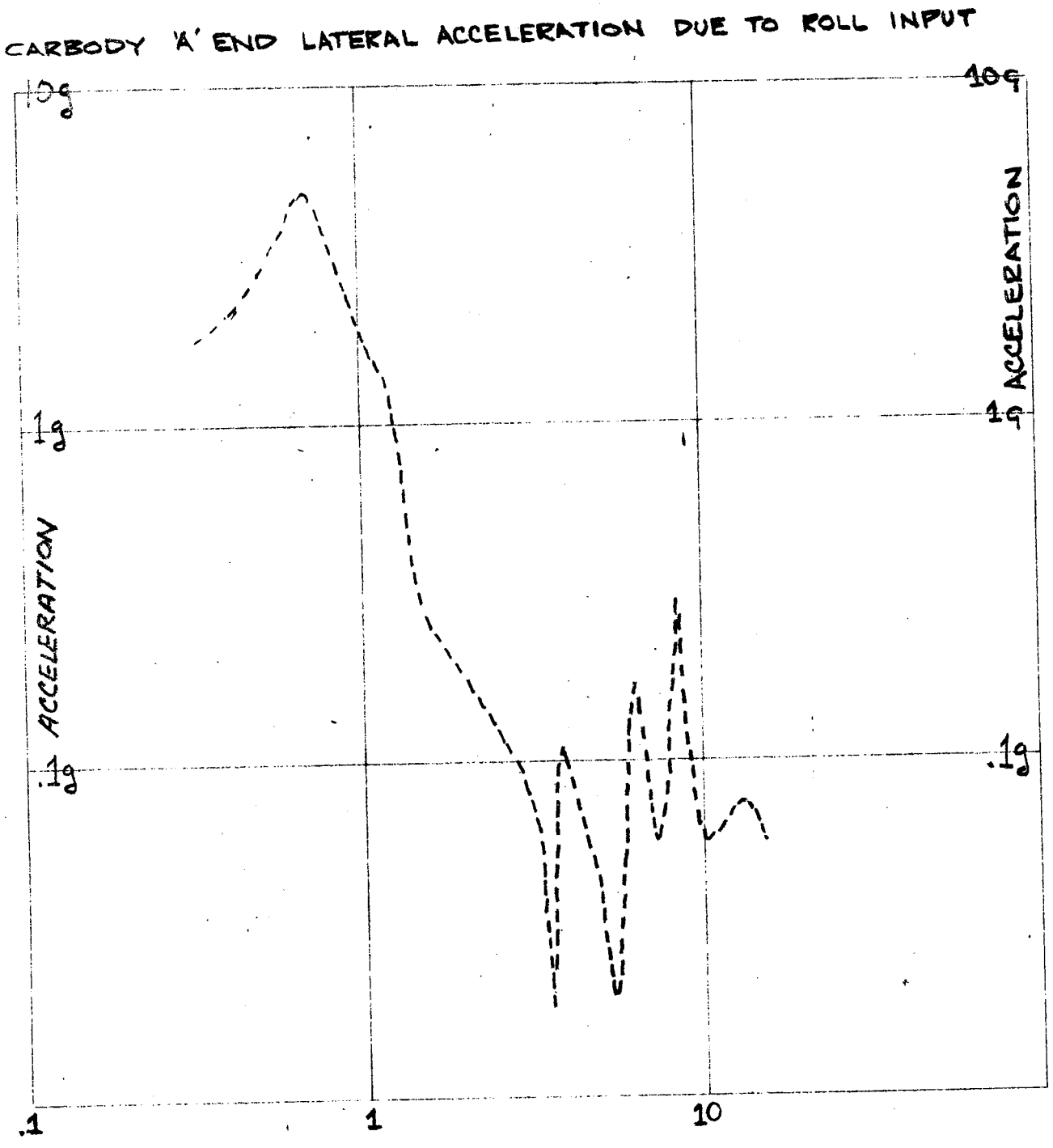

FIGURE 4.2-9

PRESENT METROLINER

CARBODY 'A' END LATERAL ACCELERATION DUE TO YAW INPUT

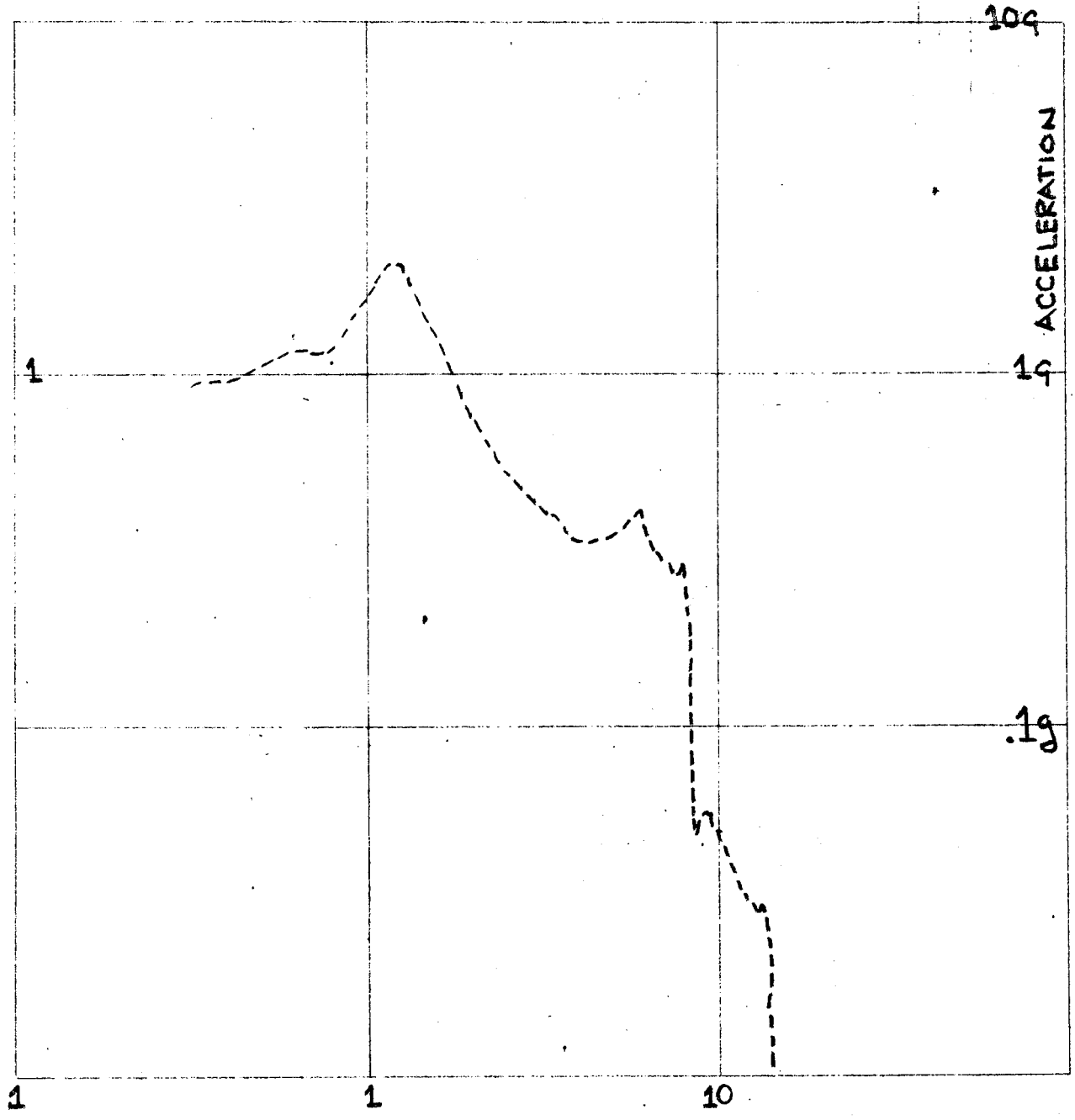

FREQUENCY – HERTZ

FIGURE 4.2-10

PRESENT METROLINER

CARBODY CENTER LATERAL ACCELERATION DUE TO LATERAL INPUT

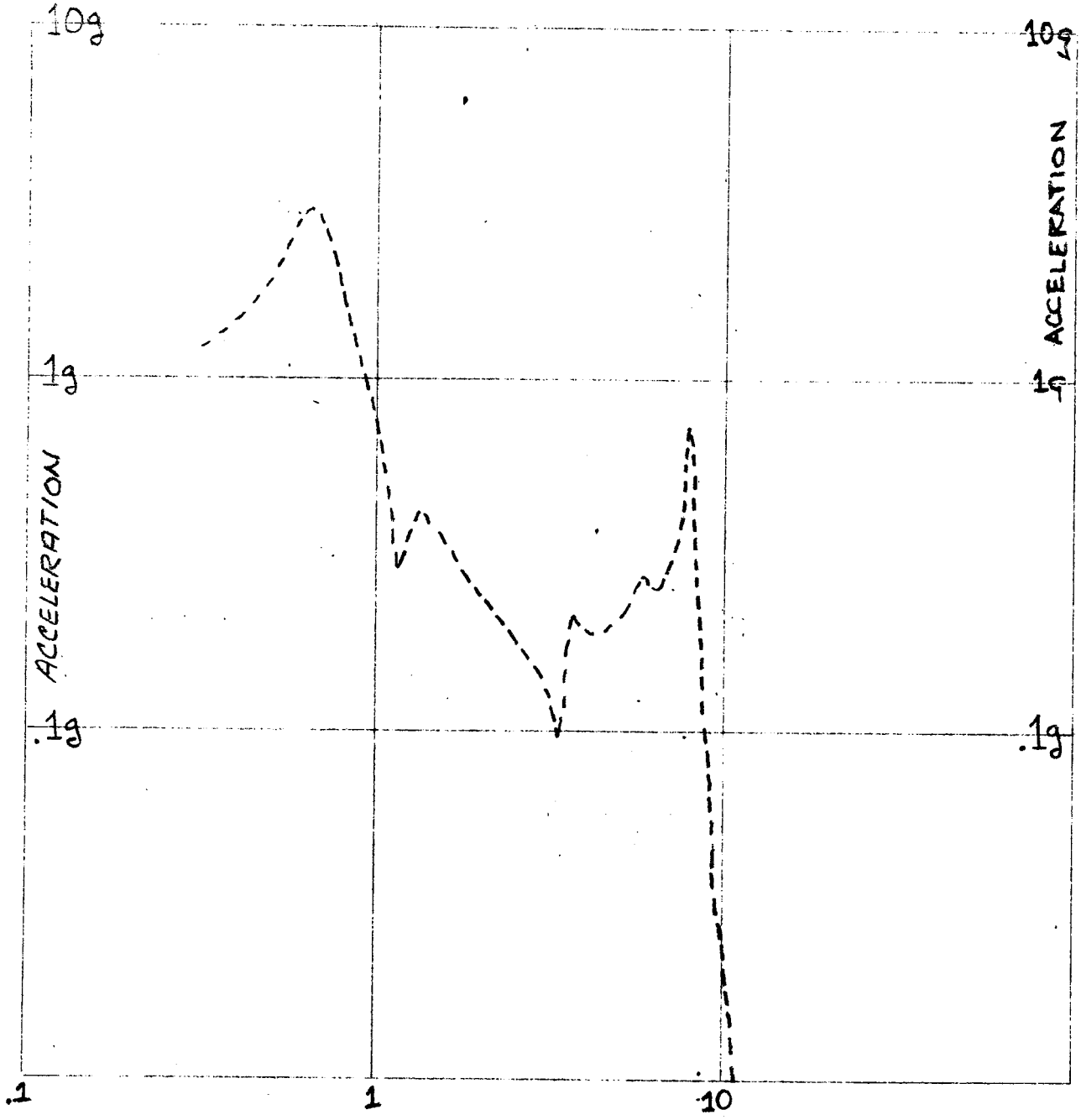

FREQUENCY - HERTZ

FIGURE 4.2-11

FIGURE 4.2-12

POWER SPECTRAL DENSITY OF LATERAL ACCELERATION OF THE CARBODY FLOOR AT THE CENTER

RUN NO. 5

FREQUENCY RESOLUTION = .1 hz

STANDARD DEVIATION = .023 gs

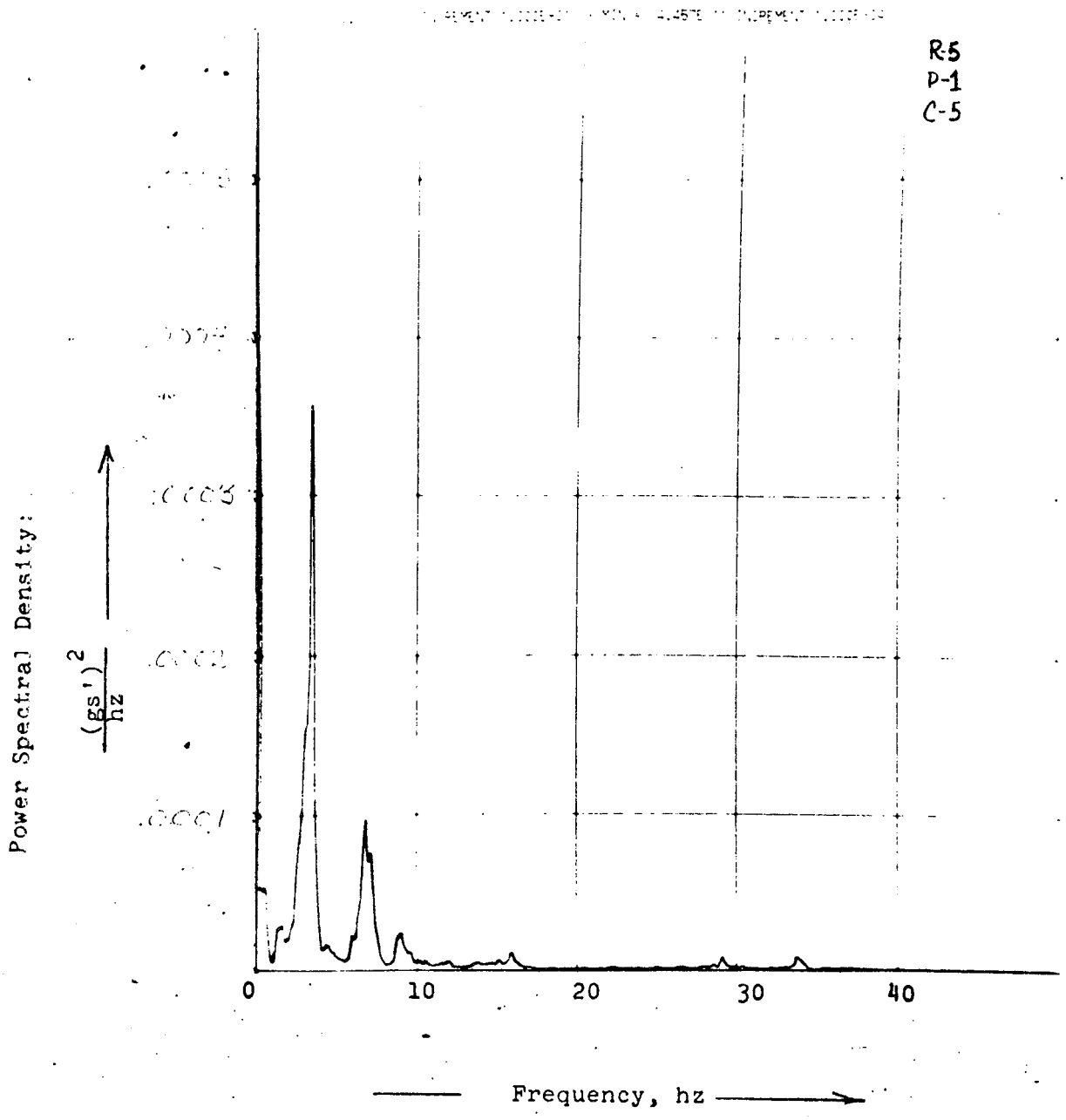

PRESENT METROLINER

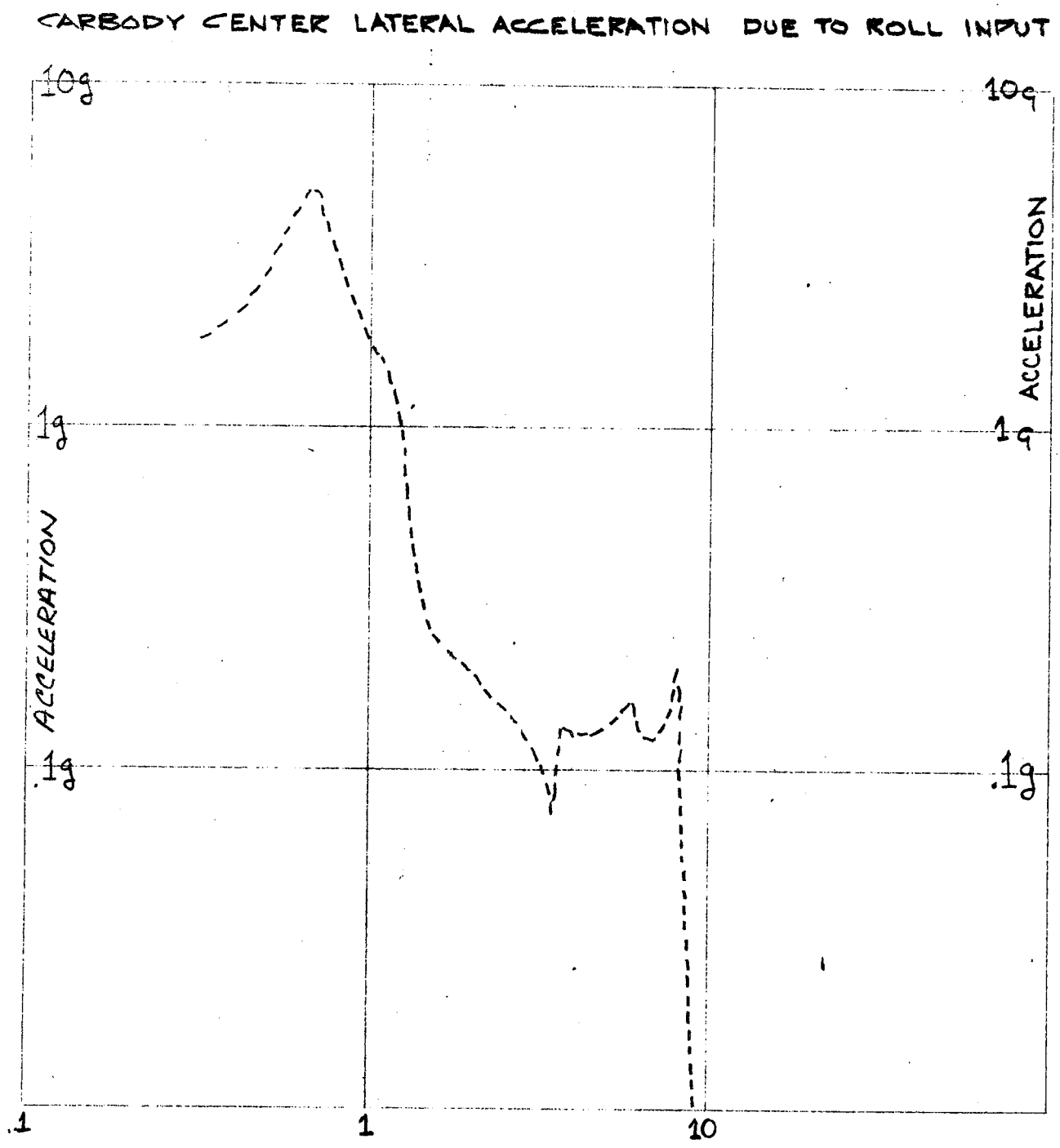

FIGURE 4.2-13

PRESENT METROLINER

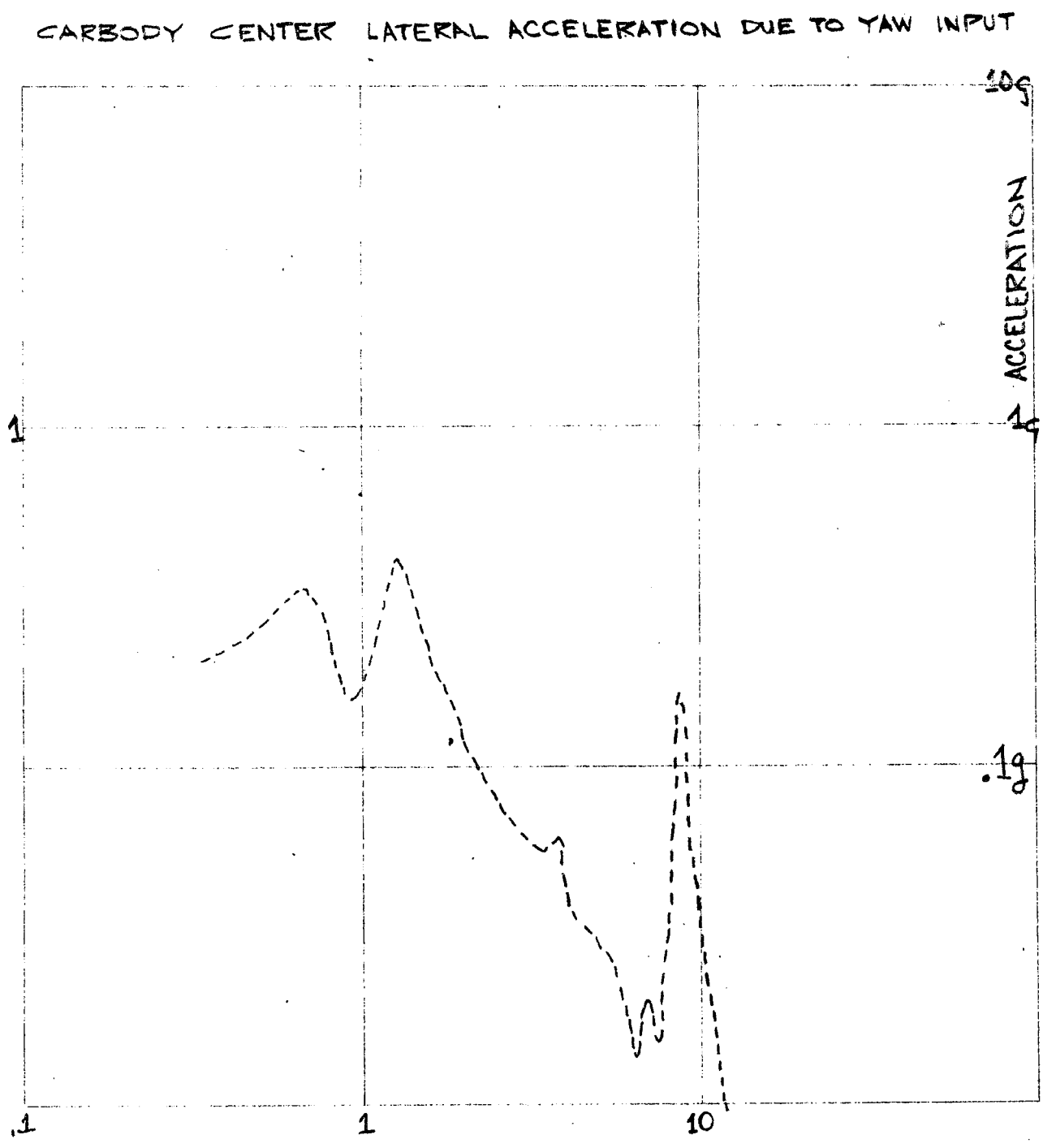

FIGURE 4.2-14

PRESENT METROLINER

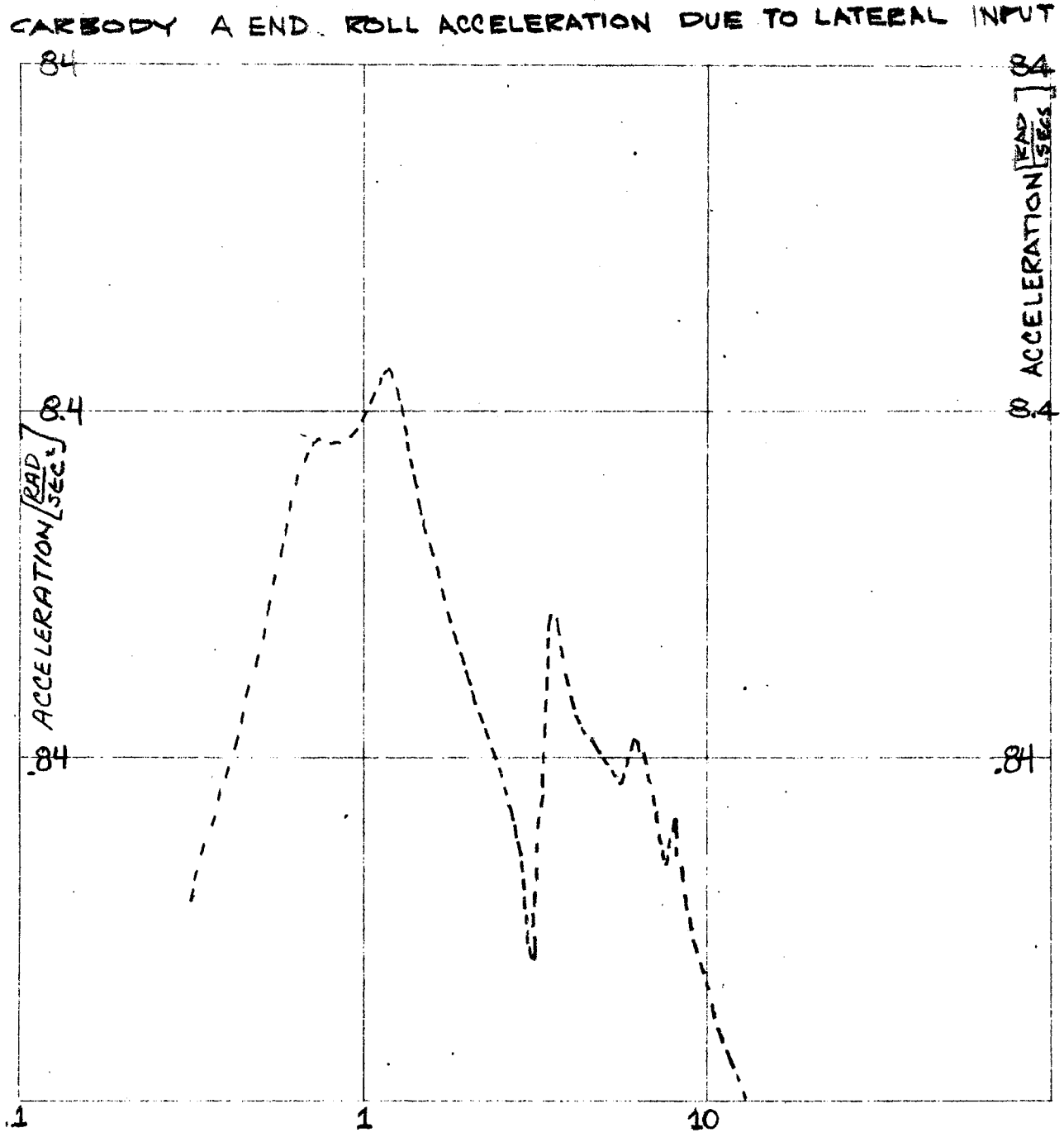

FIGURE 4.2-15

PRESENT METROLINER

CARBODY A END ROLL ACCELERATION DUE TO YAW INPUT

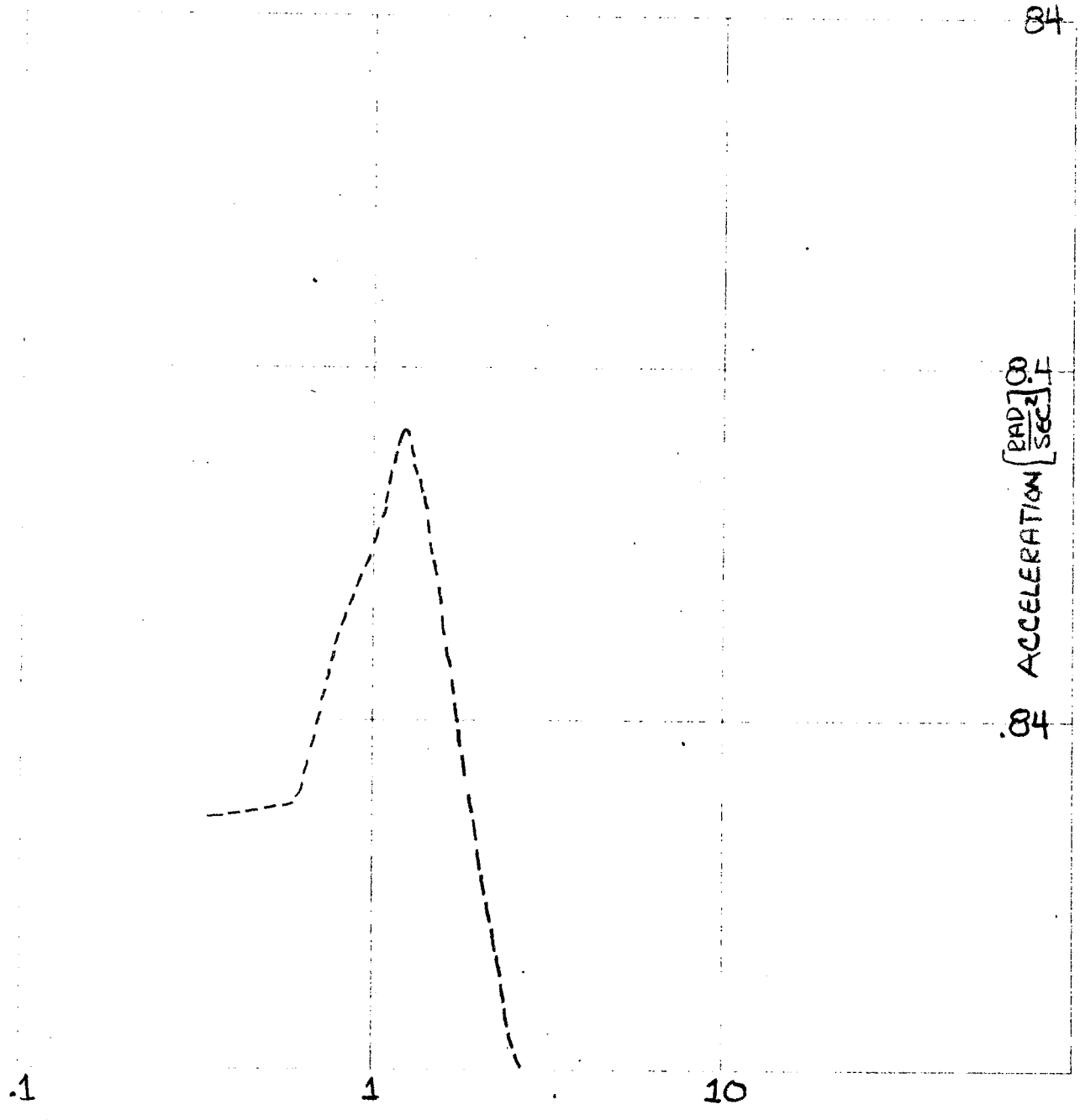

FIGURE 4.2-16

the carbody and transformer, whereas the simulated roll acceleration of the "A end" of the carbody to roll inputs, Figure 4.2-17, is influenced primarily by the upper carbody roll-lateral mode.

The simulated transformer acceleration to lateral, roll, and yaw inputs, Figures 4.2-18, 4.2-19, and 4.2-20 respectively, is dominated by the lateral-roll carbody modes and the roll-lateral modes of the transformer. The measured lateral acceleration at the bottom of the transformer in track section, Figure 4.2-21, is dominated by energy at 3.4 hertz corresponding to the dominate lateral track disturbance of 39 foot wave length and the lower transformer lateral-roll mode.

In addition to the dynamic performance of the lateral system described previously, two other conditions observed during the road test significantly influence the lateral ride.

Through track section six, the lateral unbalance force, due to exceeding the balance speed of the curve (a common occurrence on the Metroliner route), was sufficient to force the secondary lateral suspension into contact with the lateral bumper stop. Through this section of track, the standard deviation of the lateral acceleration of the carbody over the "A end" truck was .065 gs as compared to .025 gs on the baseline track section five. In the center of the carbody, the standard deviation of the lateral acceleration was .049 gs as compared to .023 gs on the baseline track section five.

PRESENT METROLINER

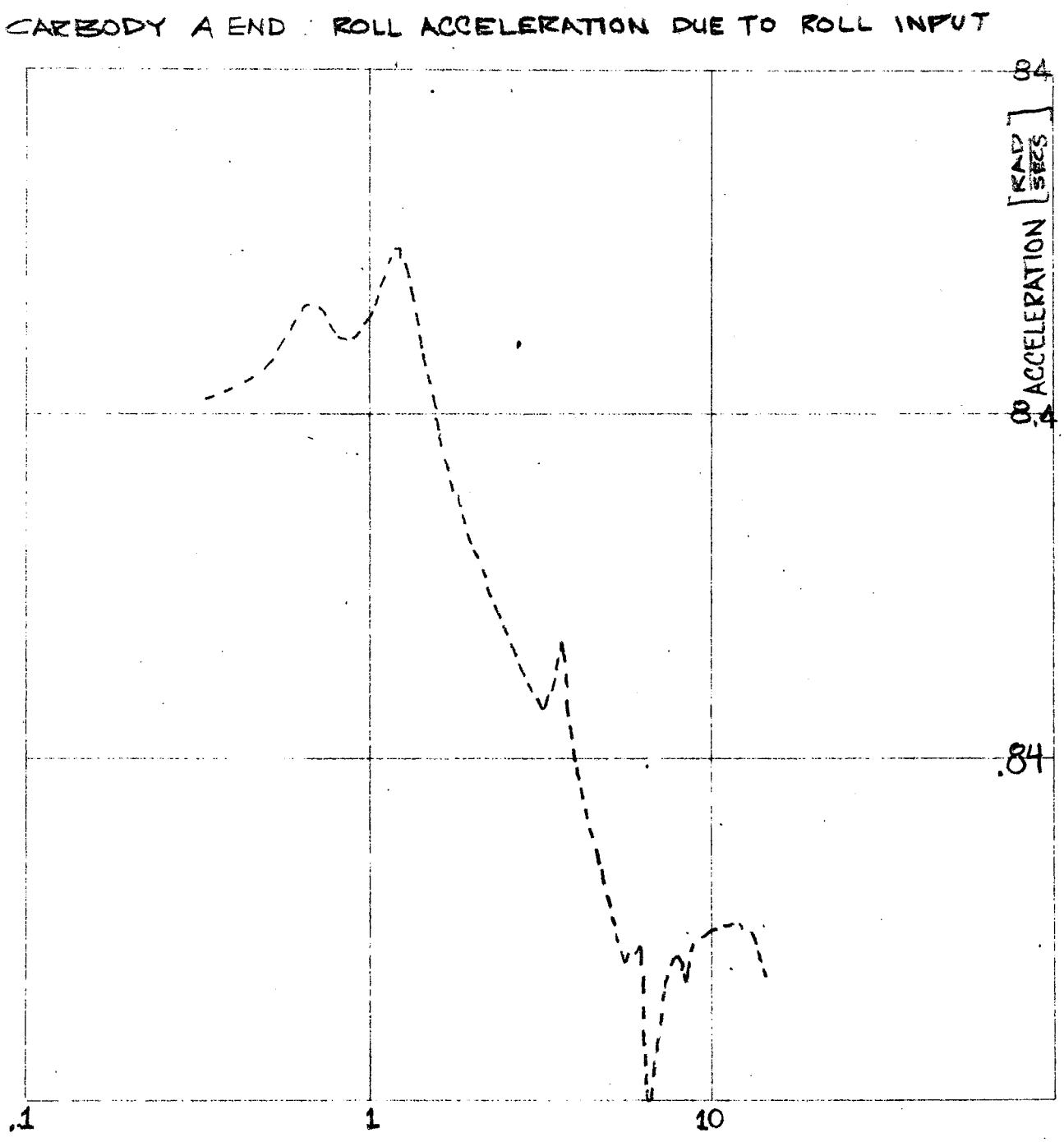

FIGURE 4.2-17

PRESENT METROLINER

TRANSFORMER LATERAL ACCELERATION DUE TO LATERAL INPUT

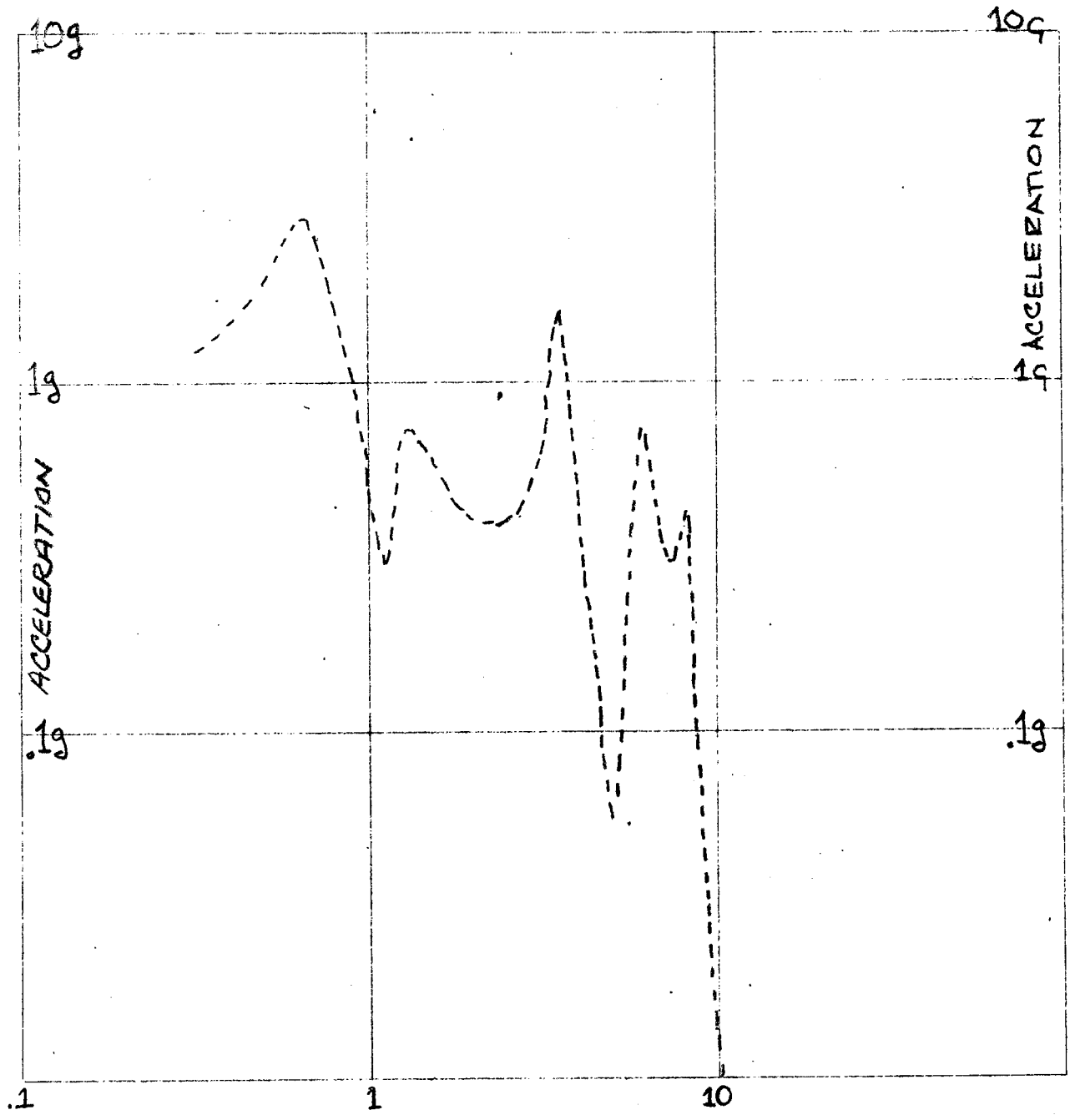

FIGURE 4.2-18

PRESENT METROLINER

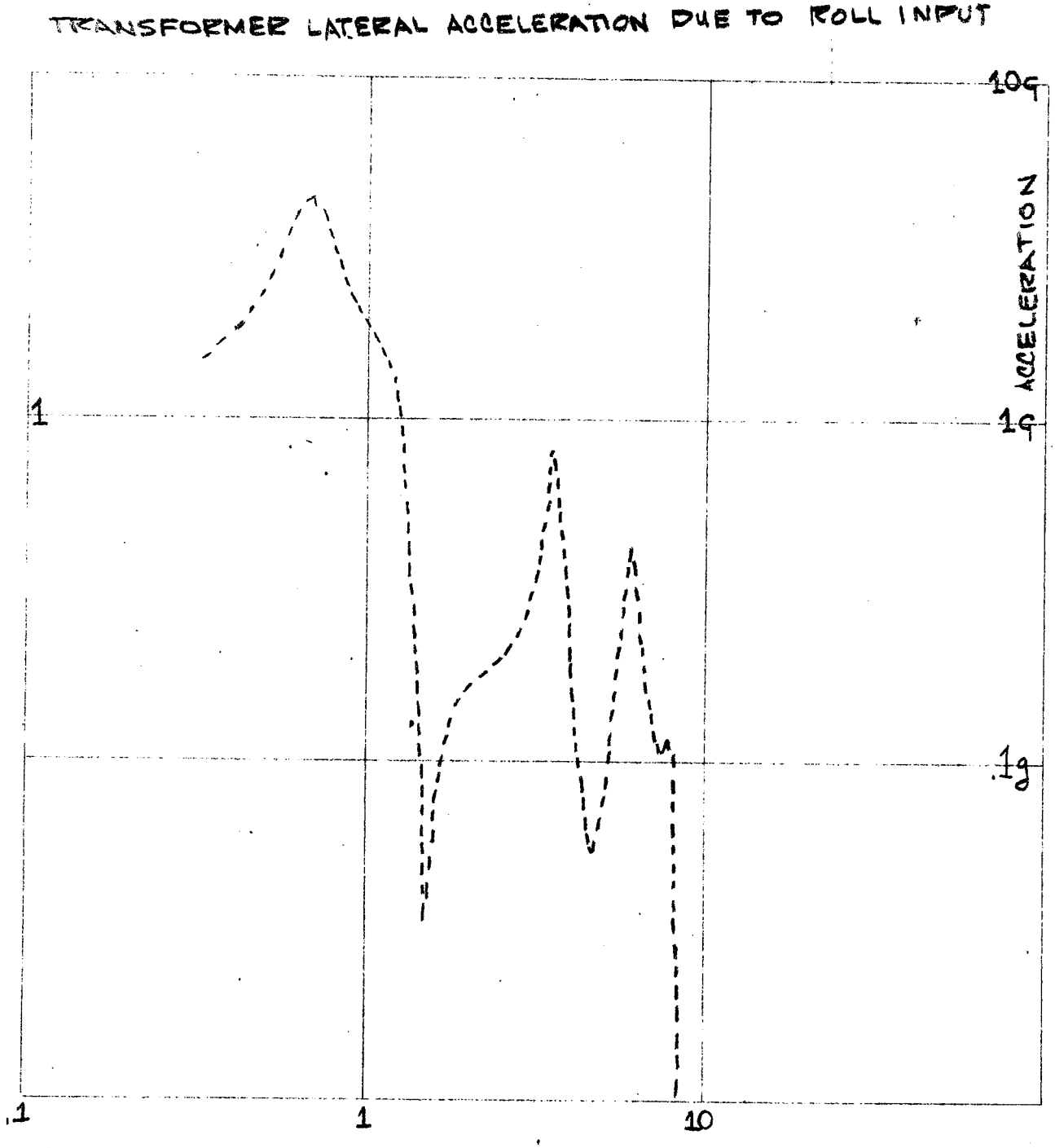

FIGURE 4.2-19

PRESENT METROLINER

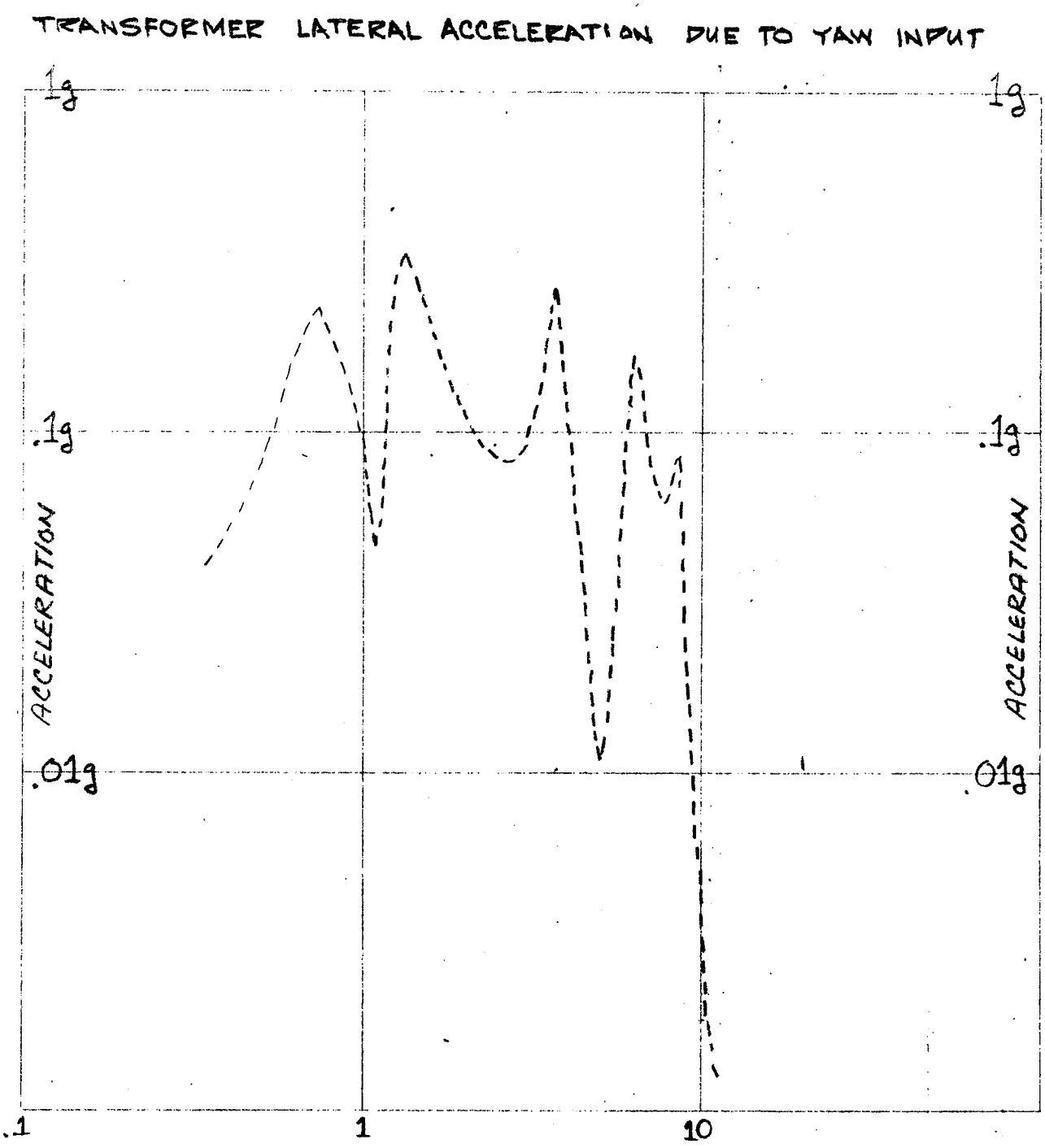

FIGURE 4.2-20

FIGURE 4.2-21

POWER SPECTRAL DENSITY OF LATERAL ACCELERATION OF BOTTOM OF POWER TRANSFORMER MOUNTED TO CARBODY NEAR CENTER

RUN NO. 5

FREQUENCY RESOLUTION = .1 hz

STANDARD DEVIATION = .061 gs

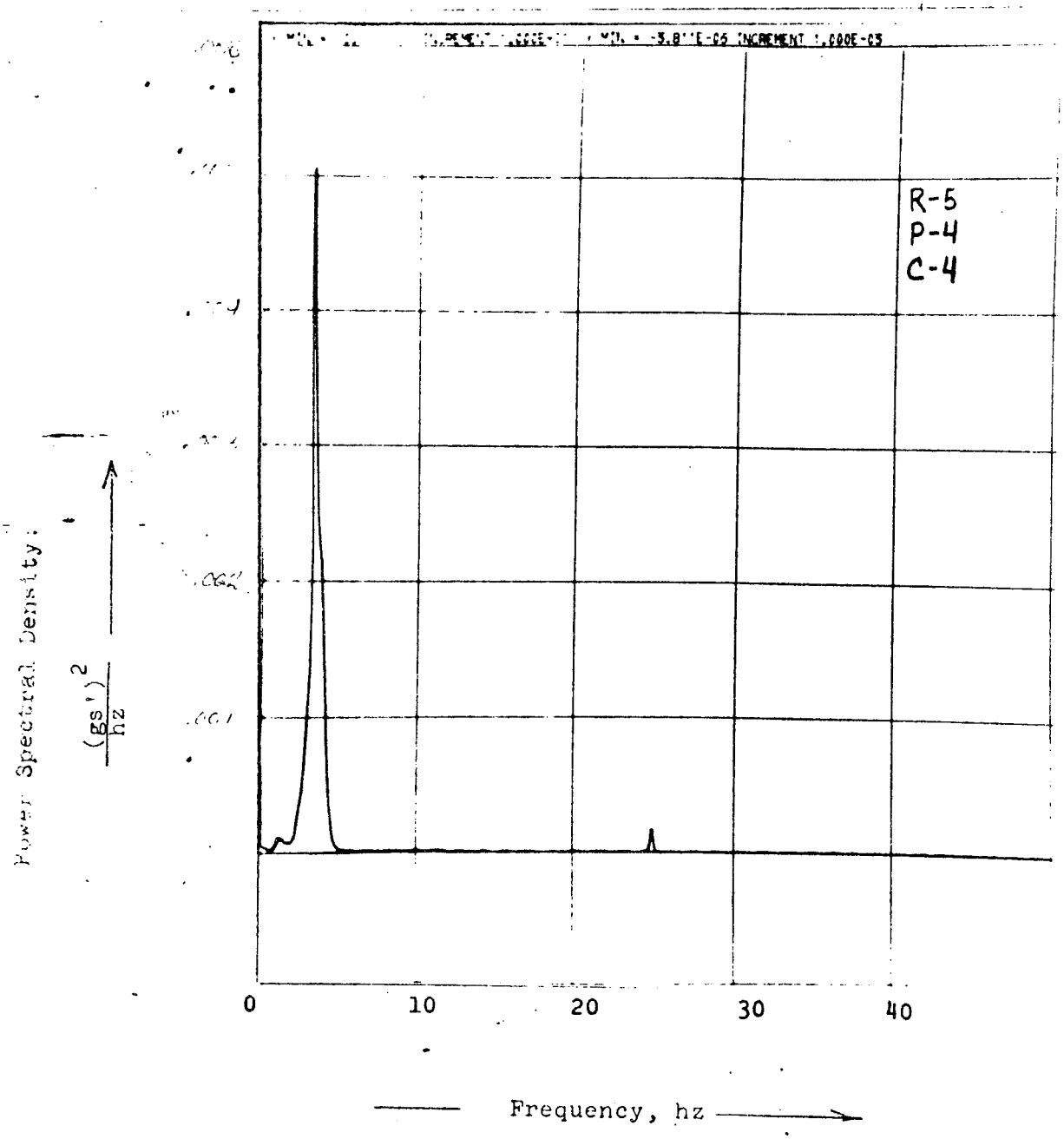

During road test section eight, a lateral instability of the wheel set was observed. This instability resulted in a large yaw and lateral acceleration of the wheel and axle assembly at 4 hertz, as shown in Figure 4.2-22 and Figure 4.2-23. This input dominates the performance of the lateral system as shown in Figures 4.2-24, 4.2-25, 4.2-26, and 4.2-27. Under this condition, the standard deviation of the lateral acceleration of the carbody over the "A end" truck was .046 gs as compared to .025 gs on the baseline track section five. In the center of the carbody, the standard deviation of the lateral acceleration was .034 gs as compared to .023 gs for the baseline track section five.

4.3 Summary of Present Metroliner Performance

Table 4.3-1 is a summary of present Metroliner resonances.

The major results of the present Metroliner performance are:

- The truck frame assembly is not isolating the track irregularities at frequencies below 13 hertz vertically and 9 hertz laterally.

- The power transformer is acting dynamically independent of the remainder of the system and has a measurable effect on the carbody vertical and lateral accelerations.

- The carbody rigid body resonances and the vertical bending resonance has a major effect on ride quality.

- The longitudinal response of the carbody to pitch inputs is not negligible.

- Spring surge has an appreciable effect on ride quality

FIGURE 4.2-22

POWER SPECTRAL DENSITY OF AVERAGE YAW ACCELERATION OF JOURNAL BOXES ON "A" END TRUCK (1/2 the difference in lateral acceleration of the journal boxes.)

RUN NO. 8

FREQUENCY RESOLUTION = .2 hz

STANDARD DEVIATION = .25 gs

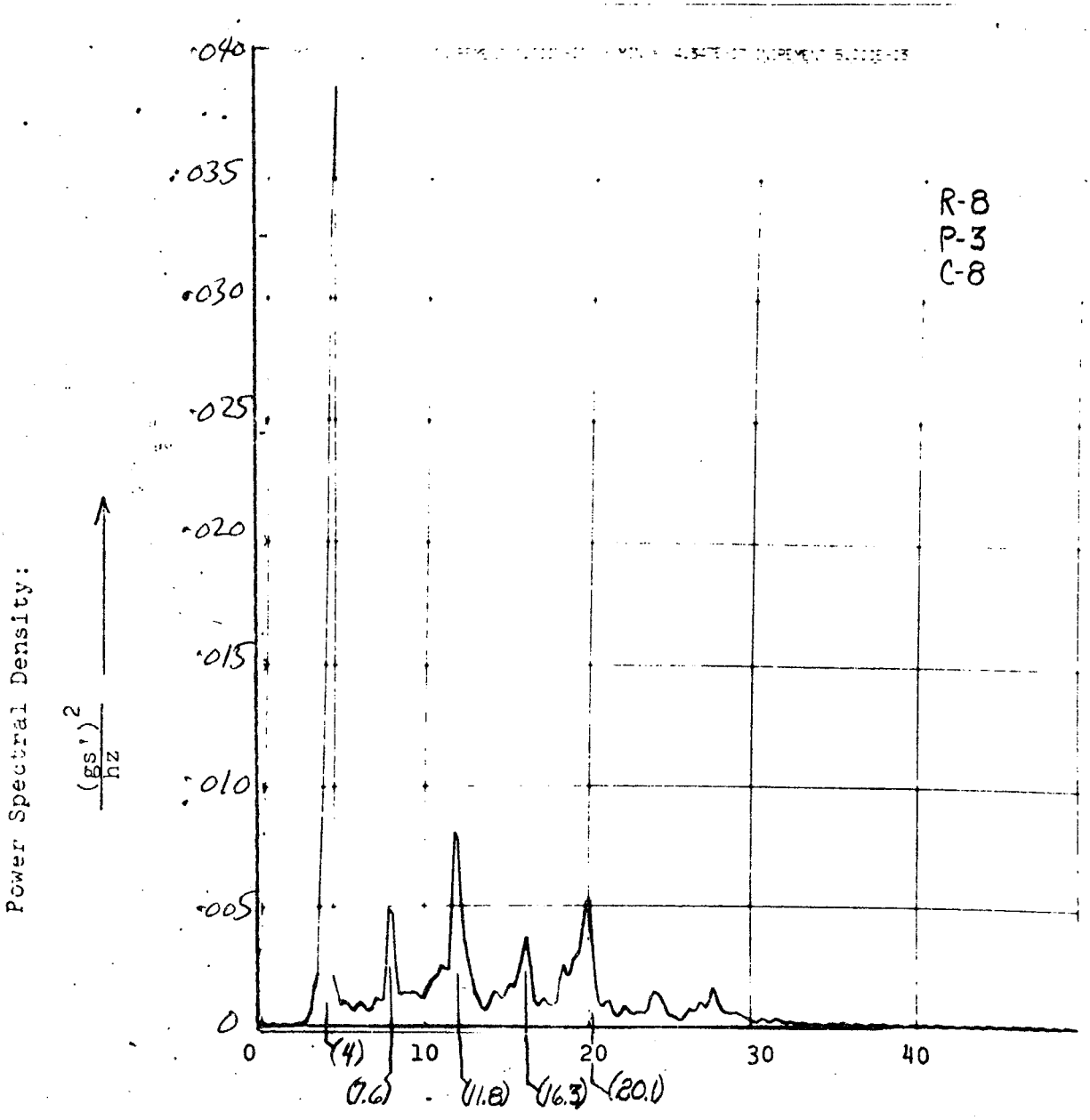

FIGURE 4.2-23

POWER SPECTRAL DENSITY OF AVERAGE LATERAL ACCELERATION OF JOURNAL BOXES ON "A" END TRUCK

RUN NO. 8

FREQUENCY RESOLUTION = .2 hz

STANDARD DEVIATION = .36 gs

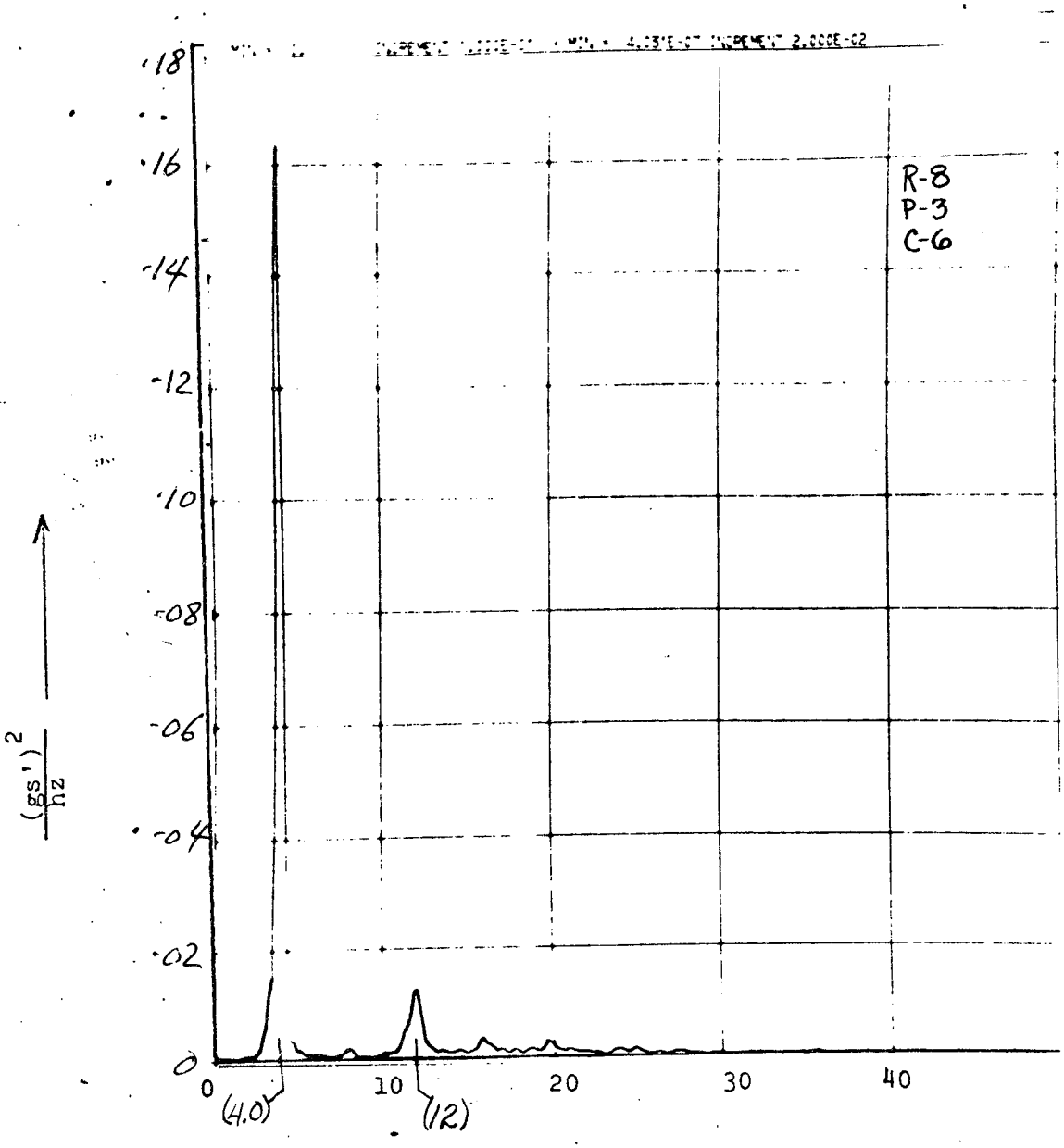

FIGURE 4.2-24

POWER SPECTRAL DENSITY OF YAW ACCELERATION OF TRUCK FRAME ON "A" END TRUCK (1/2 the difference in lateral acceleration over the journal boxes.)

RUN NO. 8

FREQUENCY RESOLUTION = .2 hz

STANDARD DEVIATION = .40 gs

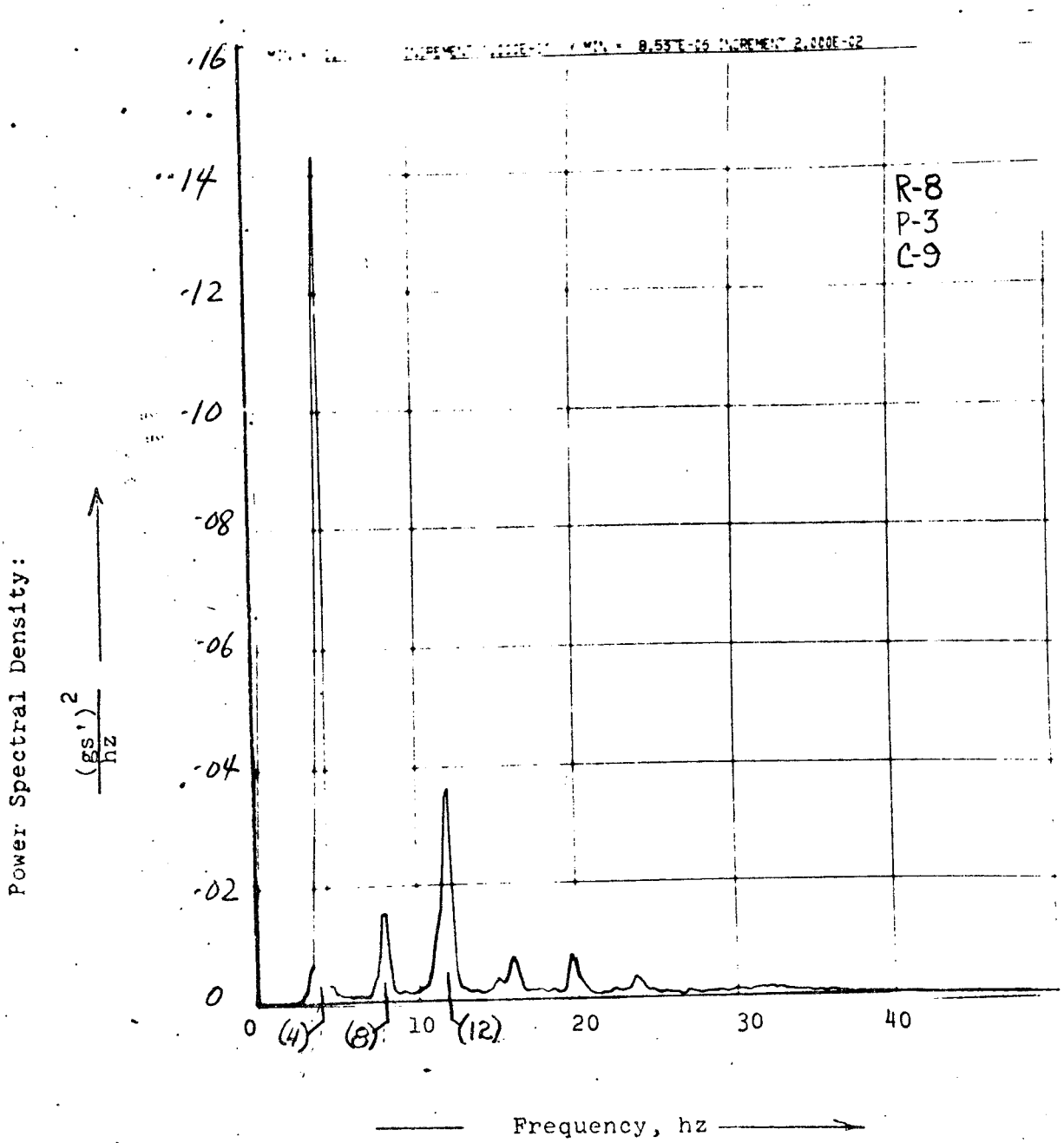

FIGURE 4.2-25

POWER SPECTRAL DENSITY OF LATERAL ACCELERATION

OF CARBODY FLOOR OVER "A" END RIGHT BOLSTER SPRING

RUN NO. 8

FREQUENCY RESOLUTION = .2 hz

STANDARD DEVIATION = .046 gs

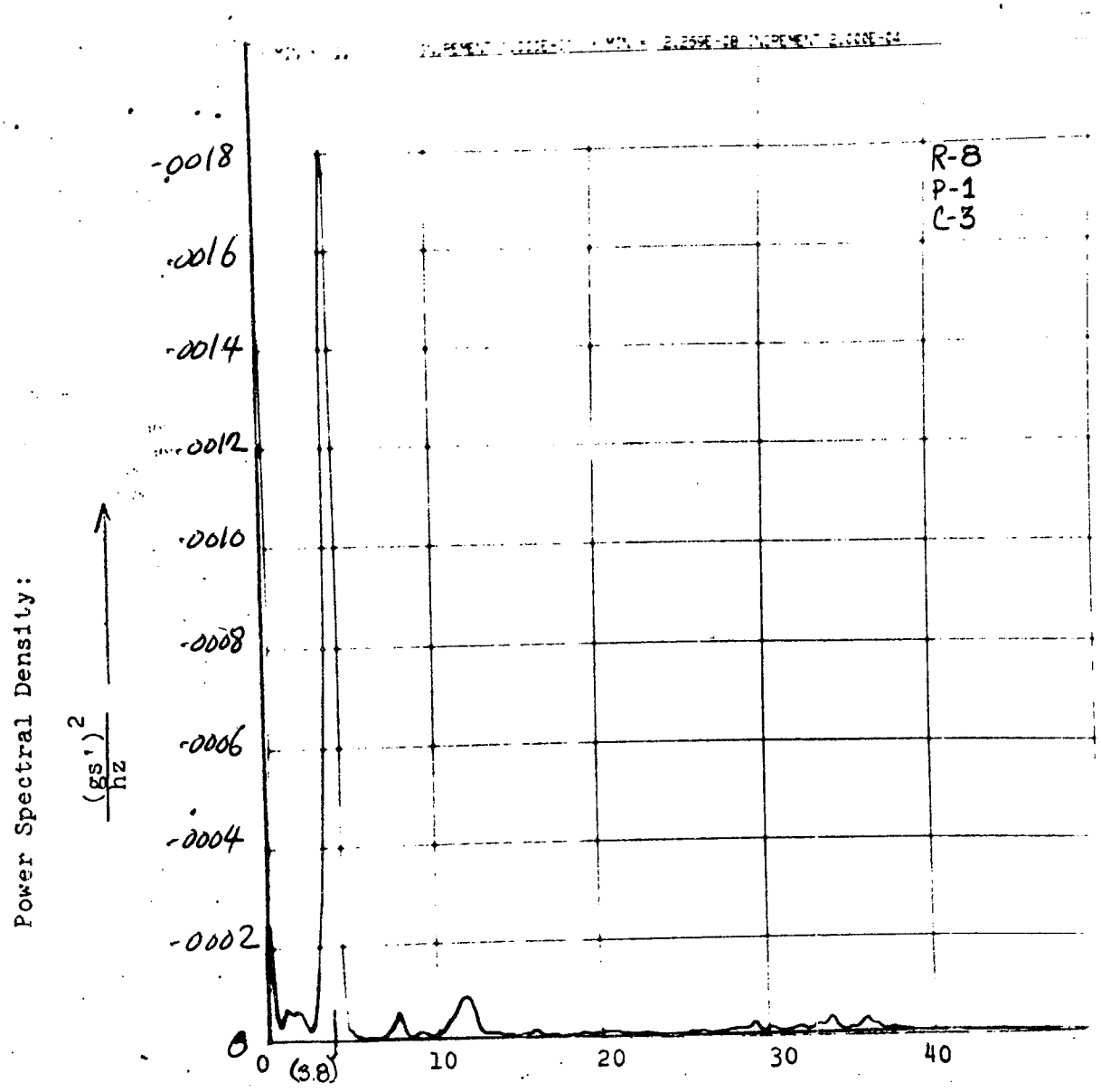

FIGURE 4.2-26

POWER SPECTRAL DENSITY OF LATERAL ACCELERATION OF THE CARBODY FLOOR AT THE CENTER

RUN NO. 8

FREQUENCY RESOLUTION = .2 hz

STANDARD DEVIATION = .034 gs

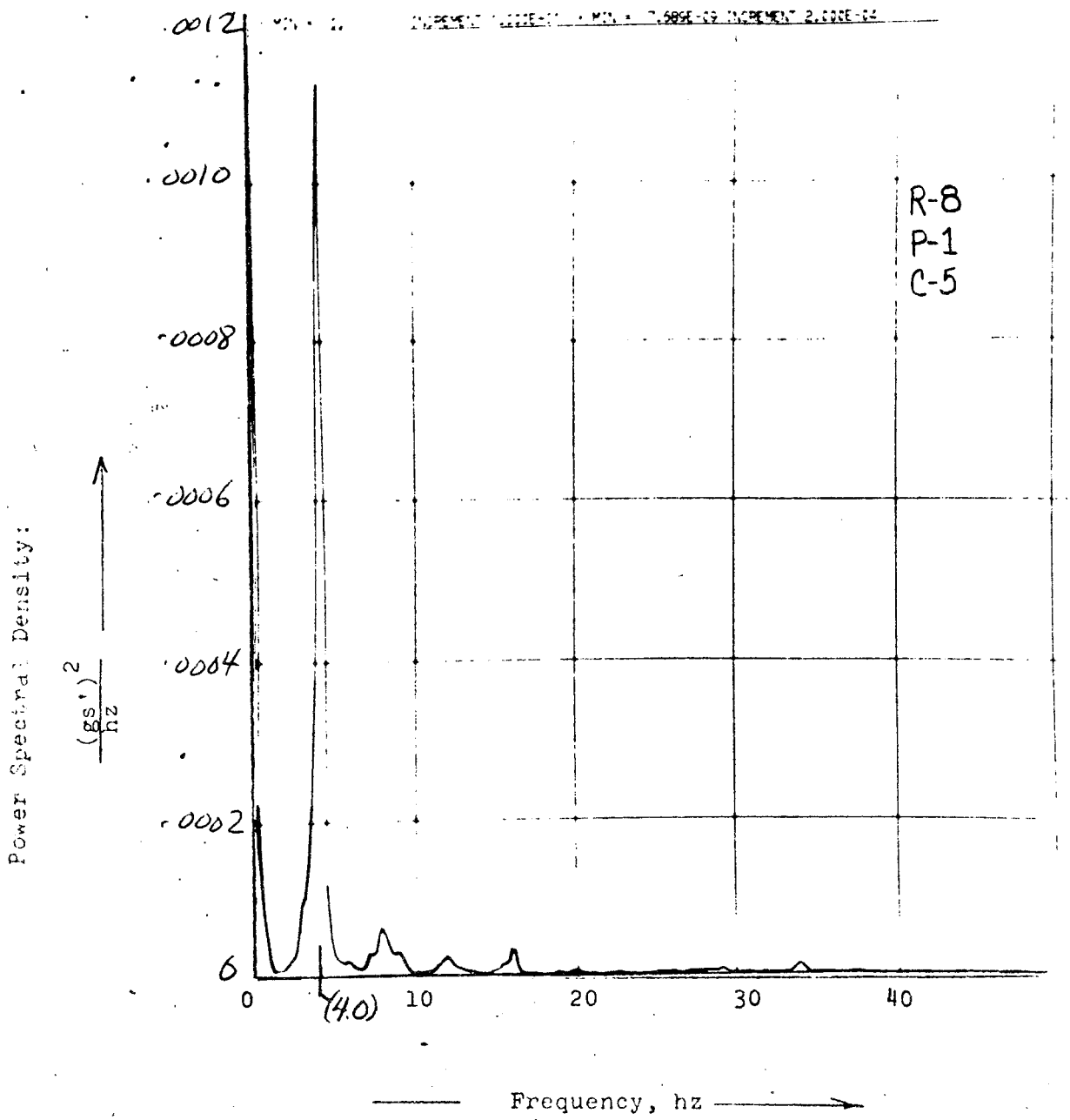

FIGURE 42-27

POWER SPECTRAL DENSITY OF LATERAL ACCELERATION OF BOTTOM OF POWER TRANSFORMER MOUNTED TO CARBODY NEAR CENTER

RUN NO. 8

FREQUENCY RESOLUTION = .2 hz

STANDARD DEVIATION = .22 gs

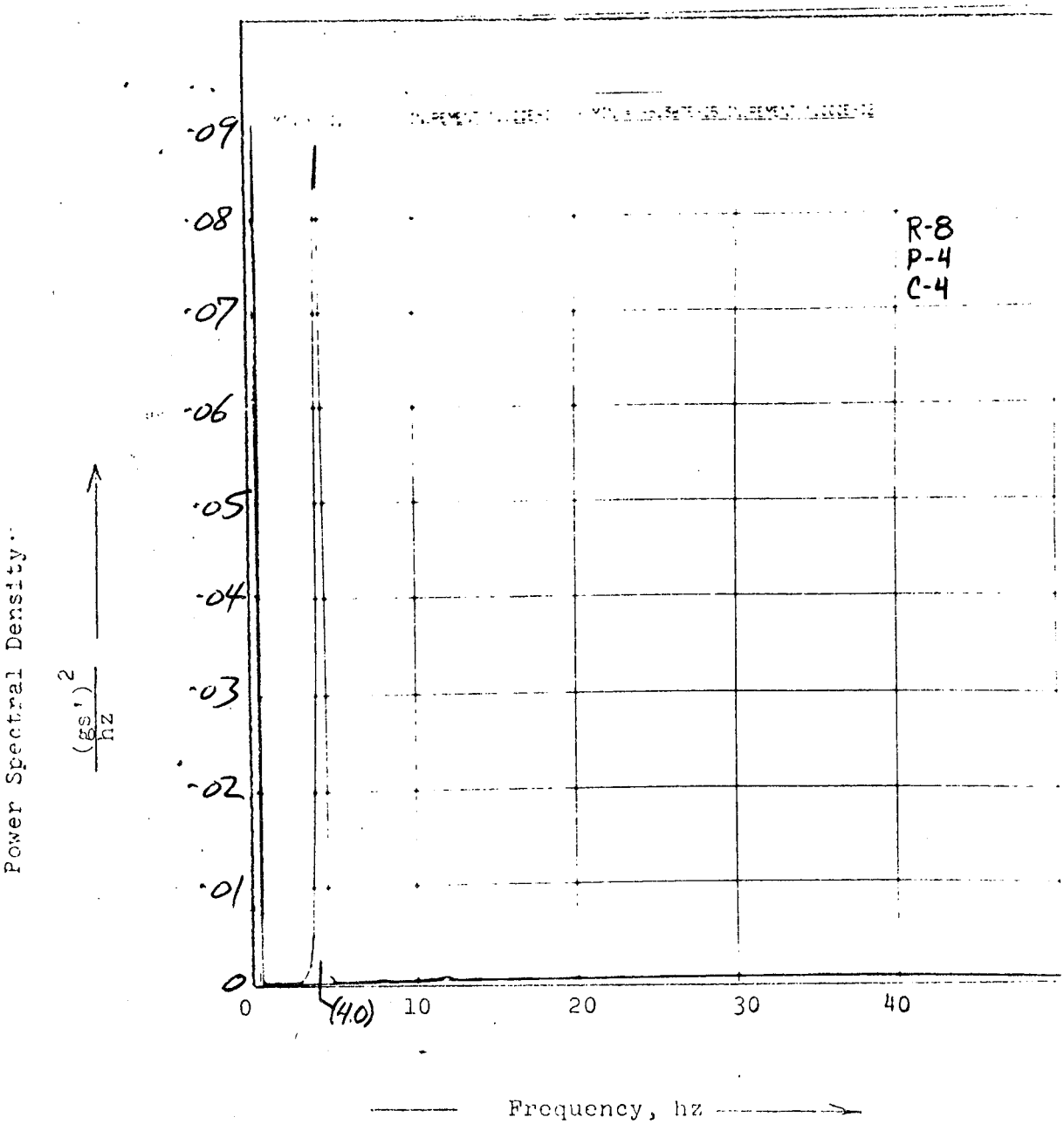

Table 4.3-1

Present Metroliner Resonances

Mode	Frequency - hertz
Carbody - lower lateral - roll	.6 to .7
Carbody - vertical	1.05
Carbody - upper lateral - roll	1.2 to 1.3
Carbody - pitch	1.32
Carbody - longitudinal	2.3
Transformer - lower lateral - roll	3.4 to 3.6
Transformer - vertical	4.6
Transformer - upper lateral - roll	6.0
Truck frame - lower lateral - roll	6.1
Carbody - vertical bending	6.8 to 7.5
Truck - longitudinal	7.5
Carbody - lateral bending	8.0
Truck frame - vertical	9.5
Truck frame - upper lateral - roll	1.3

at frequencies of 34 to 36 hertz.

- A lateral dynamic instability of the wheel set occurred infrequently during the road test and appreciably affects the ride quality.

- The lateral unbalance forces are sufficient to force the secondary lateral suspension into the suspension stops, appreciably affecting the ride quality.

5.0 MODIFIED DESIGN

The design modifications of the present Metroliner are limited to the modification or replacement of existing suspension components. Within this constraint, parametric studies were performed on the effects of modification to the transformer suspension system and the truck primary and secondary suspension system.

The goal of the transformer study was to achieve a set of parameters where the transformer interacted with the carbody vertical and lateral bending modes as a damped dynamic absorber. Additionally, the location of the lower lateral-roll resonance of the transformer at 3.4 hertz to 3.6 hertz should be moved as the dominate lateral track input occurs at this frequency at a train speed of 100 M.P.H. The transformer parametric study resulted in a set of suspension parameters tabulated in Table 5.0-1. Figures 5.0-1, 5.0-2 and 5.0-3 show a comparison of the simulated performance due to the modified transformer parameters under vertical inputs. At the "A end" of the car, the transformer modification reduces

TABLE 5.0-1

MODIFIED TRANSFORMER SUSPENSION PARAMETER

Total System	Present	Modified
Vertical Stiffness	28,800#/in.	43,200#/in.
Lateral Stiffness	27,000#/in.	57,600#/in.
Longitudinal Stiffness	260,000#/in.	388,700#/in.
Vertical Damping	72#sec./in.	384#sec./in.
Lateral Damping	72#sec./in.	220#sec./in.
Longitudinal Damping	72#sec./in.	90#sec./in.

MODIFIED DESIGN

CARBODY "A END" VERTICAL ACCELERATION DUE TO VERTICAL INPUT

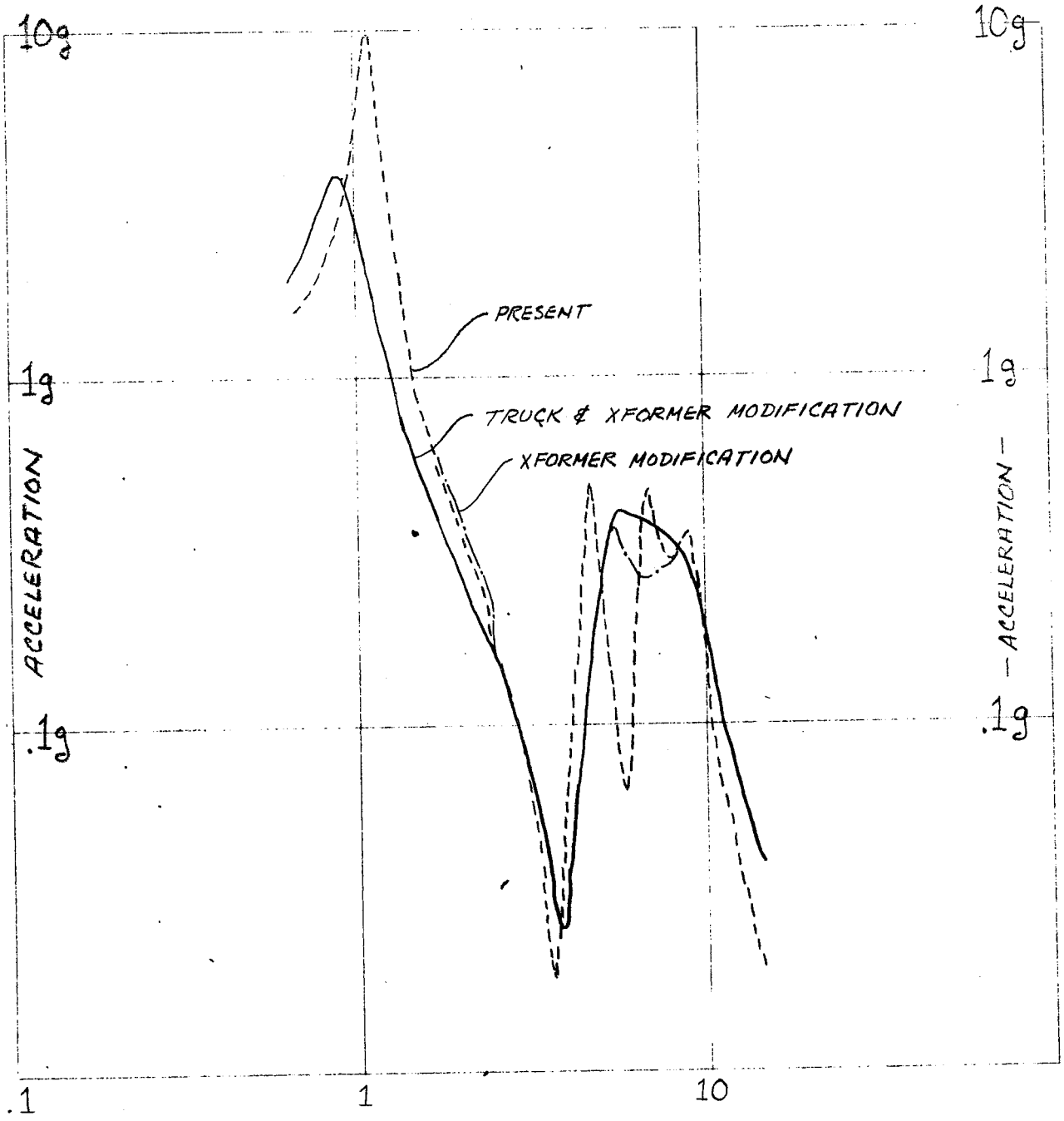

FIGURE 5.0-1

MODIFIED DESIGN

CARBODY CENTER VERTICAL ACCELERATION DUE TO VERTICAL INPUT

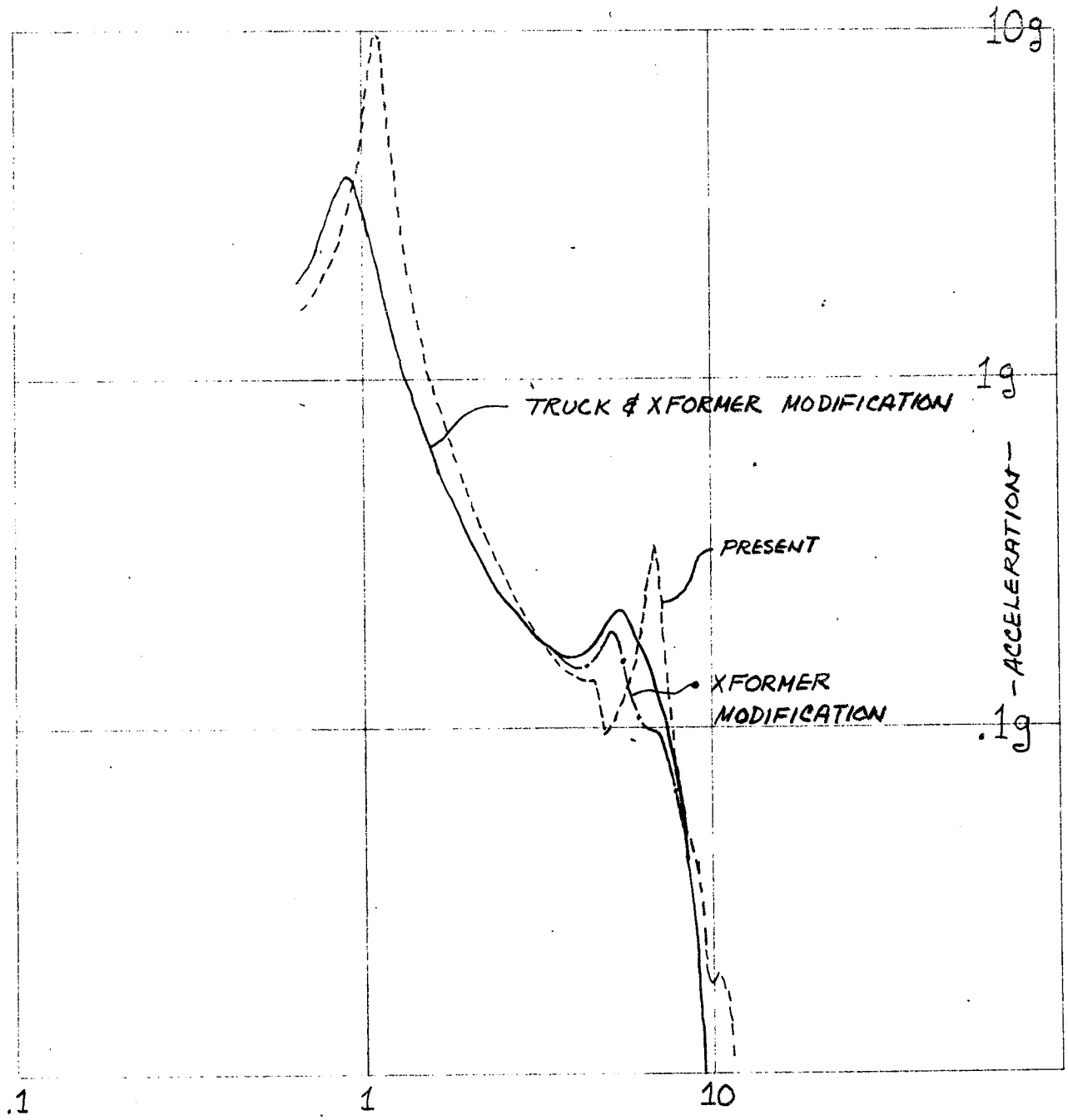

FIGURE 5.0-2

MODIFIED DESIGN

TRANSFORMER VERTICAL ACCELERATION DUE TO VERTICAL INPUT

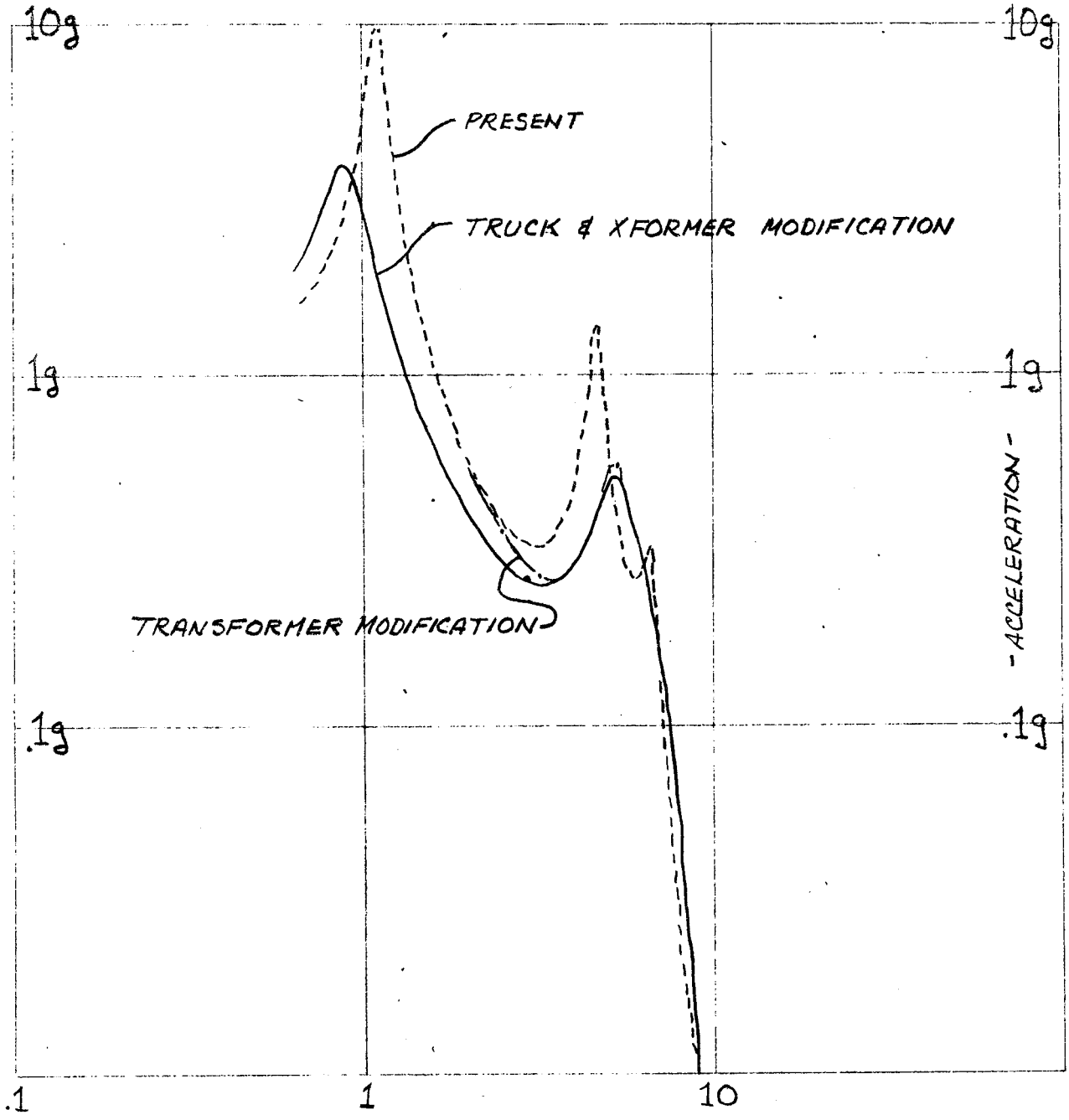

FIGURE 5.0-3

the magnitude of acceleration peaks presently at 4.6 hertz and 7.0 hertz, and shifts the peaks to 5.5 hertz and 9 hertz at reduced magnitude. The performance below 2.5 hertz is maintained at its present level. In the center of the carbody, Figure 5.0-2, the present 7.0 hertz acceleration peak is considerably reduced, with the peak shifted to 5.0 hertz.

Figures 5.0-4 through 5.0-12 show the simulated lateral performance with the modified transformer. The major improvement is the movement of the 3.6 hertz lateral-roll transformer resonance, which significantly reduces the lateral response in the 3.5 to 4.5 hertz range.

The parametric study on the primary and secondary suspension of the truck was performed with the transformer at the modified set of suspension parameters. The emphasis of this parametric study is on the vertical suspension. With the present journal configuration, controlled modifications to the lateral primary suspension system are difficult.

For the truck parametric study, the truck dynamic parameters were described in terms of the resonant frequency of the truck frame assembly with the carbody, and wheel and axle assembly ends of the secondary and primary suspension fixed. The term "9.5 hertz truck" refers to a truck where the sum of the primary and secondary suspensions produces a 9.5 hertz resonance of the truck frame assembly. The present Metroliner has a 9.5 hertz truck.

As the vertical truck frequency is reduced, the roll stiffness of the truck suspension reduces, when the same rigid carbody

MODIFIED DESIGN

CARBODY "A END" LATERAL ACCELERATION DUE TO LATERAL INPUT

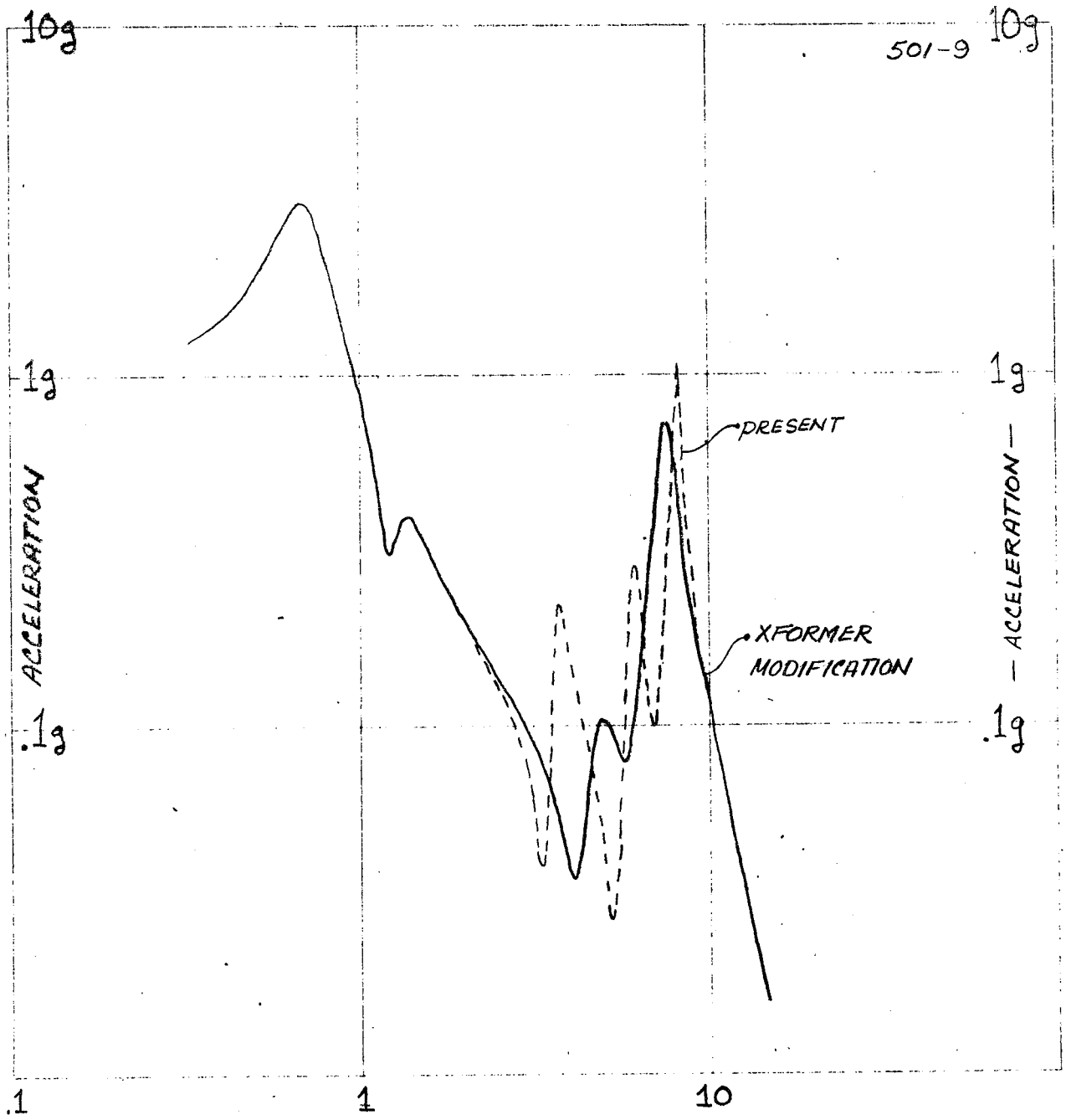

FIGURE 5.0-4

MODIFIED DESIGN

CARBODY "A END" LATERAL ACCELERATION DUE TO ROLL INPUT

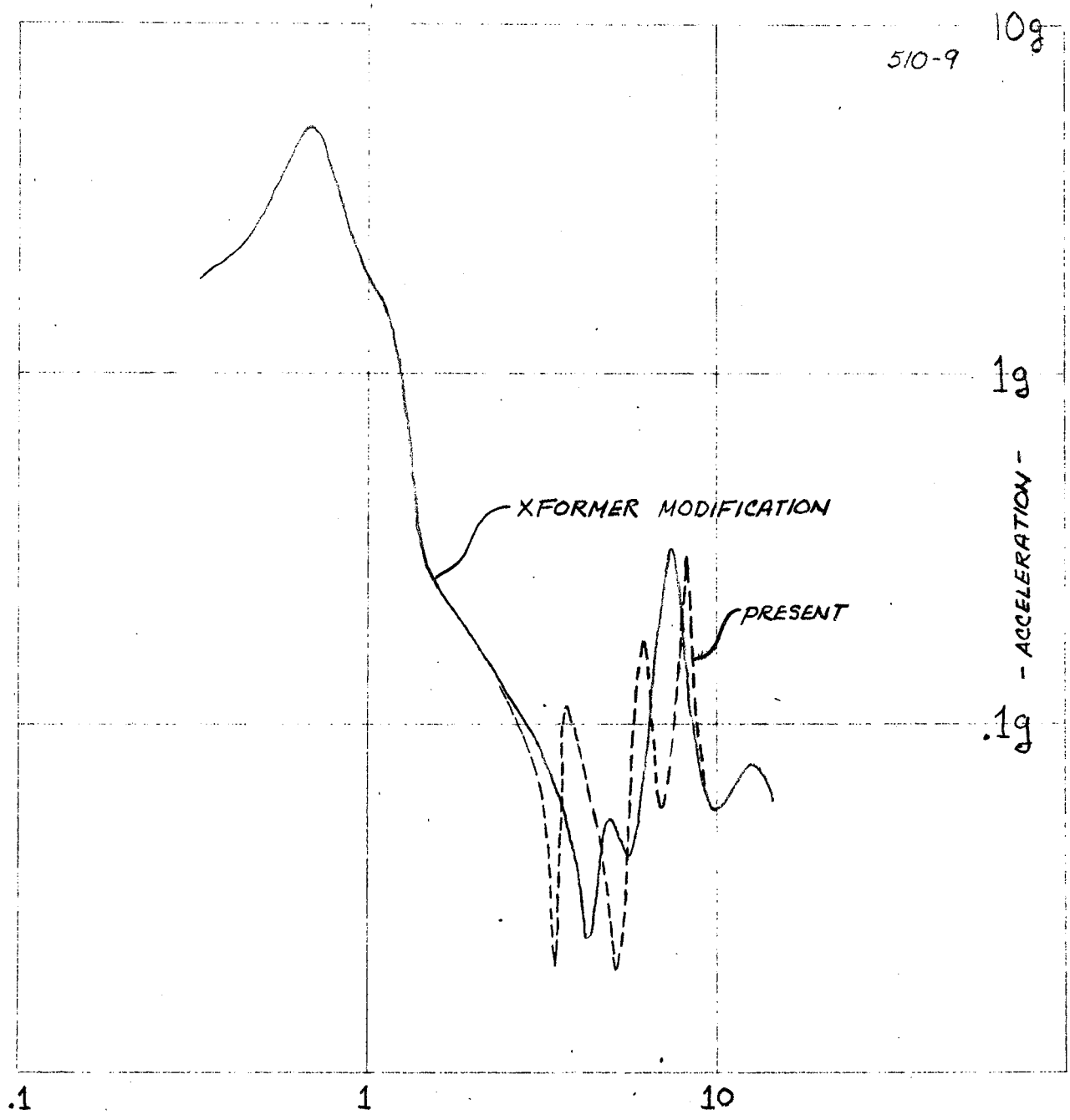

FIGURE 5.0-5

MODIFIED DESIGN

CARBODY "A END" LATERAL ACCELERATION DUE TO YAW INPUT

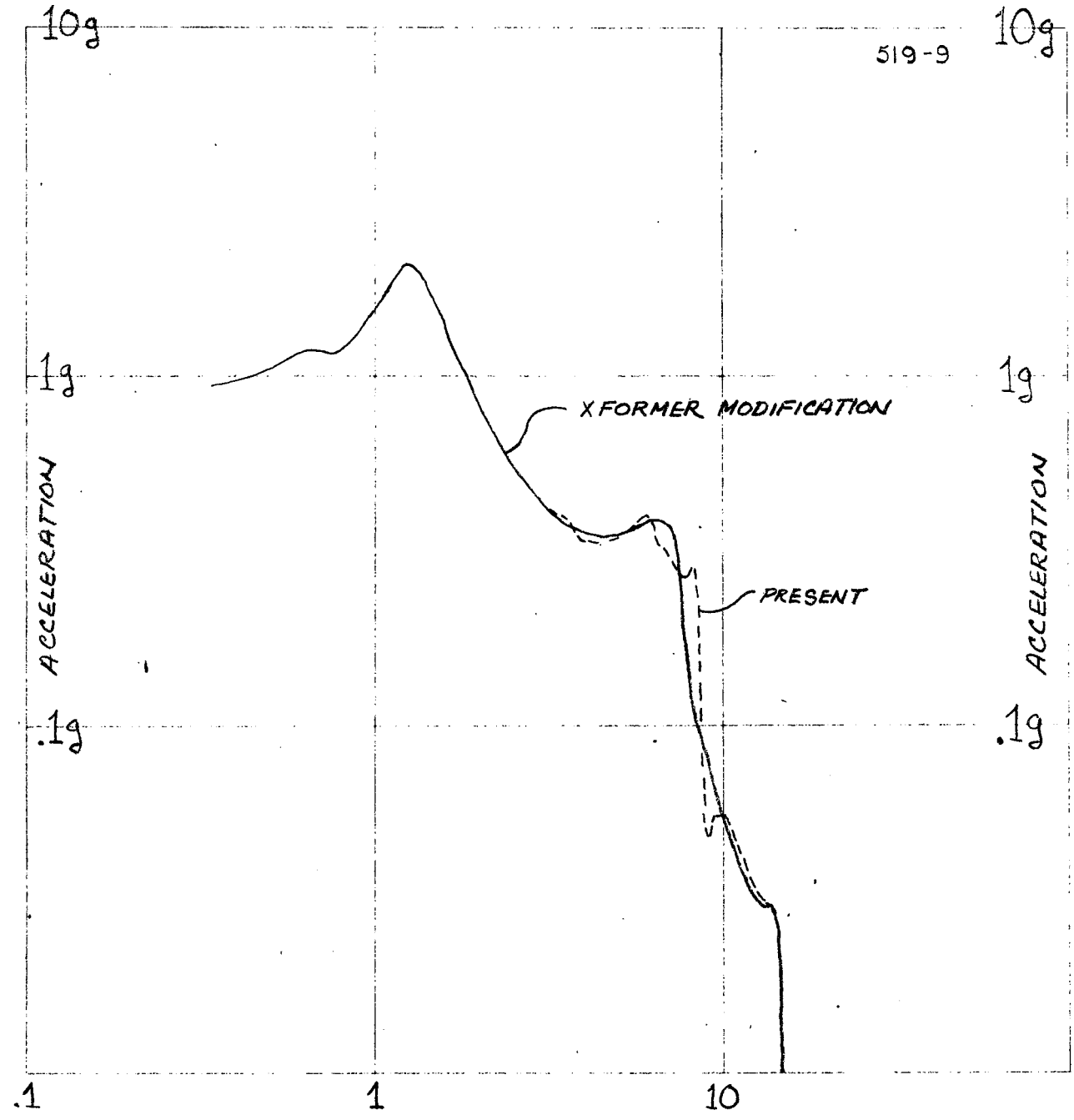

FIGURE 5.0-6

MODIFIED DESIGN

CARBODY CENTER LATERAL ACCELERATION DUE TO LATERAL INPUT

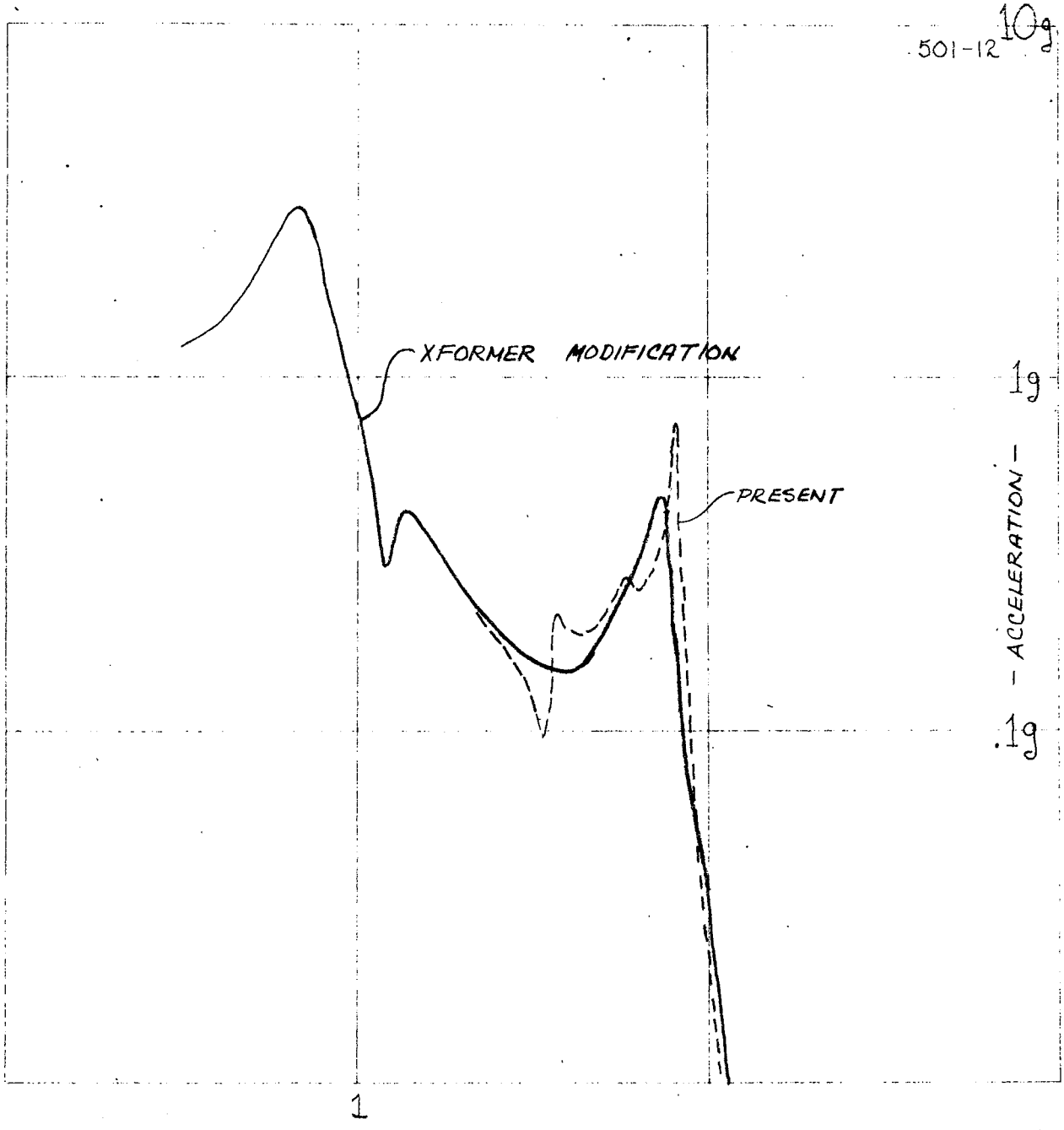

FIGURE 5.0-7

MODIFIED DESIGN

CARBODY CENTER LATERAL ACCELERATION DUE TO ROLL INPUT

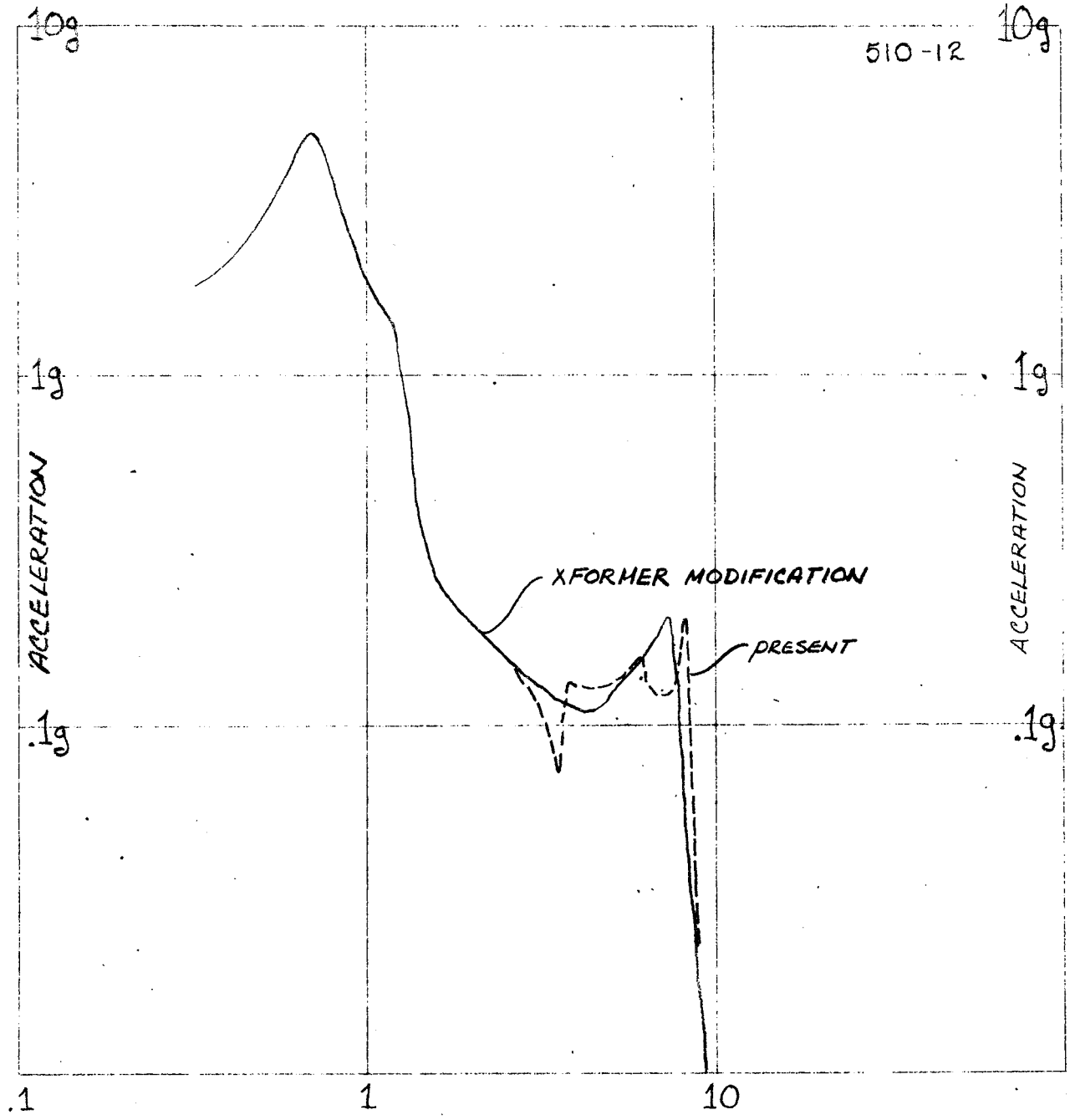

FIGURE 5.0-8

MODIFIED DESIGN

CARBODY CENTER LATERAL ACCELERATION DUE TO YAW INPUT

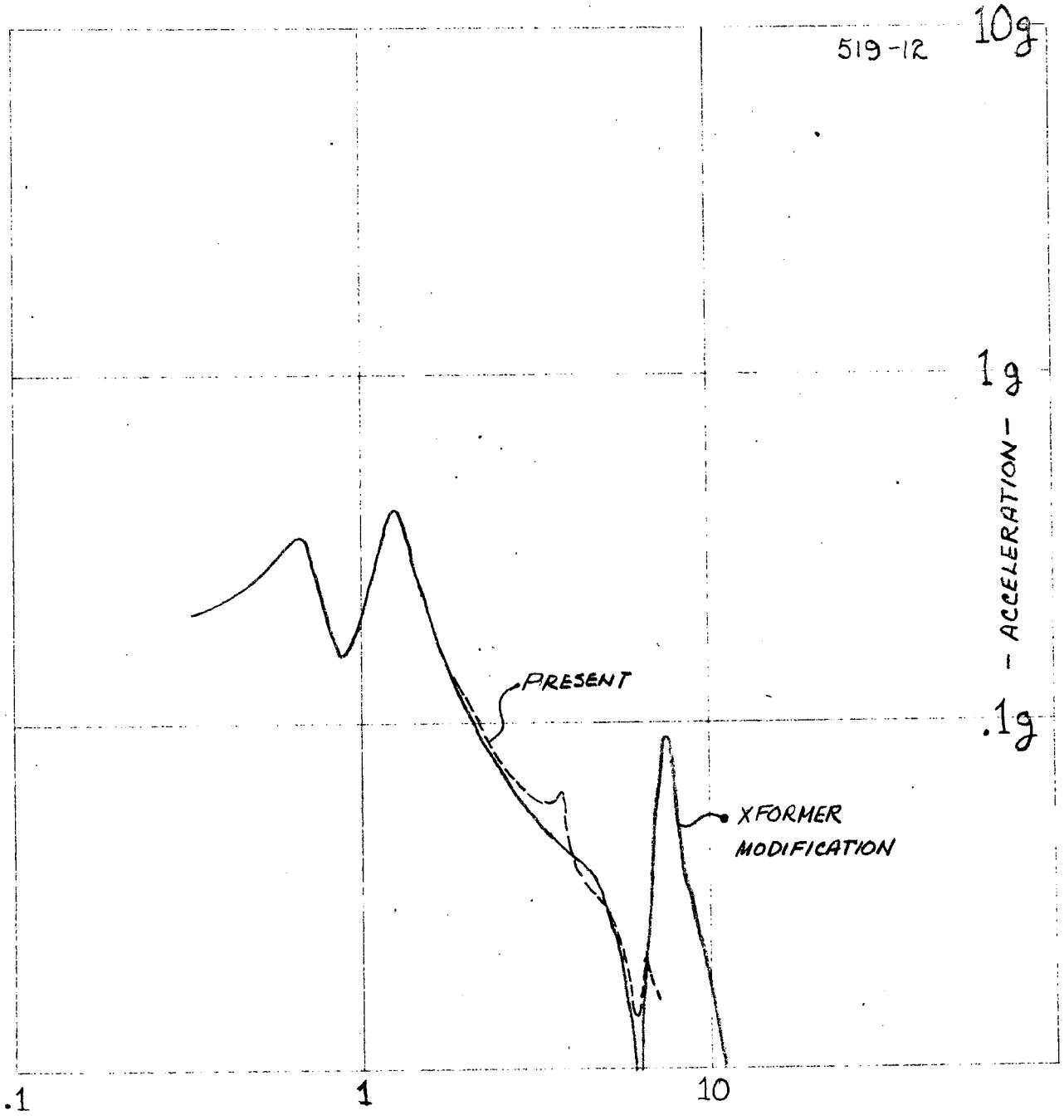

FIGURE 5.0-9

MODIFIED DESIGN

CARBODY "A END" ROLL ACCELERATION DUE TO LATERAL INPUT

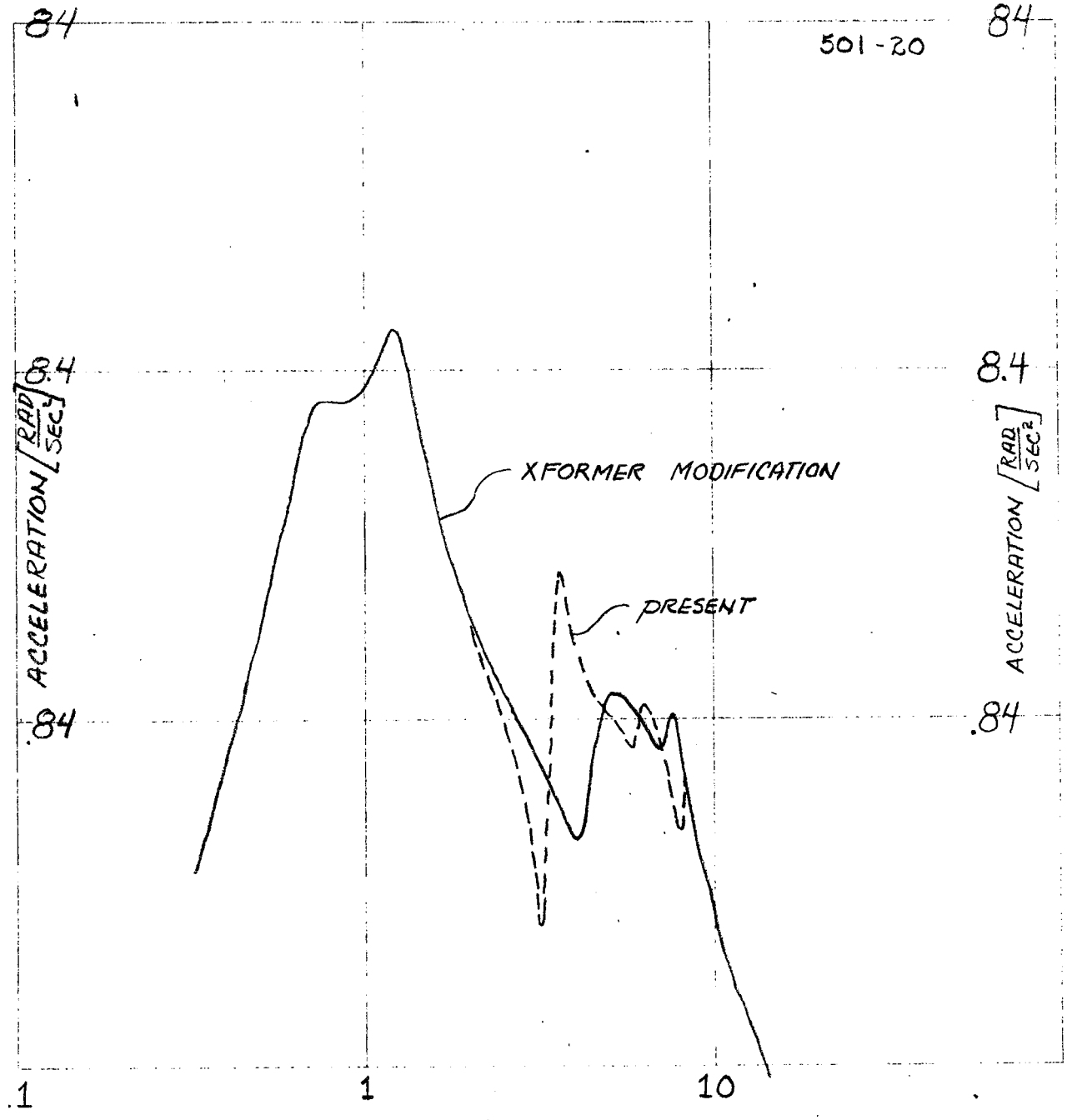

FIGURE 5.0-10

MODIFIED DESIGN

CARBODY "A END" ROLL ACCELERATION DUE TO YAW INPUT

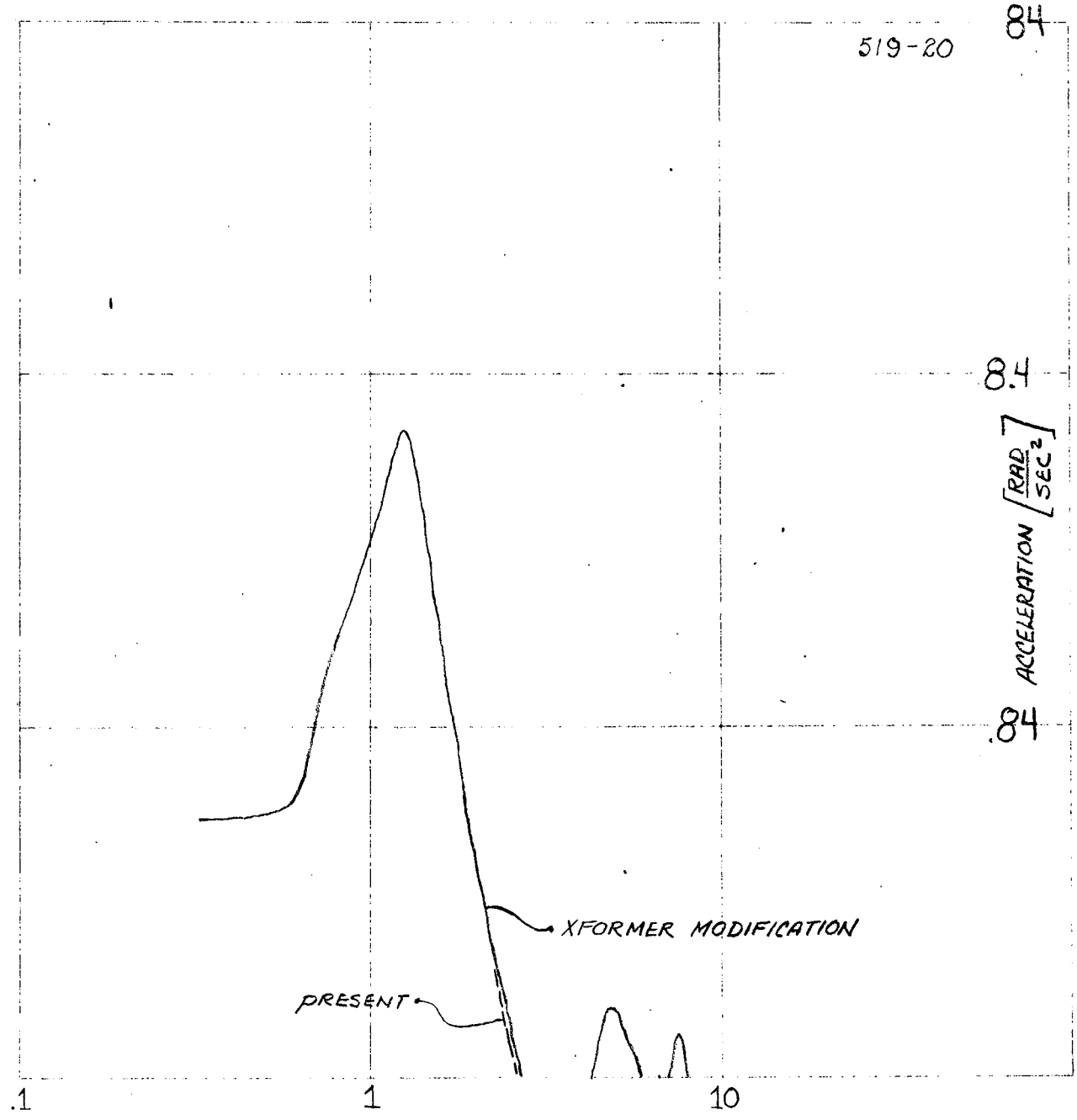

FIGURE 50-11

MODIFIED DESIGN

CARBODY "A END" ROLL ACCELERATION DUE TO ROLL INPUT

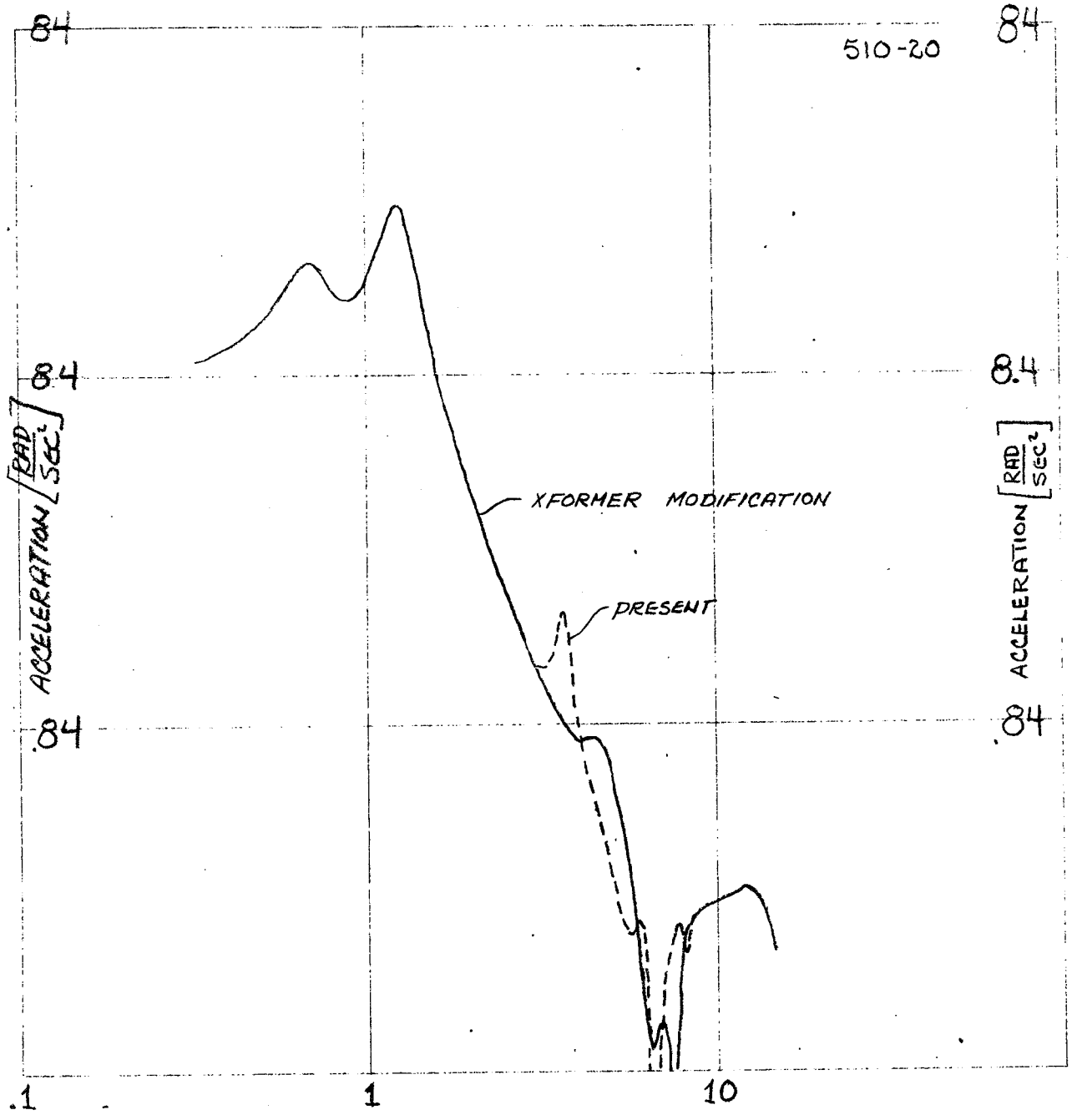

FIGURE 5.0-12

resonances are maintained. In order to maintain reasonable roll rates, the allowable truck frequency variations for the modified design were small. Increasing the truck frequency will increase wheel rail dynamic forces and reduce articulation. As a result, with the present truck the upper limit of truck frequency should be the present value of 9.5 hertz. A parametric study reported later in section 6.0 established that minor reductions in the truck frequency increase carbody acceleration response. Therefore, the modified truck is a 9.5 hertz truck with the damping in the primary and secondary suspension modified. Table 5.0-2 is a tabulation of the modified truck suspension parameters.

Figures 5.0-1,5.0-2,5.0-3, and 5.0-13 through 5.0-17 show the performance of the modified truck with the modified transformer. The modified truck significantly reduces the rigid body vertical resonances of the carbody at the expense of increasing the resonances at the carbody bending resonance. The trade-off between reduced low frequency response and increased high frequency response is due to the increased damping required to control the low frequency resonance, which increases the high frequency transmissibility. In order to eliminate this trade-off, a damper whose damping reduces with frequency is required.

5.1 Recommended Modifications to Present Metroliner

In order to implement the transformer and truck modifications, the transformer suspension system and the vertical truck secondary suspension spring must be replaced. Additionally,

TABLE 5.0-2

MODIFIED TRUCK SUSPENSION SYSTEM PARAMETERS

Primary Suspension System per Truck	Present	Modified
Vertical Stiffness	109,000#/in.	109,000#/in.
Lateral Stiffness	55,800#/in.	55,800#/in.
Longitudinal Stiffness	55,800#/in.	96,000#/in.
Vertical Damping	260#sec./in.	560#/in.
Lateral Damping	260#sec./in.	260#/in.
Longitudinal Damping	260#sec./in.	784#/in.
Secondard Suspension System per Truck		
Vertical Stiffness	7,740#/in.	5,500#/in.
Lateral Stiffness	3,386#/in.	3,386#/in.
Longitudinal Stiffness	96,660#/in.	96,600#/in.
Vertical Damping	115#sec./in.	280#sec./in.
Lateral Damping	173#sec./in.	173#sec./in.
Longitudinal Damping	78#sec./in.	780#sec./in.

MODIFIED DESIGN

TRUCK FRAME VERTICAL ACCELERATION DUE TO VERTICAL INPUT

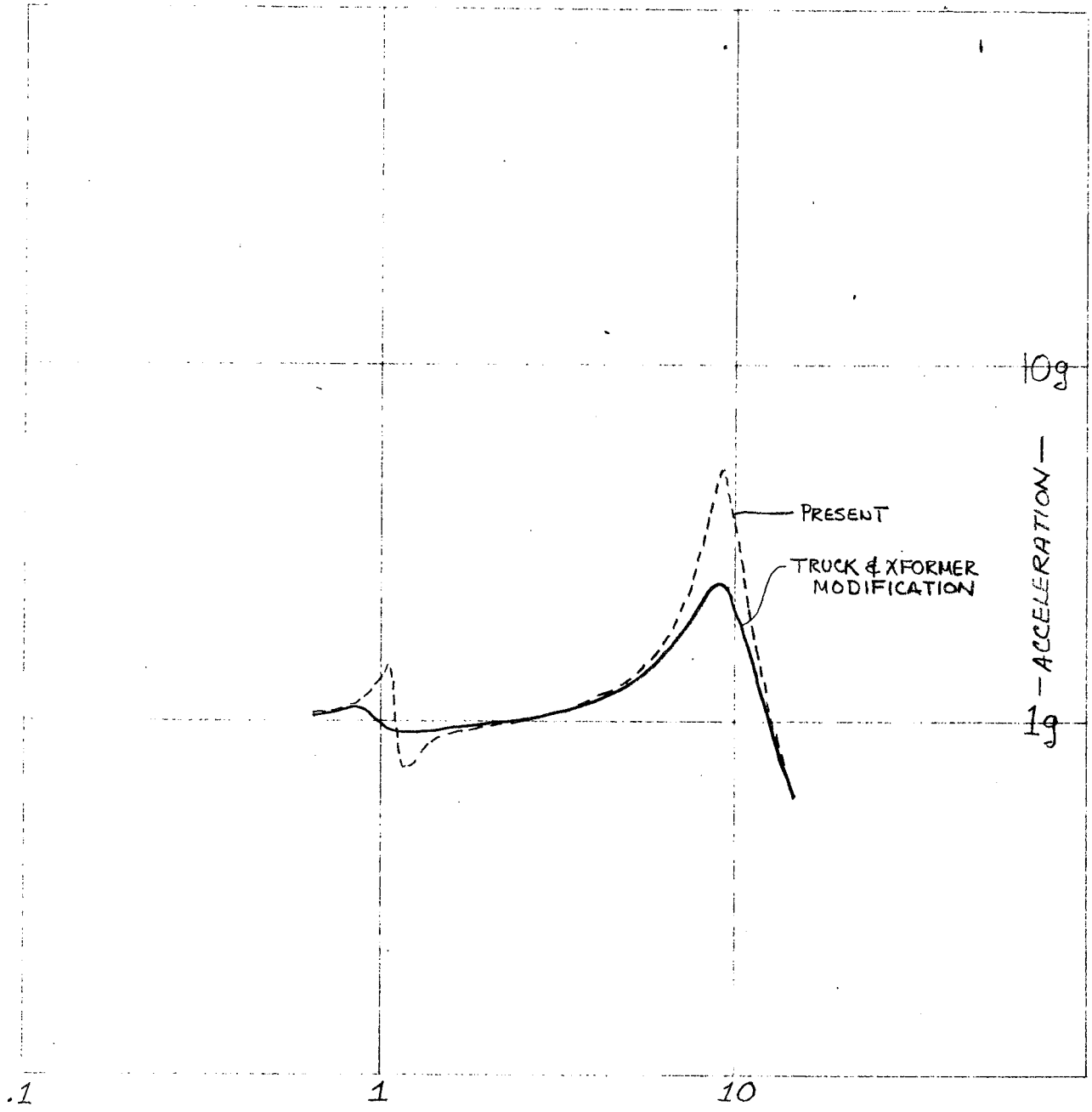

FIGURE 5.0-13

MODIFIED DESIGN

TRUCK FRAME LONGITUDINAL ACCELERATION DUE TO PITCH INPUT

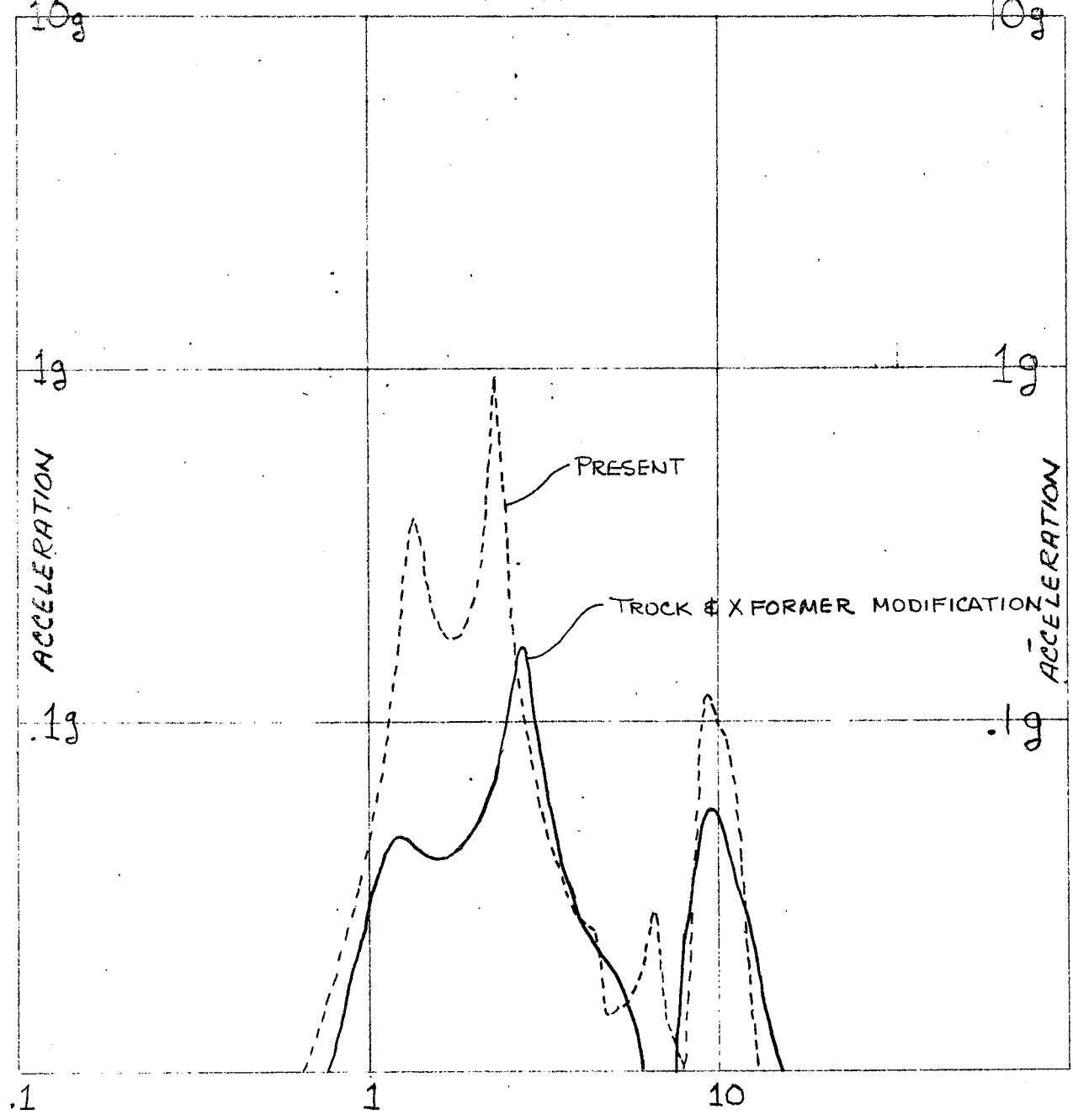

FIGURE 5.0-14

MODIFIED DESIGN

CARBODY "A END" VERTICAL ACCELERATION DUE TO PITCH INPUT

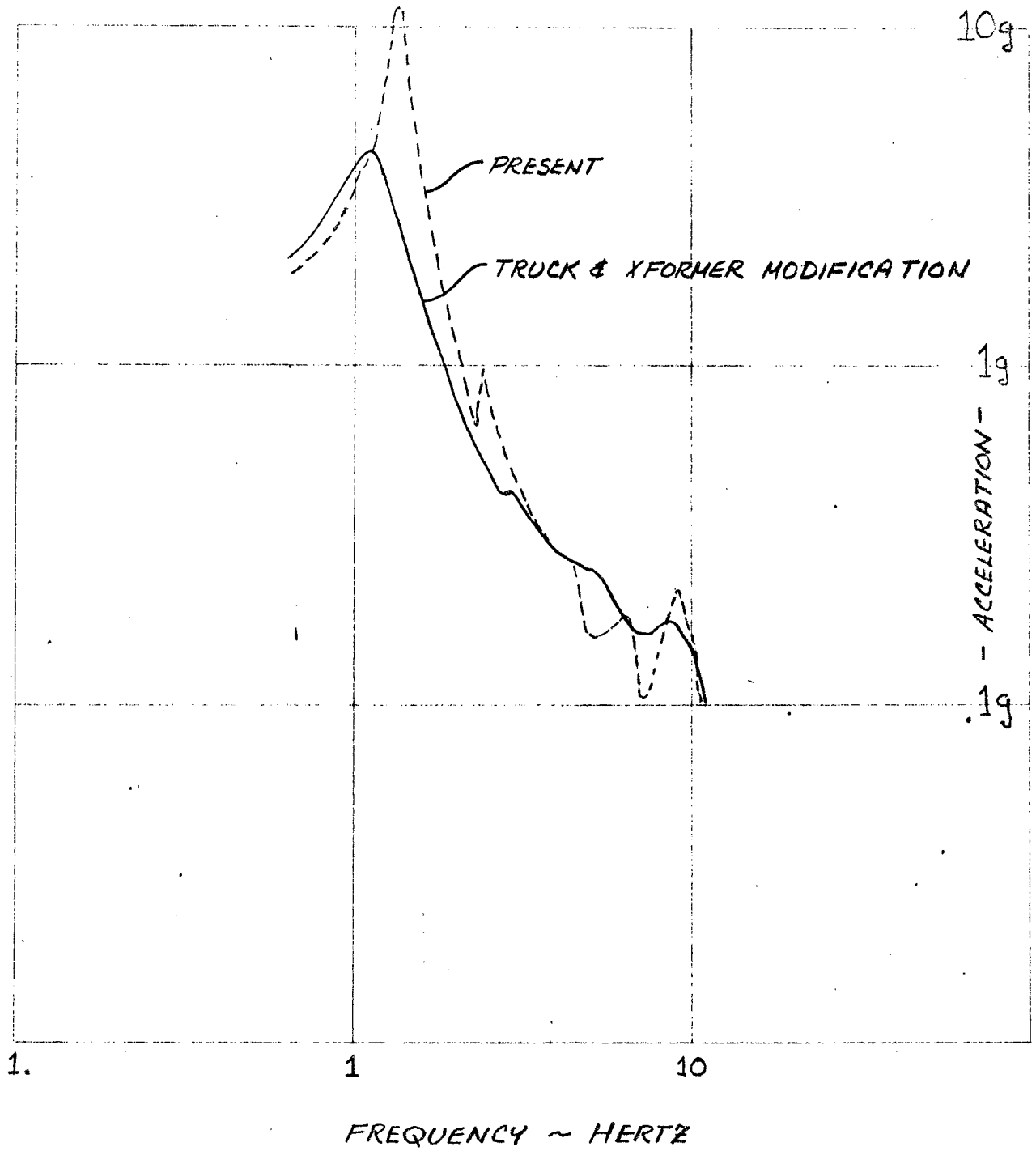

FIGURE 5.0-15

MODIFIED DESIGN

CARBODY CENTER VERTICAL ACCELERATION DUE TO PITCH INPUT

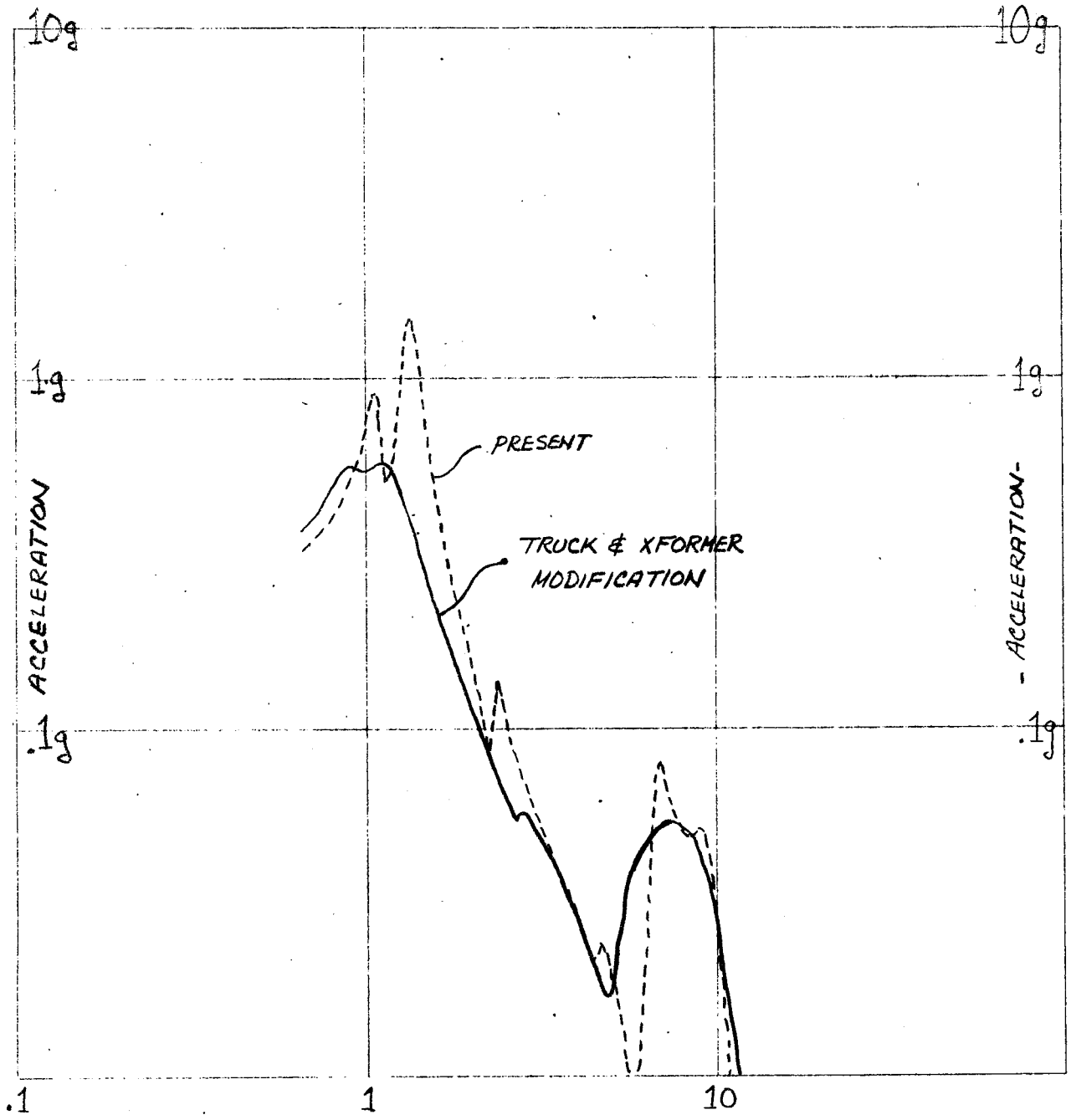

FIGURE 5.0-16

MODIFIED DESIGN

CARBODY LONGITUDINAL ACCELERATION DUE TO PITCH INPUT

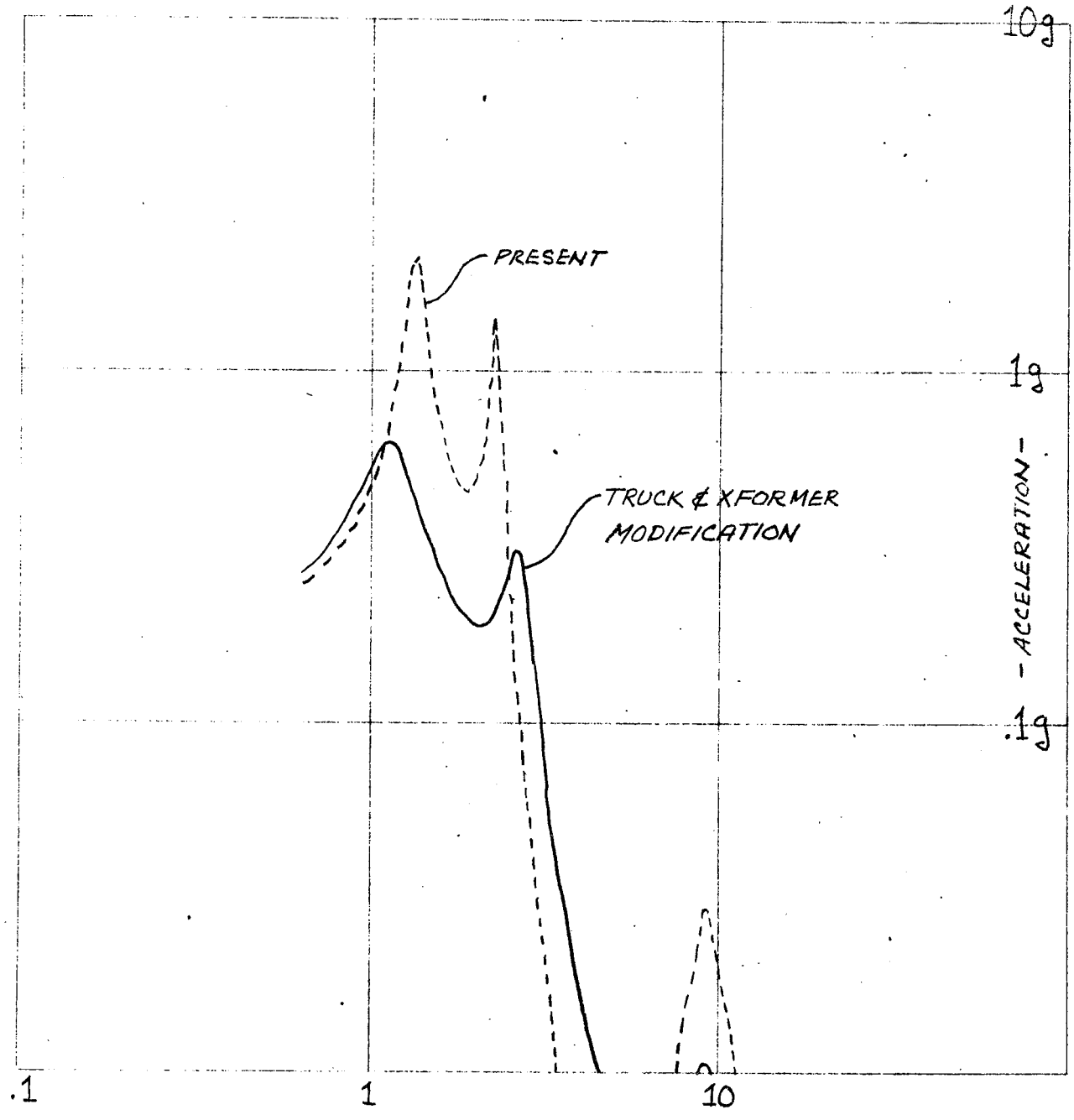

FIGURE 5.0-17

more damping will be required in the vertical and longitudinal primary and secondary suspension systems.

The first recommended modification is to replace the transformer suspension. This will reduce the response of the carbody to the dominate lateral and vertical track inputs discussed in section 3.4. The new transformer suspension will probably require either friction or hydraulic dampers, since the amount of damping in elastomeric materials is not sufficient.

The second recommended modification is to add dampers to the anchor rods as the benefits longitudinally are appreciable and the modification relatively simple.

Before completing the truck modifications by replacing the bolster spring and adding damping, some consideration should be given to replacement with a diaphragm-type air spring and a damper spring combination to give reduced damping at high frequencies. The use of a diaphragm-type air spring will eliminate the spring surge and will provide a more uniform buildup of lateral stiffness to minimize the the transistion into the lateral suspension stops. In the consideration of an air spring, particular attention should be placed on its performance when deflated to insure safe operation.

6.0 NEW TRUCK DESIGN

For the development of the new truck, the transformer suspension system was modified as described in section 5.0.

The allowable variation of the vertical truck frequencies in the development of the new truck was not limited by roll stiffness consideration, since it was assumed that in a new truck design roll stabilizing devices could be incorporated which would not affect the vertical stiffness of the truck suspension systems. In addition, the vertical truck frequency was not limited by wheel-rail dynamic forces and articulation, since it was assumed in a new design, reduction in unsprung weight and alternate methods of articulation might offset the effects of a high frequency truck.

The truck frame weight of the new truck was assumed comparable to the present truck, since the new truck would incorporate the existing traction equipment and the static and dynamic load requirements of the new truck are identical to the present truck.

The effect of vertical truck frequency on the vertical railcar performance is shown in Figures 6.0-1 and 6.0-2. For this investigation 4.0 hertz, 6.6 hertz, 9.5 hertz and 18 hertz trucks were simulated. The truck damping was optimized for each configuration. For comparison purposes the carbody rigid body resonance frequency and damping were held constant. As the vertical truck frequency is reduced from the present value of 9.5 hertz, the peak acceleration in the 4 hertz to 10 hertz range in the center and end of the carbody increases first and then reduces to a value considerably lower than present value. As a result, when

EFFECT OF TRUCK FREQUENCY

CARBODY "A END" VERTICAL ACCELERATION DUE TO VERTICAL INPUT

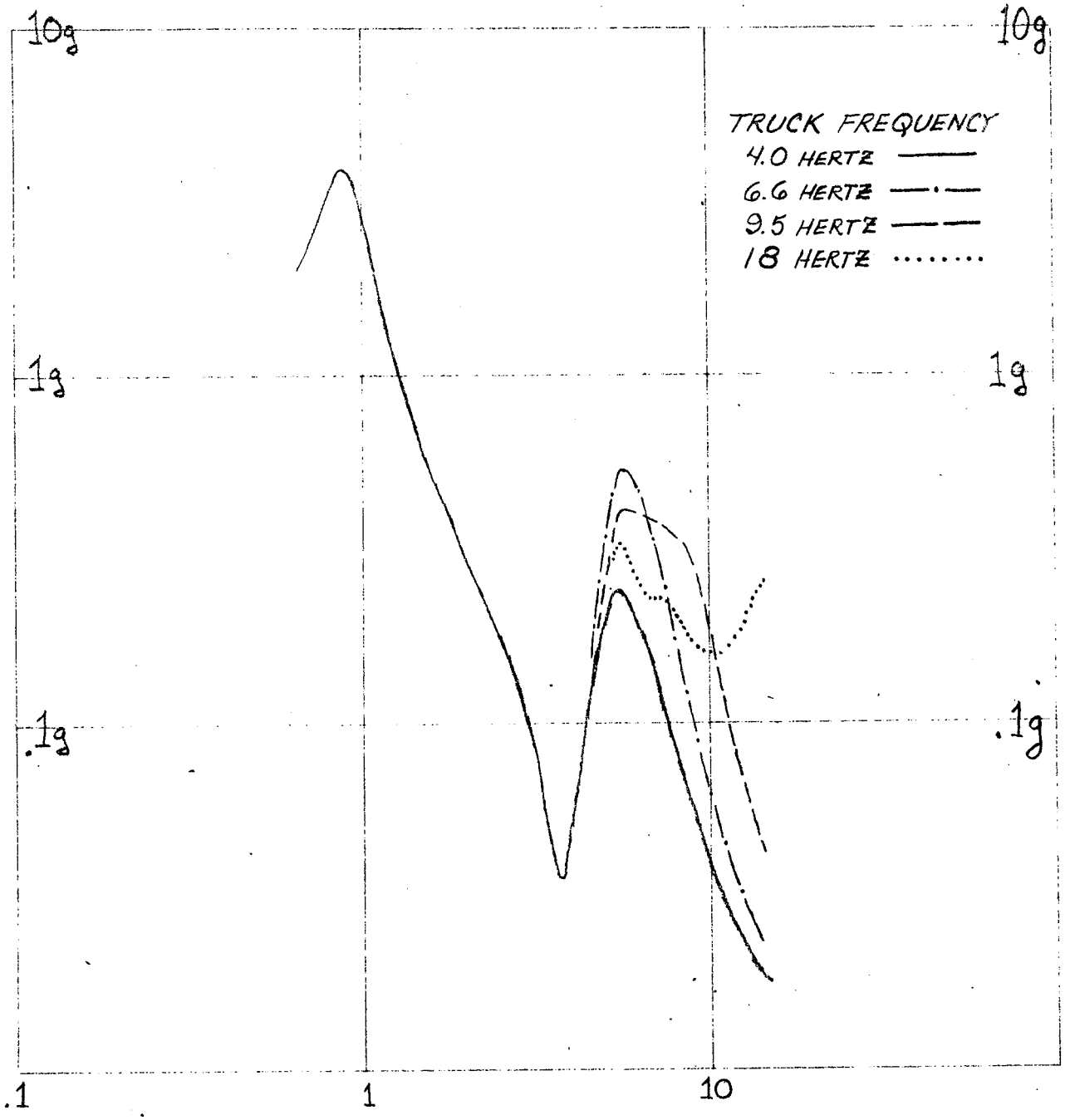

FIGURE 6.0-1

EFFECT OF TRUCK FREQUENCY

CARBODY CENTER VERTICAL ACCELERATION DUE TO VERTICAL INPUT

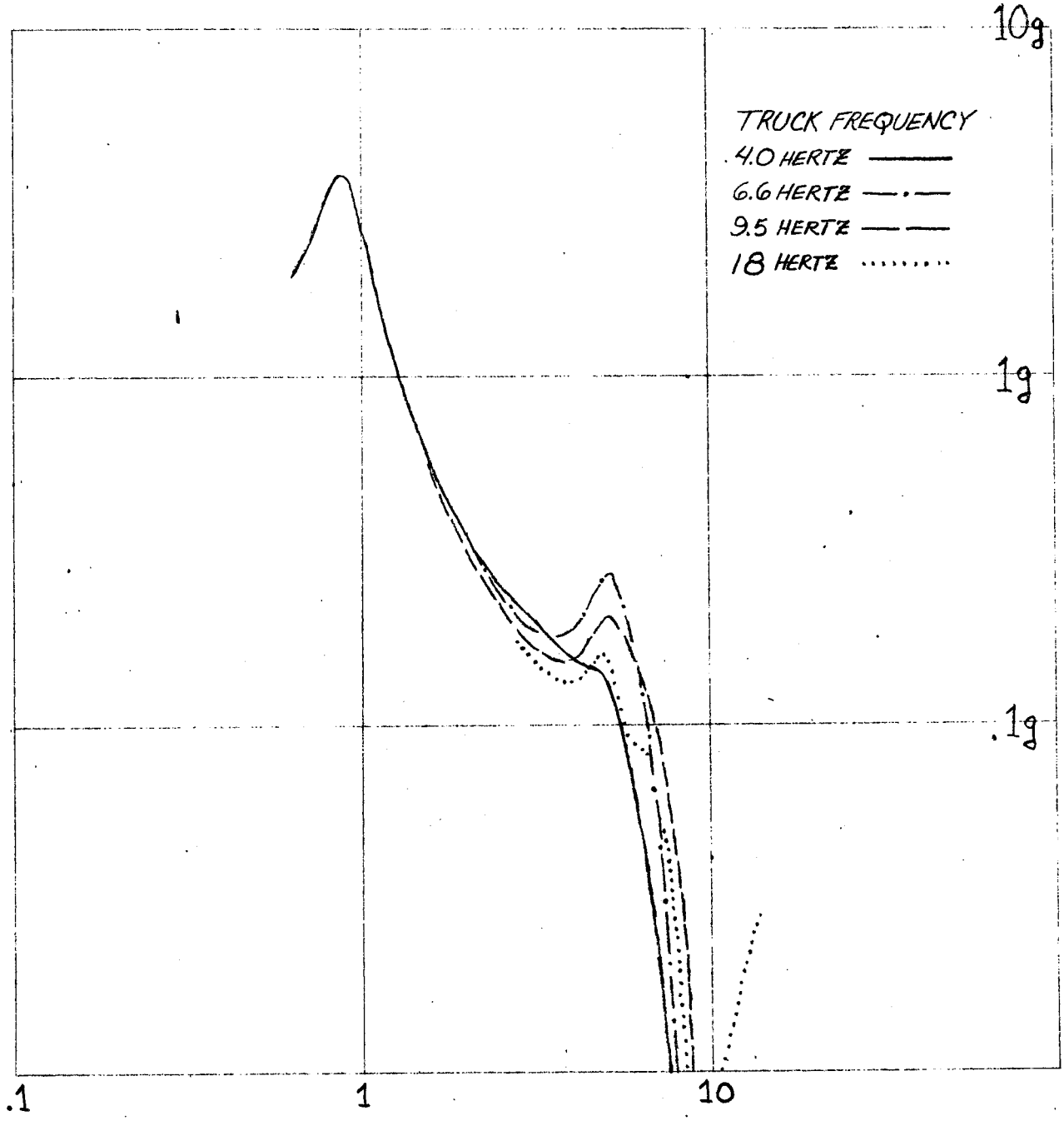

FIGURE 6.0-2

considering the modified design, small reductions in the vertical truck frequency are undesirable. As the vertical truck frequency increases above the present value of 9.5 hertz, the peak accelerations in the 4 hertz to 10 hertz range in the center and end of the carbody reduced, at the expense of increased acceleration above 10 hertz.

As a result of this study, it was concluded that the new truck should have a vertical truck frequency as low as practical and a roll stabilizing device must be incorporated in the new truck to maintain the required roll stiffness of the truck suspension system.

Results of the lateral simulation indicated that as in the vertical case, the lateral truck frequency should be as low as practical. The achievement of the low frequency lateral truck, assumes dynamic stability can be maintained.

Table 6.0-1 is a tabulation of the truck suspension parameters for the recommended new low frequency truck configuration. For this design a roll stabilizing device is simulated in the primary suspension by increasing the lateral spacing of the primary springs from 79 inches to 200 inches.

In Figure 6.0-3 through 6.0-30 the vertical and lateral performance of the recommended low frequency truck are compared to the present truck. On the same figures, the performance of the high frequency truck is shown for comparison purposes. Table 6.0-2 is a tabulation of the truck suspension parameters for the high frequency truck.

TABLE 6.0-1

RECOMMENDED LOW FREQUENCY TRUCK SUSPENSION PARAMETERS

Primary Suspension System per Truck	Present	Low Freq. Truck
Vertical Stiffness	109,000#/in.	10,700#/in.
Lateral Stiffness	55,800#/in.	13,980#/in.
Longitudinal Stiffness	55,800#/in.	96,660#/in.
Vertical Damping	260#sec./in.	686#/in.
Lateral Damping	260#sec./in.	570#/in.
Longitudinal Damping	260#sec./in.	780#/in.
Secondard Suspension System per Truck		
Vertical Stiffness	7,740#/in.	10,700#/in.
Lateral Stiffness	3,386#/in.	4,800#/in.
Longitudinal Stiffness	96,660#/in.	96,600#/in.
Vertical Damping	115#sec./in.	343#sec./in.
Lateral Damping	173#sec./in.	285#sec./in.
Longitudinal Damping	78#sec./in.	780#sec./in.

NEW TRUCK DESIGNS

TRUCK FRAME

VERTICAL ACCELERATION DUG TO VERTICAL INPUT

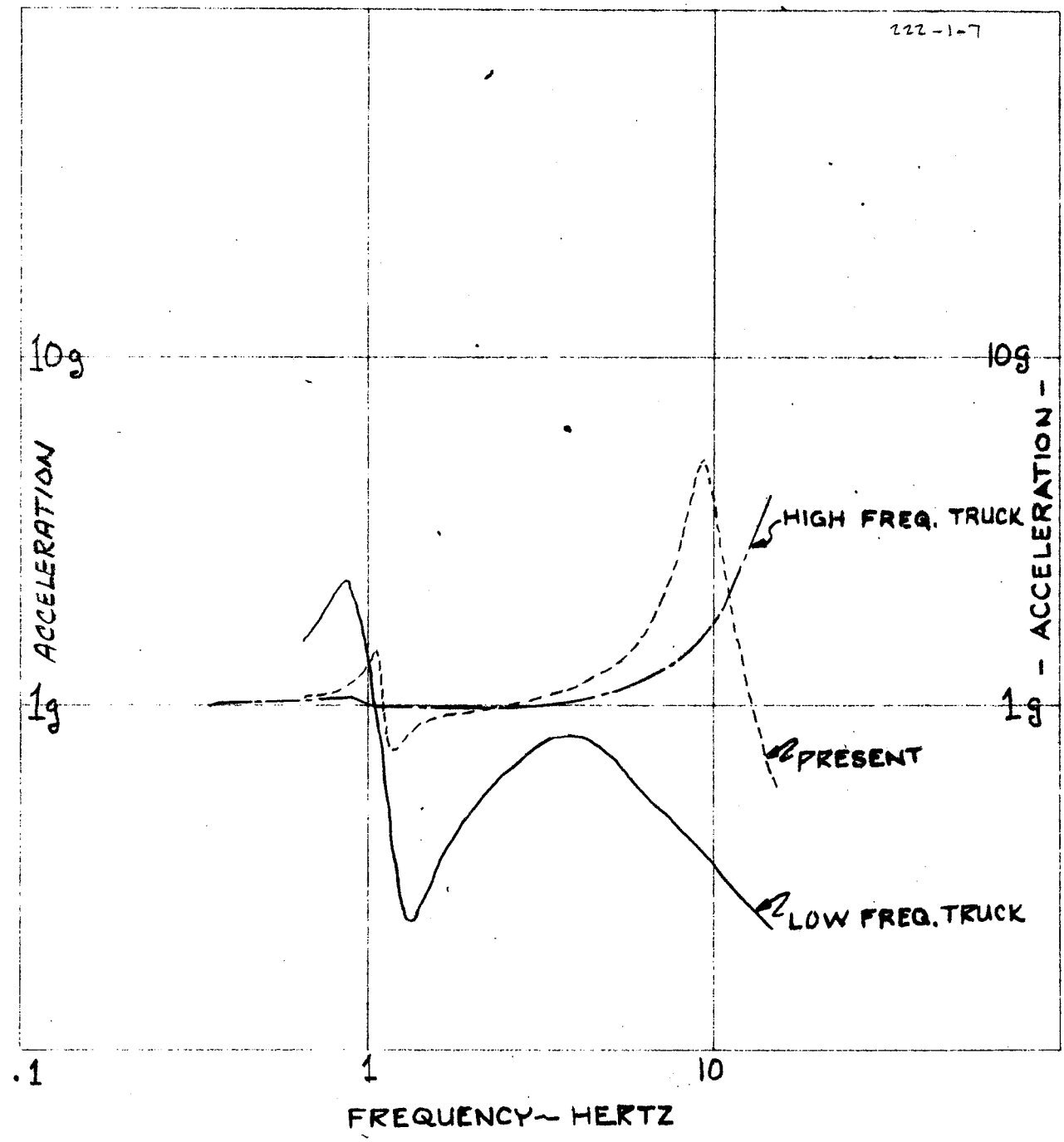

FIGURE 6.0-3

NEW TRUCK DESIGNS

TRUCK FRAME

LONGITUDINAL ACCELERATION DUE TO PITCH INPUT

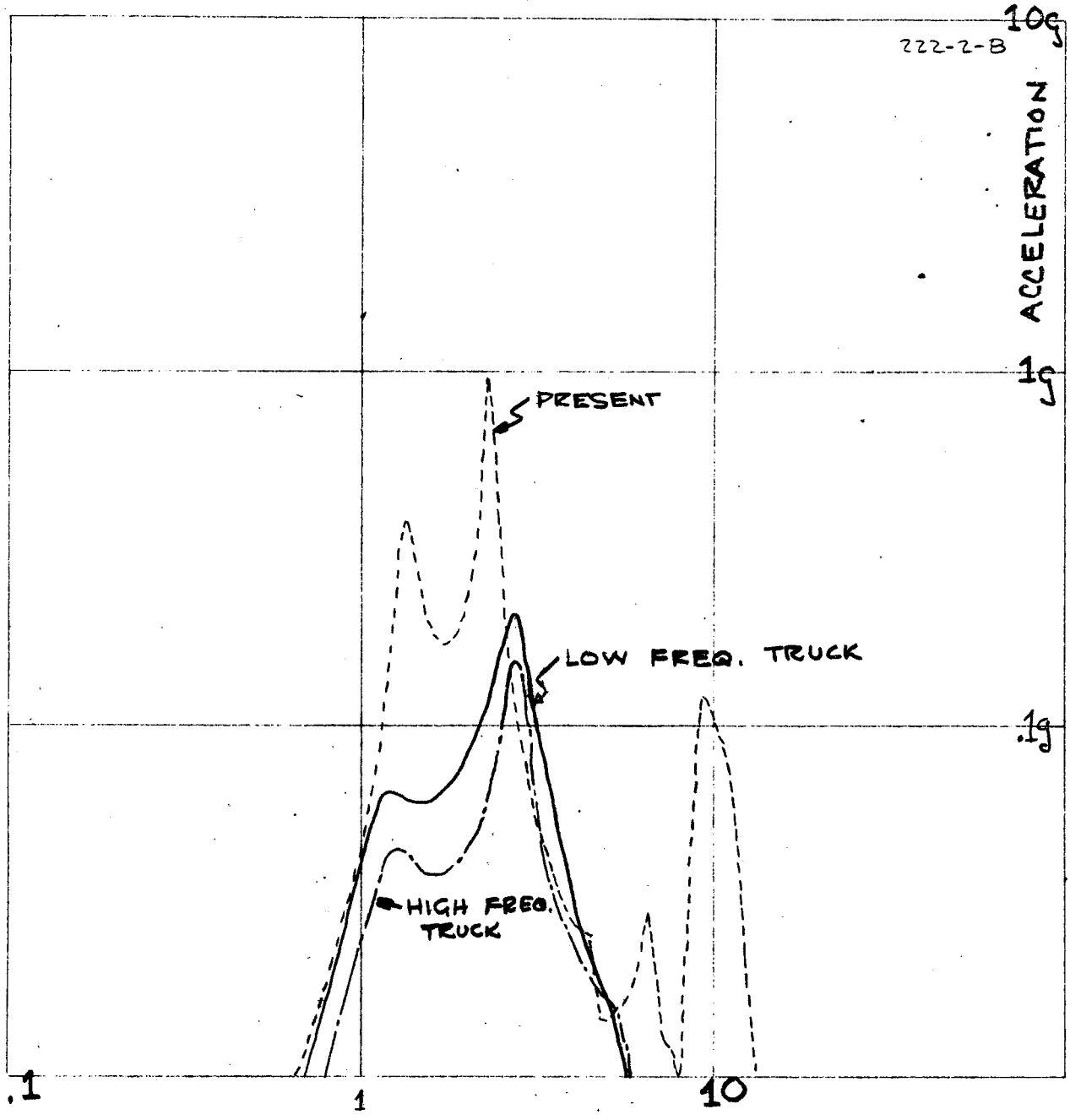

FIGURE 6.0-4

NEW TRUCK DESIGNS

CARBODY "A" END

VERTICAL ACCELERATION DUE TO VERTICAL INPUT

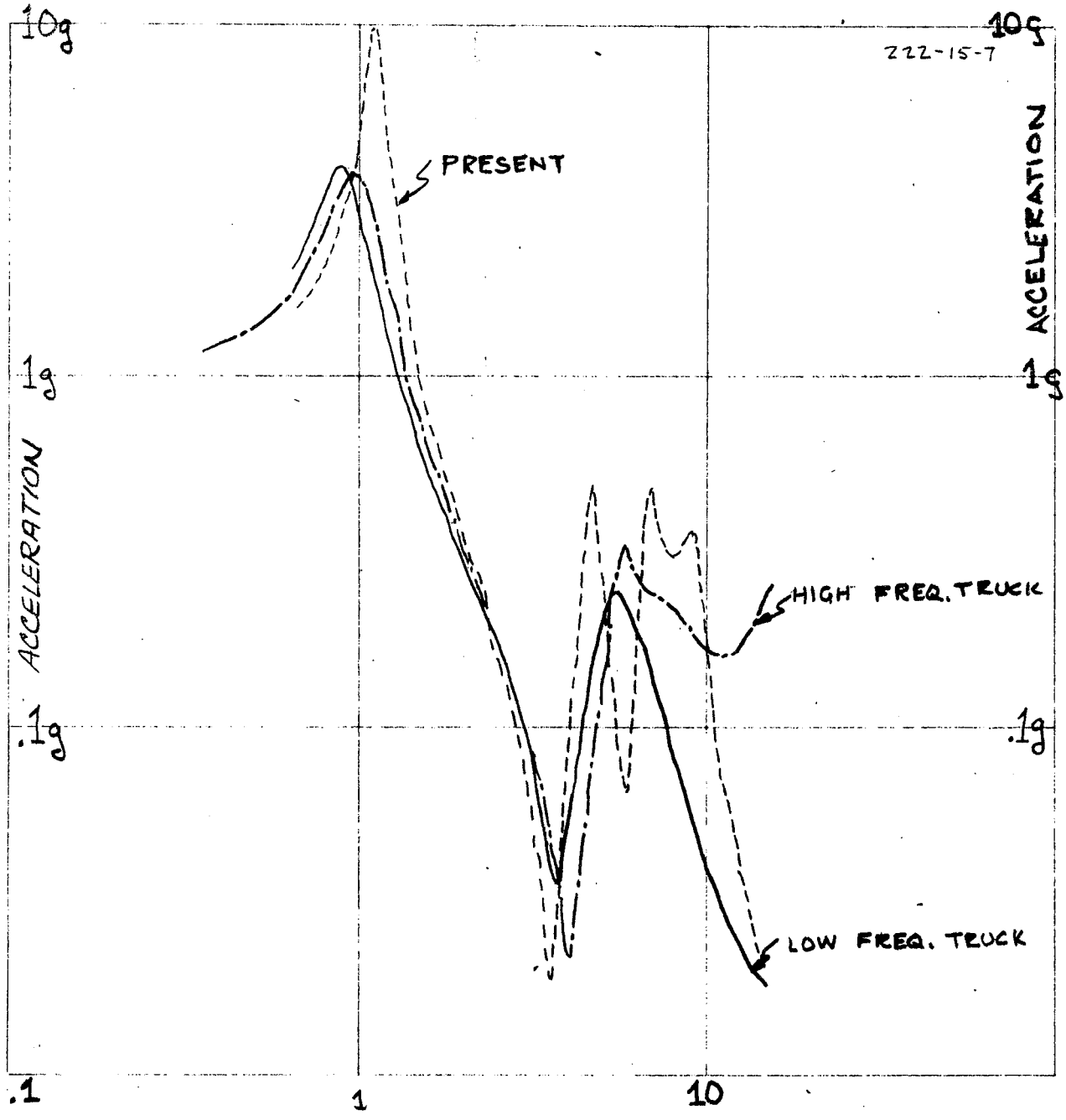

FIGURE 6.0-5

NEW TRUCK DESIGNS

CARBODY "A" END

VERTICAL ACCELERATION DUE TO PITCH INPUT

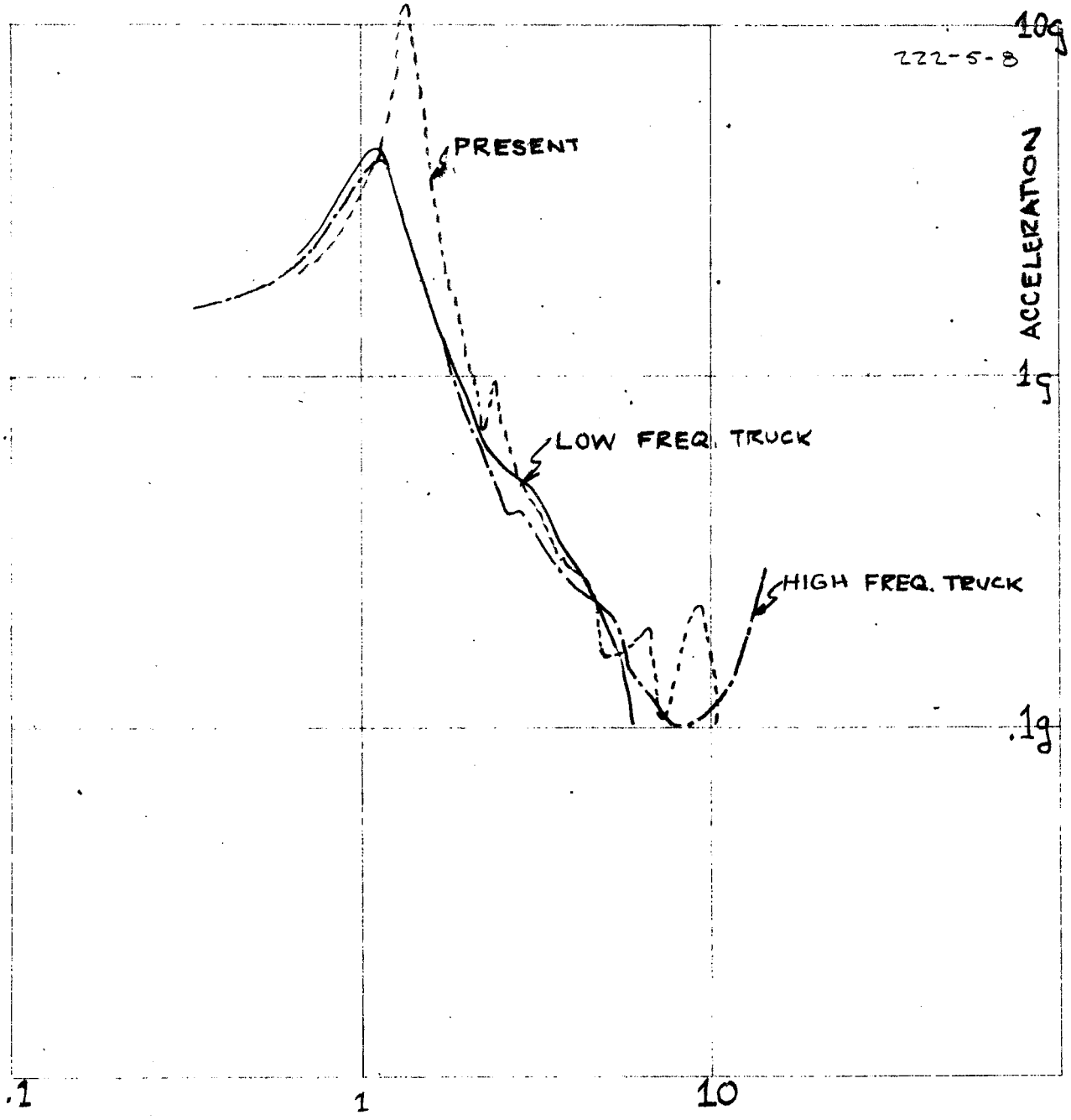

FIGURE 6.0-6

NEW TRUCK DESIGNS

CARBODY CENTER

VERTICAL ACCELERATION DUE TO VERTICAL INPUT

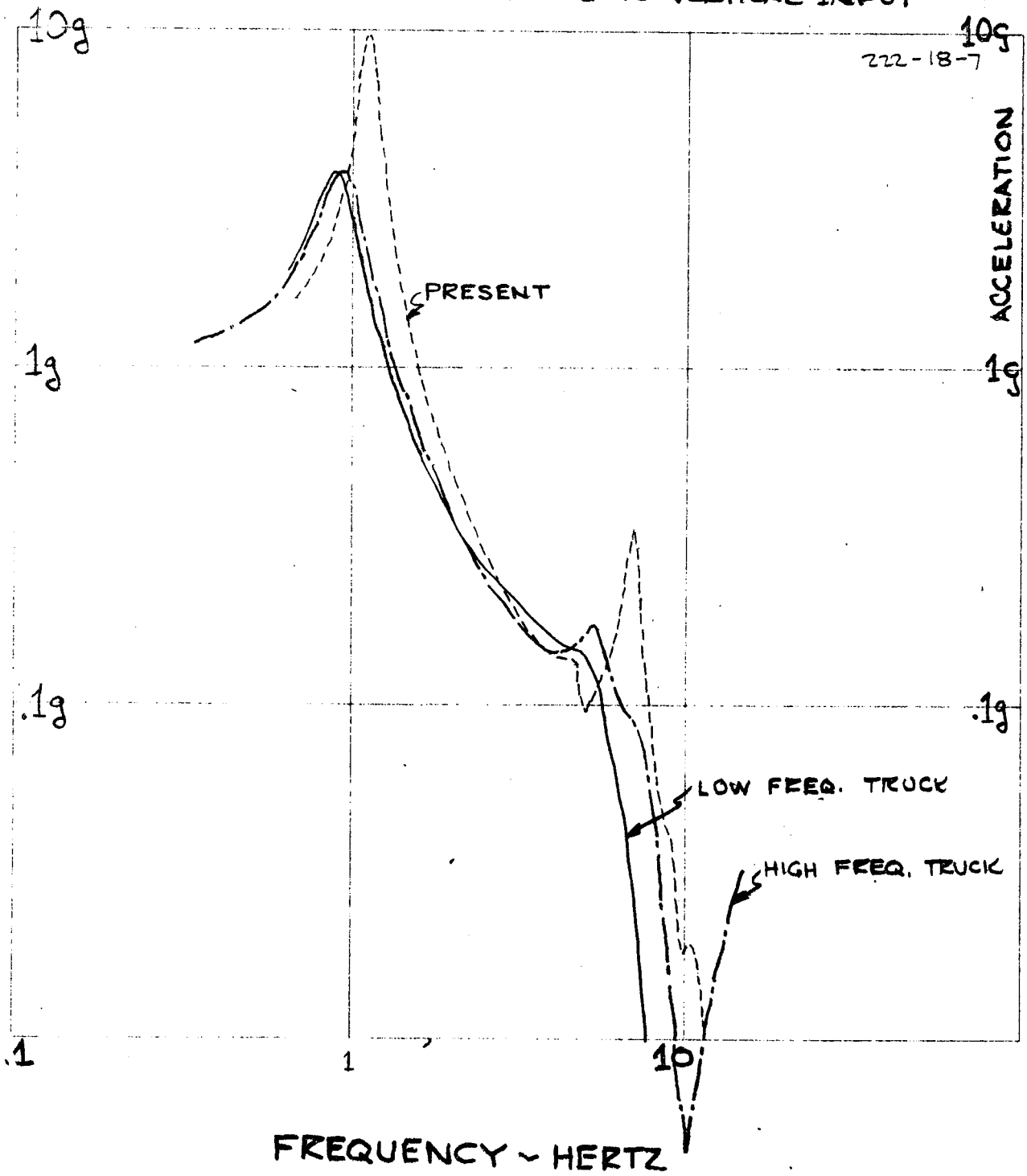

FIGURE 6.0-7

NEW TRUCK DESIGNS

CARBODY CENTER

VERTICAL ACCELERATION DUE TO PITCH INPUT

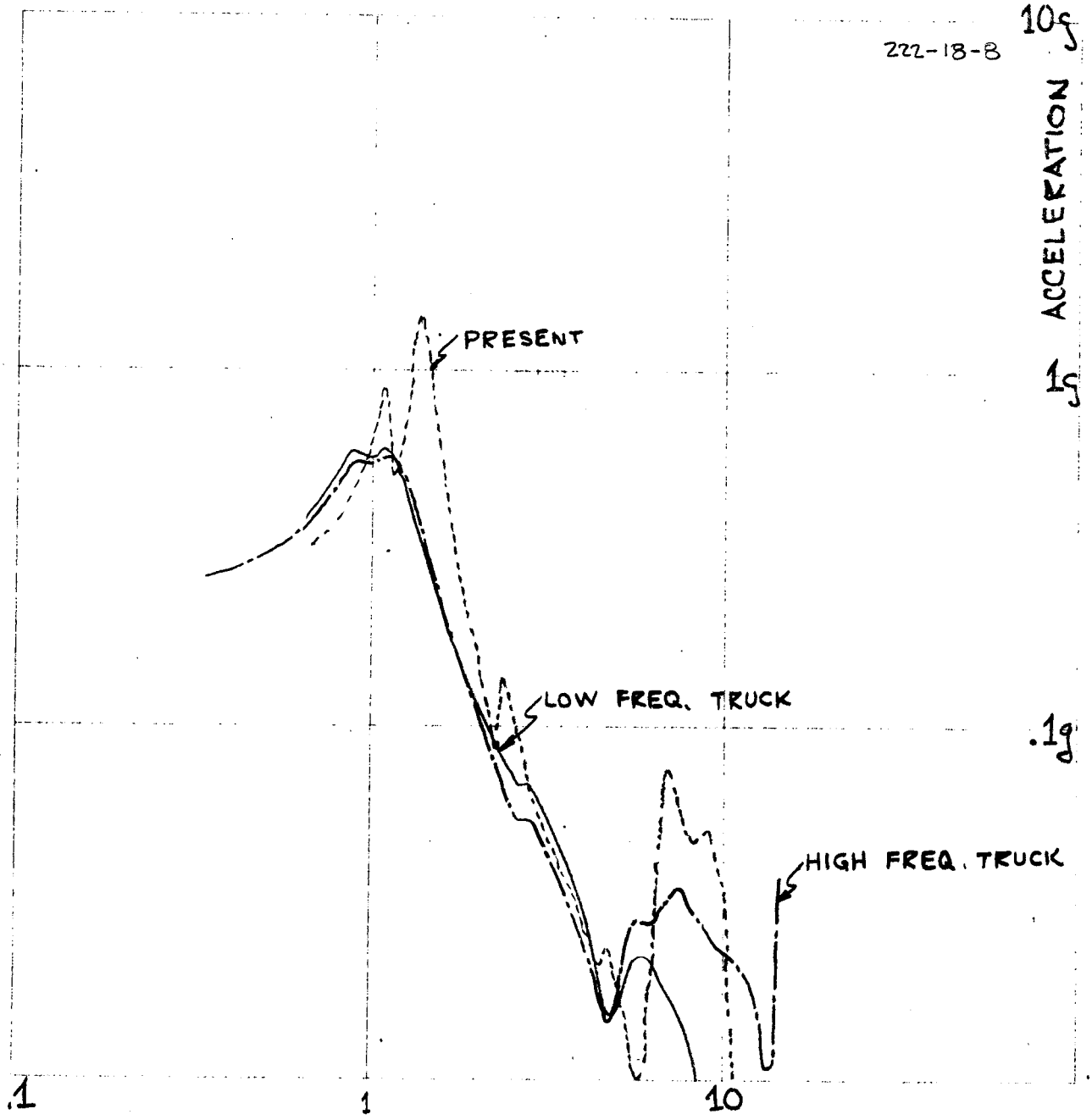

FIGURE 6.0-8

NEW TRUCK DESIGNS

CARBODY

LONGITUDINAL ACCELERATION DUE TO PITCH INPUT

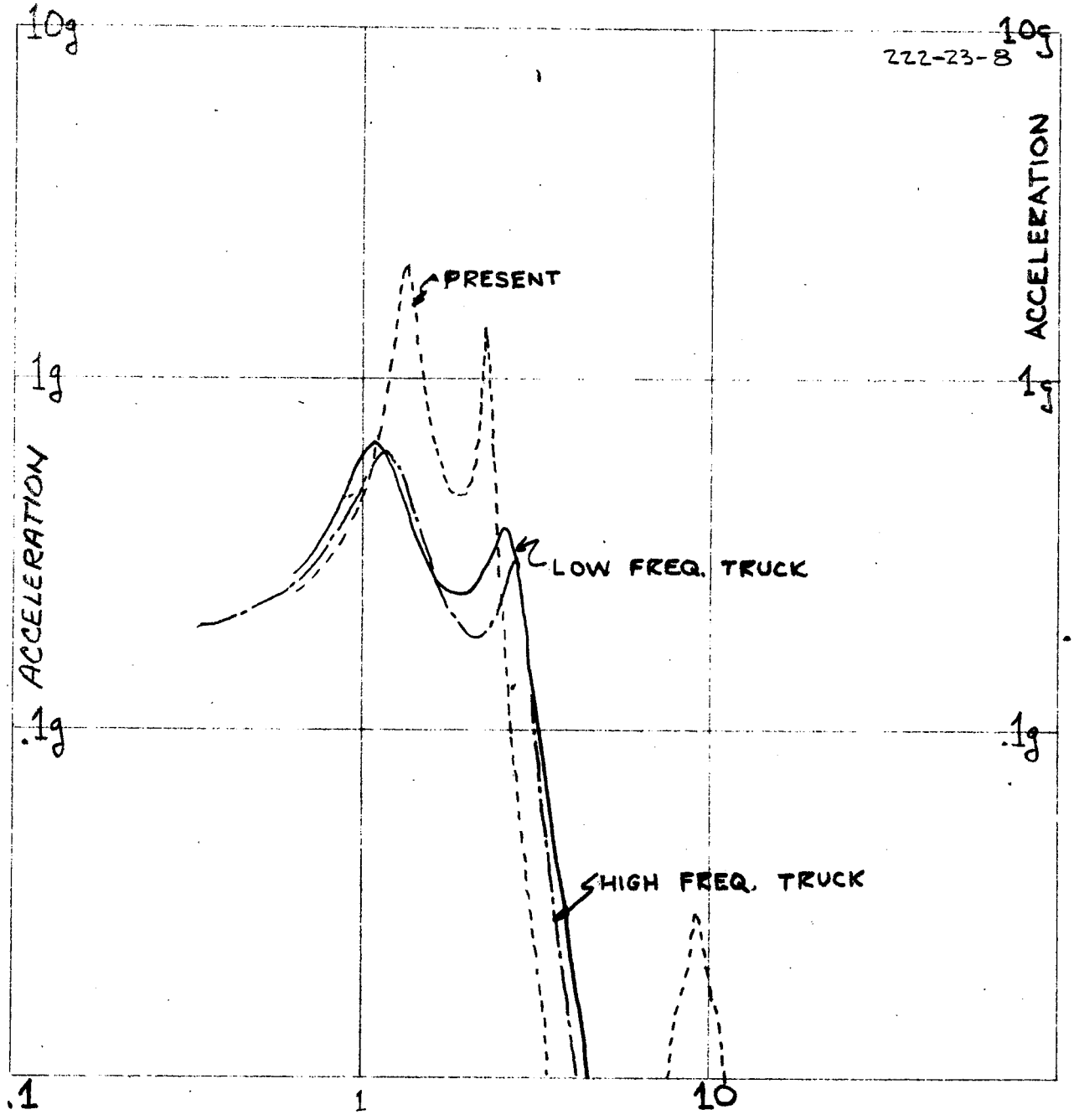

FIGURE 6.0-9

NEW TRUCK DESIGNS

TRANSFORMER

VERTICAL ACCELERATION DUE TO VERTICAL INPUT

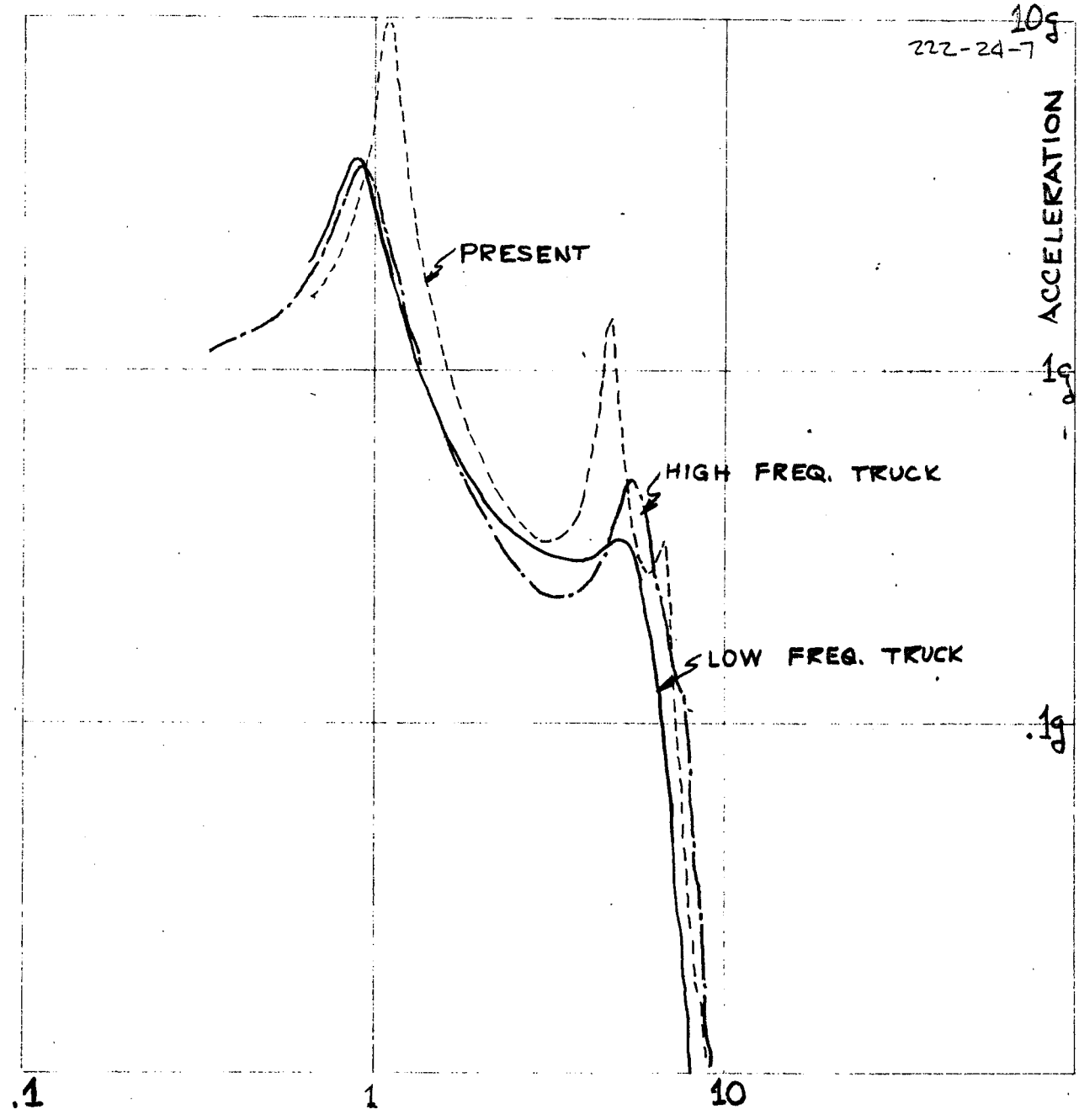

FIGURE 6.0-10

NEW TRUCK DESIGNS

TRANSFORMER

VERTICAL ACCELERATION DUE TO PITCH INPUT

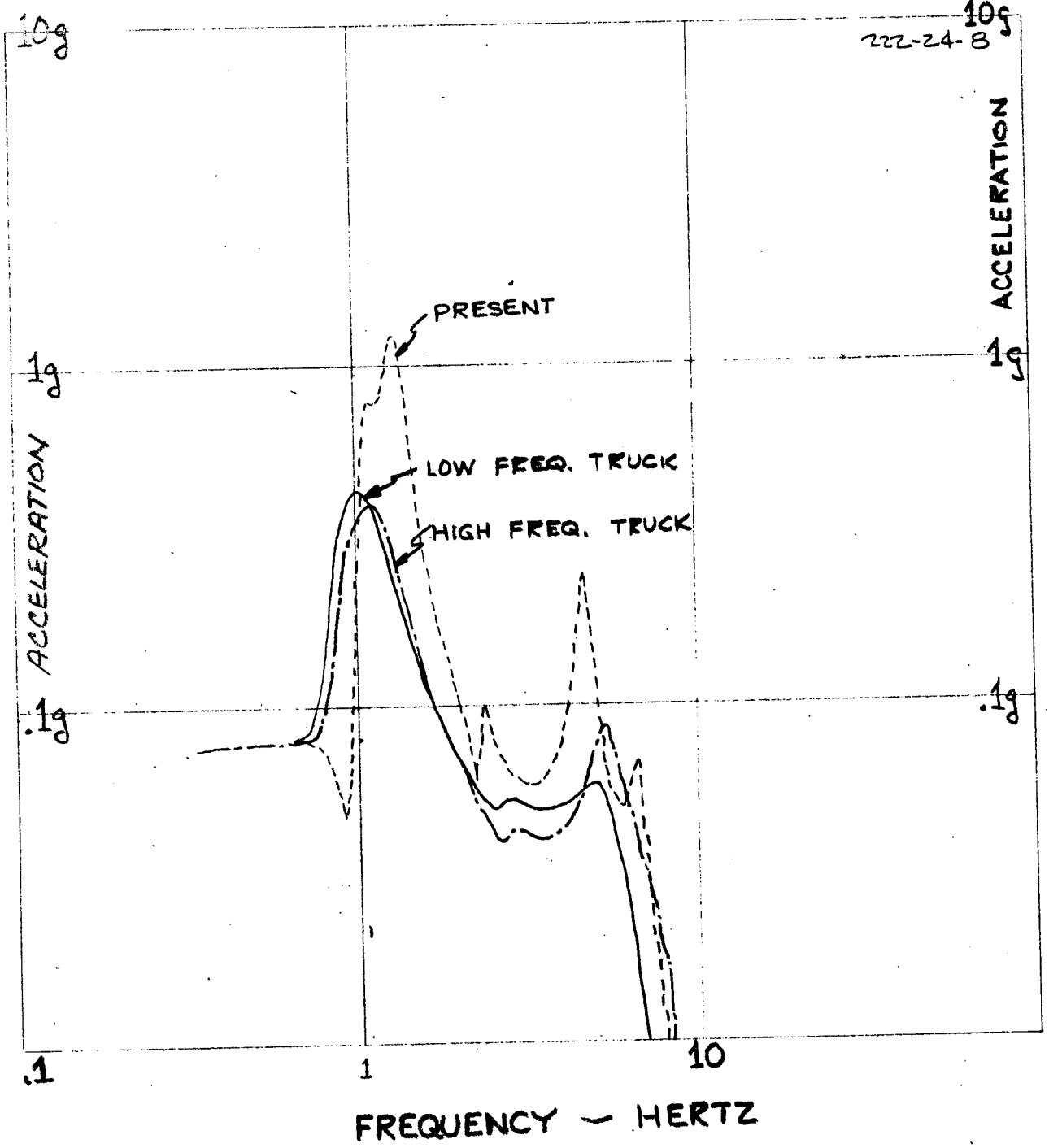

FIGURE 6.0-11

NEW TRUCK DESIGNS

TRANSFORMER

LONGITUDINAL ACCELERATION DUE TO PITCH INPUT

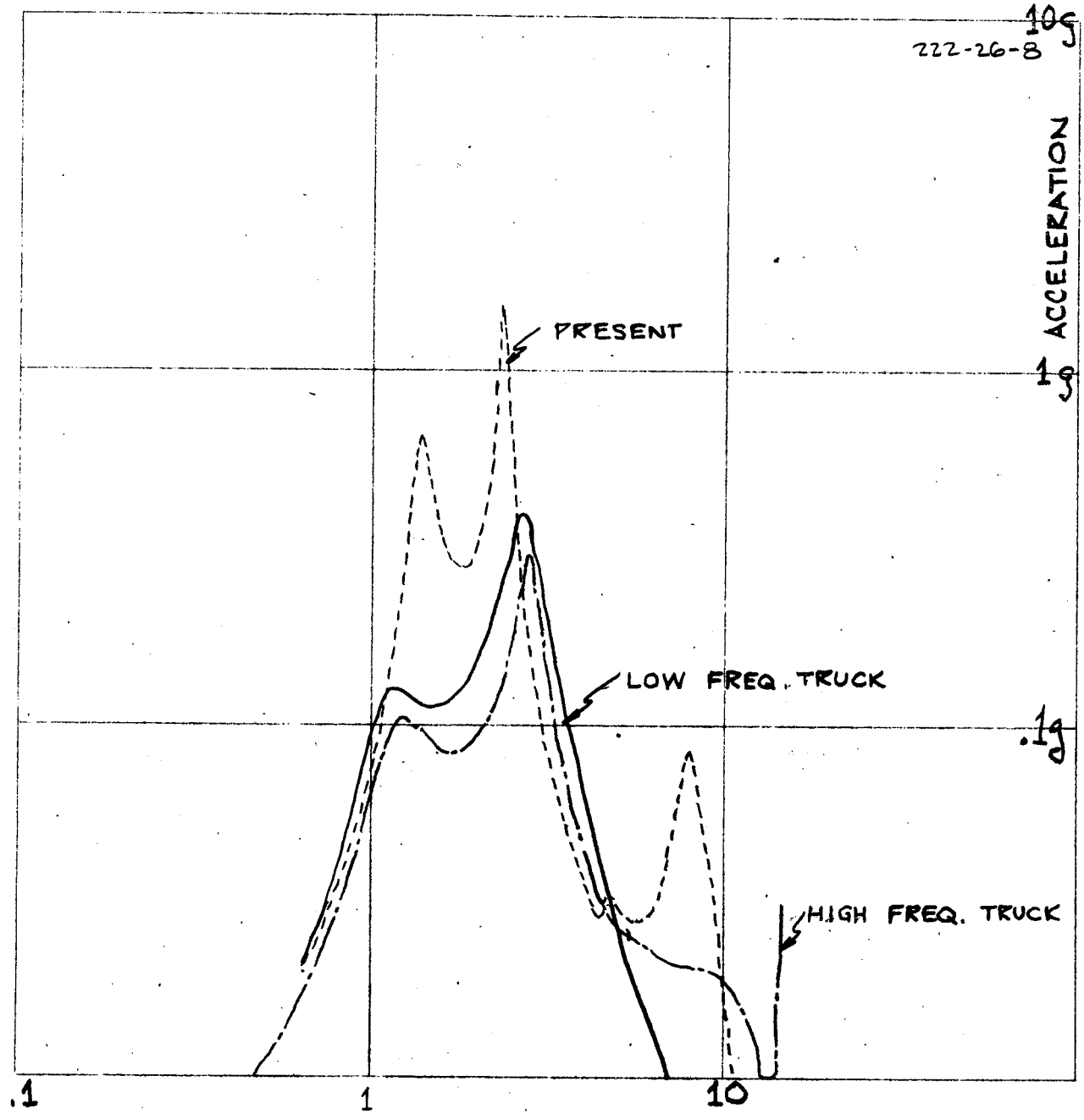

FIGURE 6.0-12

NEW TRUCK DESIGNS

TRUCK FRAME

LATERAL ACCELERATION DUE TO LATERAL INPUT

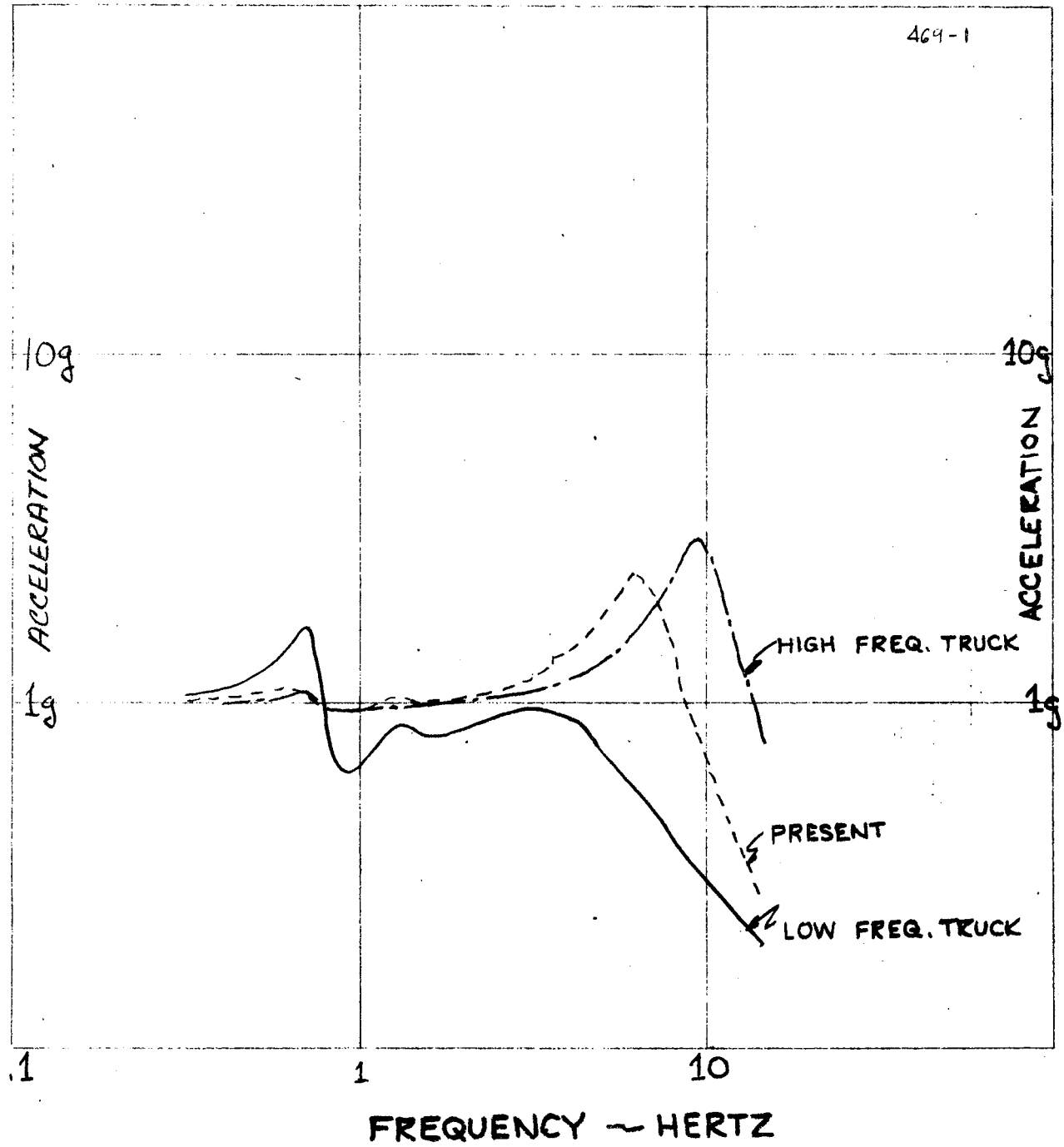

FIGURE 6.0-13

NEW TRUCK DESIGNS

TRUCK FRAME

LATERAL ACCELERATION DUE TO ROLL INPUT

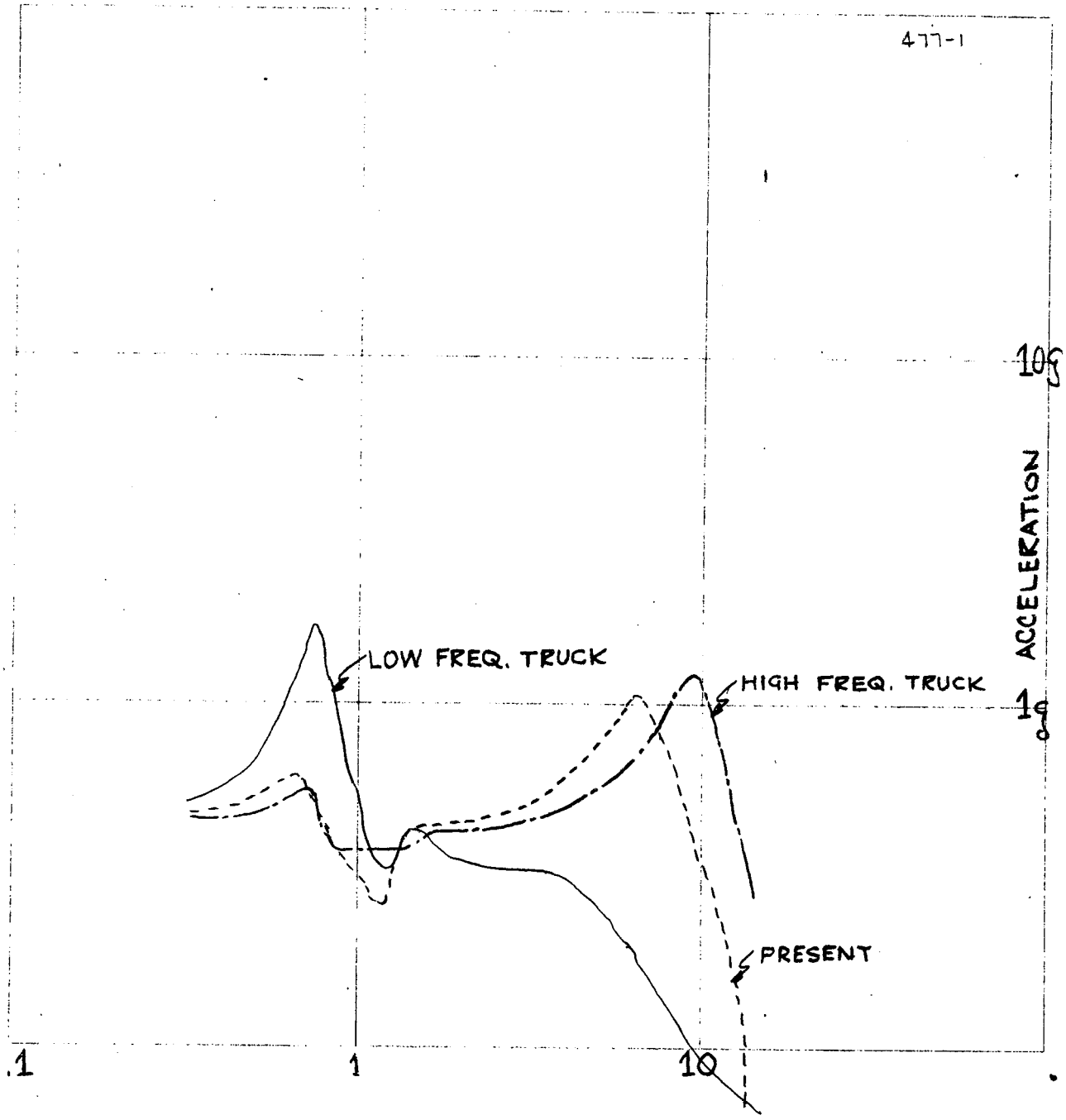

FIGURE 6.0-14

NEW TRUCK DESIGNS

TRUCK FRAME

LATERAL ACCELERATION DUE TO YAW INPUT

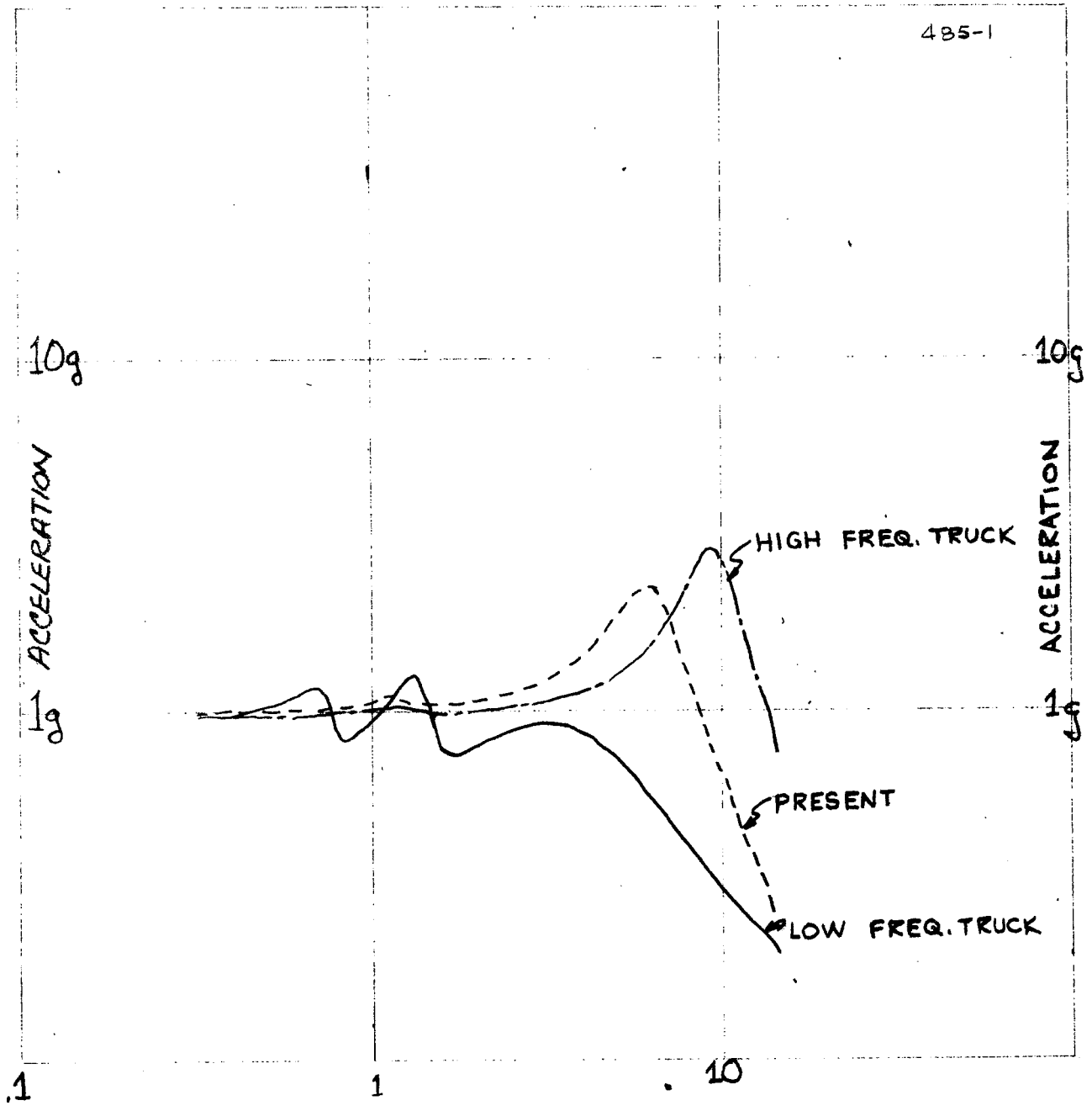

FIGURE 6.0-15

NEW TRUCK DESIGNS

TRUCK FRAME

ROLL ACCELERATION DUE TO ROLL INPUT

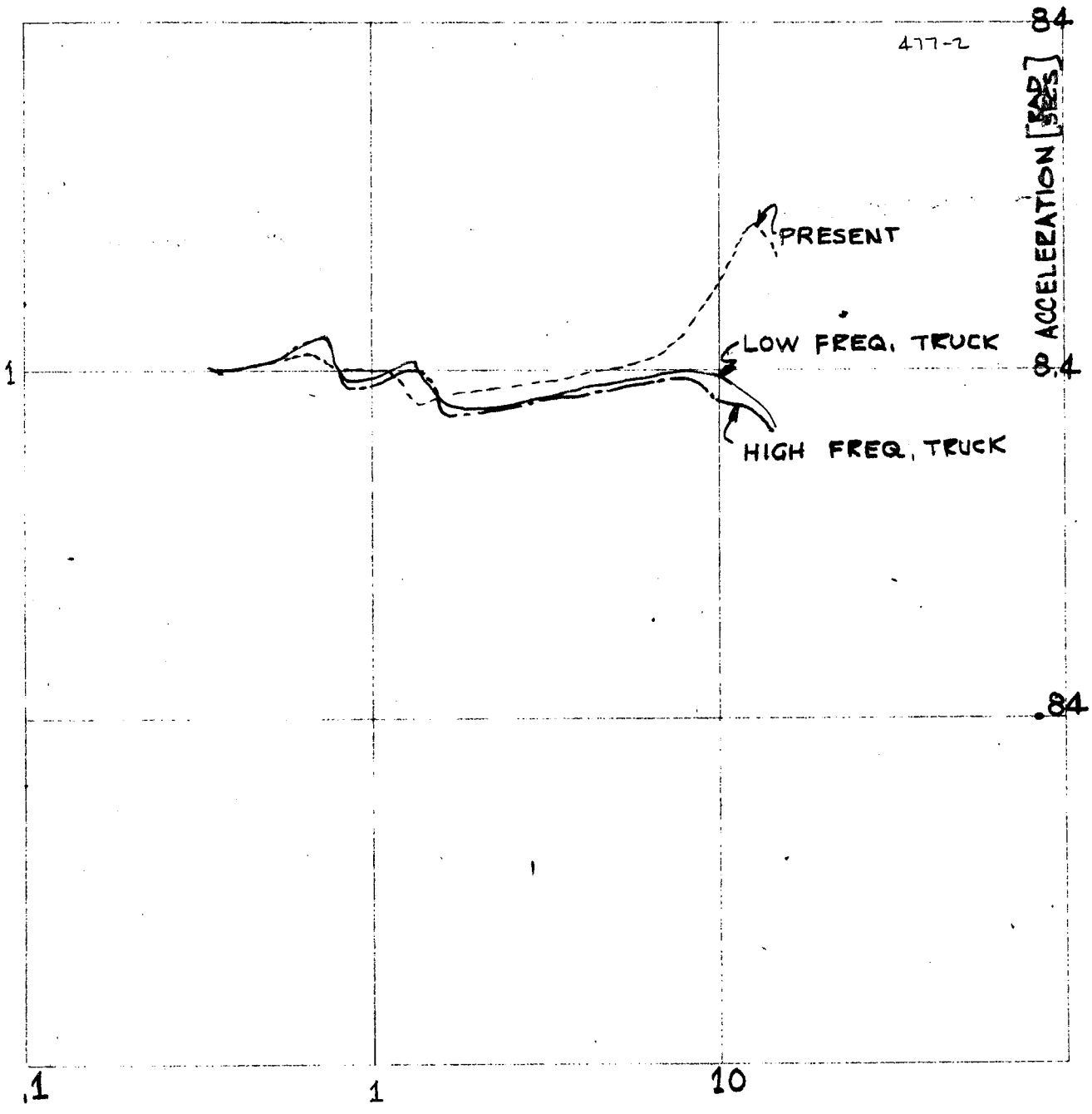

FIGURE 6.0-16

NEW TRUCK DESIGNS

TRUCK FRAME

ROLL ACCELERATION DUE TO LATERAL INPUT

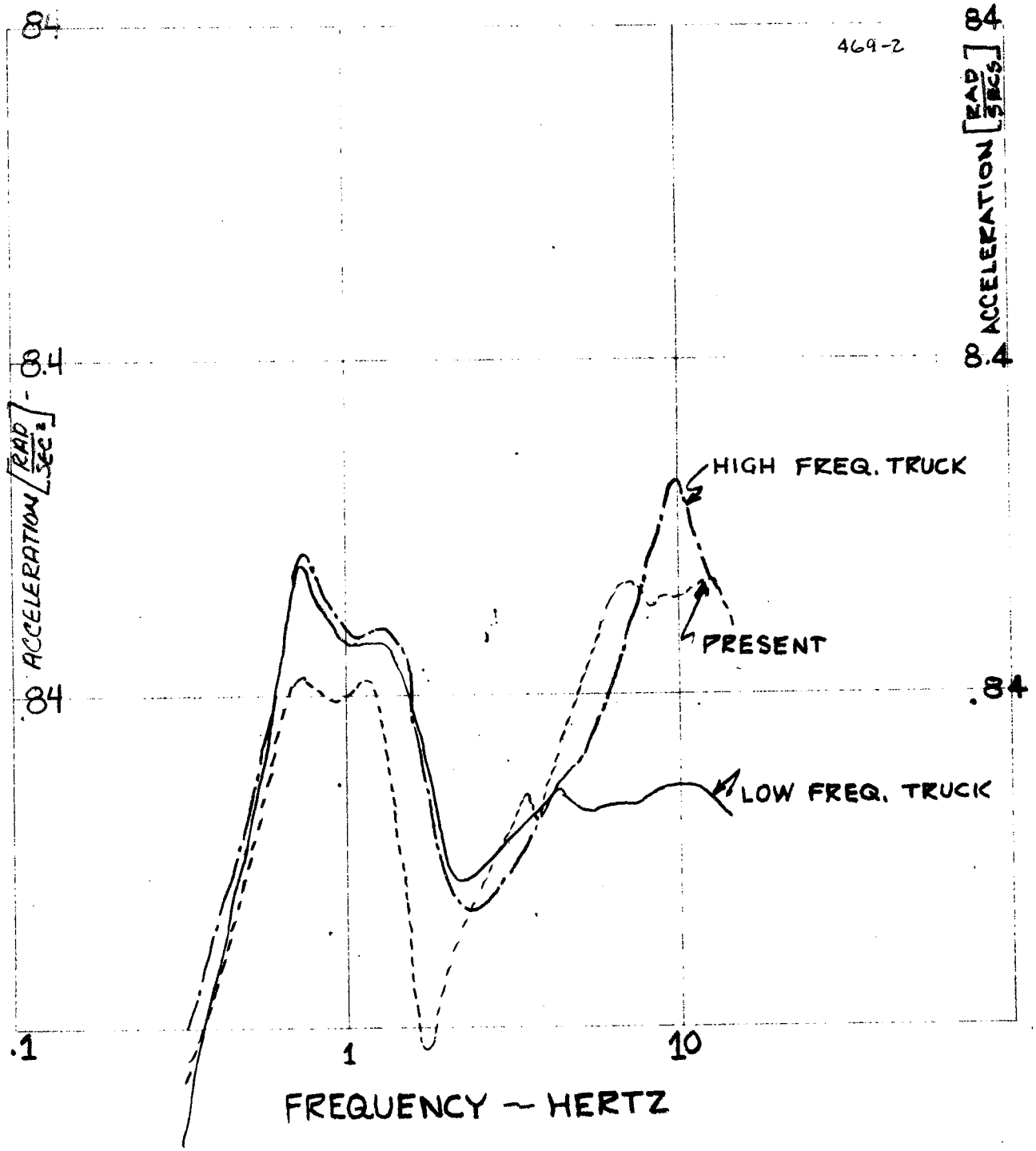

FIGURE 6.0-17

NEW TRUCK DESIGNS

TRUCK FRAME

ROLL ACCELERATION DUE TO YAW INPUT

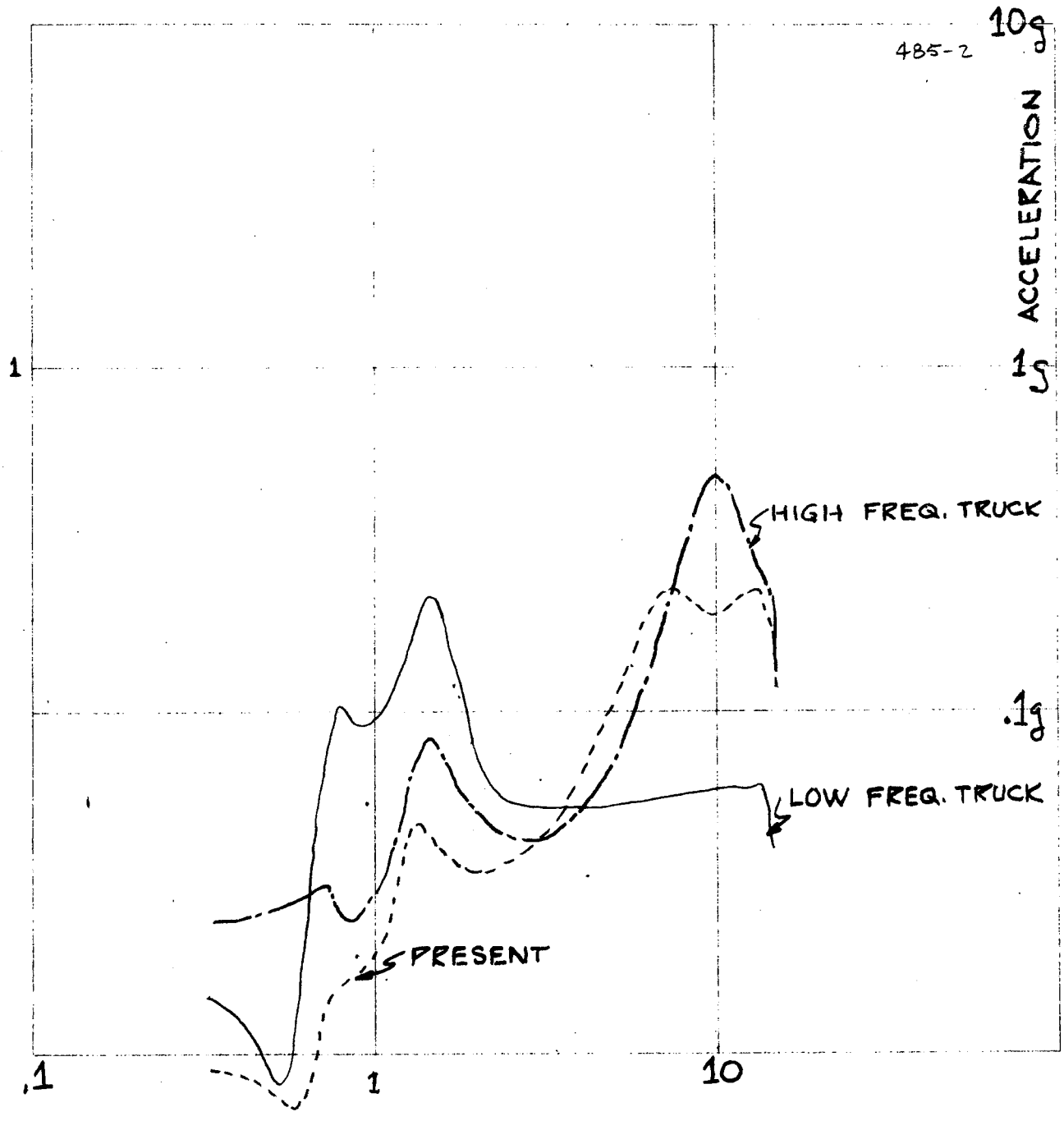

FIGURE 6.0-18

NEW TRUCK DESIGNS

CARBODY "A" END

LATERAL ACCELERATION DUE TO LATERAL INPUT

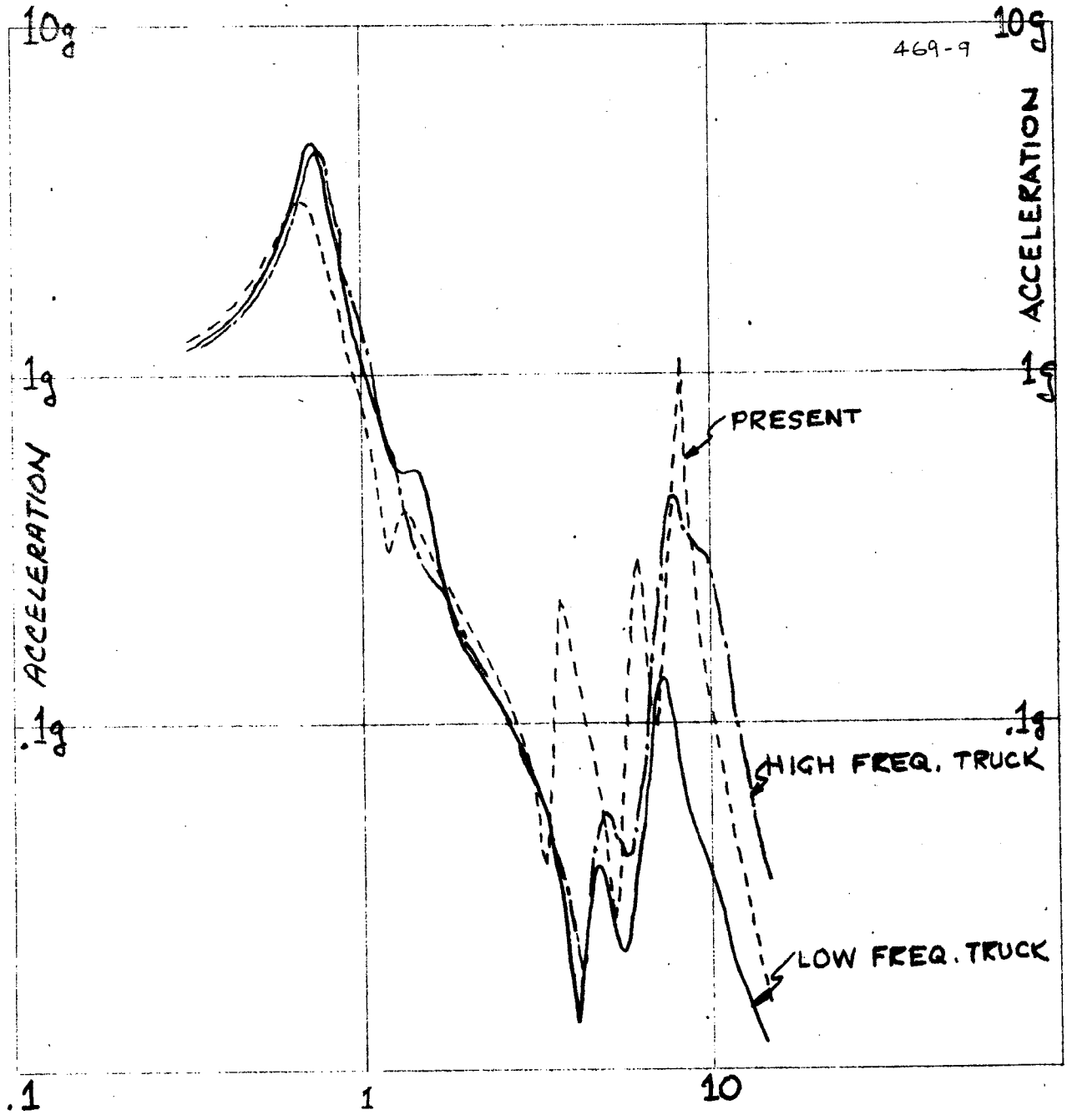

FIGURE 6.0-19

NEW TRUCK DESIGNS

CARBODY "A" END

LATERAL ACCELERATION DUE TO ROLL INPUT

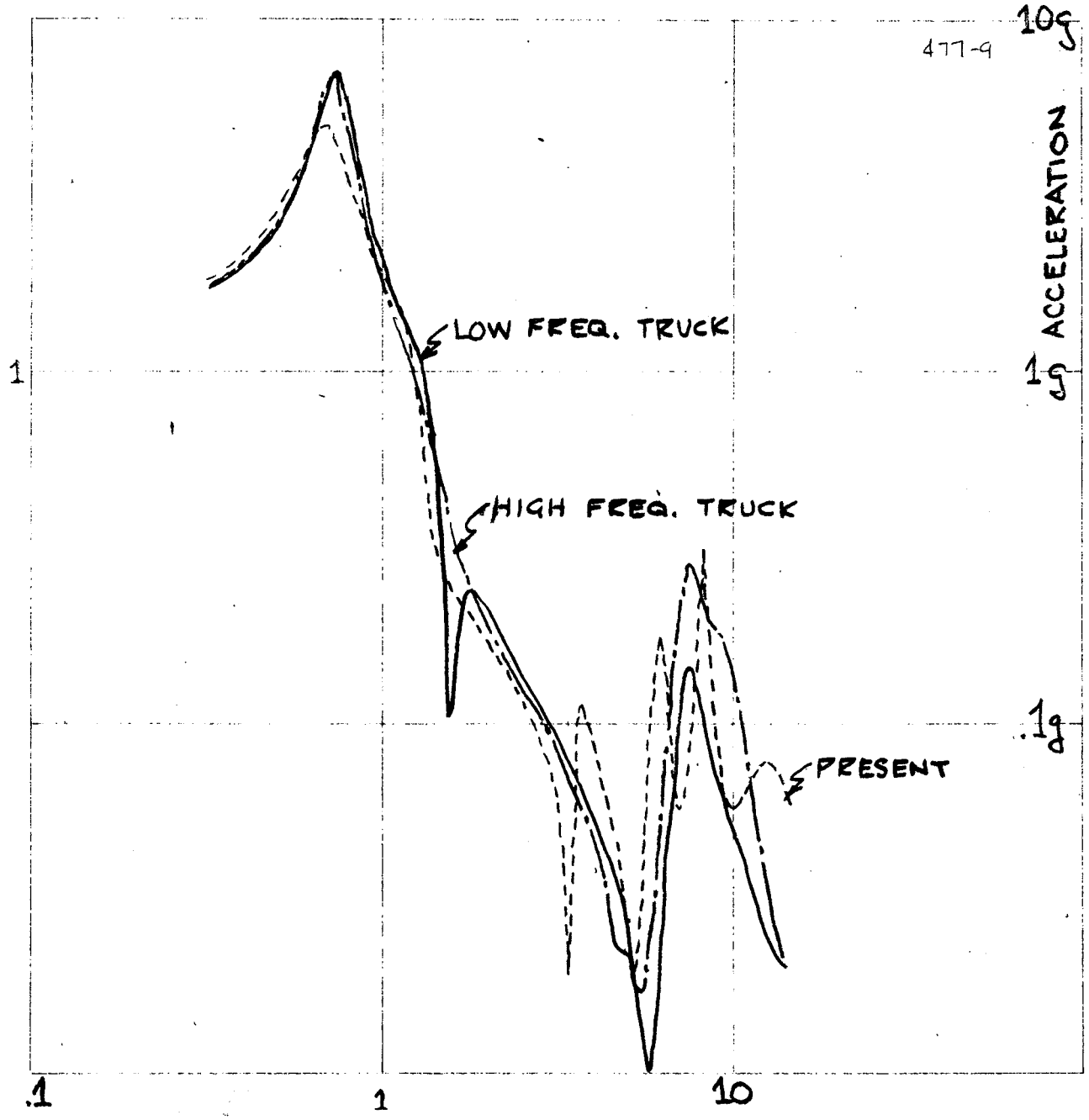

FIGURE 6.0-20

NEW TRUCK DESIGNS

CARBODY "A" END

LATERAL ACCELERATION DUE TO YAW INPUT

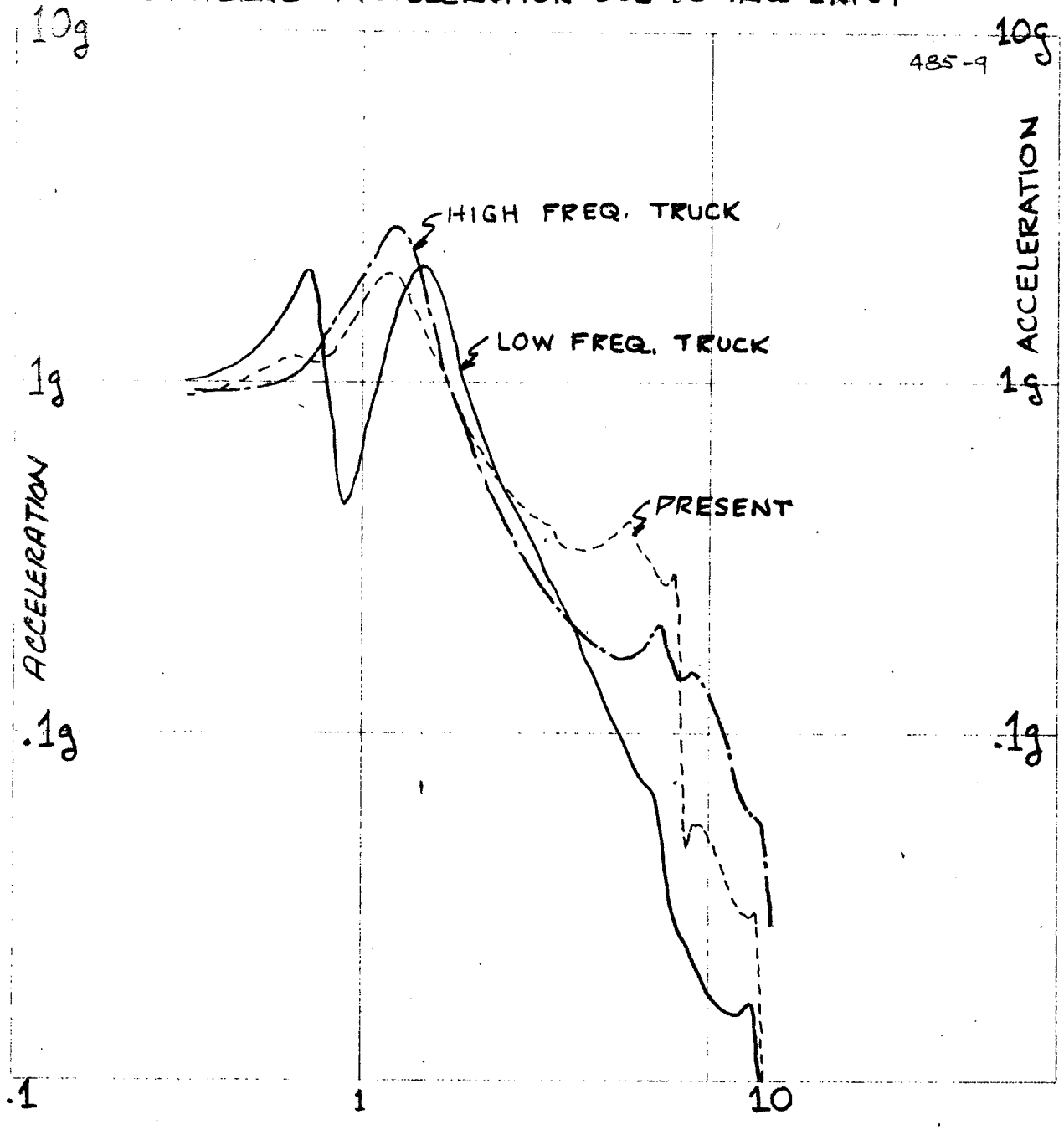

FIGURE 6.0-21

NEW TRUCK DESIGNS

CARBODY CENTER

LATERAL ACCELERATION DUE TO LATERAL INPUT

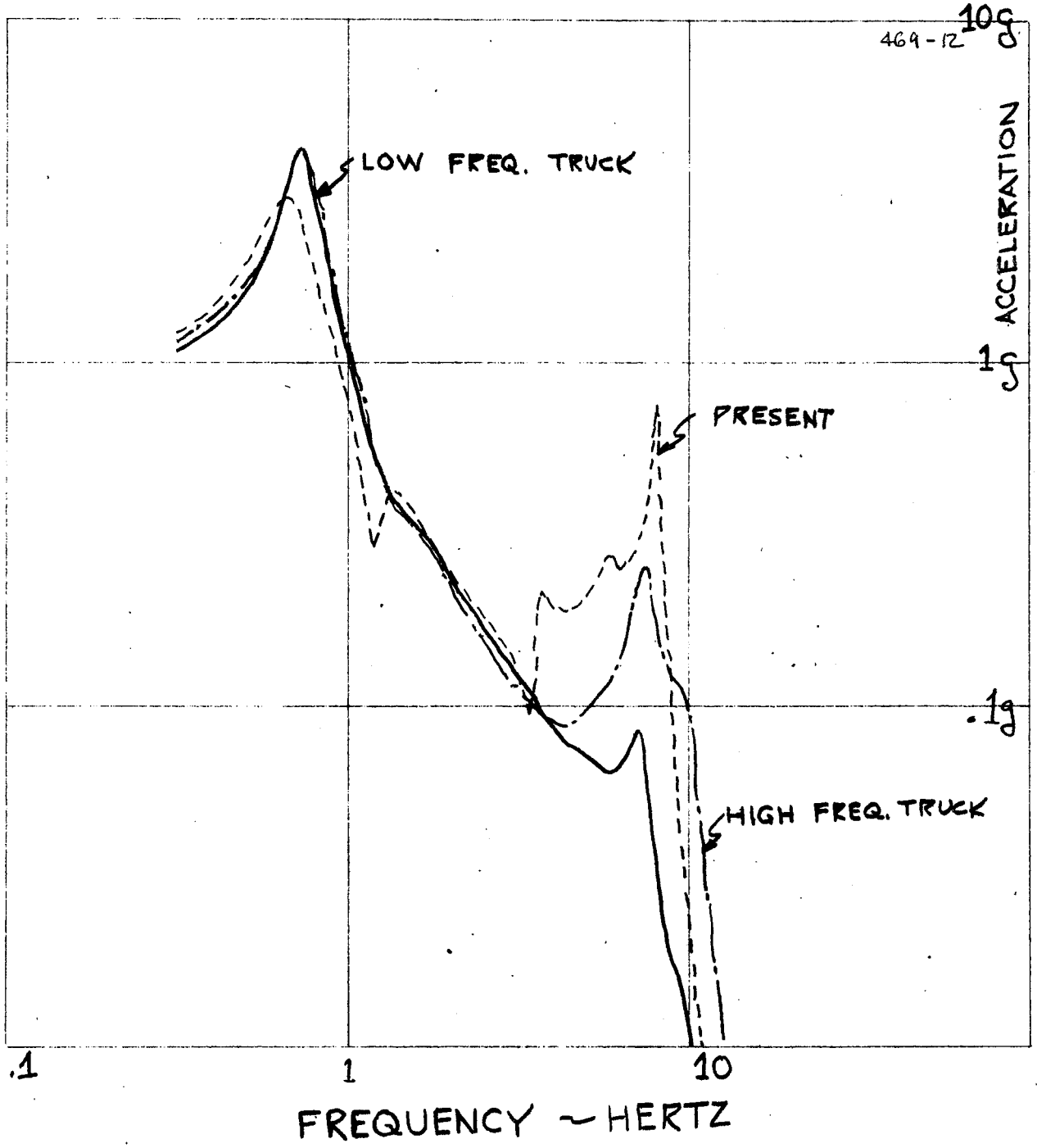

FIGURE 6.0-22

NEW TRUCK DESIGNS

CARBODY CENTER

LATERAL ACCELERATION DUE TO ROLL INPUT

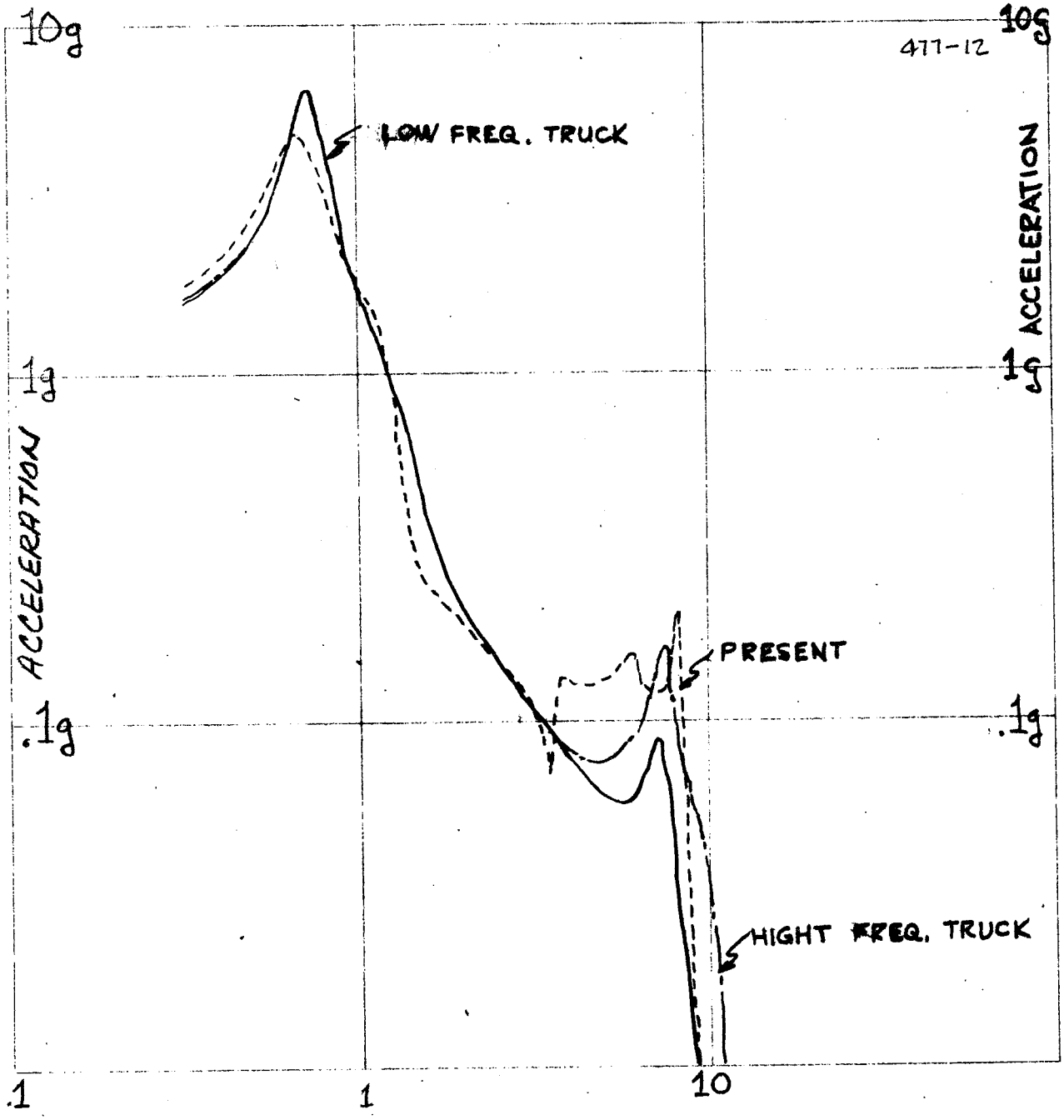

FREQUENCY – HERTZ

FIGURE 6.0-23

NEW TRUCK DESIGNS

CARBODY CENTER

LATERAL ACCELERATION DUE TO YAW INPUT

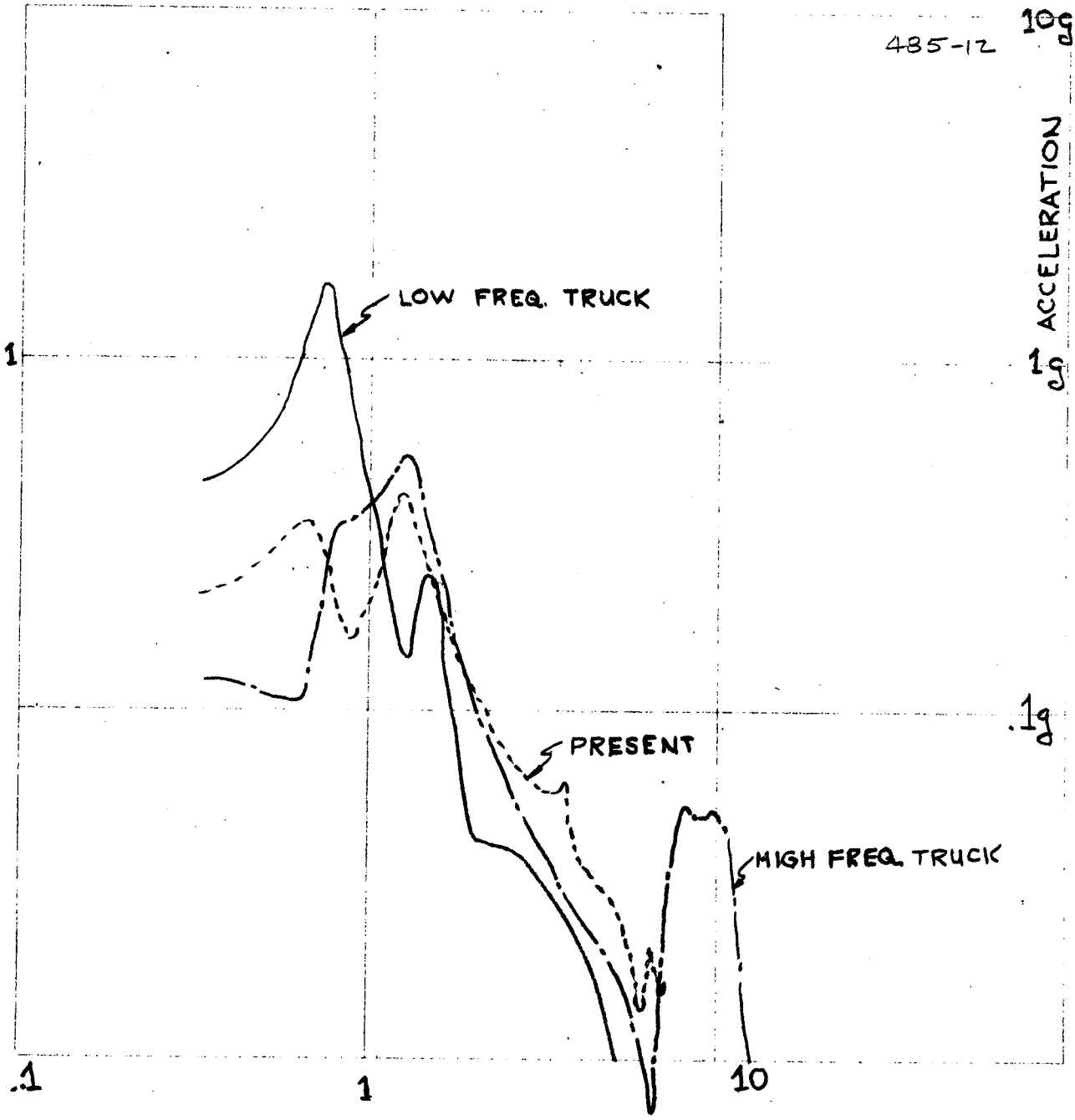

FIGURE 6.0-24

NEW TRUCK DESIGNS

CARBODY "A" END

ROLL ACCELERATION DUE TO LATERAL INPUT

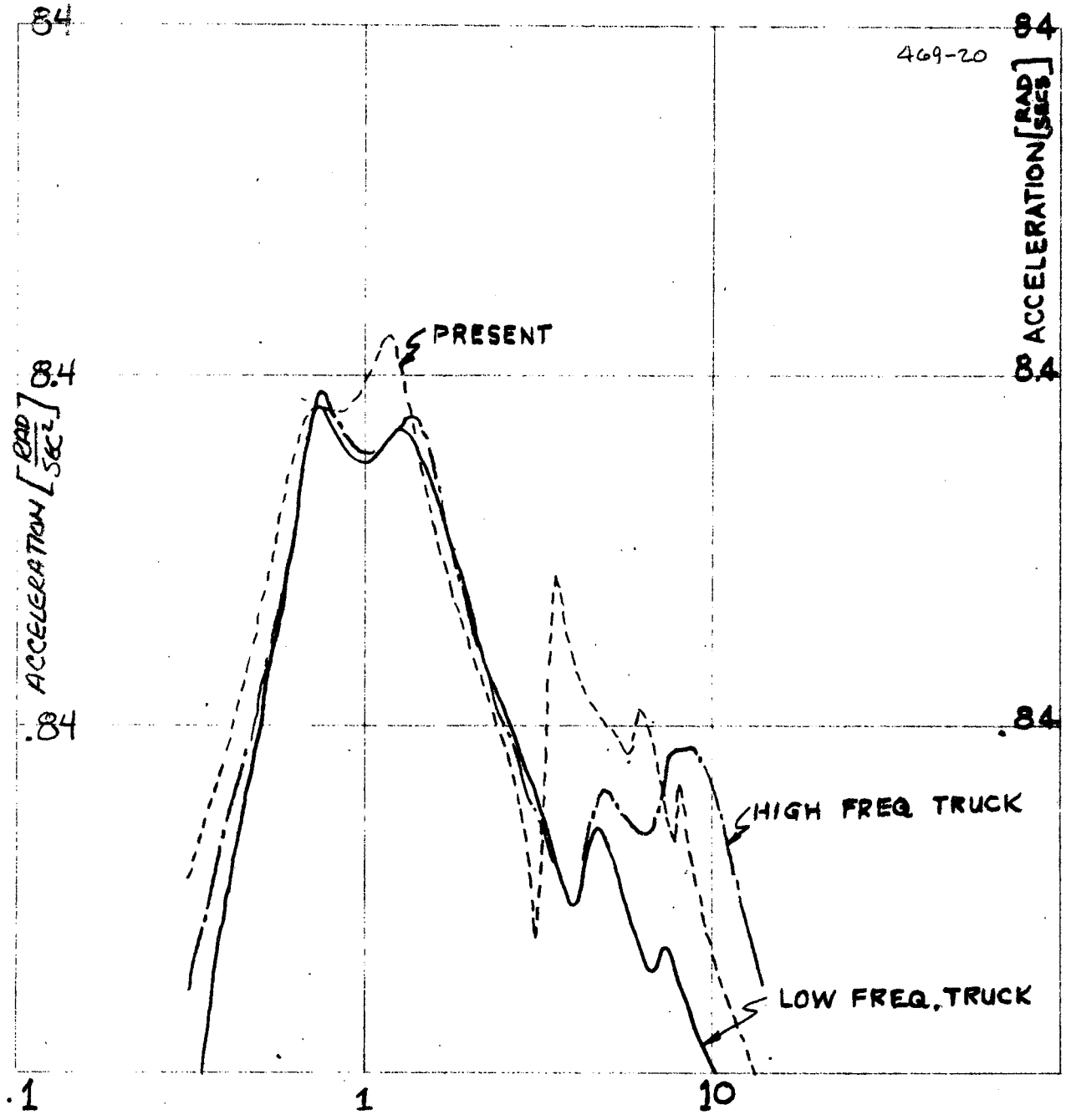

FREQUENCY ~ HERTZ

FIGURE 6.0-25

NEW TRUCK DESIGNS

CARBODY A END

ROLL ACCELERATION DUE TO YAW INPUT

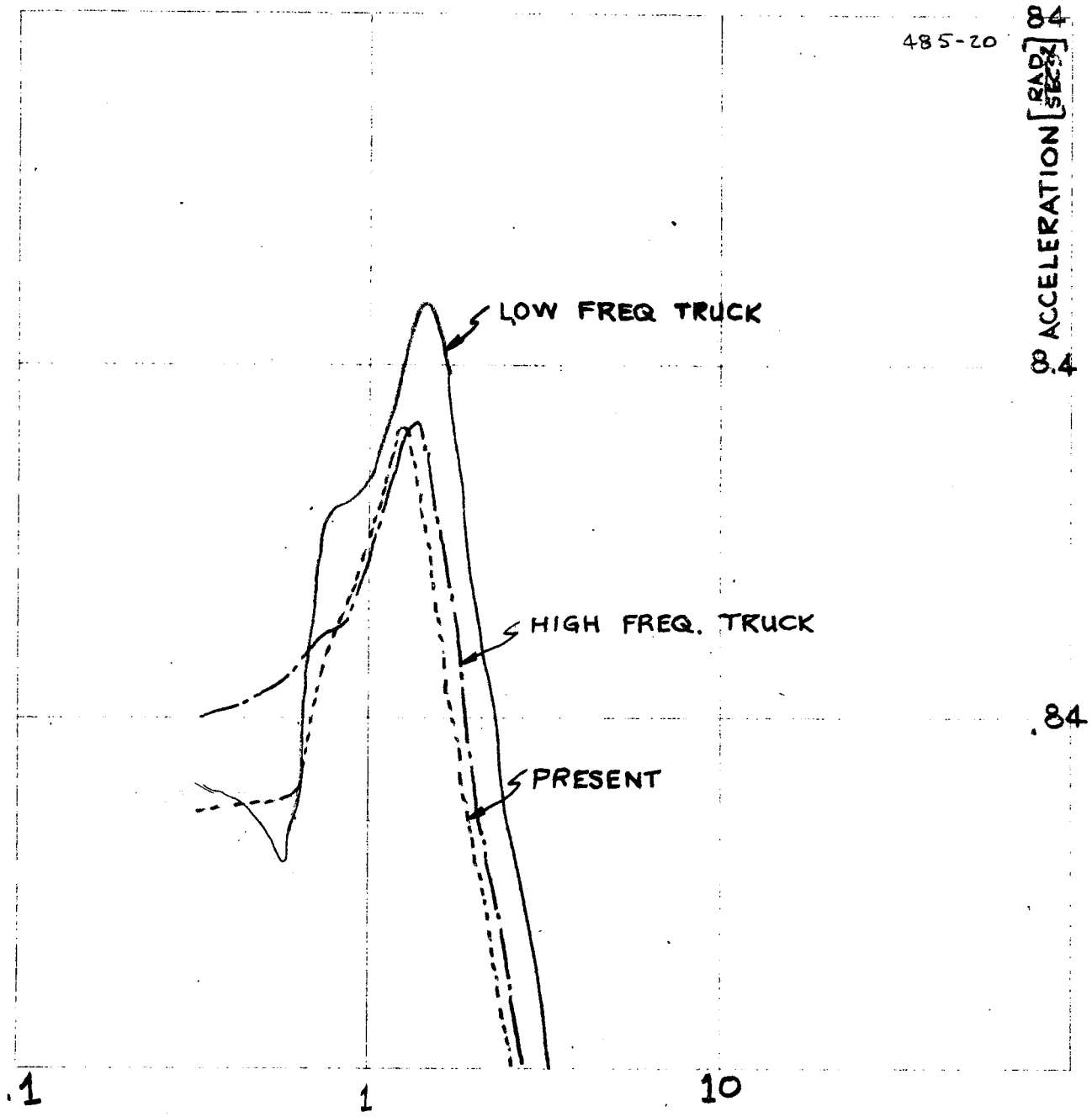

FIGURE 6.0-26

NEW TRUCK DESIGNS

CARBODY "A" END

ROLL ACCELERATION DUE TO ROLL INPUT

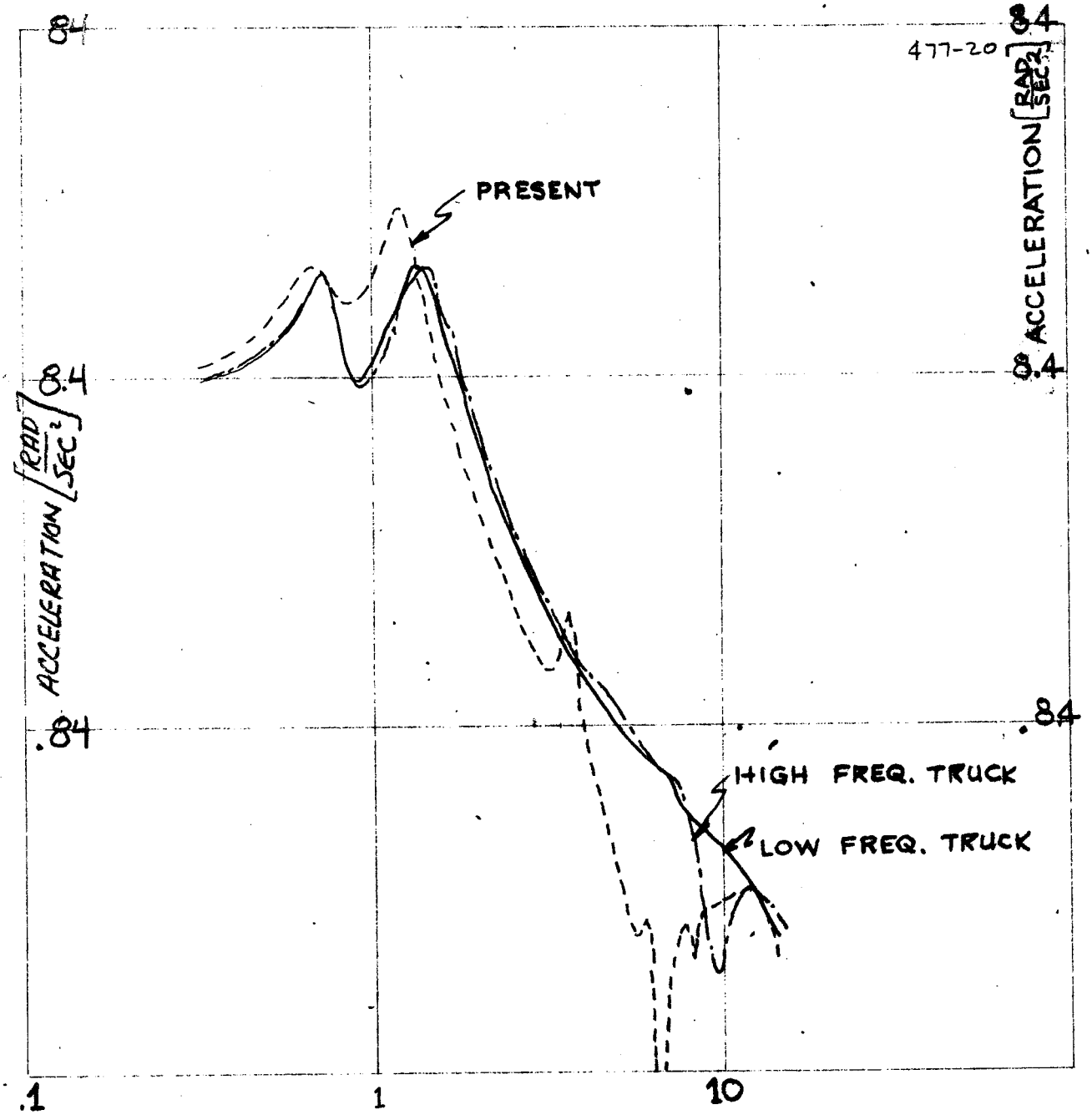

FREQUENCY – HERTZ

FIGURE 6.0-27

NEW TRUCK DESIGNS

TRANSFORMER

LATERAL ACCELERATION DUE TO LATERAL INPUT

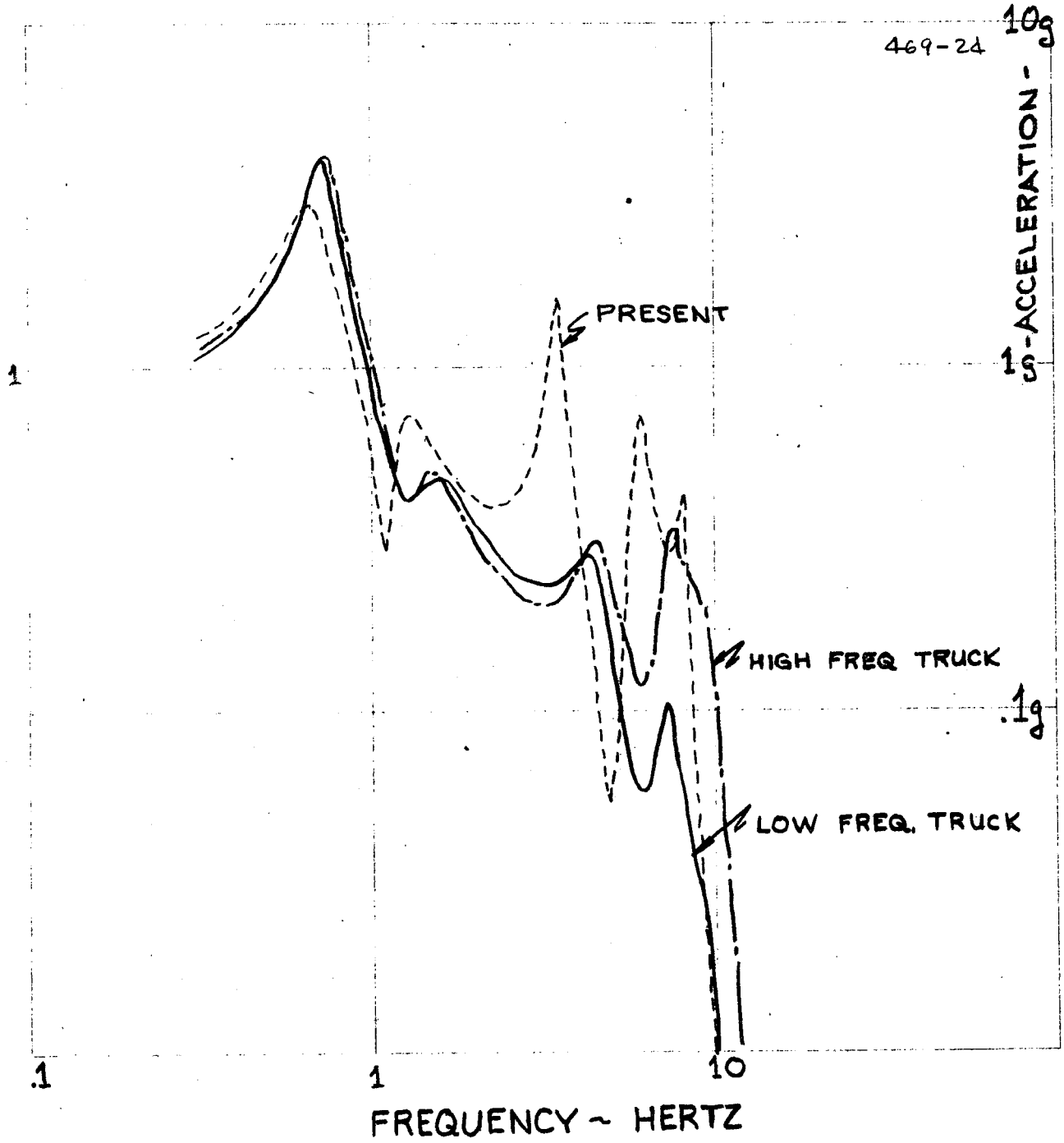

FIGURE 6.0-28

NEW TRUCK DESIGNS

TRANSFORMER

LATERAL ACCELERATION DUE TO ROLL INPUT

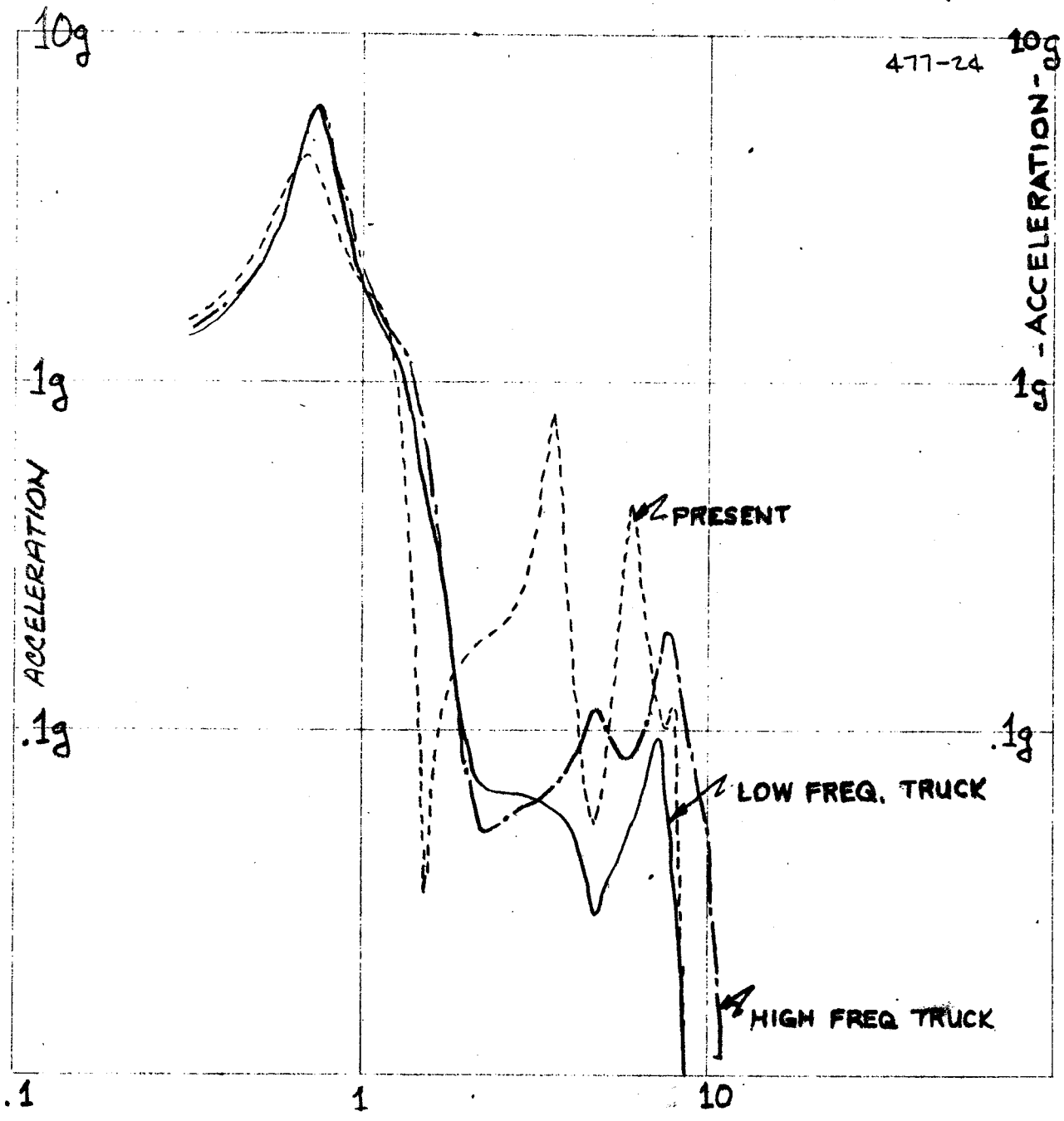

FIGURE 6.0-29

NEW TRUCK DESIGNS

TRANSFORMER

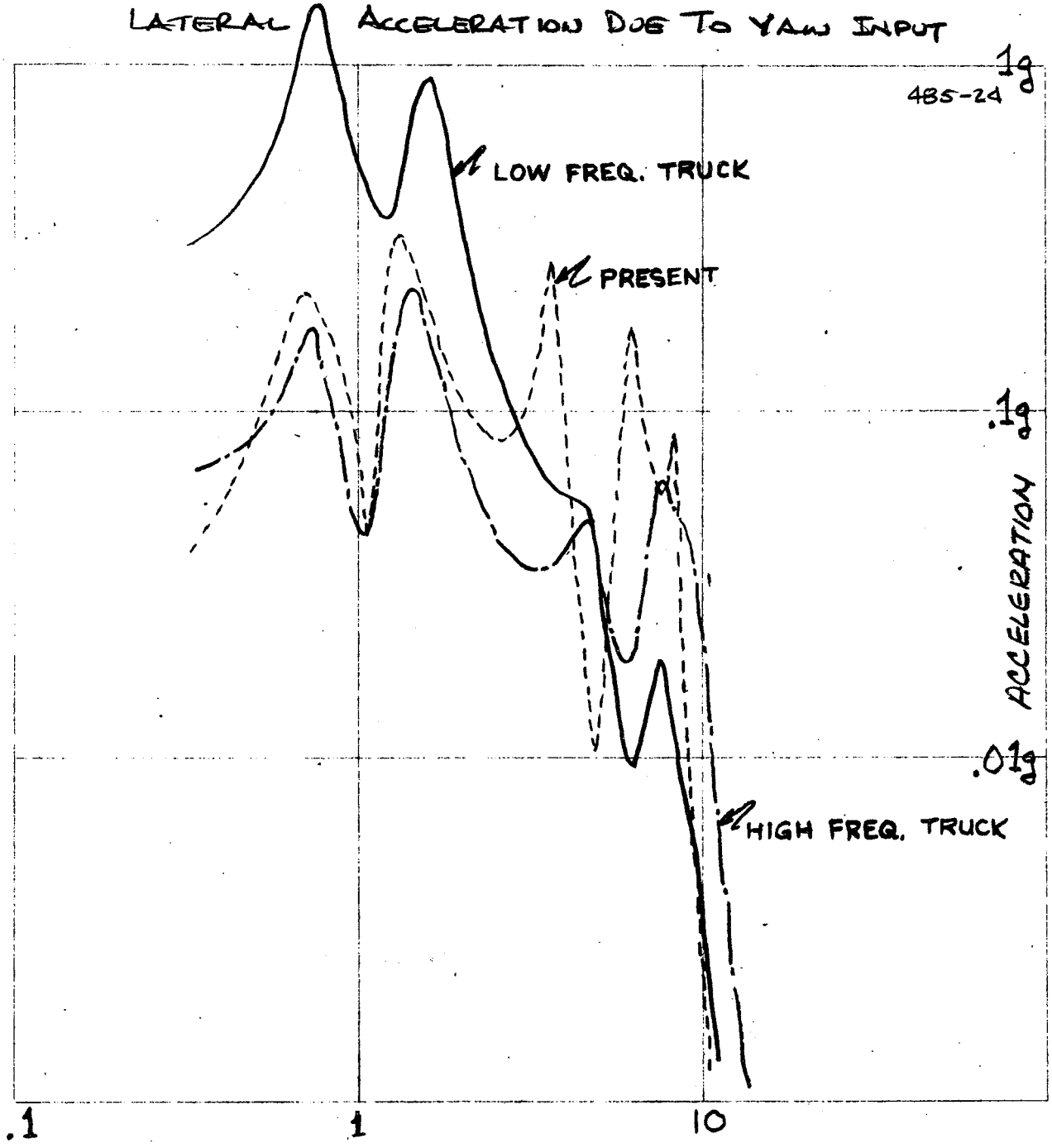

FIGURE 6.0-30

TABLE 6.0-2

SUSPENSION PARAMETERS OF VERTICAL AND LATERAL HIGH FREQUENCY TRUCKS

Primary Suspension System per Truck	High Frequency Truck for Vertical Simulation	High Frequency Truck for Lateral Simulation
Vertical Stiffness	290,000#/in.	10,700#/in.
Lateral Stiffness	---	116,000#/in.
Longitudinal Stiffness	96,000#/in.	---
Vertical Damping	533#sec./in.	686#sec./in.
Lateral Damping	---	433#sec./in.
Longitudinal Damping	686#sec./in.	---
Secondard Suspension System per Truck		
Vertical Stiffness	5,390#/in.	10,700#/in.
Lateral Stiffness	---	3,890#/in.
Longitudinal Stiffness	96,000#/in.	---
Vertical Damping	266#sec./in.	343#sec./in.
Lateral Damping	---	218#sec./in.
Longitudinal Damping	780#sec./in.	---